Summer 6-7-2012

Omics Approaches To Mammalian Cell Metabolic Engineering

Michael Betenbaugh
Johns Hopkins University

‘OMICS APPROACHES TO MAMMALIAN CELL METABOLIC ENGINEERING

Michael Betenbaugh
Chemical and Biomolecular Engineering
Johns Hopkins University
&
Novo Nordisk Foundation Center for Biosustainability
Copenhagen, Denmark

Metabolic Engineering

Thursday, June 7, 2012

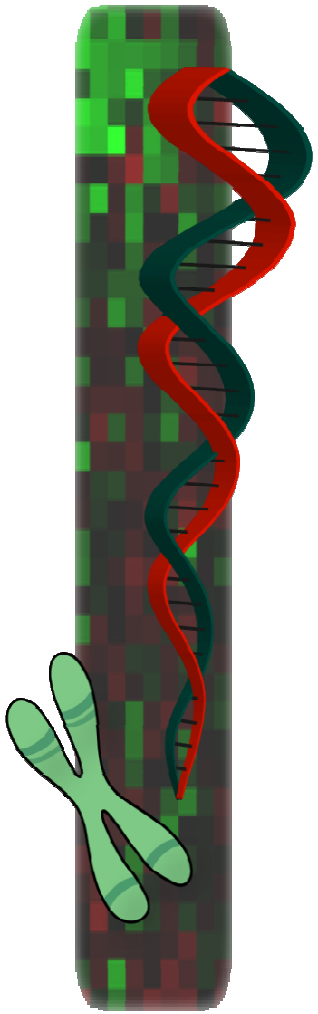

Chinese hamster ovary cells are a widely used protein production host because….

- Glycosylation patterns accepted by human immune system
- High production efficiency
- Growth to large scales in bioreactors
- Resistance to viral infection

First Step:
Decipher the Chinese Hamster Ovary Genome

Chinese Hamster

Chinese Hamster Ovary
(CHO) Cells

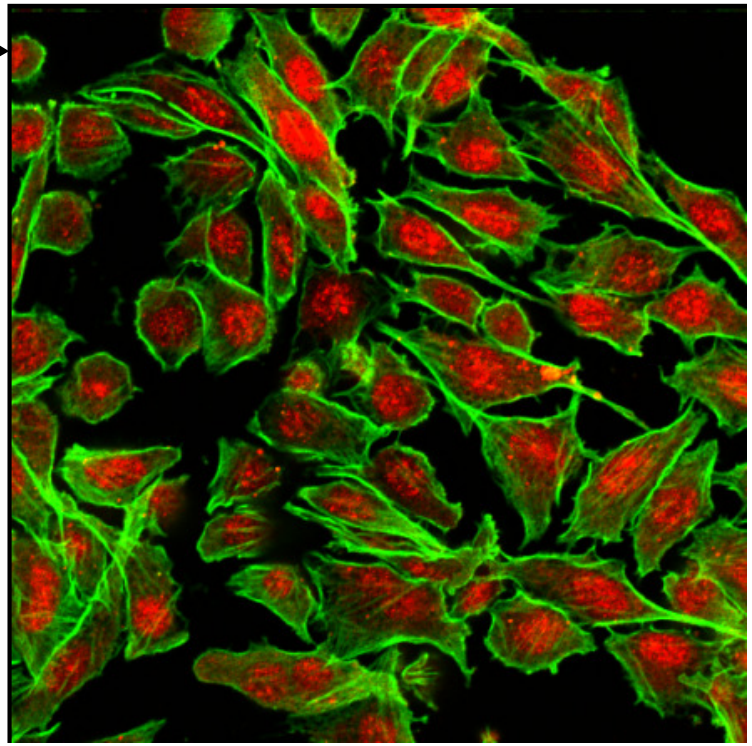

Analysis and Application of Gene Function in Chinese Hamster Ovary (CHO)

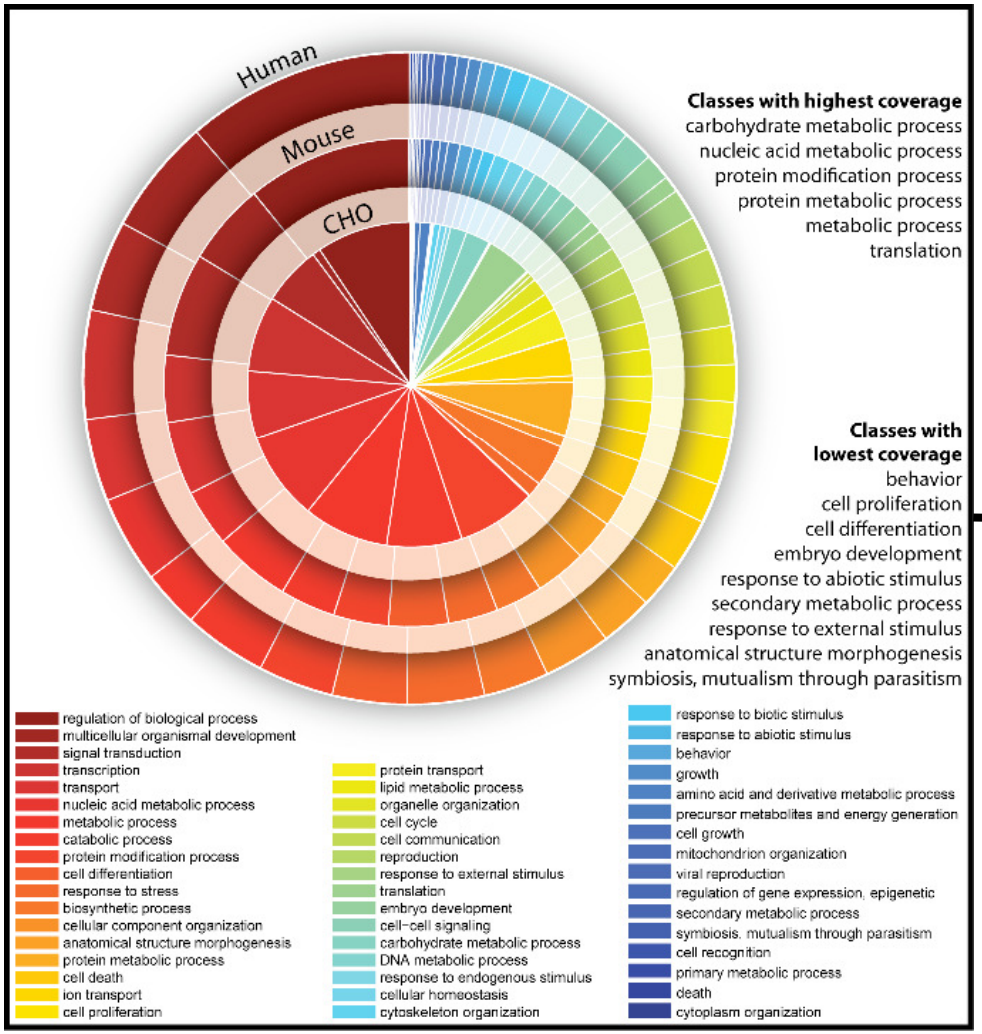

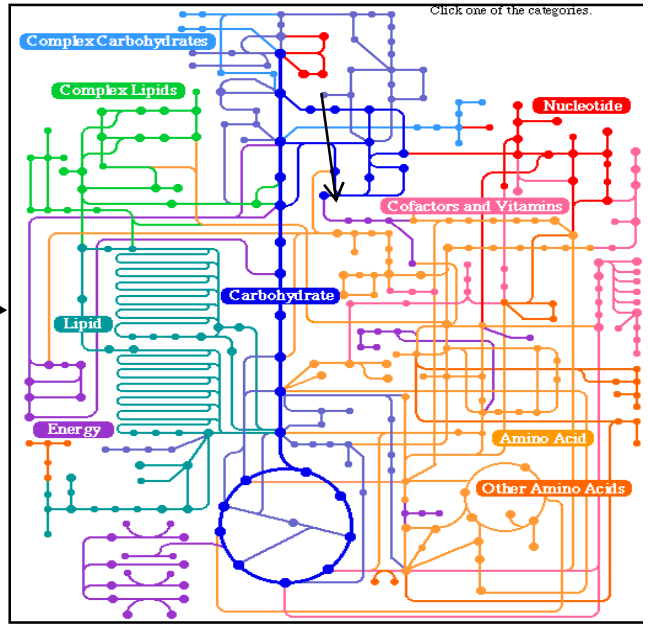

Metabolic Reconstructions w/ B. Palsson Group

Xu et al , Nature Biotechnoloy (2011)

Post-translational Processing: The Addition of Sugars Chains etc. to Proteins

Polypeptide Struc

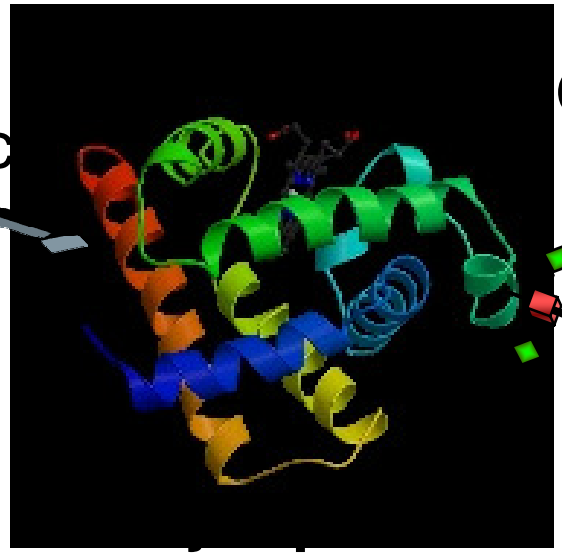

Glycosylation (*N*-glycan):
Attached sugar group

Biotherapeutics are Glycoproteins

*Polypeptide chain of amino acids

*Attached sugar (glycan) chains: glycosylation

CHO N-linked Glycosylation Pathways

Sialylation
α(2,6) linkage possible
Not expressed.

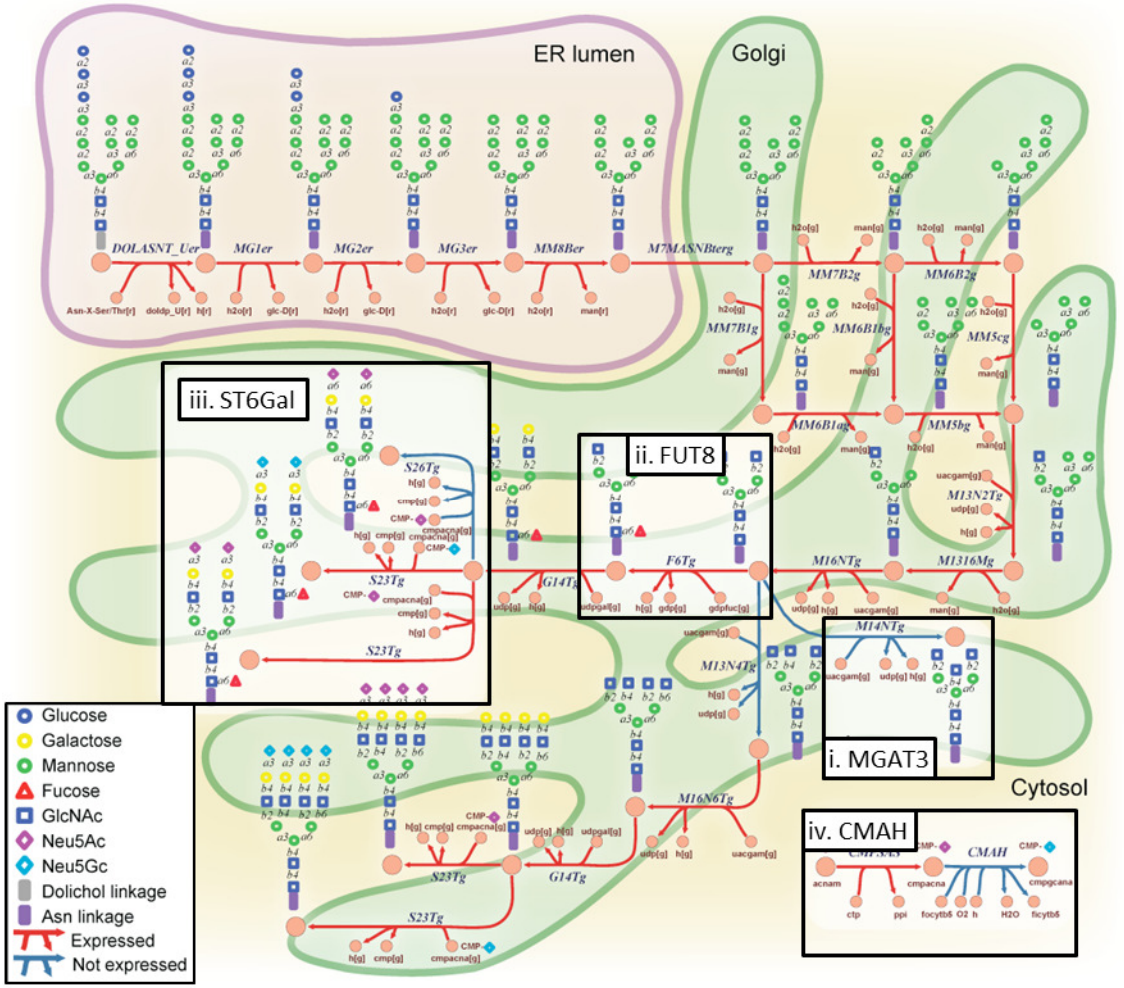

Only fucosyltransferases FUT8 and O-FUT

Bisecting (ß4) GlcNAc
LEC10 gain of function

Neu5Ac->Neu5Gc
No expression,
lower Neu5Gc less
immunogenic
response in humans.

Xu et al , Nature Biotechnol., (2011)

Can We Prevent Death Phase in Cell Culture?

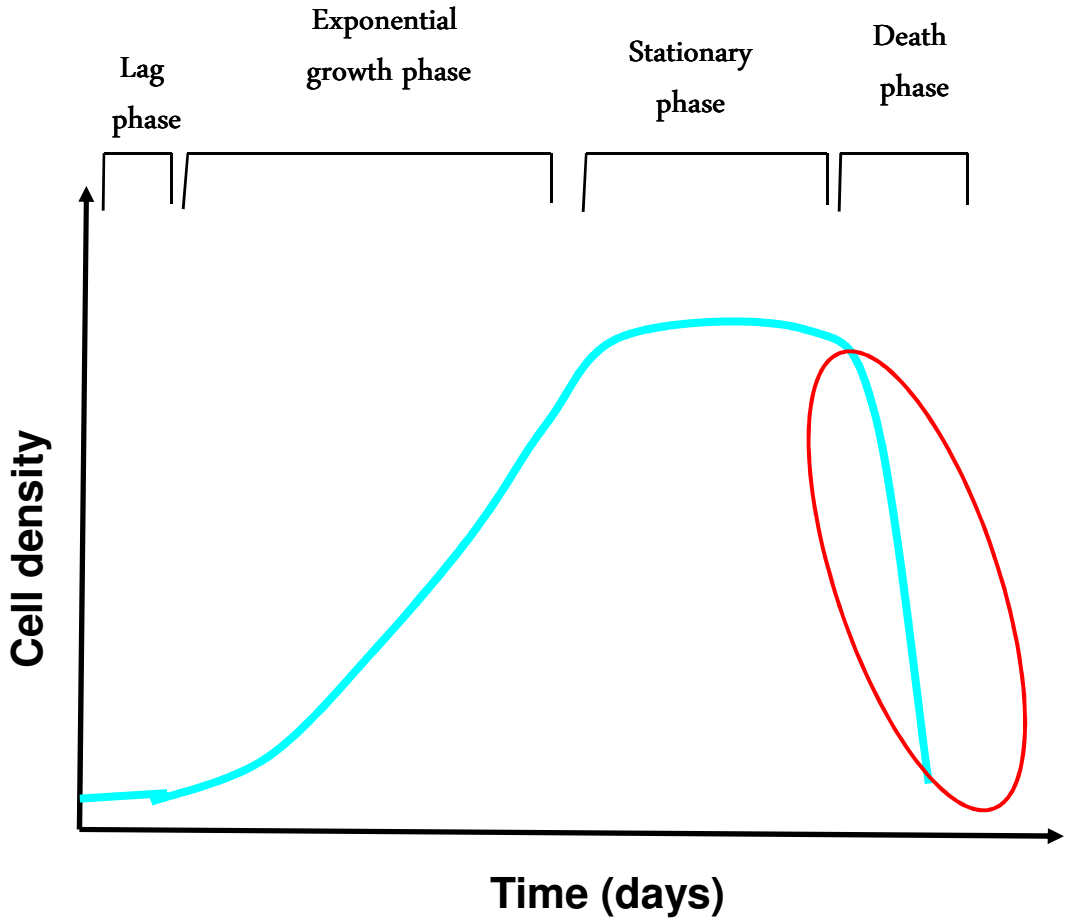

Death phase: number of viable (living cells) in the stationary phase culture decreases due to cell death

Apoptotic Detection Examples

Healthy Chinese Hamster Ovary (CHO) cell

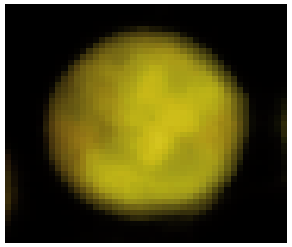

Apoptotic CHO cell

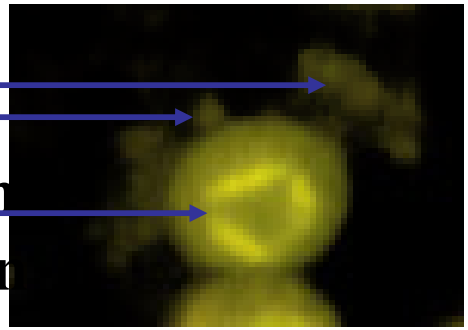

Acridine Orange Staining

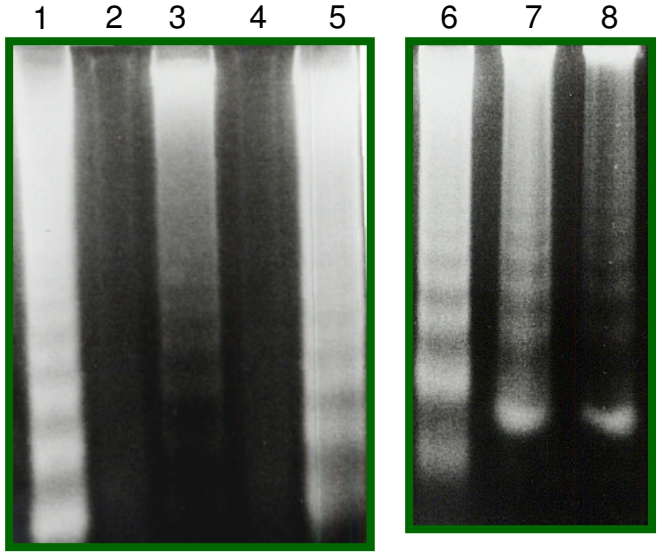

CHO cells (3 and 7) and
Baby Hamster Kidney (BHK)
(5 and 8) undergo DNA fragmentation

Does Nutrient Depletion Stimulate Apoptosis

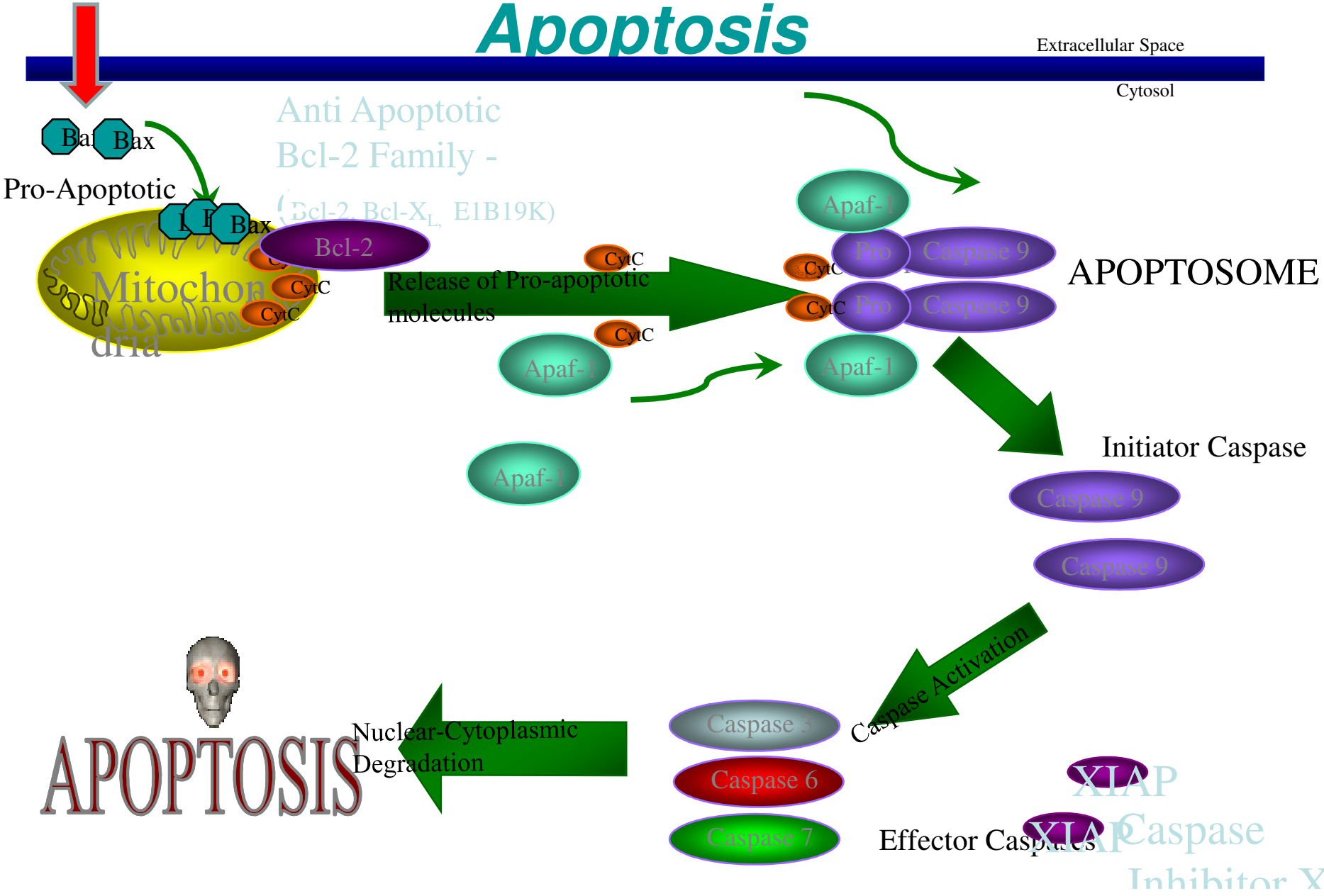

Comparison of Cell Viability in Depleted (Spent) and Nutrient Rich (Fresh) Media

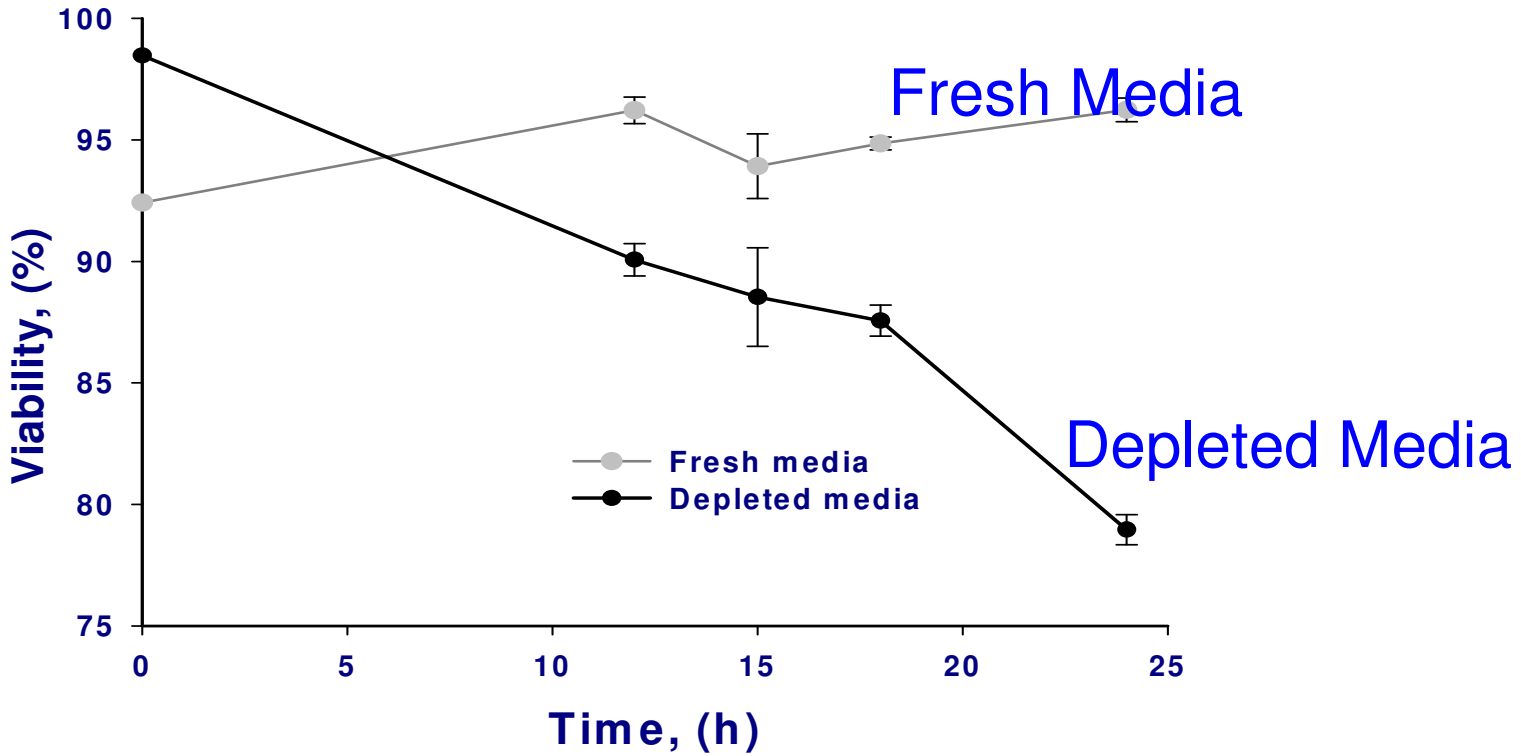

Alex Druz and Yossi Shiloach

Rapid decline (hours) of cell viability for cells Resuspended in spent media

Are CHO Apoptosis Pathways activated in Depleted Media:
Measurement of Caspase Activity

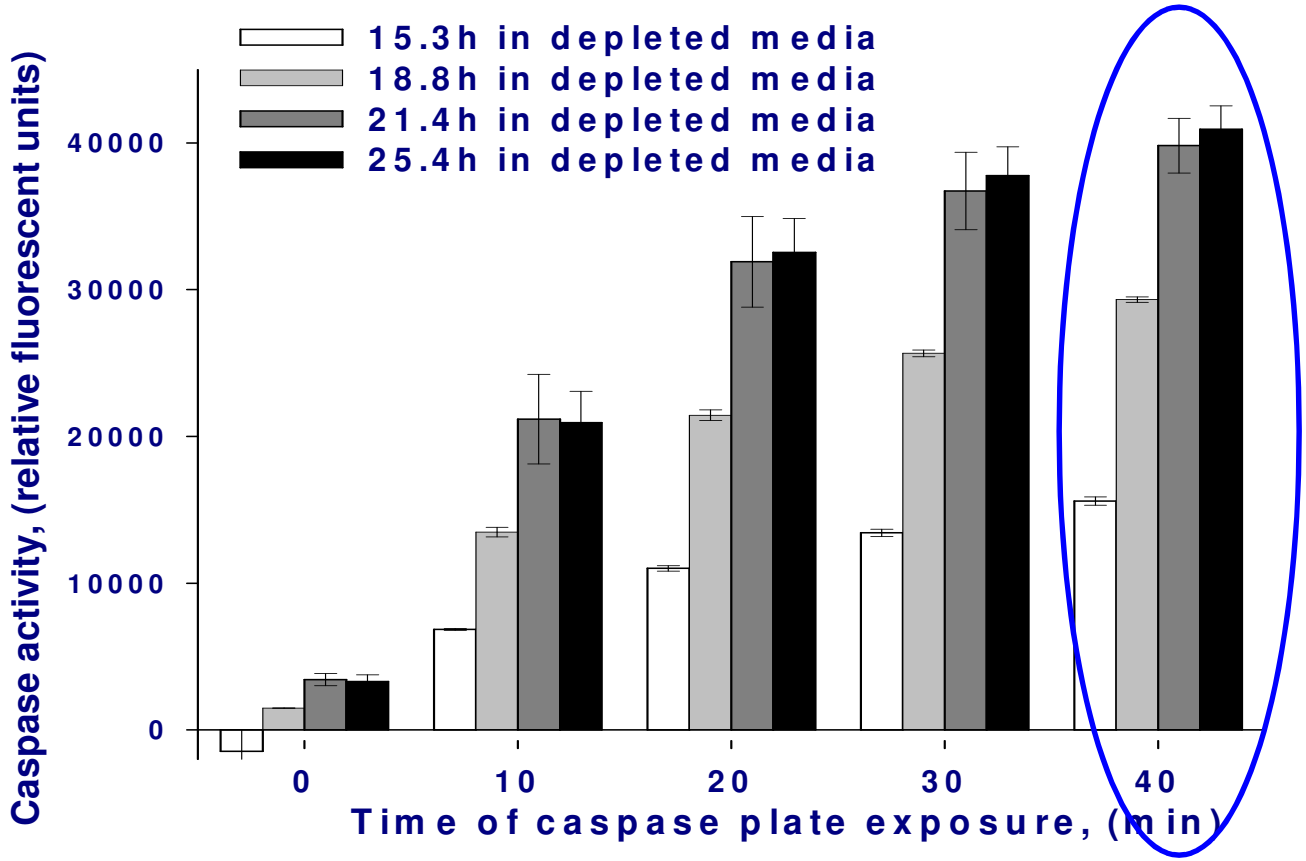

Caspase activity (apoptosis) increased for cells exposed for longer periods (20-25 hours) in depleted (spent) media

Higher Antibody Biotherapeutic Yields in Chinese hamster cells expressing anti-apoptotic genes

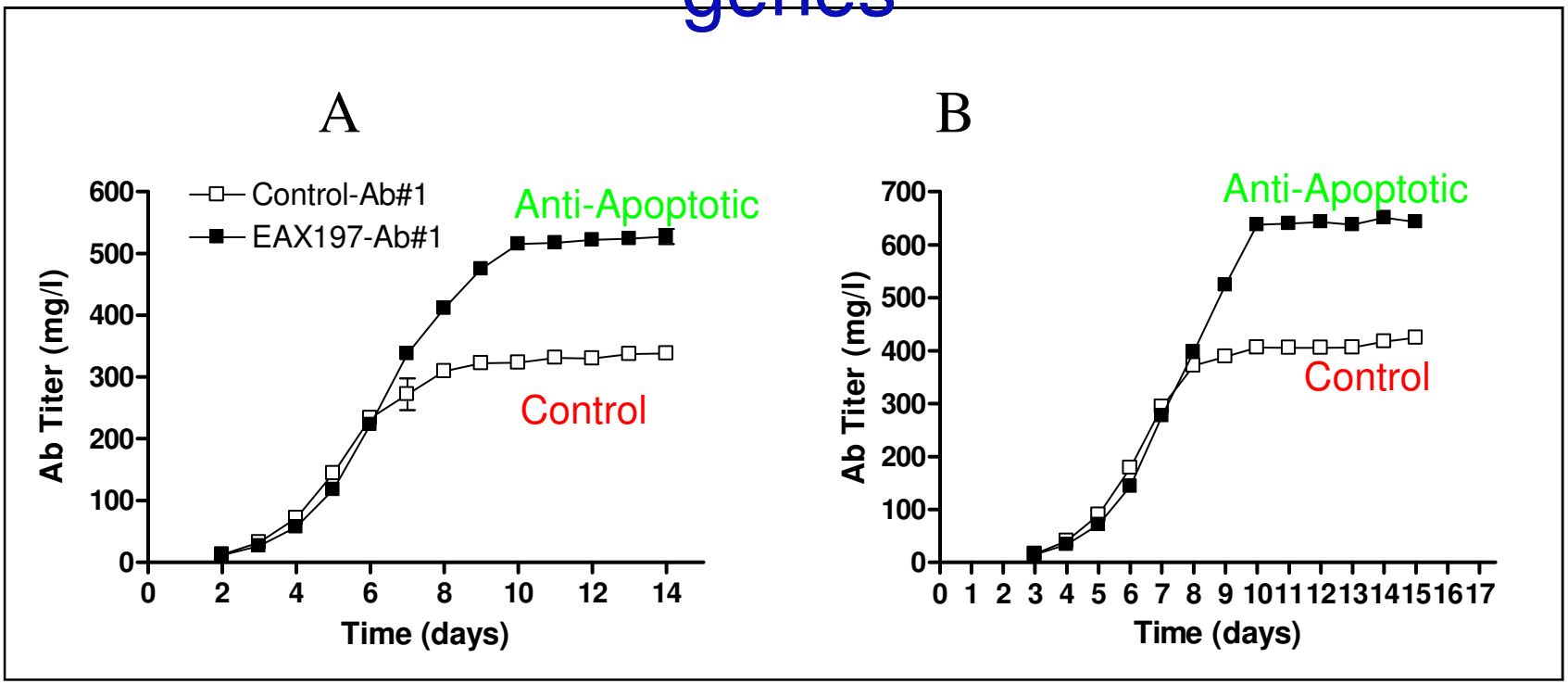

Dorai et al., Biotechnol. Bioeng.,

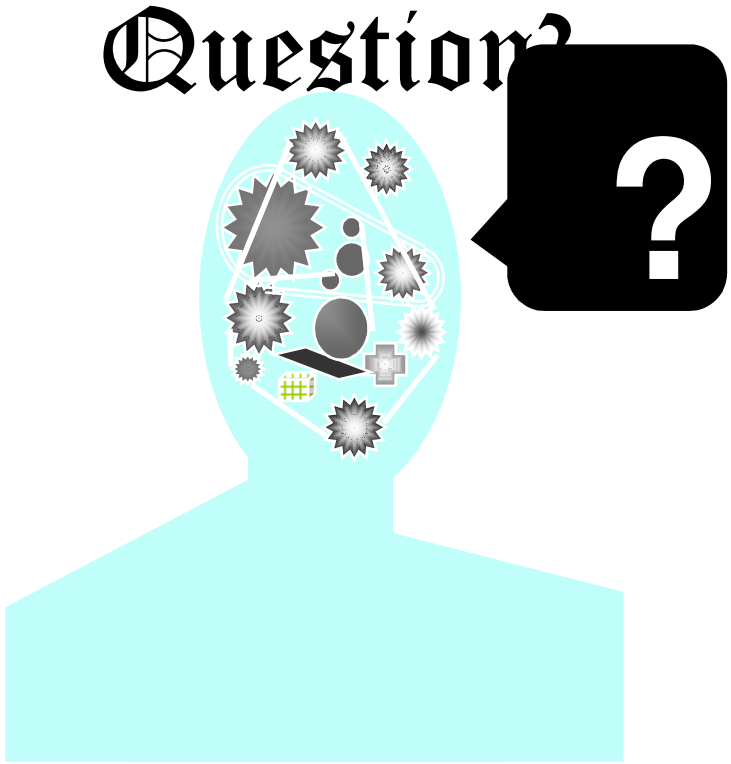

Can we apply
‘Omics approaches to help interpret
mammalian cell performance for biotechnology

Are MicroRNAs involved in Regulating Apoptosis Cascade in Mammalian cells

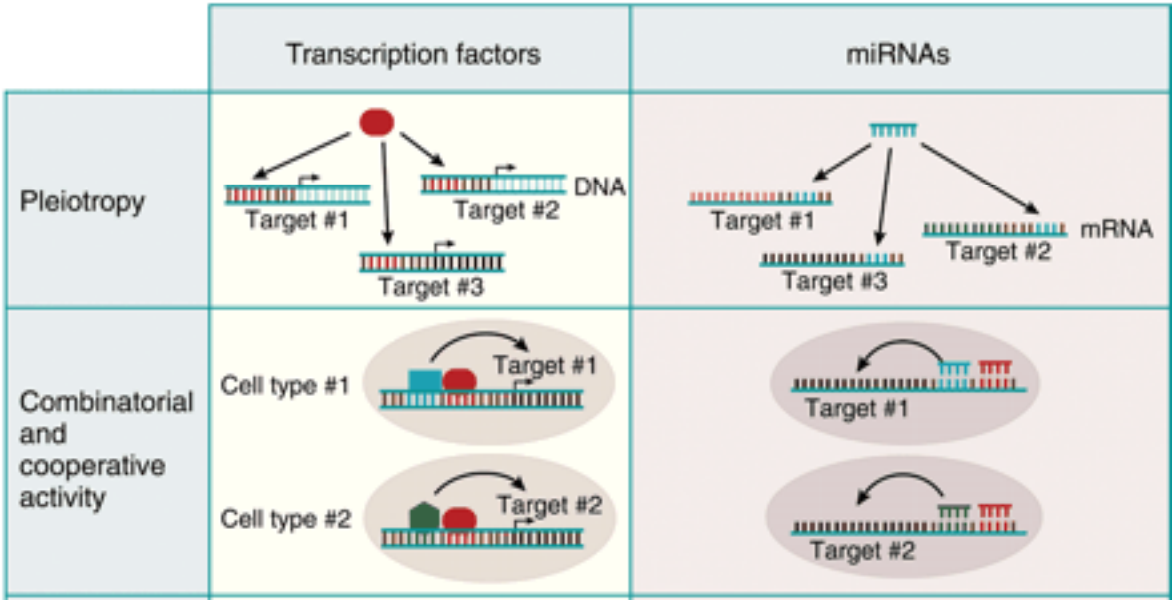

Microarray Analysis of MicroRNA: Fresh and Depleted Media

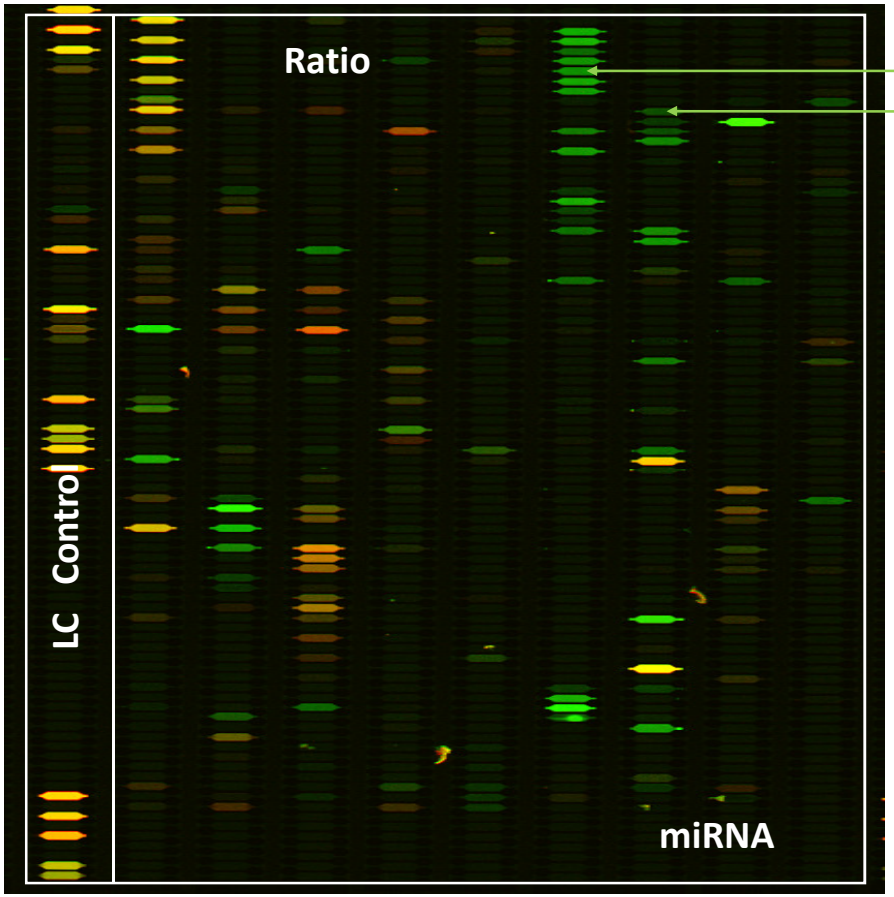

mmu-miR-466h

mmu-miR-669c

(A) Microarray map of overlaid images of miRs in fresh (labeled red) and depleted (labeled green) conditions.

MicroRNAs including mouse (mmu) microRNA (mir)-466h and mmu-mir-669c upregulated in depleted media

Location of microRNAs within cluster

Mouse miR ID (mmu-)	Variant	Mature miR sequence	Fresh media relative fluorescent signal	Depleted media relative fluorescent signal	Up-regulation in depleted media (times)	p-value
miR-297a	-	AUGUAUGUGUGCAUGUGCAUGU	14±4	1412±220	101±13	0.039
miR-466a	3p	UAUACAUACACGCACACAUAAGA	8±1	203±30	25±1	0.050
miR-466b	3-3p	AAUACAUACACGCACACAUAAGA	5±1	209±39	42±1	0.035
miR-466d	3p	UGUGUGUGCGUACAUGUACAUG	10±1	648±122	65±6	0.039
	5p	UAUACAUACACGCACACAUAG	8±2	552±92	69±6	0.050
miR-466f	3p	CAUACACACACACAUACACAC	19±1	5056±105	266±8	0.009
	5p	UACGUGUGUGUGCAUGUGCAUG	102±13	22200±5982	218±31	0.036
miR-466g	-	AUACAGACACAUGCACACACA	51±9	14935±4286	293±32	0.038
miR-466h	**-**	**UGUGUGCAUGUGCUUGUGUGUA**	**29±4**	**13105±2366**	**452±19**	**0.023**
miR-467a	minor	AUAUACAUACACACACCUACAC	44±1	9567±2001	217±40	0.025
miR-467b	minor	AUAUACAUACACACACCAACAC	72±8	14451±2817	201±17	0.027
miR-467e	minor	AUAUACAUACACACACCUAUAU	14±2	1056±38	75±8	0.022
miR-669a	-	AGUUGUGUGUGCAUGUUCAUGU	7±0	57±3	8±0	0.016
miR-669b	-	AGUUUUGUGUGCAUGUGCAUGU	8±0	46±1	6±0	0.003
miR-669c	**-**	**AUAGUUGUGUGUGGAUGUGUGU**	**23±4**	**2870±299**	**125±9**	**0.023**
miR-669d	-	ACUUGUGUGUGCAUGUAUAUGU	7±0	1511±463	216±66	0.038
miR-669e	-	UGUCUUGUGUGUGCAUGUUCAU	12±0	4090±971	341±81	0.027
miR-669f	-	CAUAUACAUACACACACACGUAU	44±1	13444±4267	306±90	0.037
miR-669h	3p	UAUGCAUAUACACACAUGCACA	8±0	326±6	41±1	0.007
miR-669i	-	UGCAUAUACACACACUGCAUAC	13±1	39±1	2±0	0.048

- **18 detected members of mouse miR 297-669 cluster were up-regulated in CHO cells in**

MicroRNA and gene upregulation in glucose-deprived media

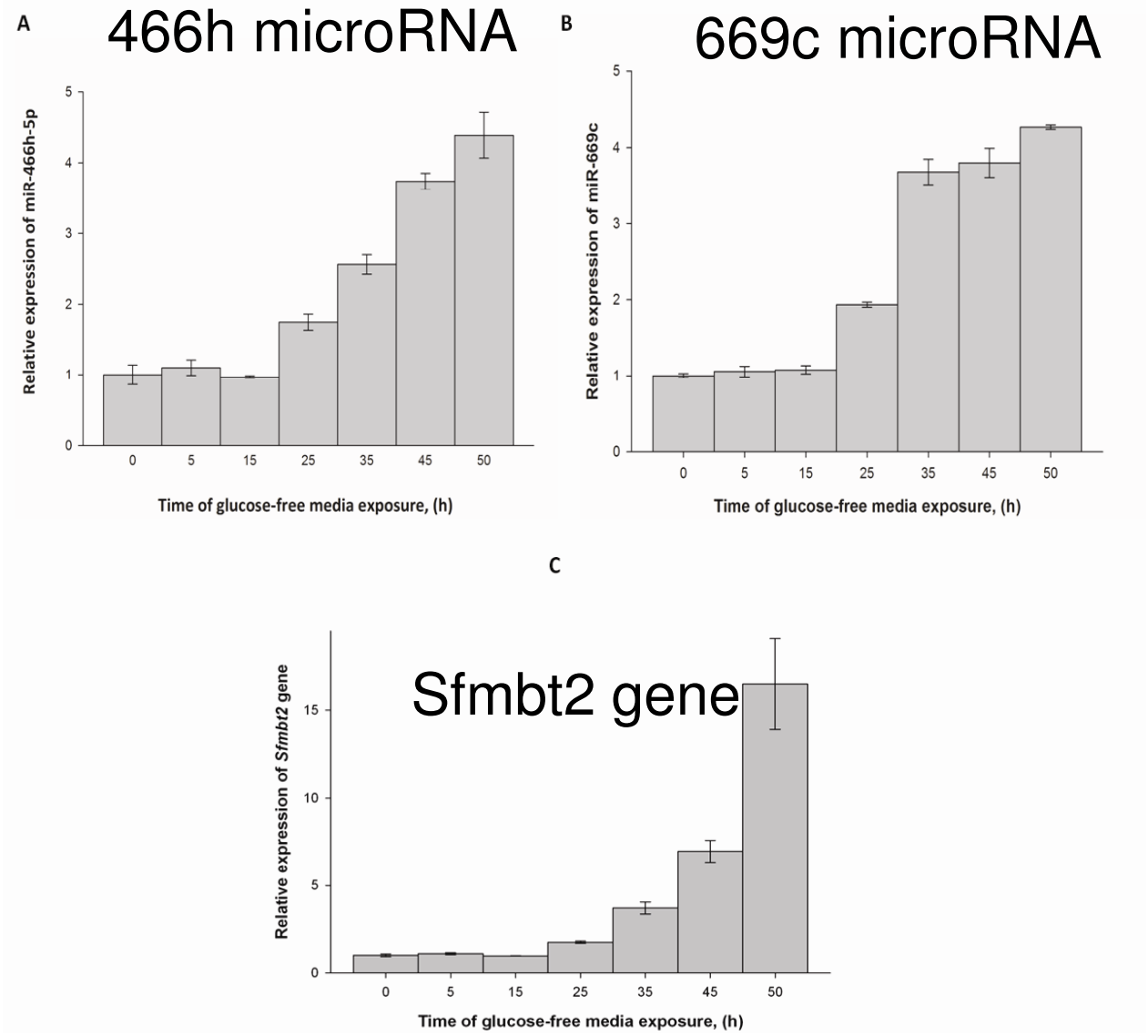

Micro-RNA cluster miR 297-669 is intronic and co-expresses 466h and 669c together with the Sfmbt2 gene

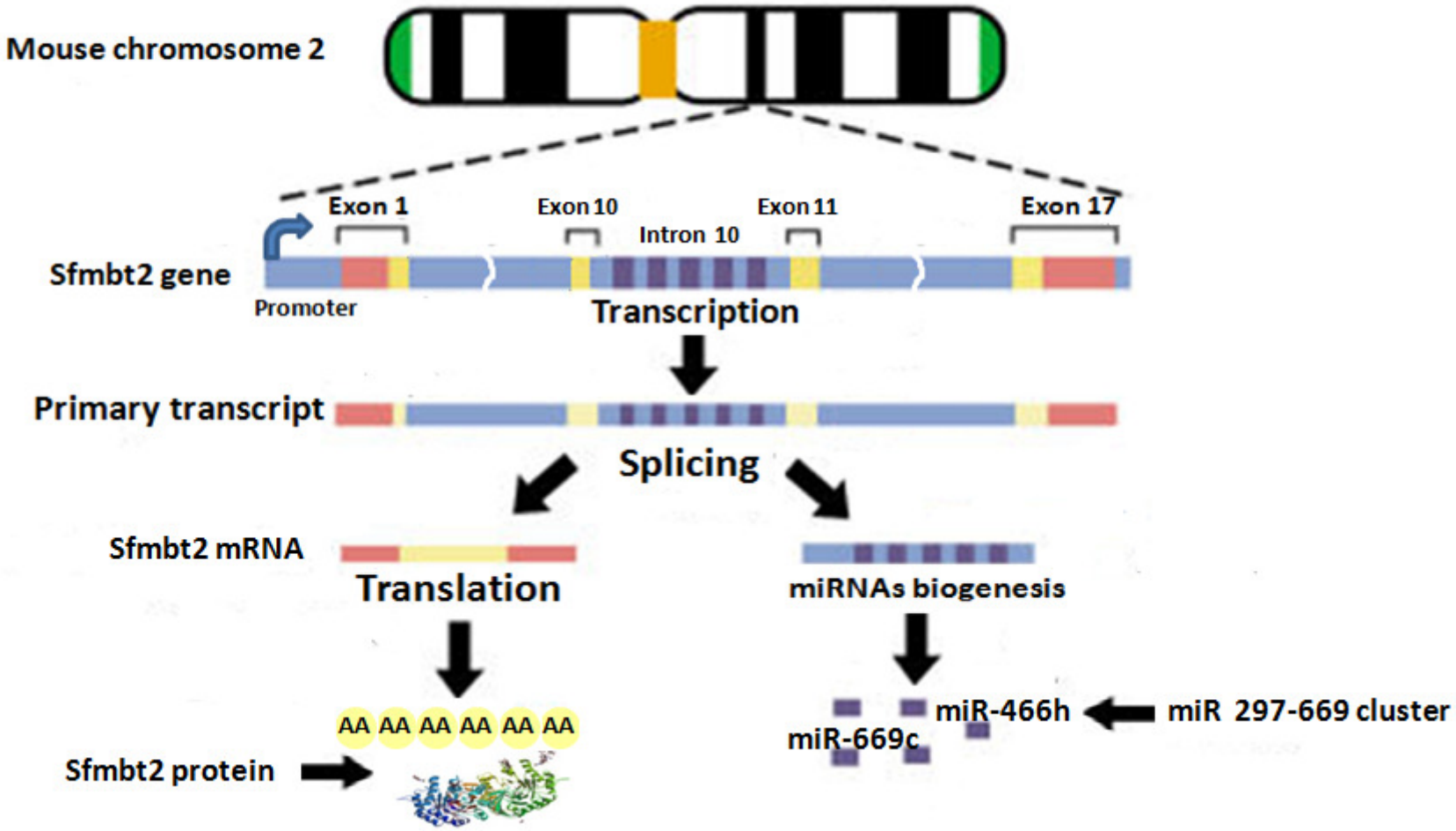

Effect of glucose deprivation on oxidative stress and reactive oxygen species (ROS) accumulation

A

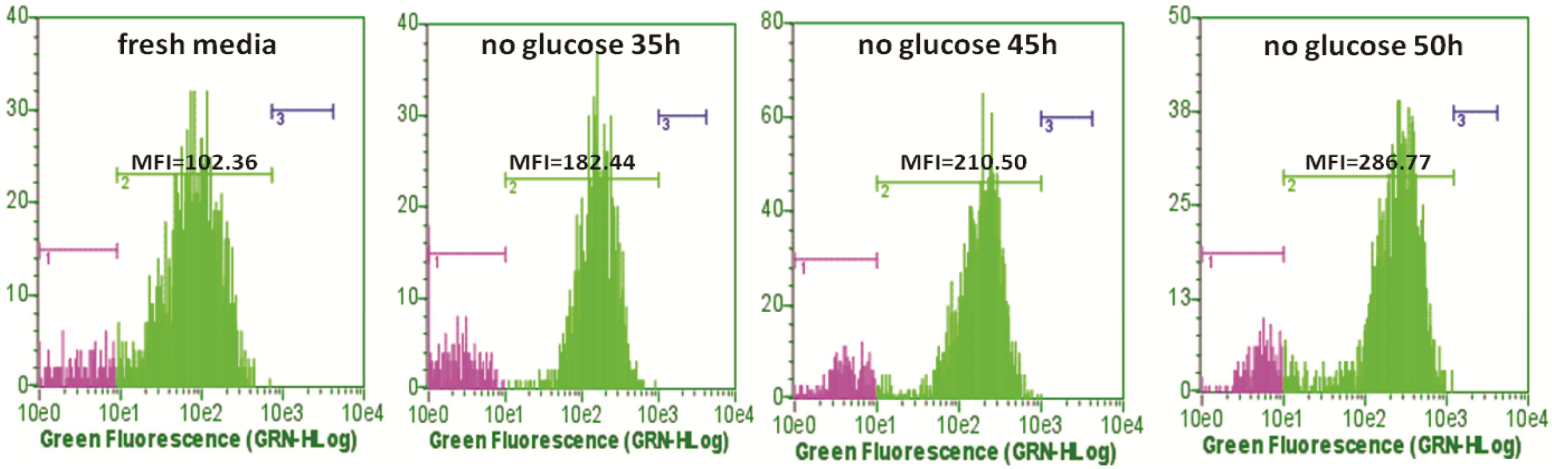

B

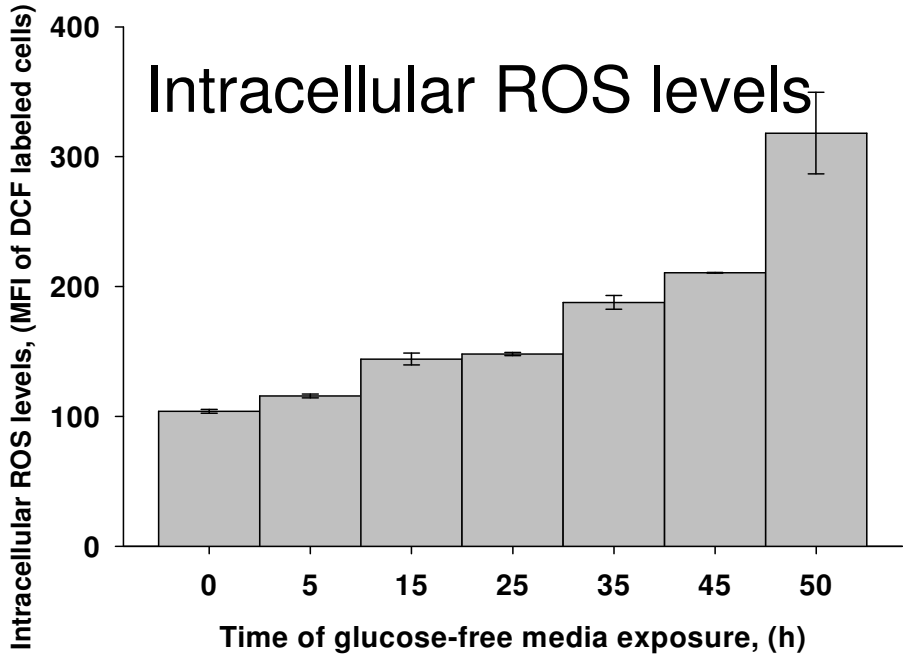

(A) Green fluorescence is proportional to intracellular ROS levels following glucose deprivation

(B*) Intracellular ROS levels increase with time of exposure to glucose free-media*

Effect of oxidative stress (glucose depletion or hydrogen peroxide) on miR-466h

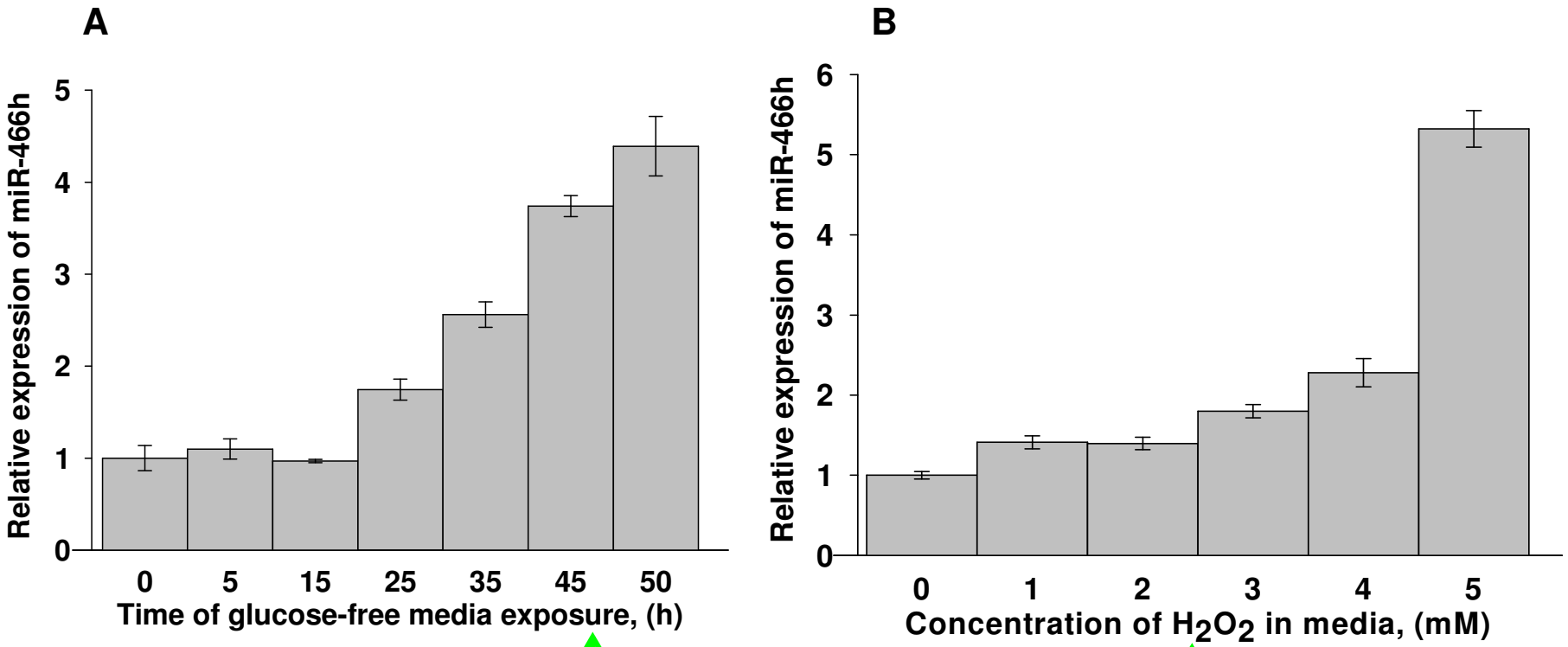

(B) miR-466h activated by exogenous oxidative stress → H_2O_2

(A) miR-466h also activated by exposure to glucose-free media

Other effects of glucose depletion:

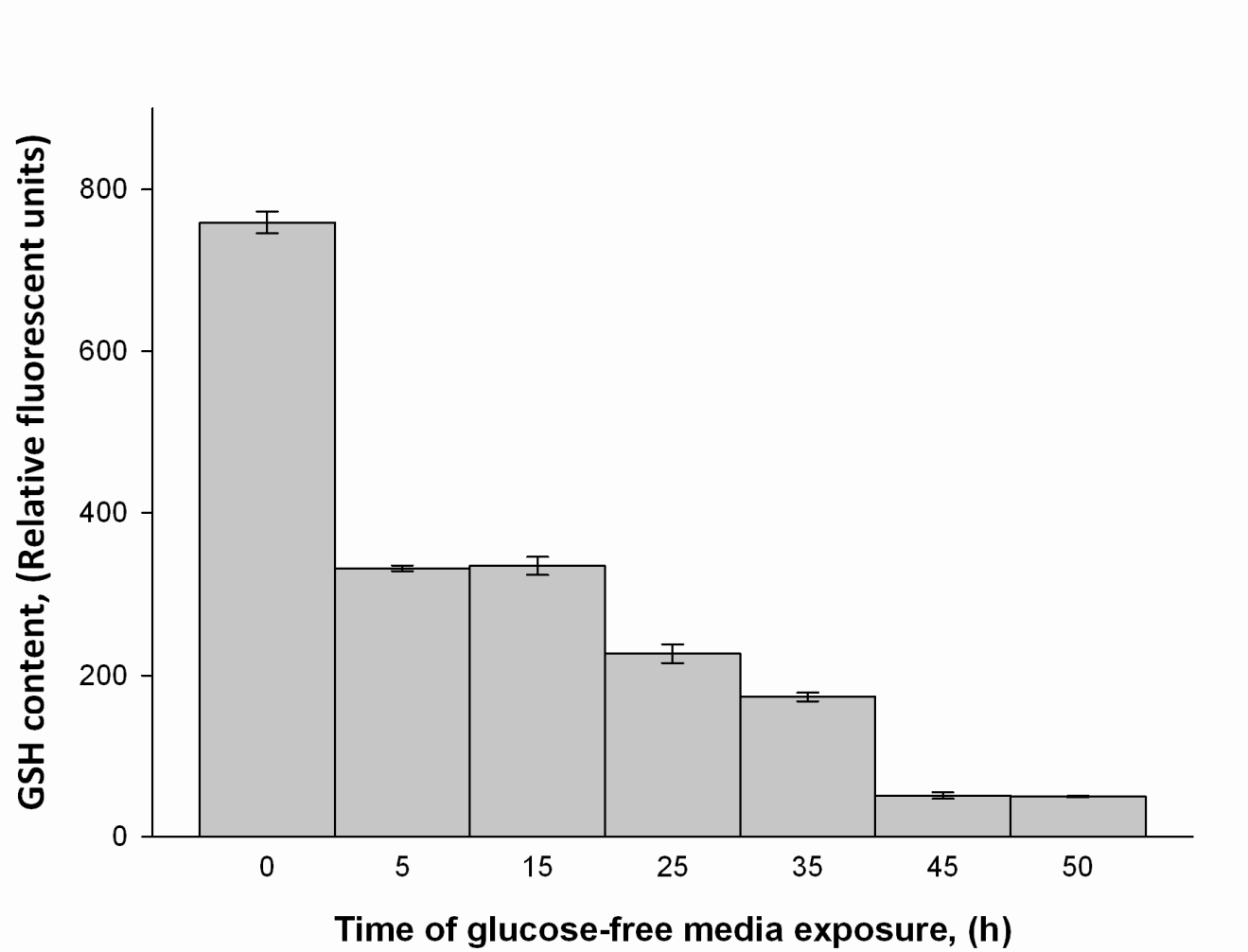

Depletion of glucose lowers
intracellular glutathione (GSH) levels in cell lines

Effect of glucose deprivation on histone deacetylase (HDAC) activity

Histone Deacetylase Activity

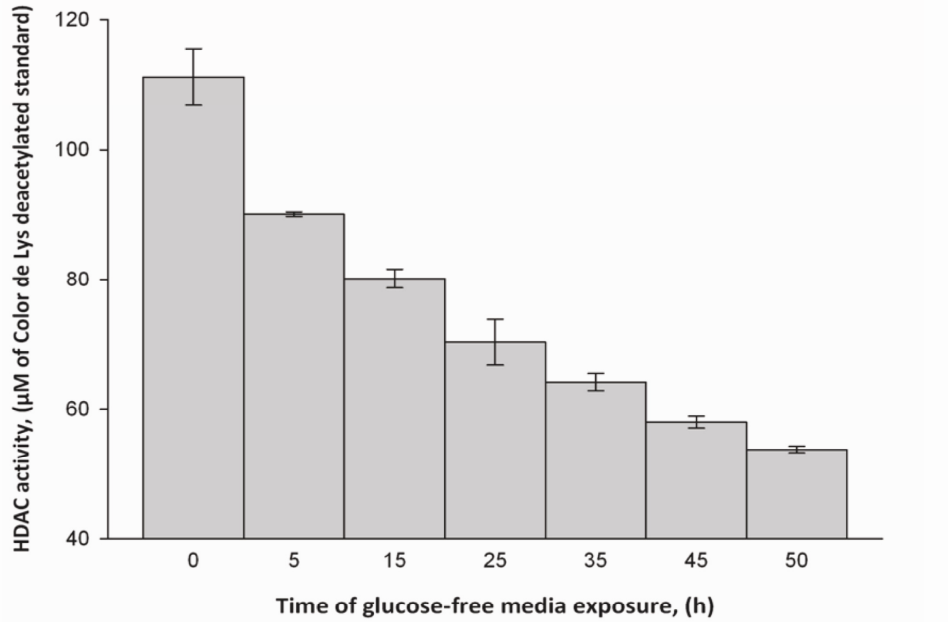

Time in glucose free medium

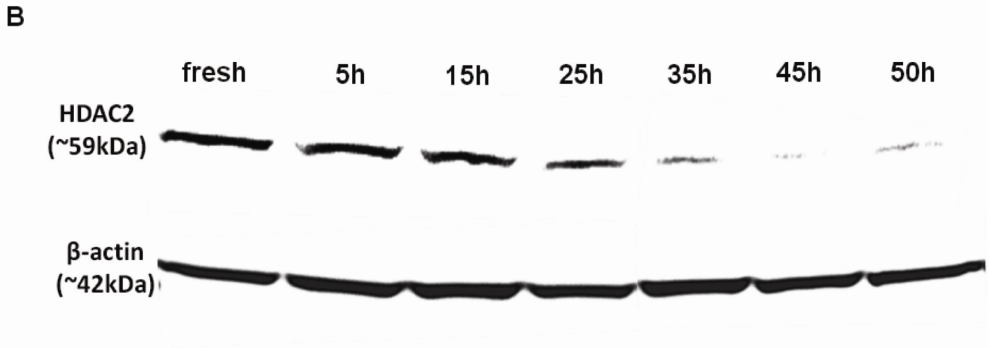

HDAC activity *decreases* following glucose deprivation

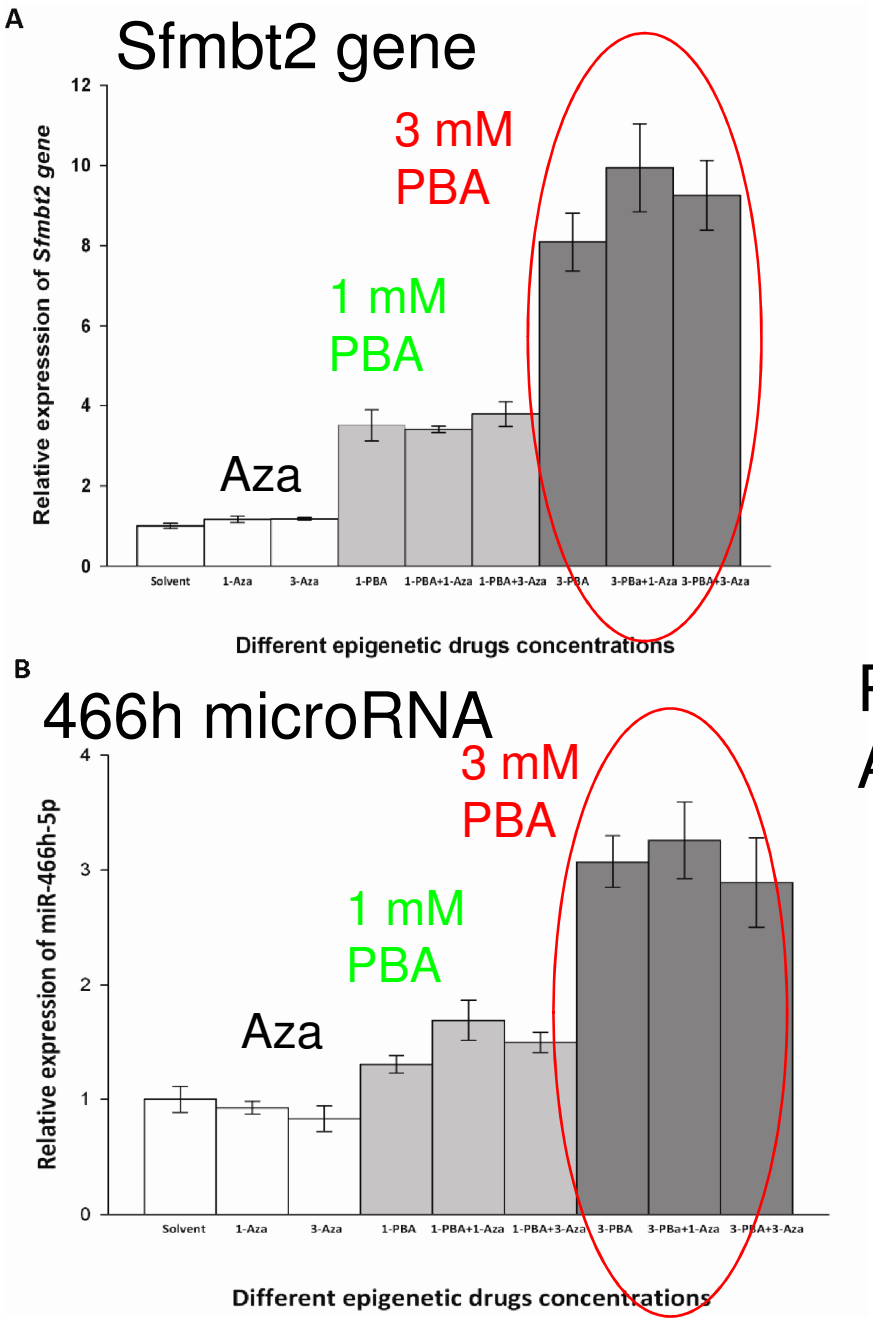

Effect of chemical HDAC inhibitor or demethylating agent on expression of *Sfmbt2* gene and miR-466h

PBA = HDAC Inhibitor

Aza = DNA demethylating agent

HDAC inhibitors (PBA) increase Sfmbt2 gene and miR 466h expression

Demethylating agents have neglible effects on Sfmbt2 and 466h expression

Effect of glucose deprivation on histone acetylation

Enrichment Of ***Acetylated*** Histones Near miR-466h Promoter

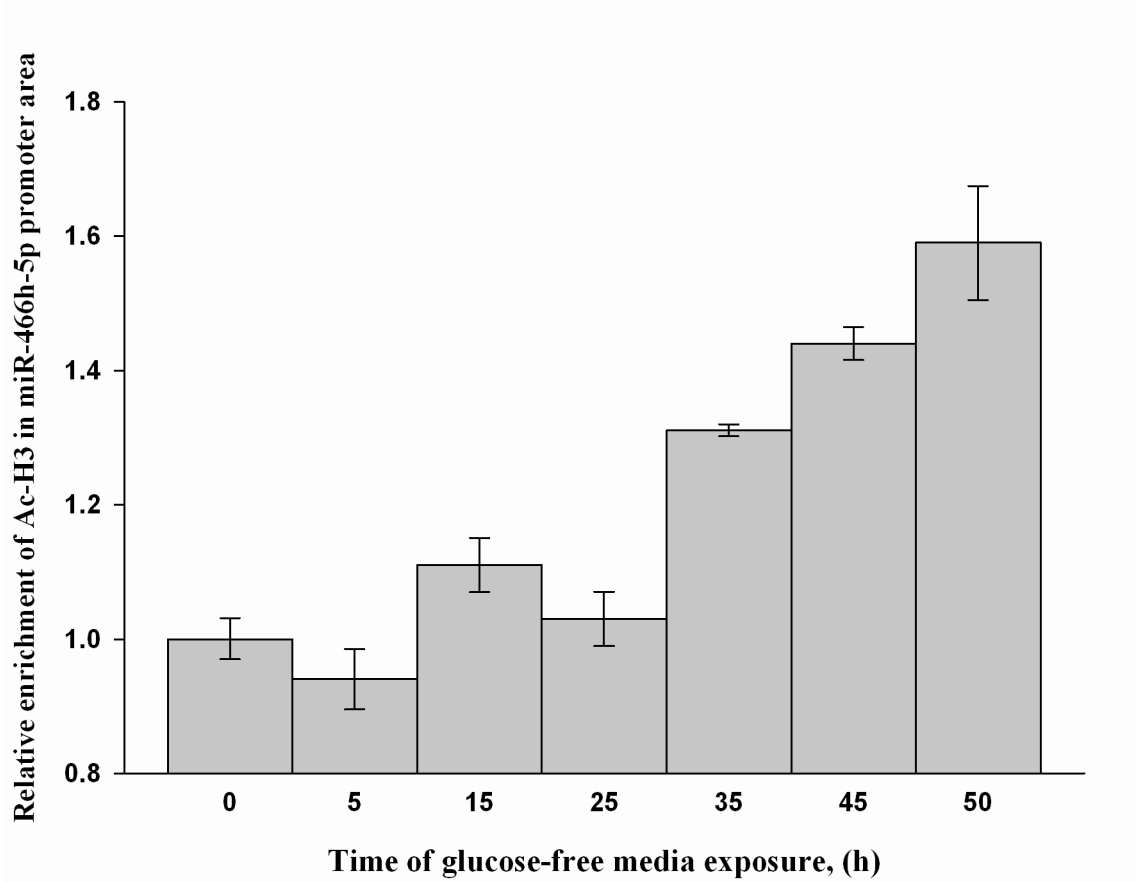

Time in glucose free medium

Glucose deprivation lowers HDAC activity and this increases acetylated histones

Pathway for MicroRNA Activation

Enrichment Of Acetylated Histones

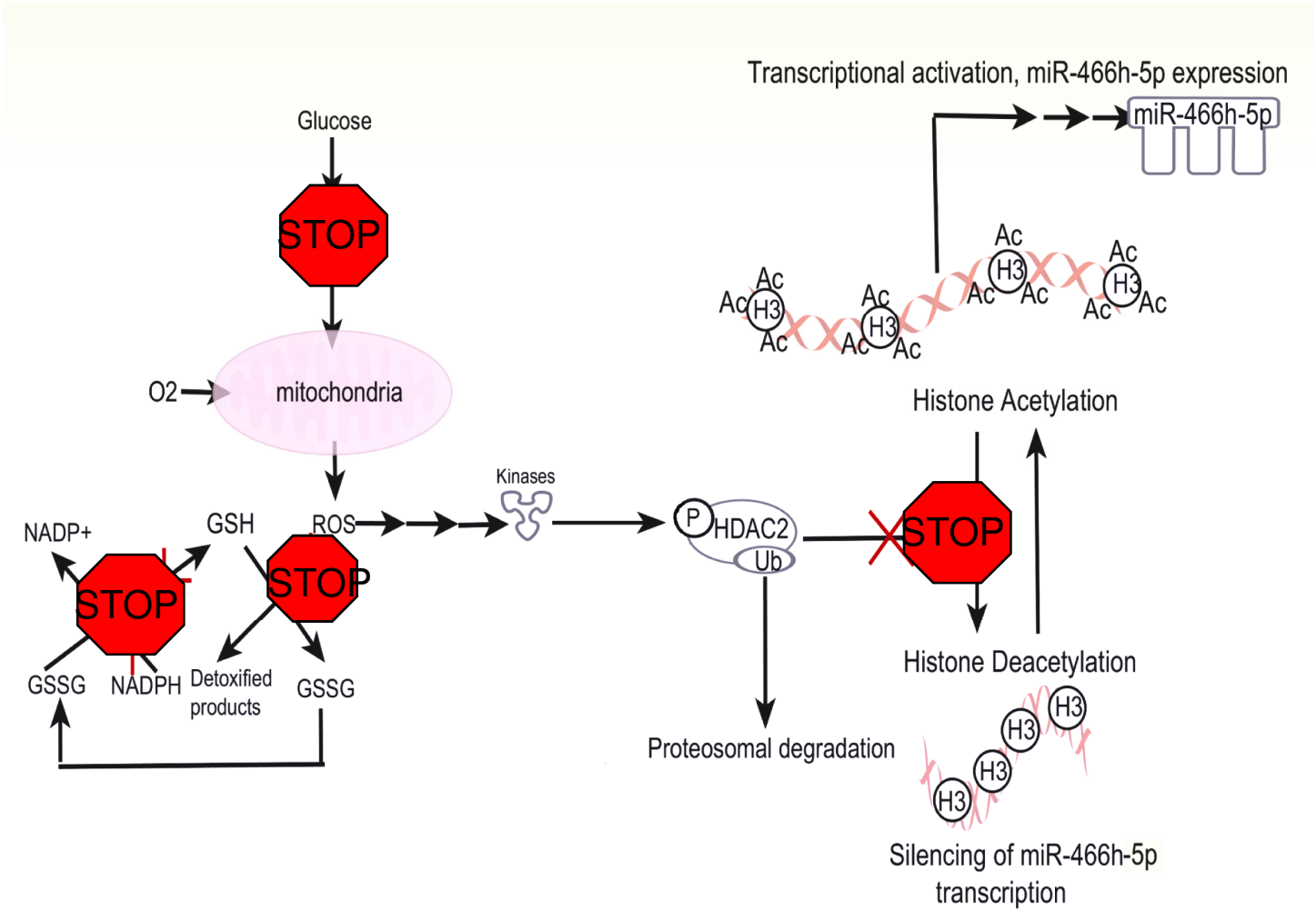

Glucose deprivation pathway leads to ROS, Histone acetylation, and microRNA activation

What are targets of MicroRNA mir-466h

- 8708 mmu-miR-466h potential targets were obtained from miRecords using bioinformatics analysis

- Targets were narrowed to 38 anti-apoptotic genes with DAVID NCBI (which classifies genes according to their biological roles)

- 9 anti-apoptotic genes were predicted to be targeted by mmu-miR-466h by 3 prediction engines

Potential targets of mir-466h

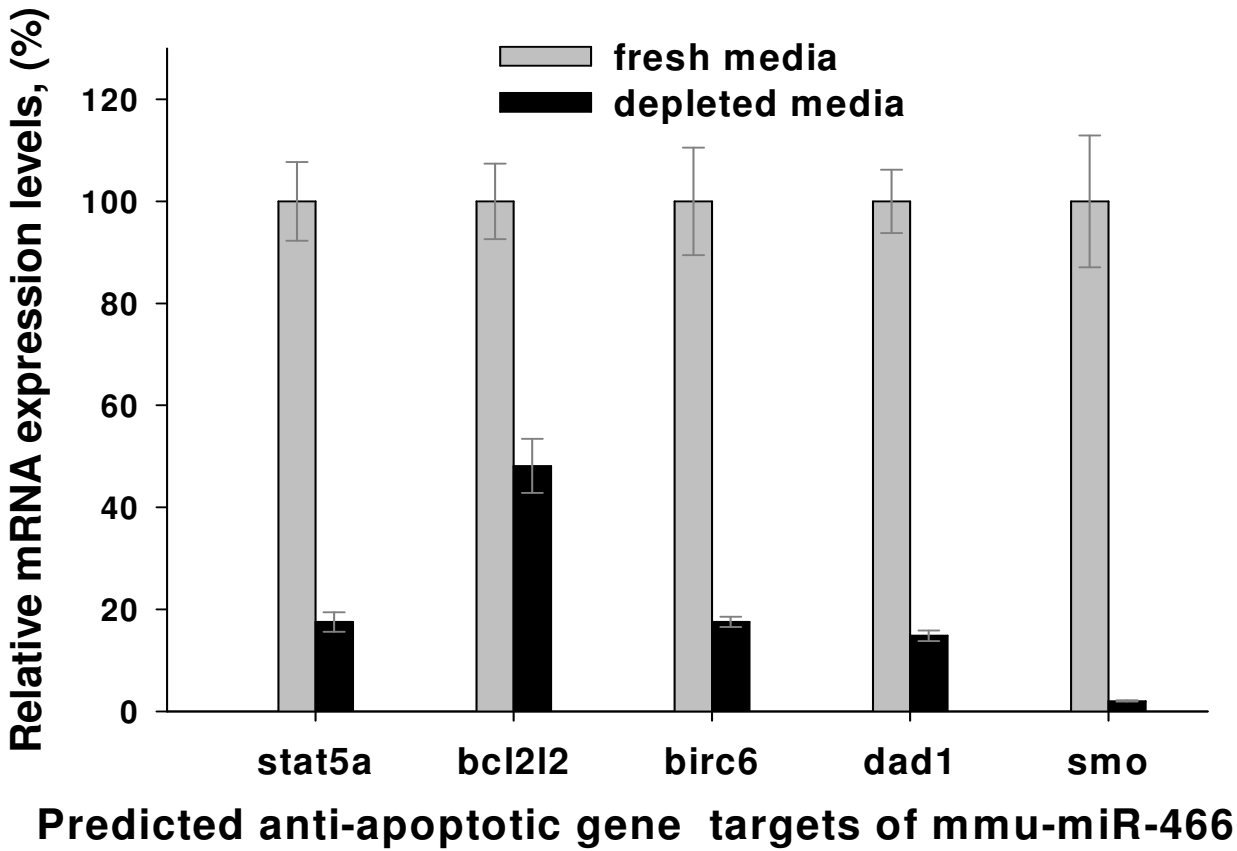

Five anti-apoptotic genes were detected in CHO and DOWN-REGULATED in nutrient-depleted conditions:
stat5a, bcl2l2, birc6, dad1, smo

MicroRNA and Apoptosis Signaling

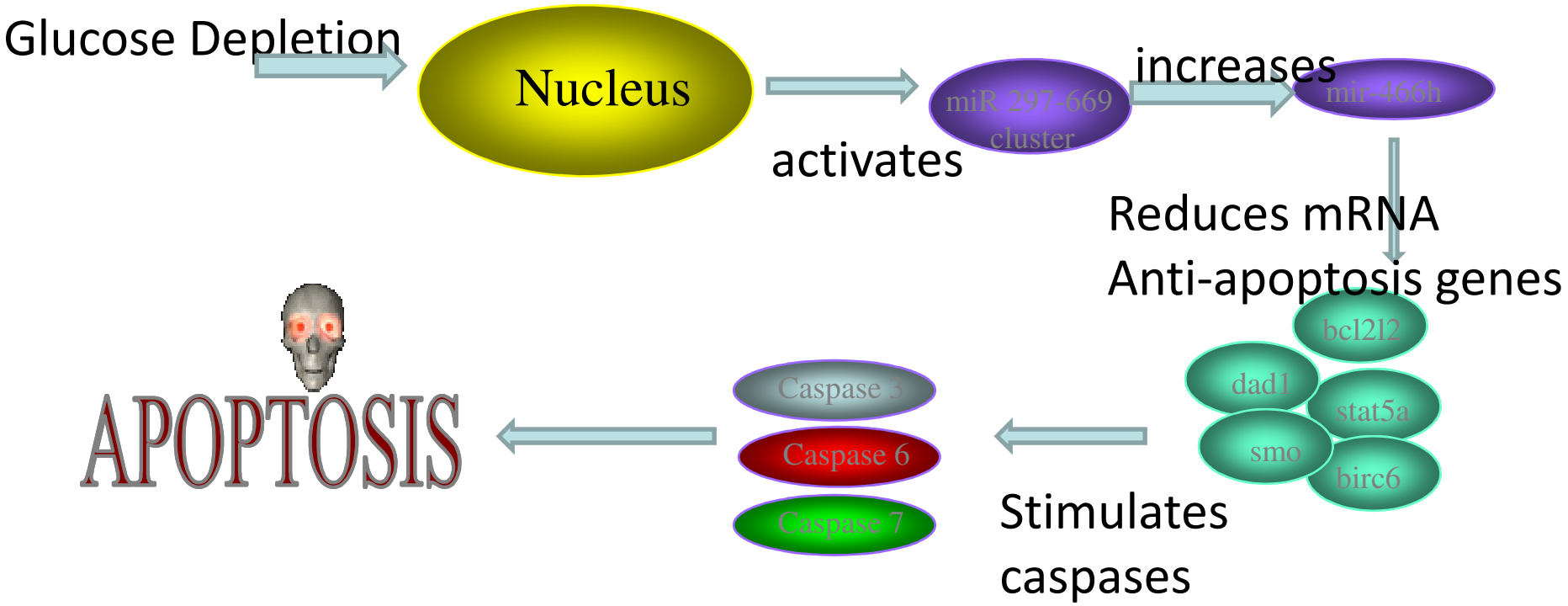

Chemical Inhibition of MicroRNA

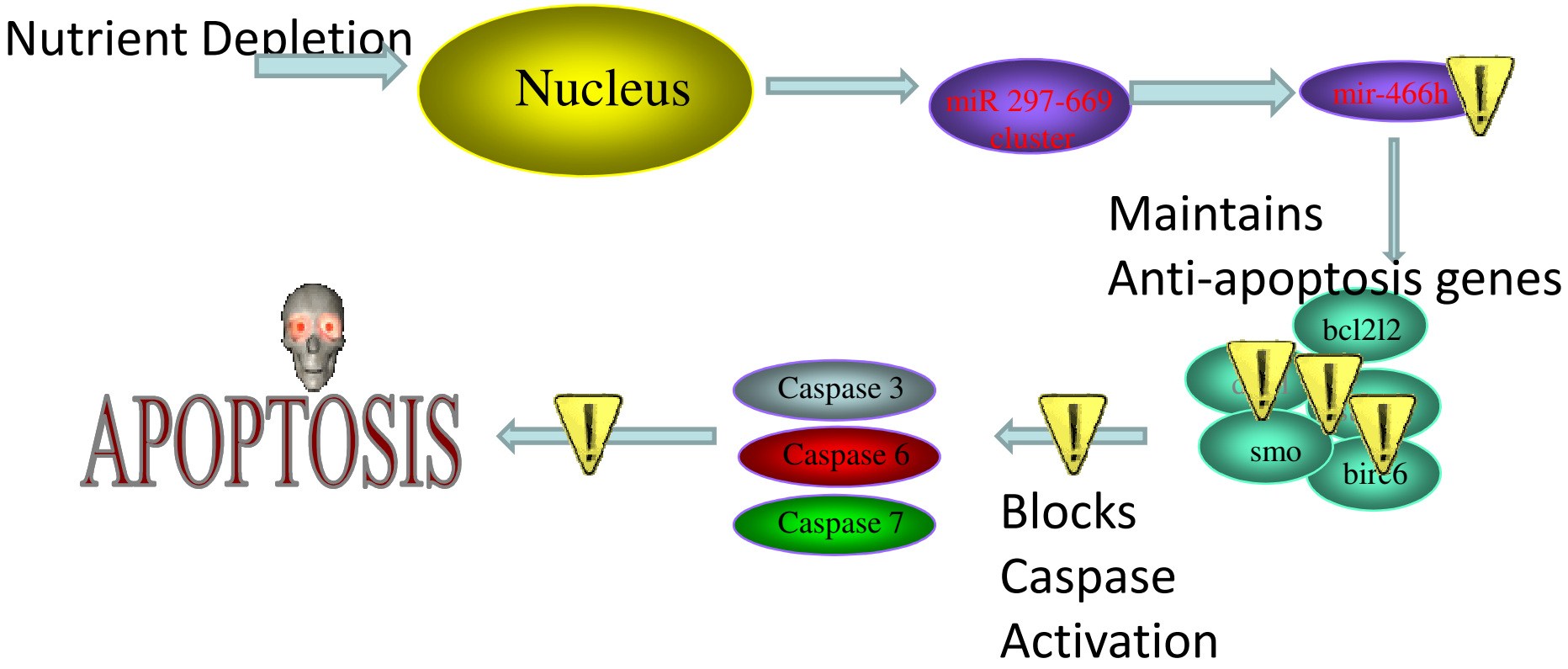

Effects of anti-mir466h

- A chemically modified single stranded oligonucleotide specific for mmu-miR-466h was added to the cells
- The levels of mmu-miR-466h in fresh media and in the depleted media, with or without anti-miR-466h, were measured
- **Compared with fresh media, mmu-miR-466h levels were 10 times higher in depleted media in the absence of the inhibitor**
- **Mir-466h levels were reduced by a factor of 4.5 in depleted media containing anti-miR-466h.**

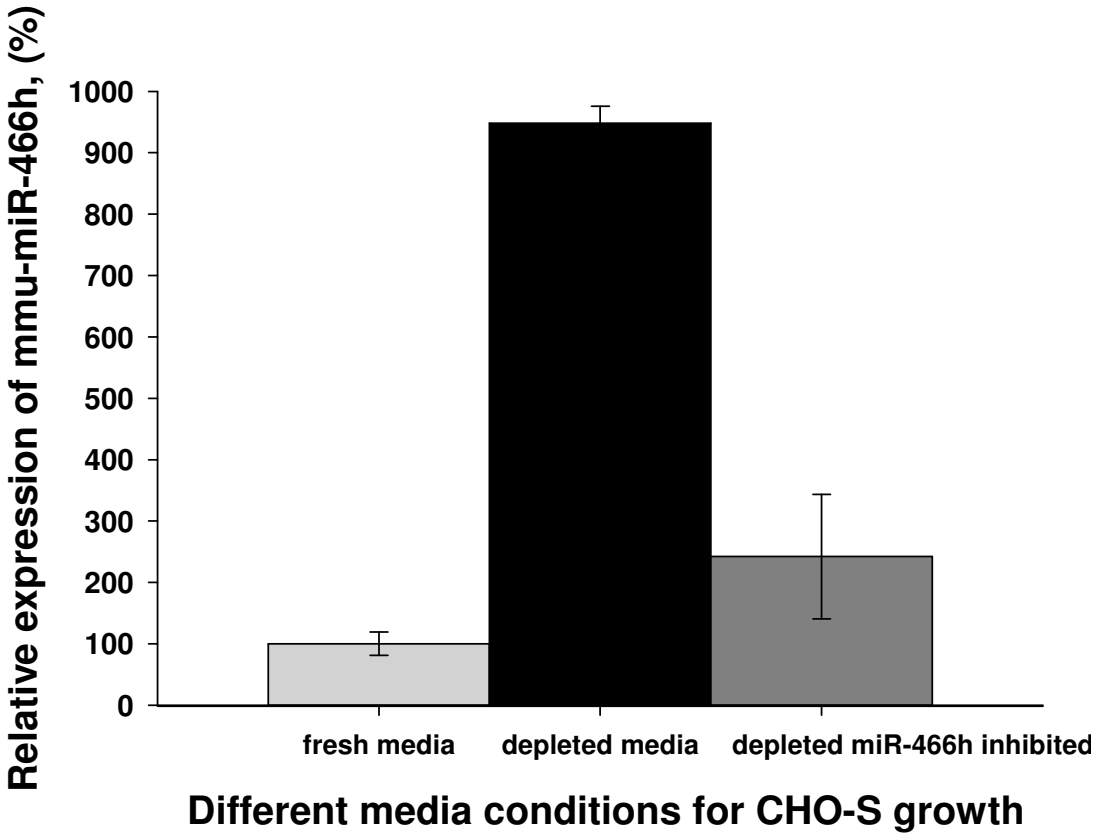

Increases in mir-466h expression levels in depleted media are inhibited by oligonucleotide

Effects of anti-mmu-mir466h on potential anti-apoptotic targets

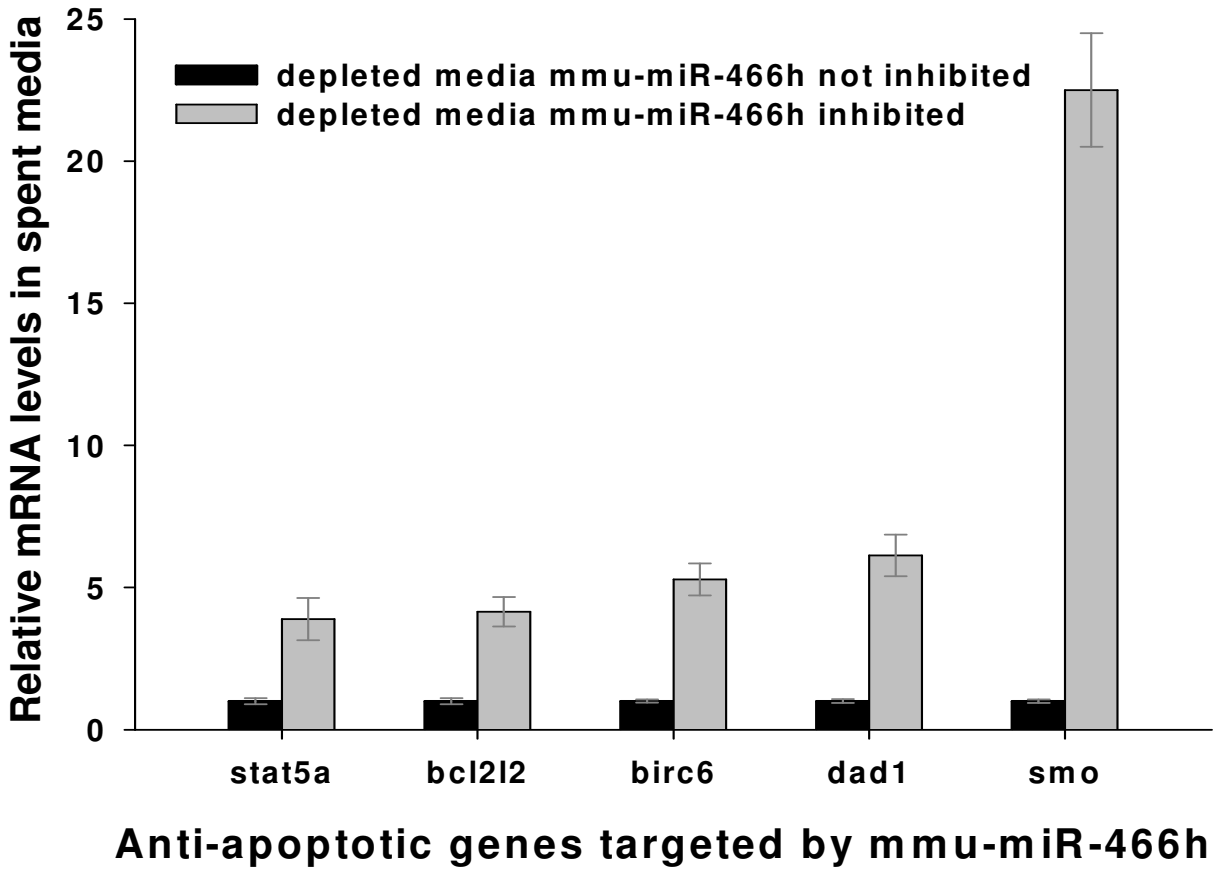

Addition of anti-mmu-mir-466h enhances mRNA levels of anti-apoptotic genes in depleted media

Does chemical inhibition of mir-466h affect apoptosis?

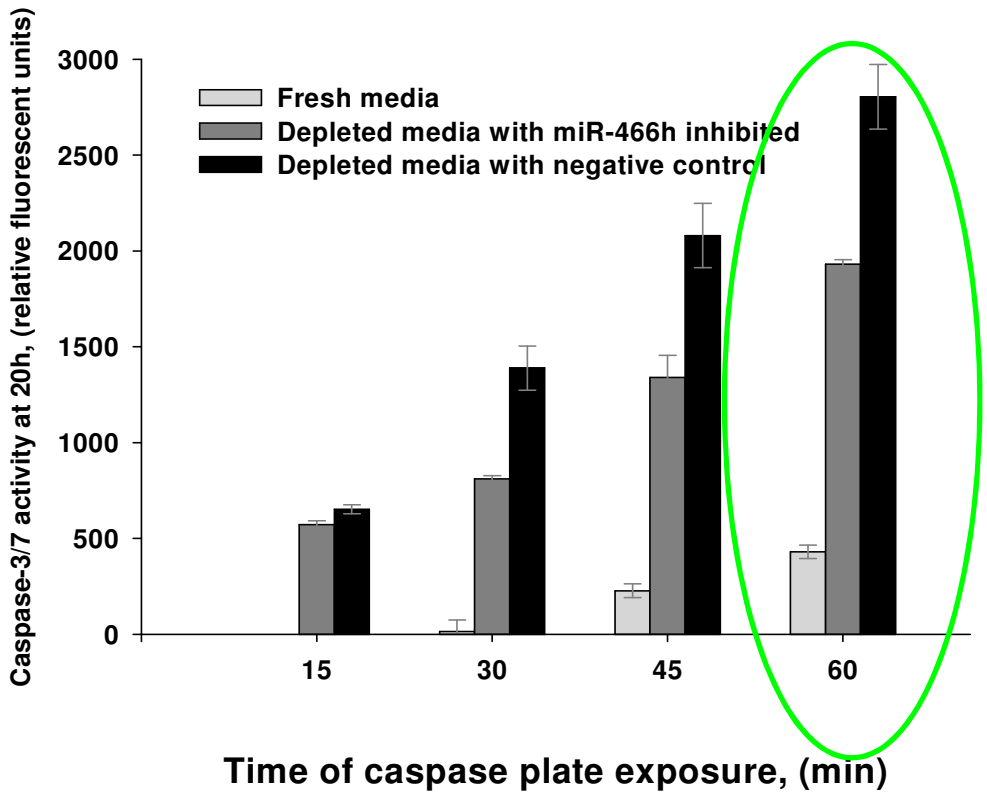

Addition of anti-mir-466h chemical to cells lowers caspase activity following nutrient depletion

Does chemical inhibition of mir-466h affect cell viability

- Cell viability in the depleted media started to decline after about 18 hours and fell to 81% by 23 hours.
- **When the cells were chemically treated with anti -miR-466h oligonucleotide, the cell viability was higher at both the 20 and 23 hours time points.**

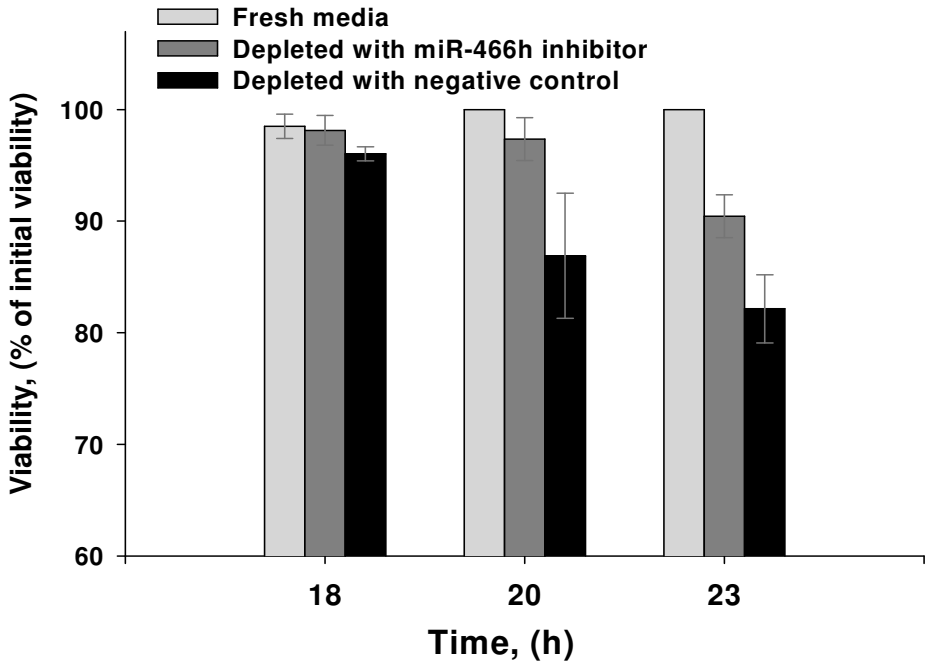

Addition of anti-mmu-mir-466h chemical to cells enhances viability following nutrient depletion

Mammalian Cell Engineering

CHO Genome: www.chogenome.org

- Host genome sequence
- Integrate protein, transcript, metabolic data
- Provide community resource for ongoing cell engineering efforts

Conclusions:

- **MicroRNAs are activated in CHO cells under nutrient depleted conditions**
- **The microRNA mmu-mir-466h has a number of anti-apoptotic gene targets**
- **Inhibition of mmu-miR-466h lowers CHO caspase activity and increases cell viability**
- **MicroRNAs may play an important role in control of multiple cellular activities for cell engineering applications**

Acknowledgements

Graduate Students:

Alex Druz

&

Deniz Baycin

Collaborators: Bernhard Palsson, Iman Famili, BGI, Kelvin Lee, Yossi Shiloach, Haimanti Dorai

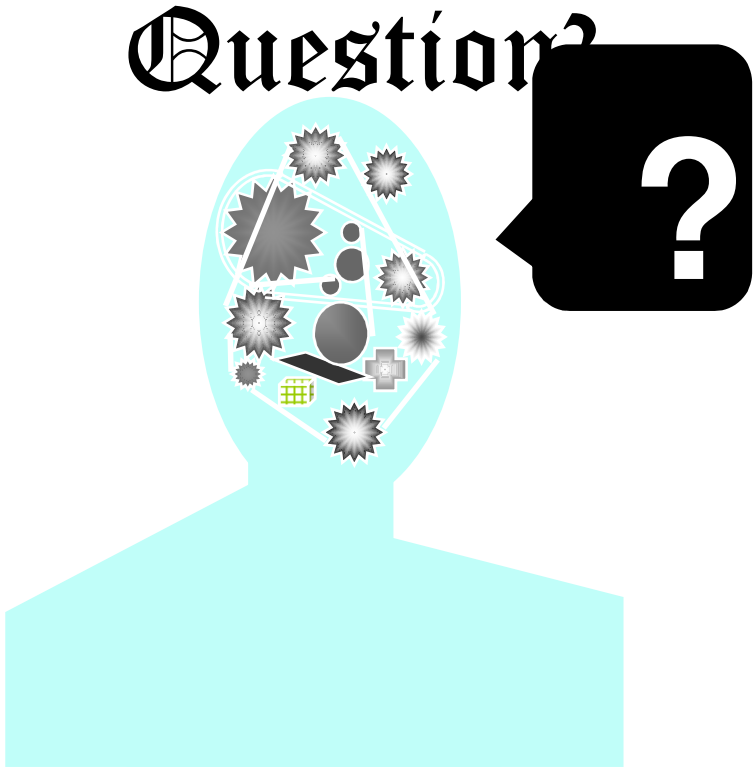

Can we apply microRNA information in cell re-engineering strategies to alter mammalian culture systems performance

Mass Spec Proteomics Analysis in CHO

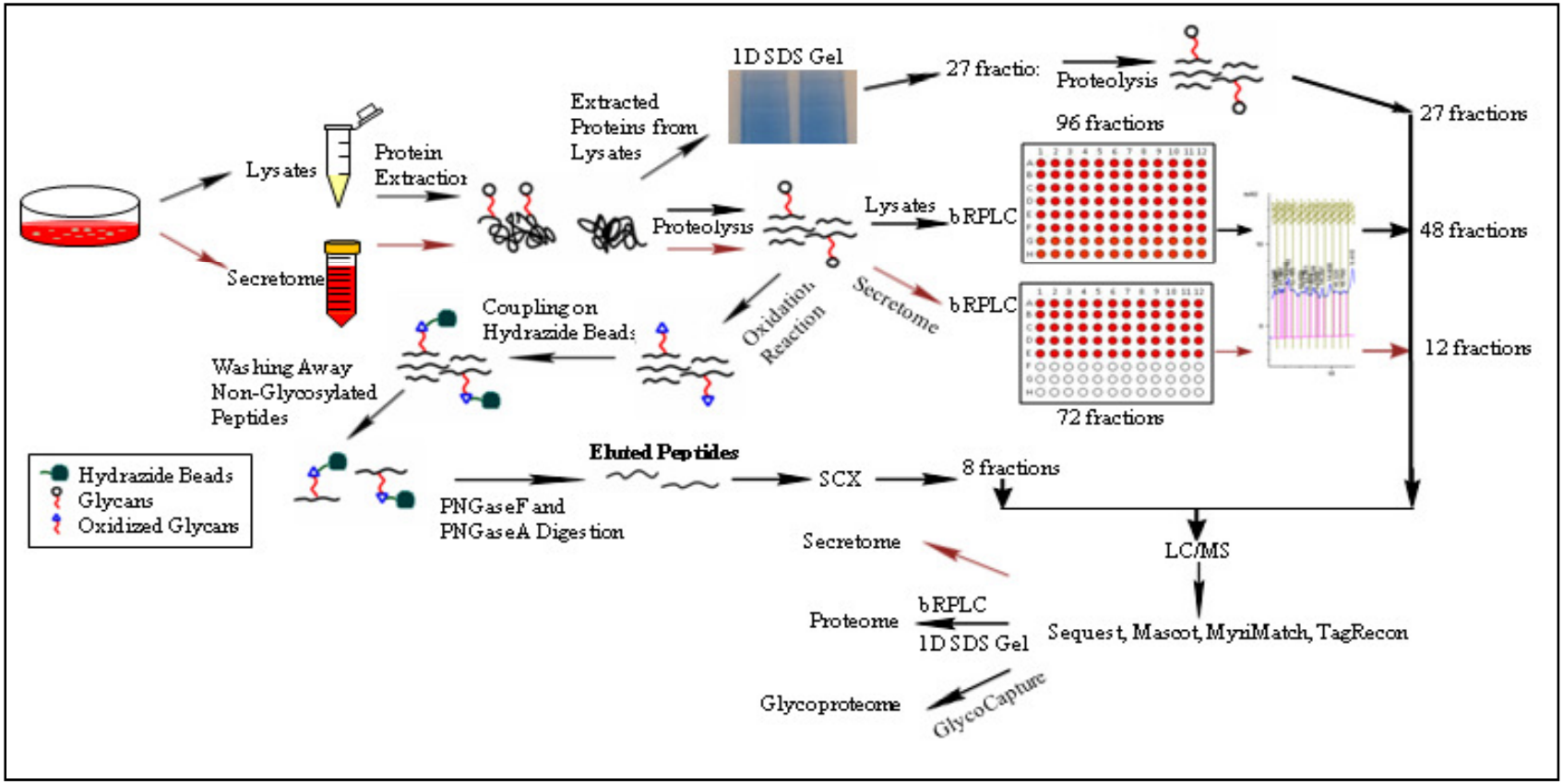

Proteomics and Glycoproteomics Database of CHO Cells

Proteome all (8300) Glycoproteome (525)

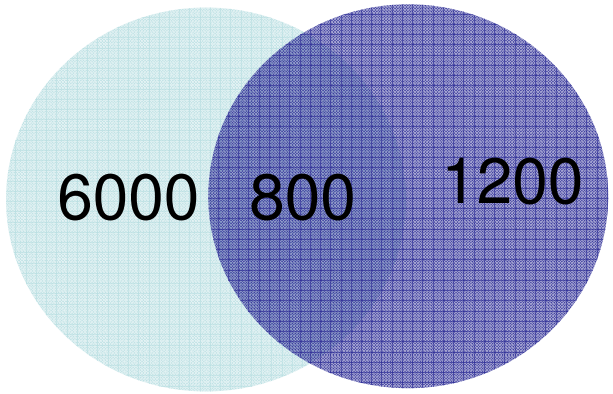

- Identified proteins include:
  - Cell adhesion molecules
  - Growth Factors
  - Receptors
  - Glycosyltransferases and glycosidases
  - Chaperones
  - Apoptosis inhibitors
  - 1292 different proteins were observed to be *N*-glycosylated

MicroRNA Biogenesis

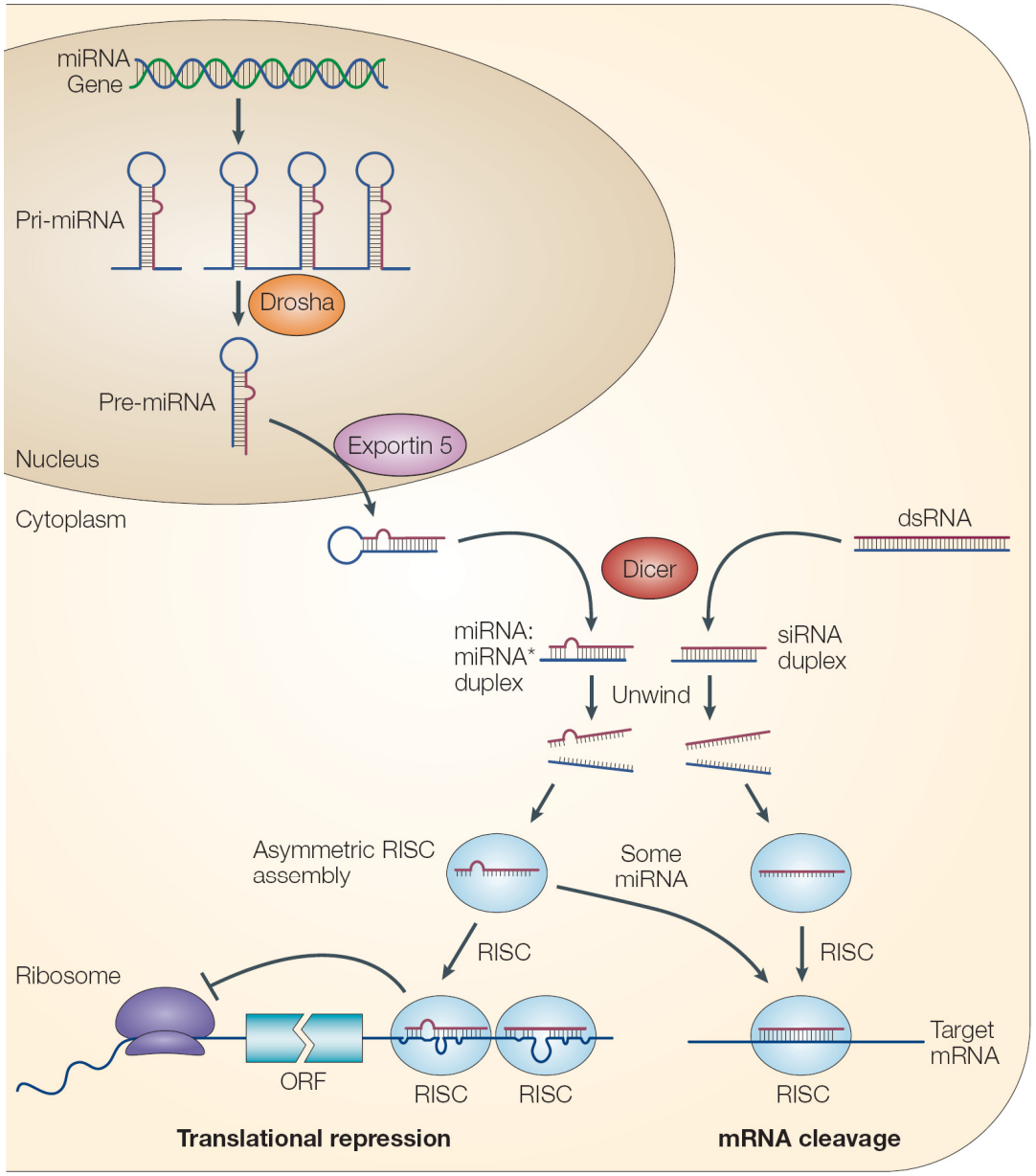

microRNA information center

www.CHOgenome.org

One-stop shopping for everything genomic related to CHO.

A community website sponsored by academic, government and industrial collaborators has organized and financially committed to share and host genome-scale information about CHO and activities for the biotechnology community.

flybase.org
wikipedia
etc.

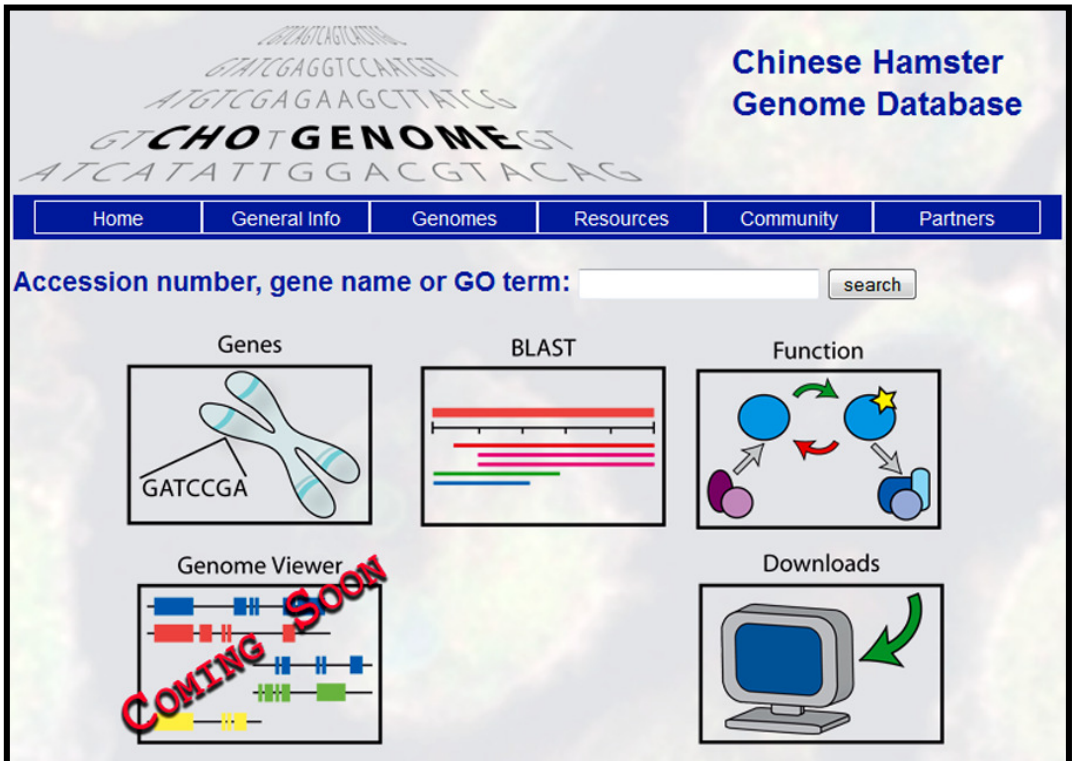

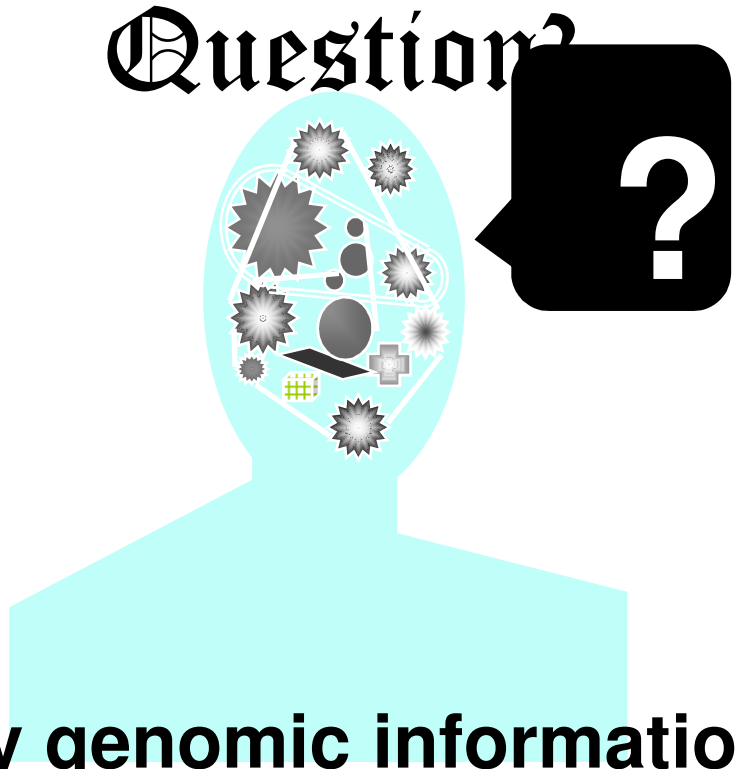

Can we apply genomic information to help us better understand and improve mammalian Cell culture?

CHO K1 Genome Assembly and Annotation

- CHO-K1 (ATCC CCL-61)
- CHO-K1 genome sequence
  - Total of 343 Gb sequence generated
  - >95-fold coverage of the CHO genome
- CHO-K1 genome assembly
  - 2.45 Gb of estimated 2.6 Gb genome assembled

CHO-K1 genome annotation

- 24,383 predicted genes
- 29,291 predicted transcripts
- 416 ncRNAs predicted

Xu et al (2011)

Comparative Genomic Features

	CHO-K1	Mouse	Rat	Human
Genome size	**2.6 Gb**	**2.6 Gb**	**2.75 Gb**	**2.9 Gb**
Chromosomes (2n)	**21**	**40**	**42**	**46**
Average GC content	**41.3%**	**41.5%**	**41.8%**	**40.9%**
Repeat content*	**38%**	**37%**	**40%**	**46%**
Predicted genes^	**24,383**	**21, 662**	**22, 416**	**20, 935**

*Repeat content: RepeatMasker against Repbase transposable element library and RepeatModeller to construct *de novo* repeat library.

^Genscan, Augustus, GlimmerHMM to predict genes which are aligned to Ensembl rel. 58). GLEAN used to reconcile gene set that was augmented with transcriptome data using Tophat and Cufflinks.

Xu et al (2011)

Functional Analysis of Gene Expression

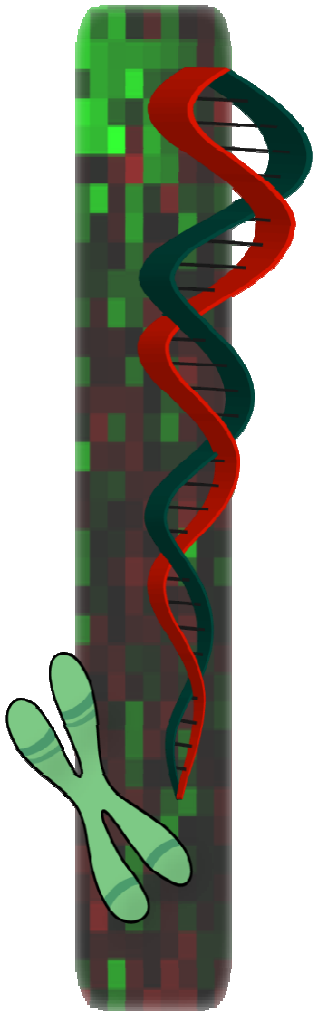

Analysis of global gene expression

- Identify human genes in these pathways
- Look for CHO homologs in genome
- Examine gene expression using RNA-Seq data

Therapeutic Glyco-products (Sugars or Glycans + Proteins) in Biotechnology

- Most Commercial Biotherapeutics
  - Cancers
  - Arthritis
  - Anemia
  - Stroke and Heart Attack
  - Genetic Disorders
  - Infertility
- Sales of 100 billion dollars
- Nearly 50% of FDA Pipeline
  - Includes Vaccines and Gene Therapy Products

N-Linked Glycosylation

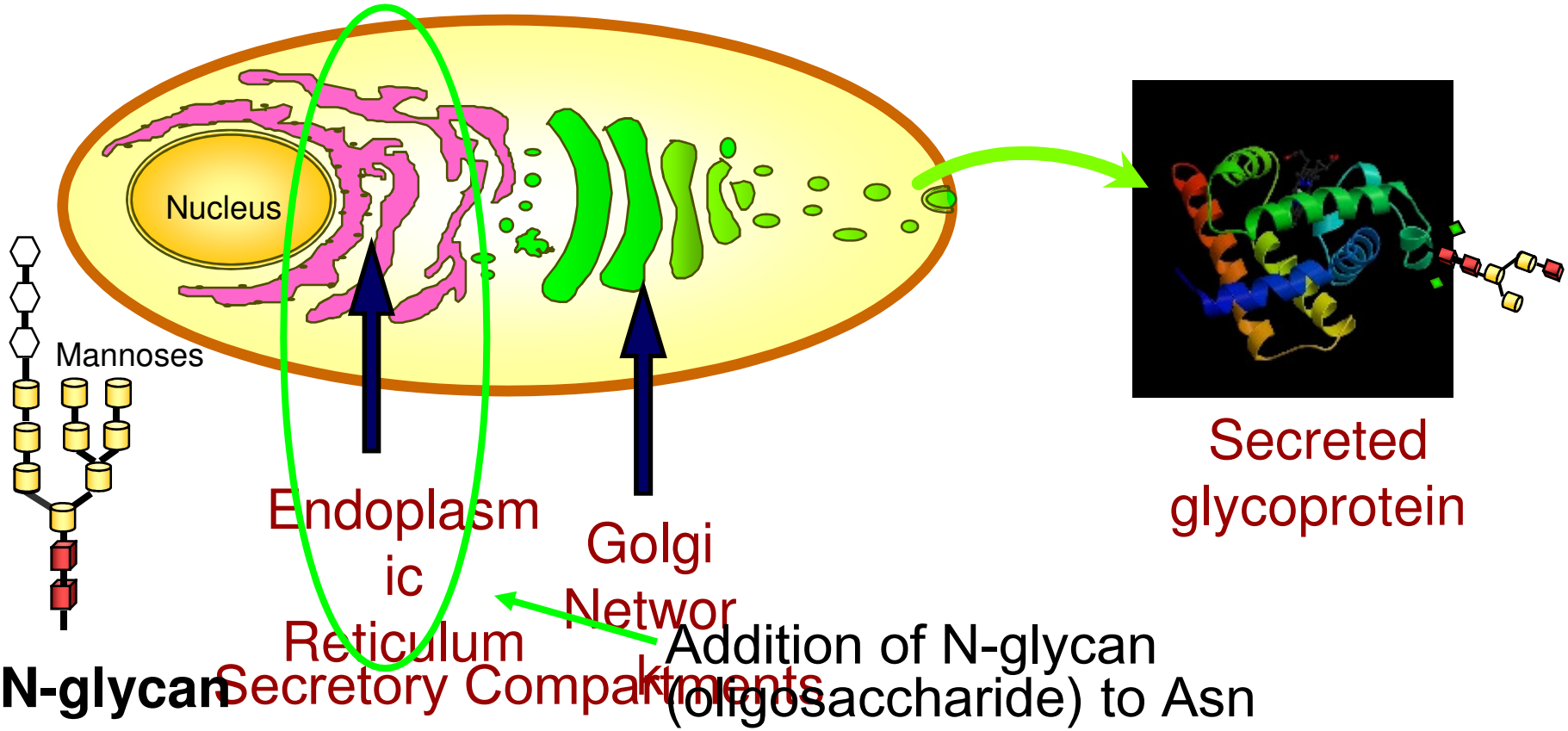

- **Large high mannose oligosaccharide (N-glycan) is linked to Asn of Asn-X-Thr/Ser of a protein in the endoplasmic reticulum (ER)**

Glycosylation Genes Expressed in CHO K1: What pathways are missing; What pathways are present?

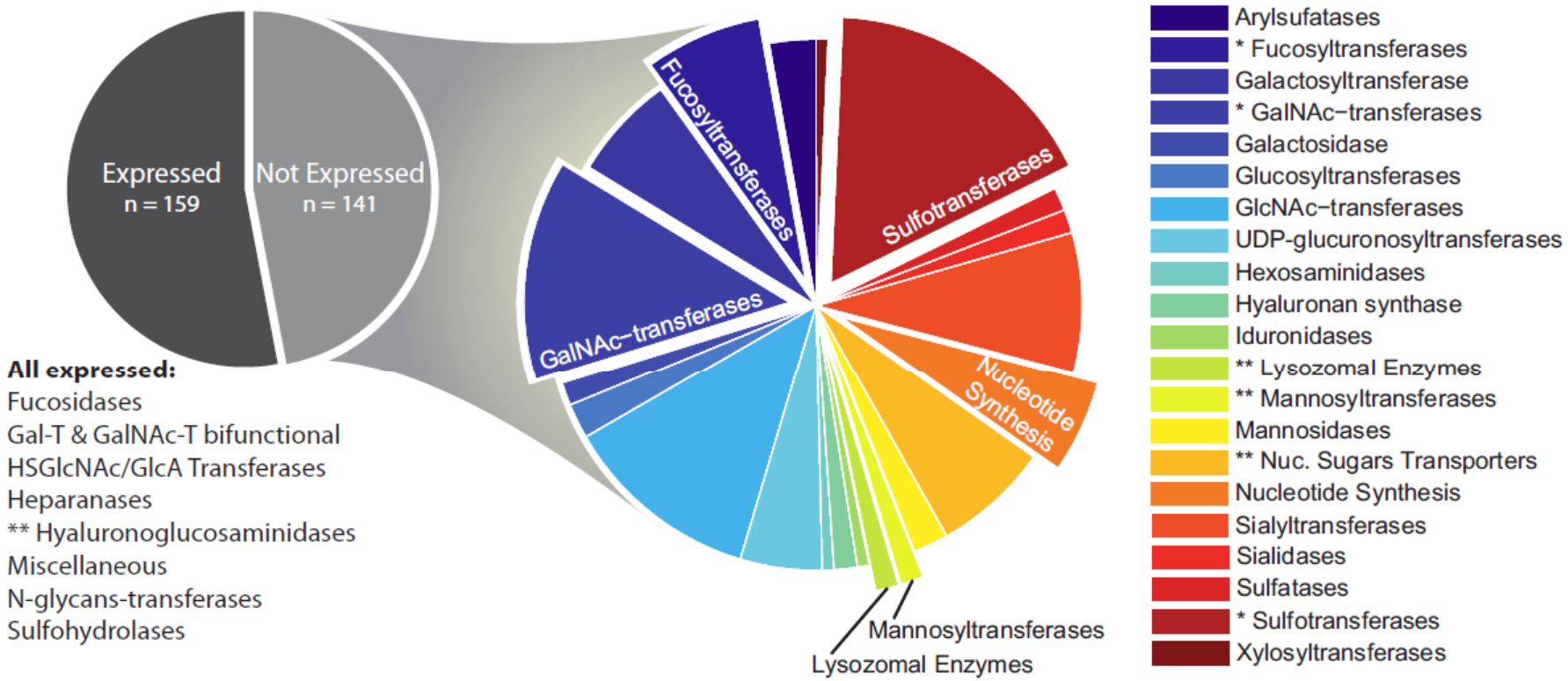

Glycosylation Processing in the Cell

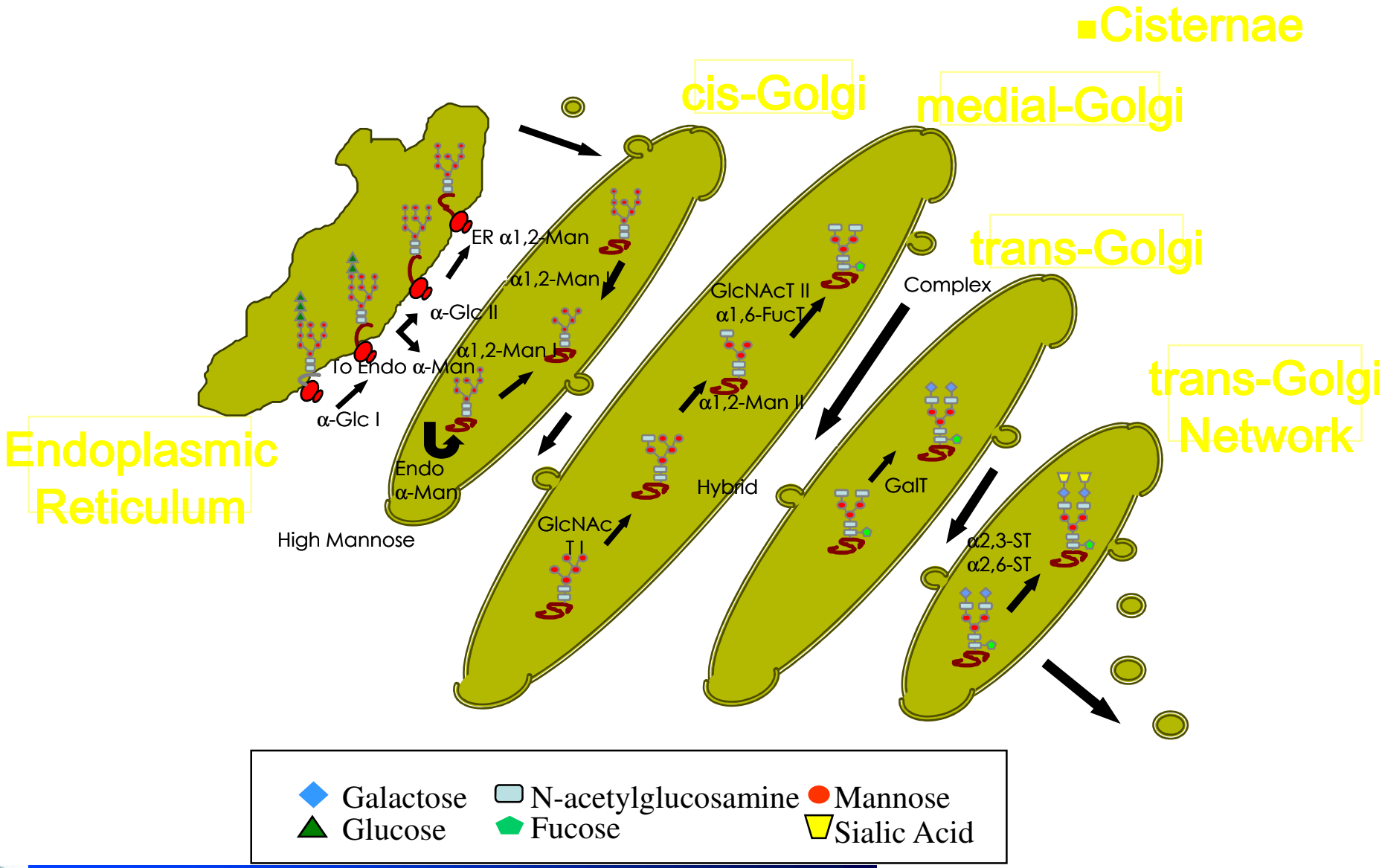

Example reaction: Sialylation of Glycoproteins

ACCEPTOR:P_n 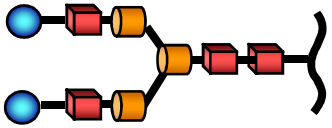

Galactose-terminated Structure √

\+

DONOR: UDP-S 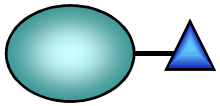

CMP- Neu5AC
CMP-Sialic acid √

\+

ENZYME: E 

Alpha 2-3 Sialic acid Transferase √

PRODUCT:P_{n+1} PRODUCT:P_{n+2}

Genome Analysis of Sialic acid Reactions in CHO

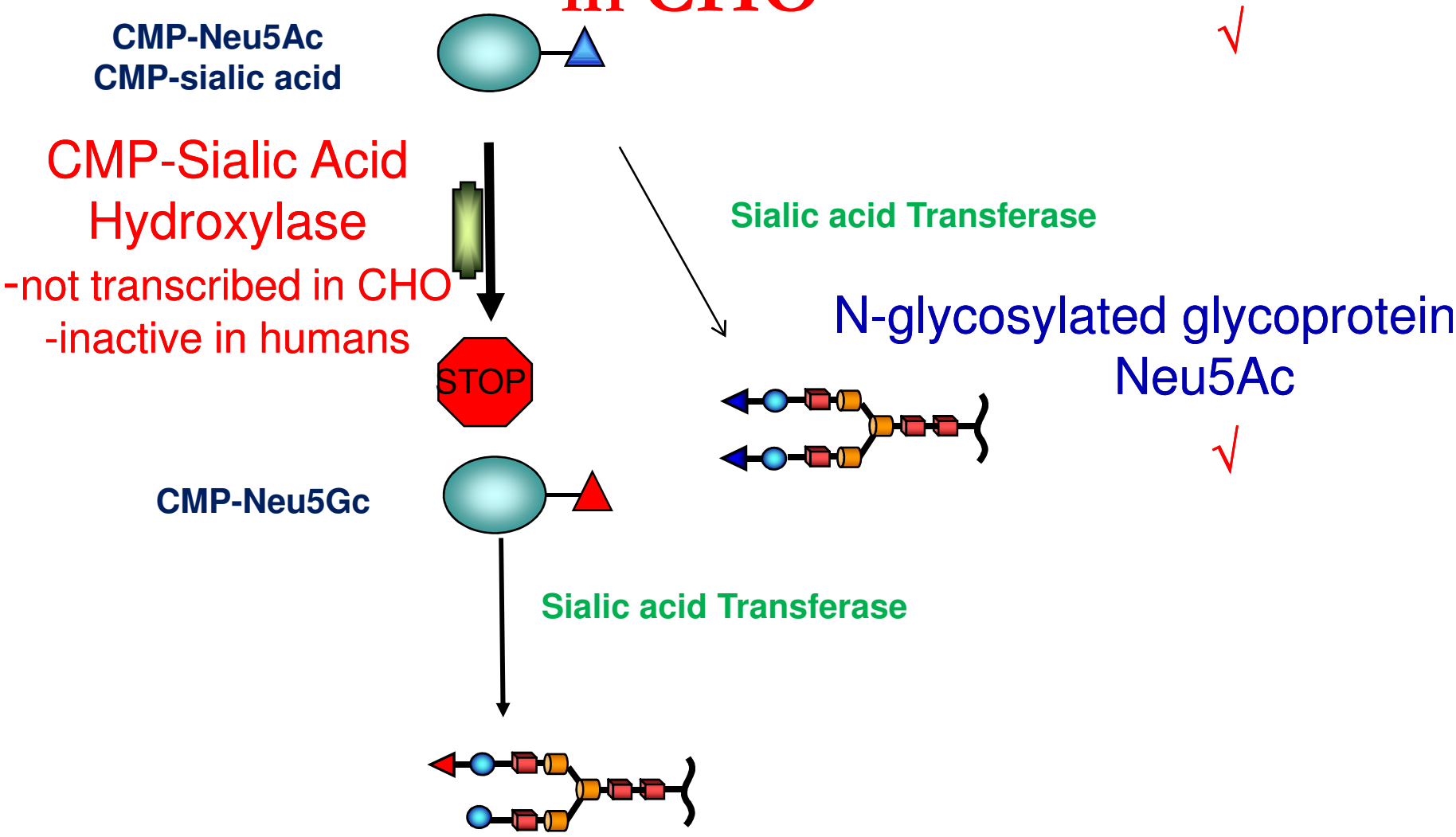

Immunogenic N-glycosylated glycoprotein with Neu5Gc √

Glycosylation Observations:
NO Bisecting GlcNAc to Block Fucose

ß4 GlcNAc from GnTIII:

GnTIII observed in CHO genome, but not transcriptome

CHO Pathway

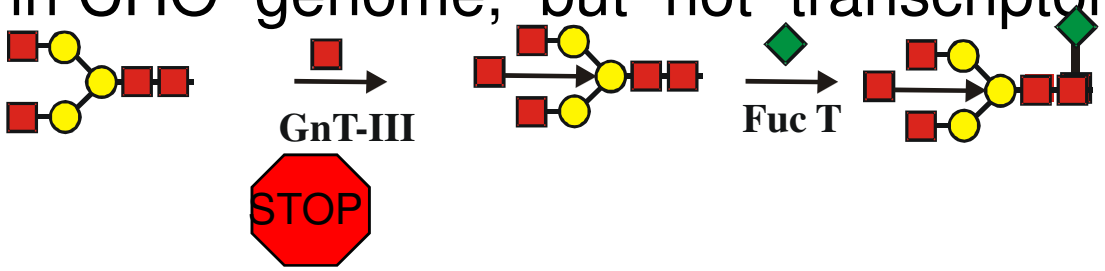

Human Pathway

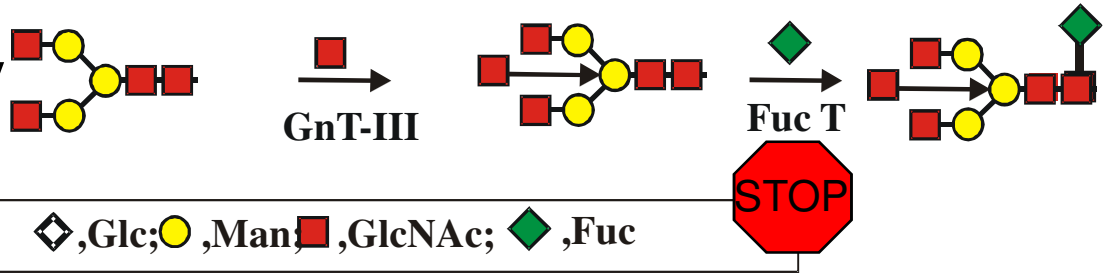

Can We Connect Transcriptomics and Proteomics Data Sets?

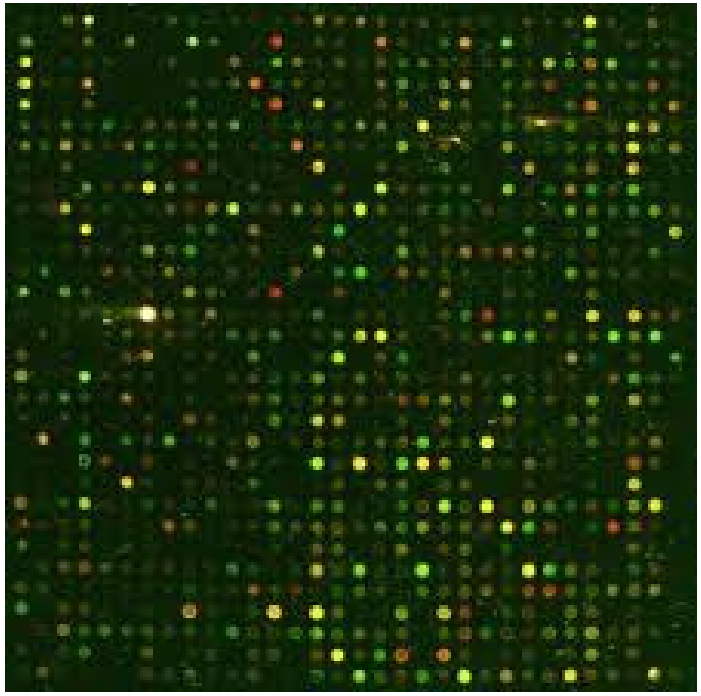

Transcriptomics Profiling

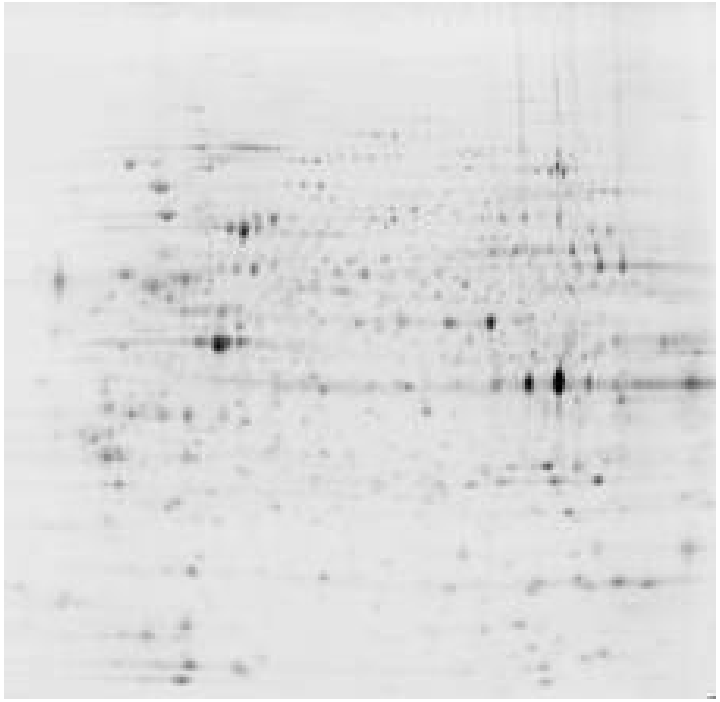

Proteomics Profiling

Baycin-Hizal et al

Amino Acid Codon Usage: CHO versus Humans

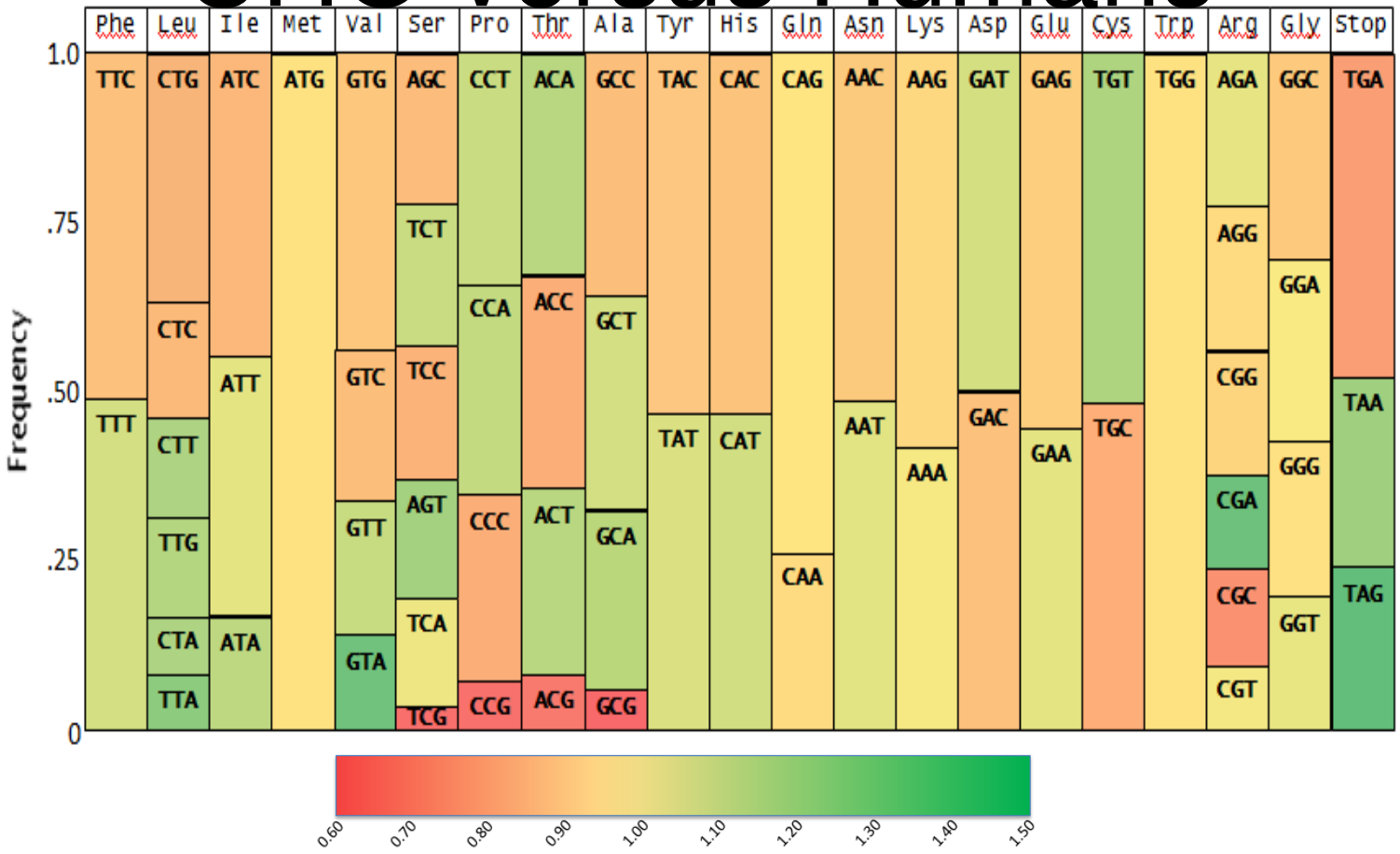

Codon frequency for CHO cells and the ratio of codon frequency in CHO cells to human.

Connecting Transcriptomics and Proteomics Data Sets?

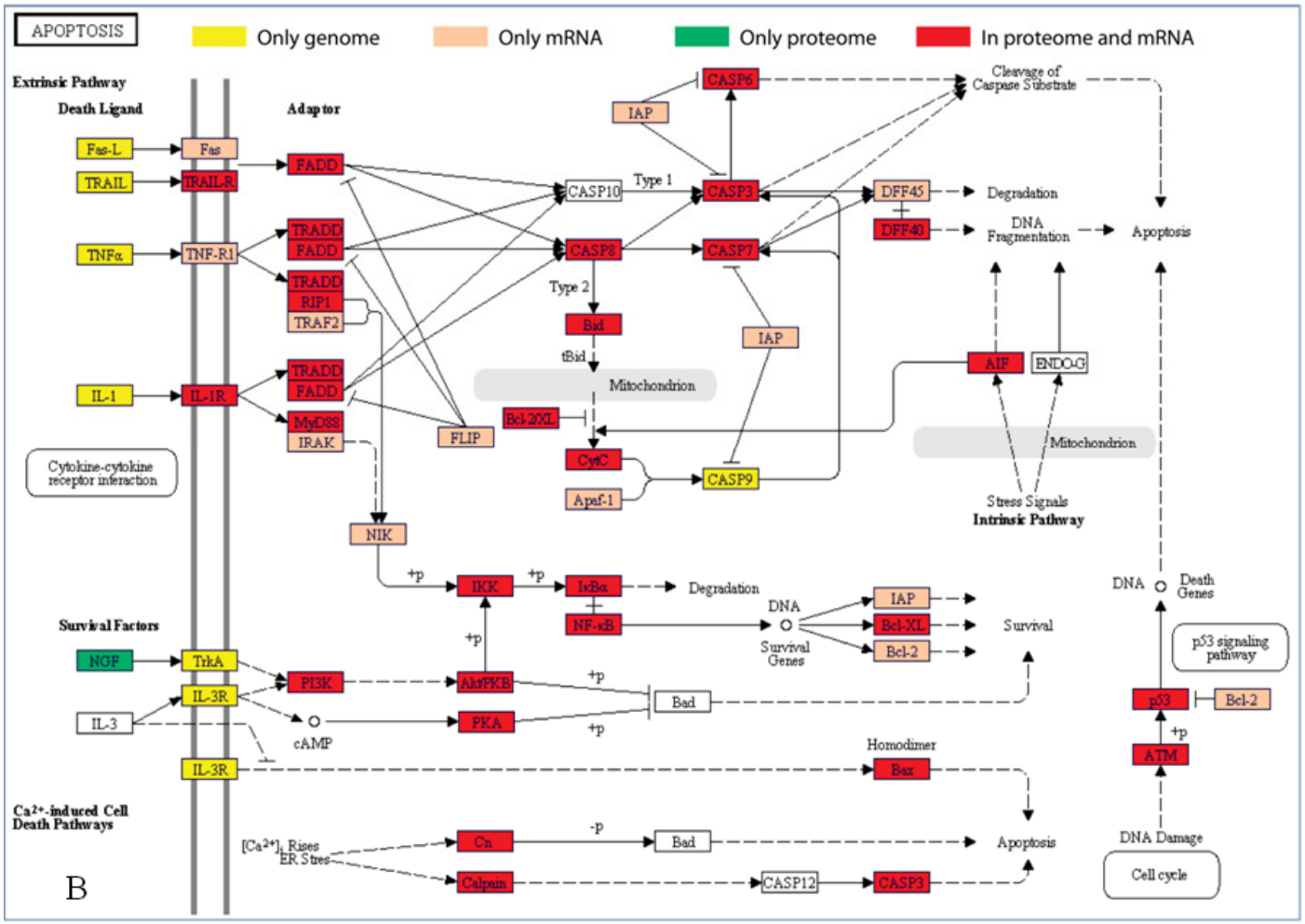

Baycin-Hizal et al

Connecting Transcriptomics and Proteomics Data Sets?

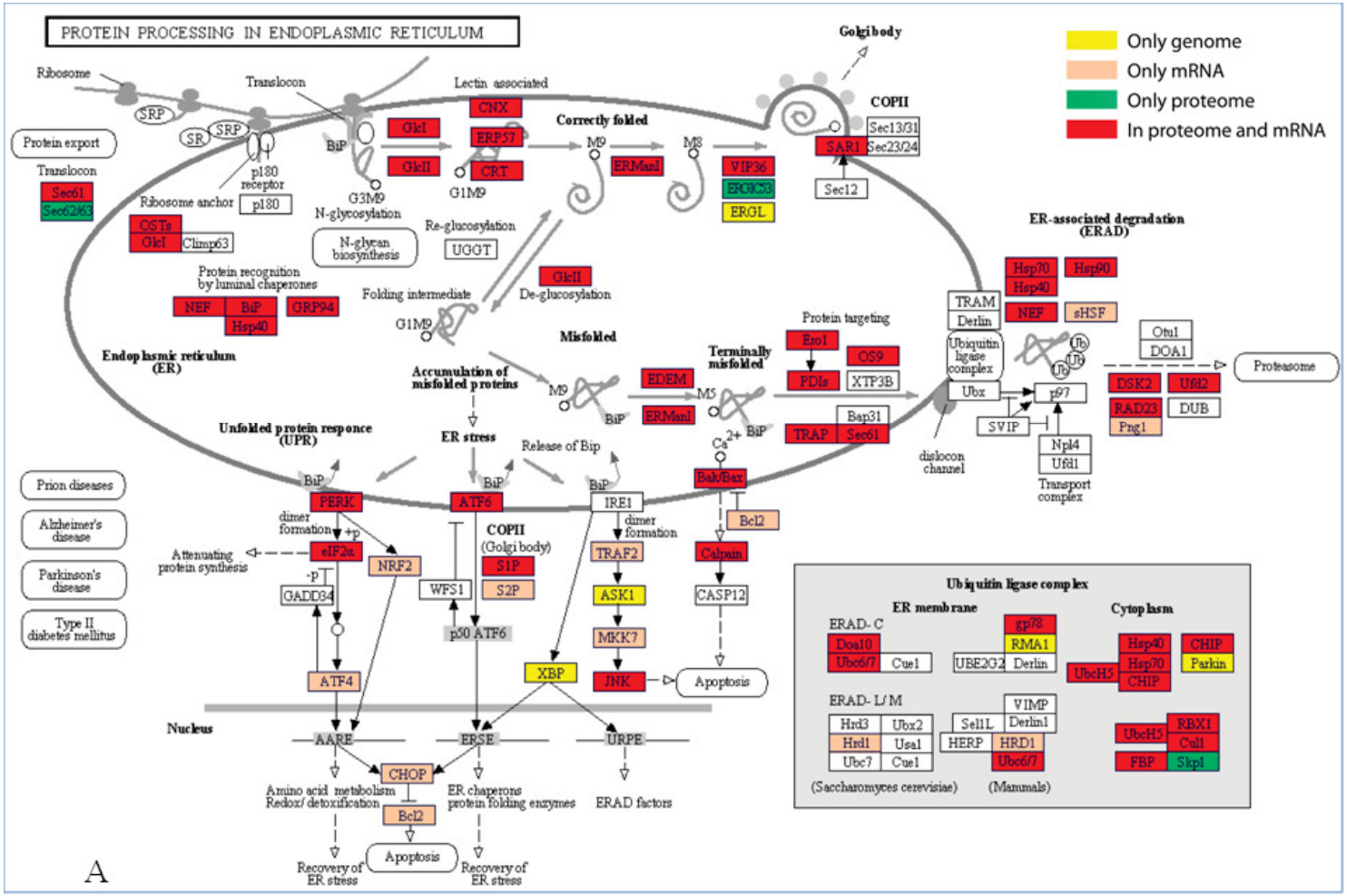

Baycin-Hizal et al

Effects of anti-mmu-mir466h on potential anti-apoptotic targets

- **mRNA level for five anti-apoptotic targets increased between 4 and 23 fold in the presence of anti-miR-466h**
- The largest relative increases in mRNA observed in *smo* and *dad1* genes
- Addition of the negative control (irrelevant anti-miR) at the same concentration generated the respective mRNA levels that were comparable to their levels without inhibitor (data not shown).

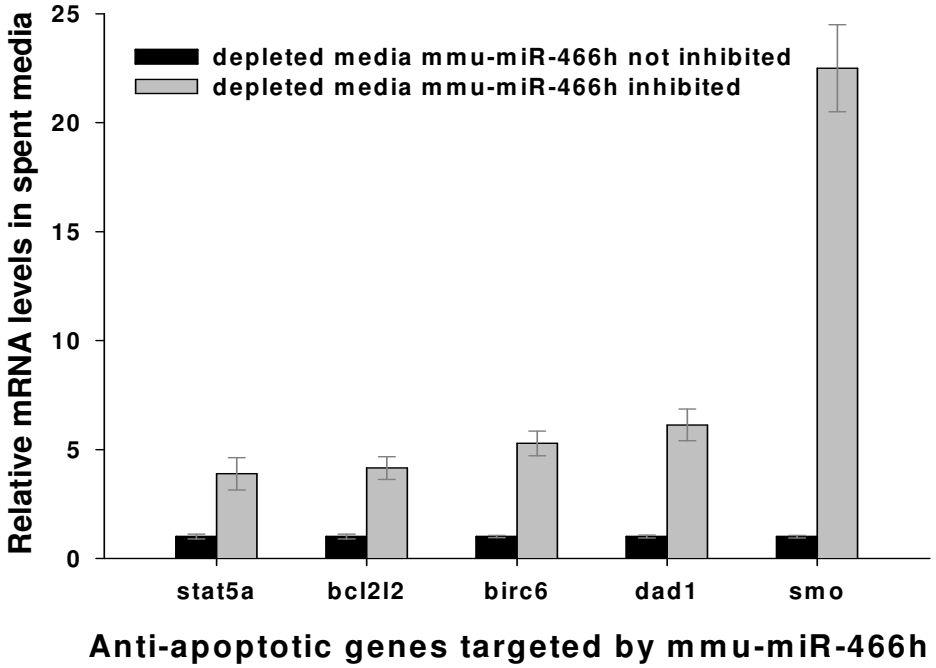

Addition of anti-mmu-mir-466h enhances mRNA levels of anti-apoptotic genes in depleted media

Does chemical inhibition of mmu-mir-466h affect apoptosis pathway?

- Caspase 3/7 activity was analyzed after 17 to 20 hours of incubation in fresh or depleted media
- Caspase activity increased only slightly in fresh medium
- No difference in caspase activity after 17 hours exposure in spent/depleted media
- After 20 hours exposure, the caspase-3/7 activity increased in depleted media
- **Addition of anti-miR-466h oligonucleotide reduced caspase activity below control**

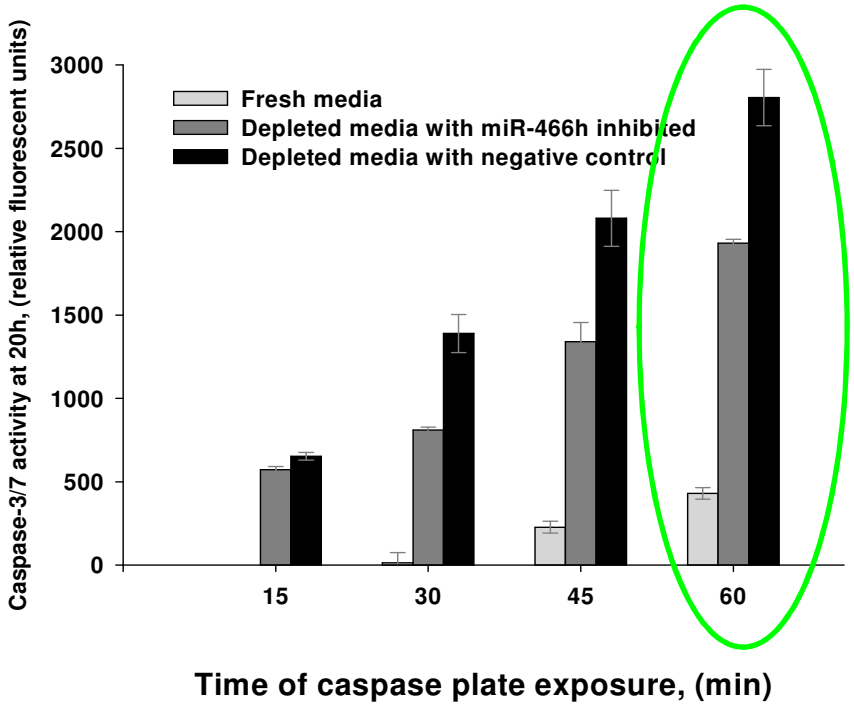

Addition of anti-mmu-mir-466h chemical to cells lowers caspase activity following nutrient depletion

Examine Potential targets of mmu-mir-

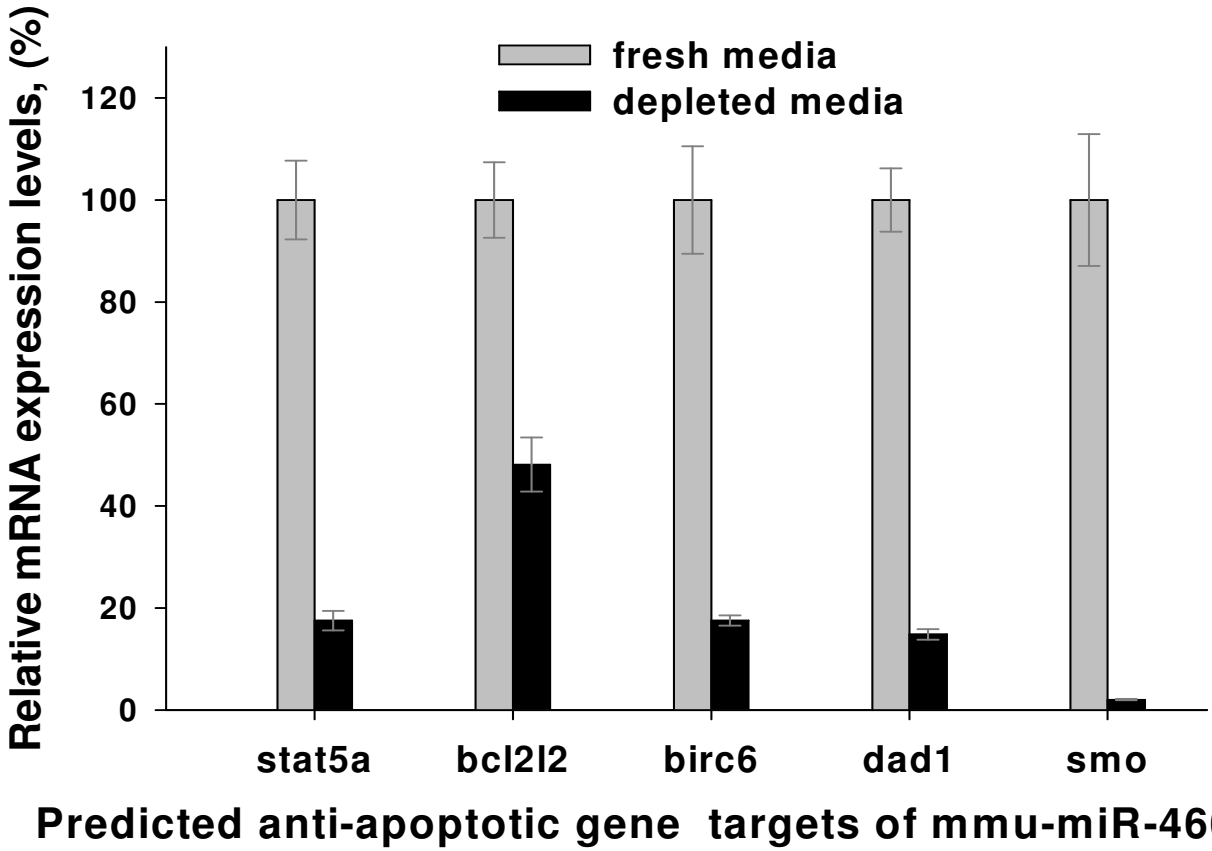

Five anti-apoptotic genes were detected in CHO and DOWN-REGULATED in nutrient-depleted conditions:
stat5a, bcl2l2, birc6, dad1, smo

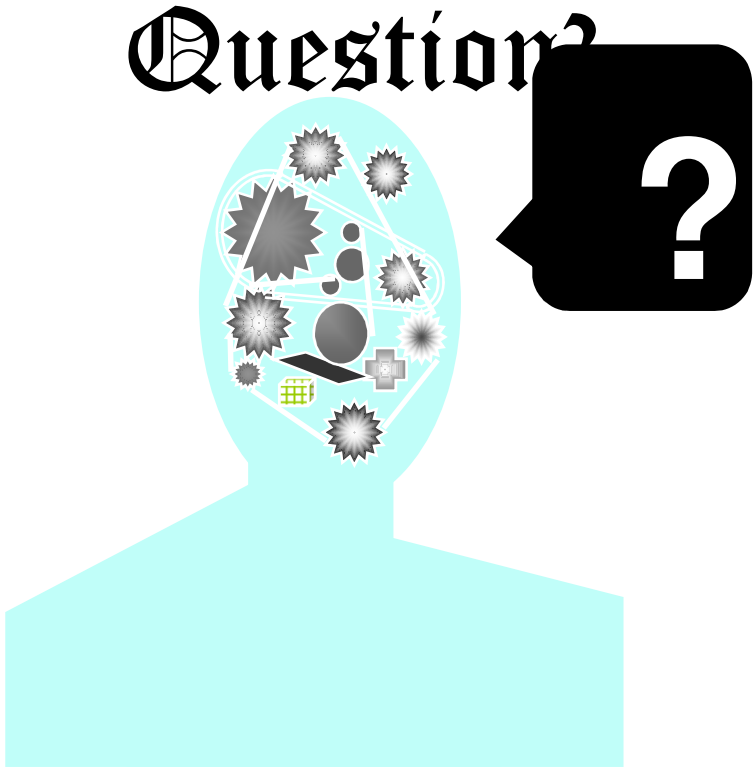

Can we apply ‘omics and cell re-engineering strategies to alter mammalian culture systems performance

Location of microRNAs within cluster

Mouse miR ID (mmu-)	Variant	Mature miR sequence	Fresh media relative fluorescent signal	Depleted media relative fluorescent signal	Up-regulation in depleted media (times)	p-value
miR-297a	-	AUGUAUGUGUGCAUGUGCAUGU	14±4	1412±220	101±13	0.039
miR-466a	3p	UAUACAUACACGCACACAUAAGA	8±1	203±30	25±1	0.050
miR-466b	3-3p	AAUACAUACACGCACACAUAAGA	5±1	209±39	42±1	0.035
miR-466d	3p	UGUGUGUGCGUACAUGUACAUG	10±1	648±122	65±6	0.039
	5p	UAUACAUACACGCACACAUAG	8±2	552±92	69±6	0.050
miR-466f	3p	CAUACACACACACAUACACAC	19±1	5056±105	266±8	0.009
	5p	UACGUGUGUGUGCAUGUGCAUG	102±13	22200±5982	218±31	0.036
miR-466g	-	AUACAGACACAUGCACACACA	51±9	14935±4286	293±32	0.038
miR-466h	**-**	**UGUGUGCAUGUGCUUGUGUGUA**	**29±4**	**13105±2366**	**452±19**	**0.023**
miR-467a	minor	AUAUACAUACACACACCUACAC	44±1	9567±2001	217±40	0.025
miR-467b	minor	AUAUACAUACACACACCAACAC	72±8	14451±2817	201±17	0.027
miR-467e	minor	AUAUACAUACACACACCUAUAU	14±2	1056±38	75±8	0.022
miR-669a	-	AGUUGUGUGUGCAUGUUCAUGU	7±0	57±3	8±0	0.016
miR-669b	-	AGUUUUGUGUGCAUGUGCAUGU	8±0	46±1	6±0	0.003
miR-669c	**-**	**AUAGUUGUGUGUGGAUGUGUGU**	**23±4**	**2870±299**	**125±9**	**0.023**
miR-669d	-	ACUUGUGUGUGCAUGUAUAUGU	7±0	1511±463	216±66	0.038
miR-669e	-	UGUCUUGUGUGUGCAUGUUCAU	12±0	4090±971	341±81	0.027
miR-669f	-	CAUAUACAUACACACACACGUAU	44±1	13444±4267	306±90	0.037
miR-669h	3p	UAUGCAUAUACACACAUGCACA	8±0	326±6	41±1	0.007
miR-669i	-	UGCAUAUACACACAUGCAUAC	18±1	39±1	2±0	0.048

- **18 detected members of mouse miR 297-669 cluster were up-regulated in CHO cells in nutrient-depleted conditions based on**

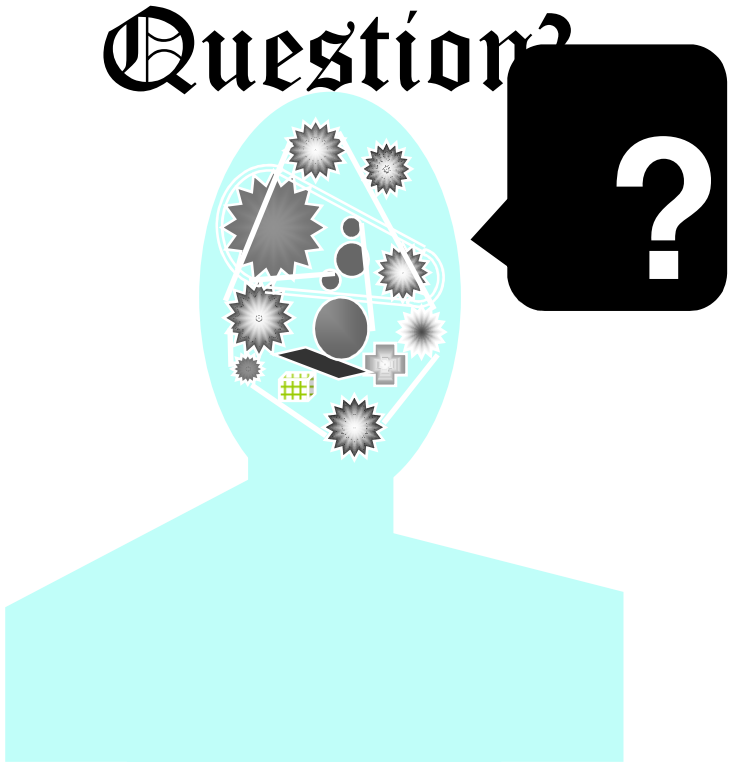

Can we apply
Omics approaches to improve or enhance these
Cell Engineering Methodologies

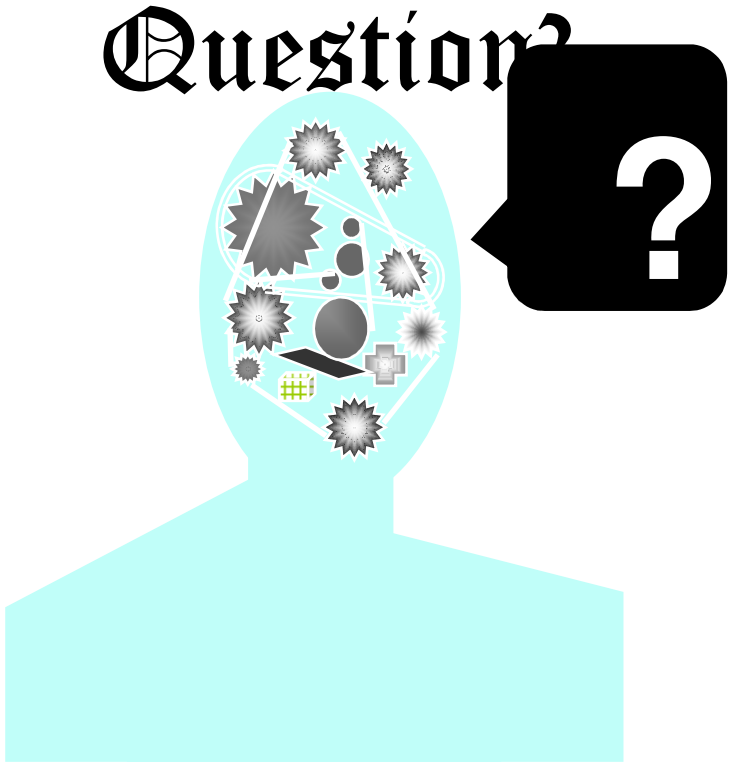

Can we apply
cell re-engineering to improve or enhance these Production Systems

A Typical Batch Growth Curve for Cell Culture

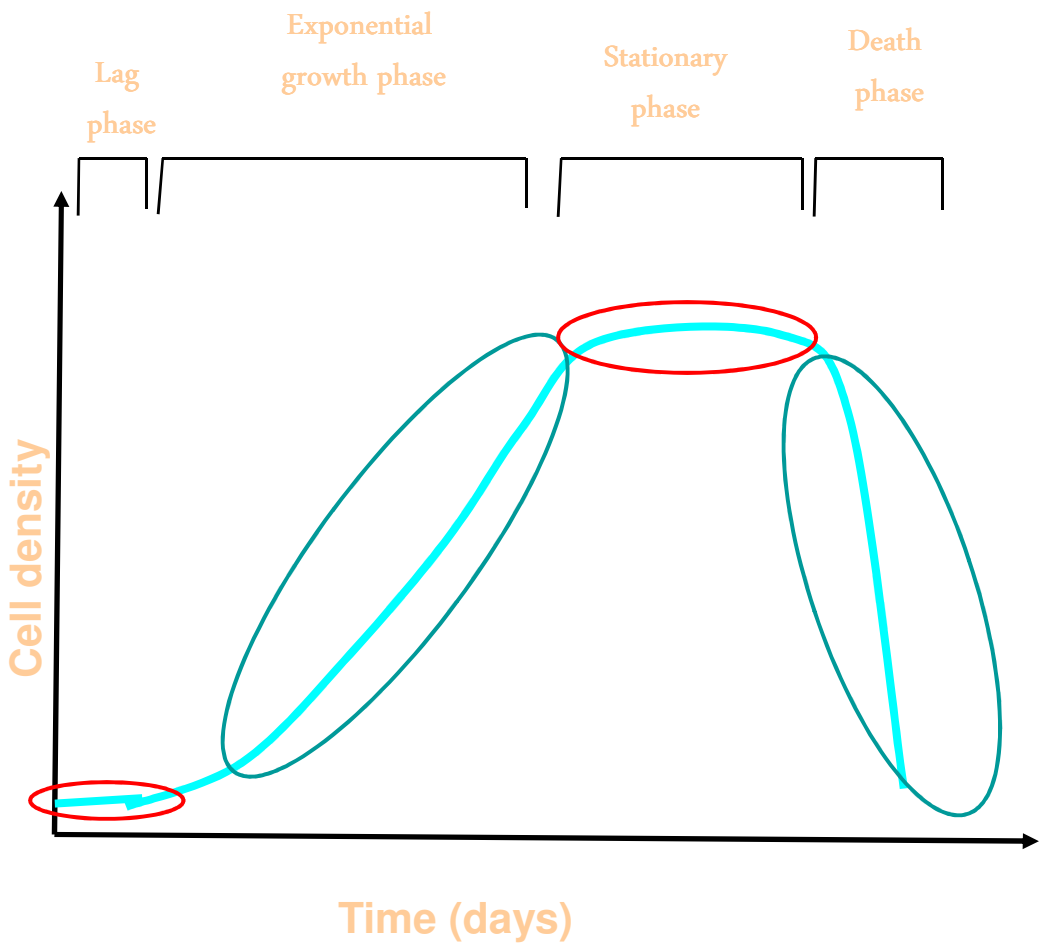

Lag phase: cells adapt to the new environment (temp, nutrients, etc.)

Exponential phase: cells dividing at a constant rate (i.e. the maximum for the species under the given conditions of temp, pH, nutrients, oxygen, etc.)

Stationary phase: cell growth ceases as nutrients are exhausted and/or waste products build up in the media

Death phase: number of viable (living cells) in the stationary phase culture decreases due to cell death

A Typical Batch Growth Curve for Cell Culture

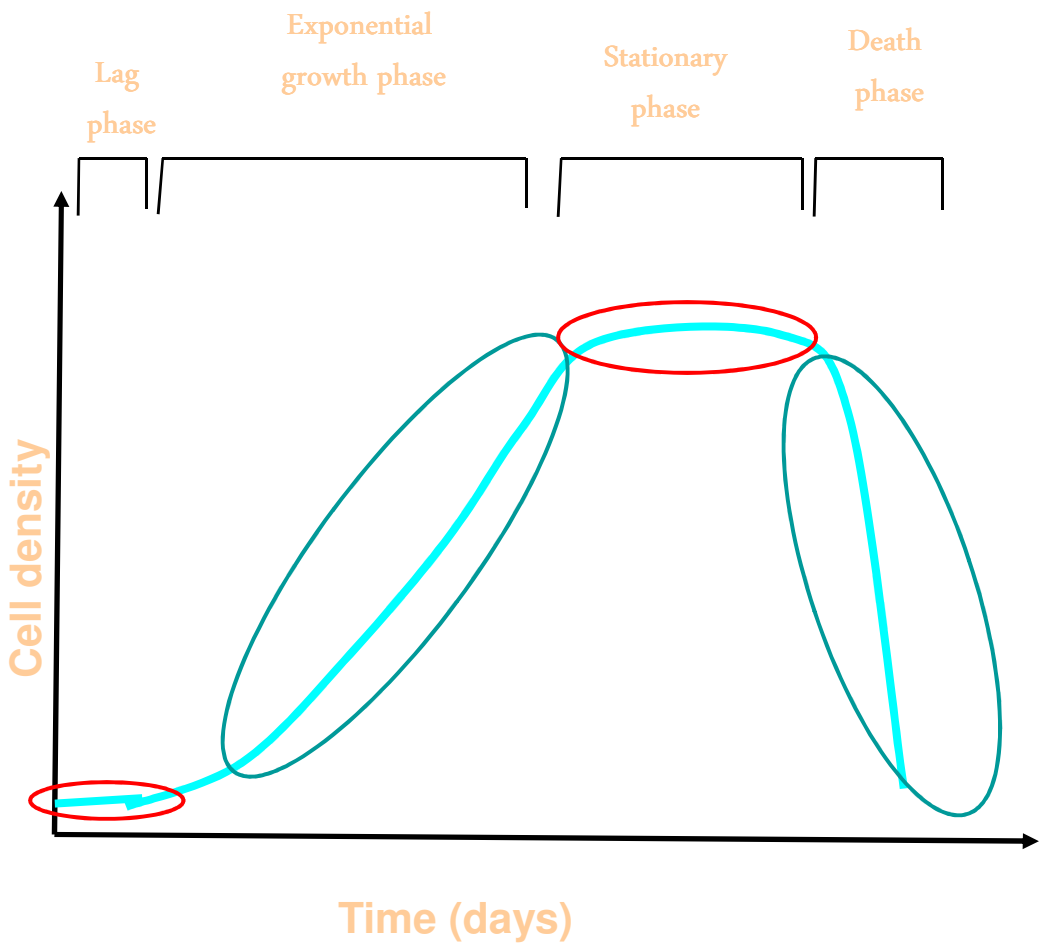

Lag phase: cells adapt to the new environment (temp, nutrients, etc.)

Exponential phase: cells dividing at a constant rate (i.e. the maximum for the species under the given conditions of temp, pH, nutrients, oxygen, etc.)

Stationary phase: cell growth ceases as nutrients are exhausted and/or waste products build up in the media

Death phase: number of viable (living cells) in the stationary phase culture decreases due to cell death

Can We Prevent Death Phase in Cell Culture?

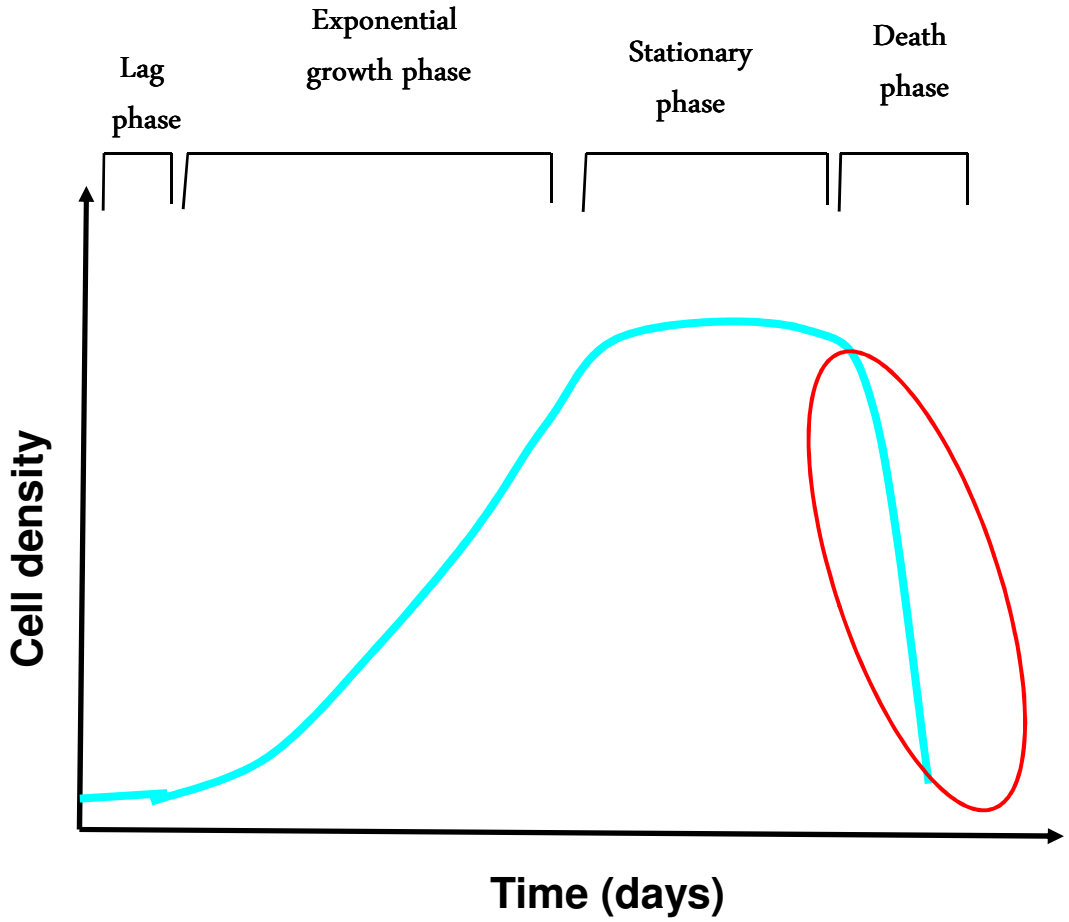

Death phase: number of viable (living cells) in the stationary phase culture decreases due to cell death

Apoptotic Detection Examples

Healthy Chinese Hamster Ovary (CHO) cell

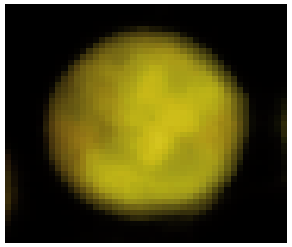

Apoptotic CHO cell

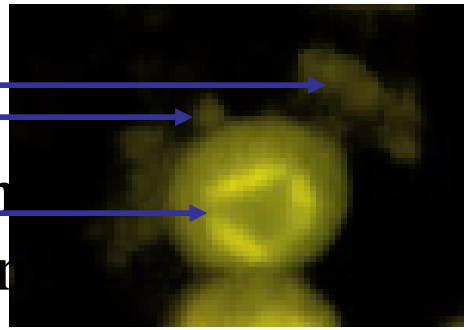

Acridine Orange Staining

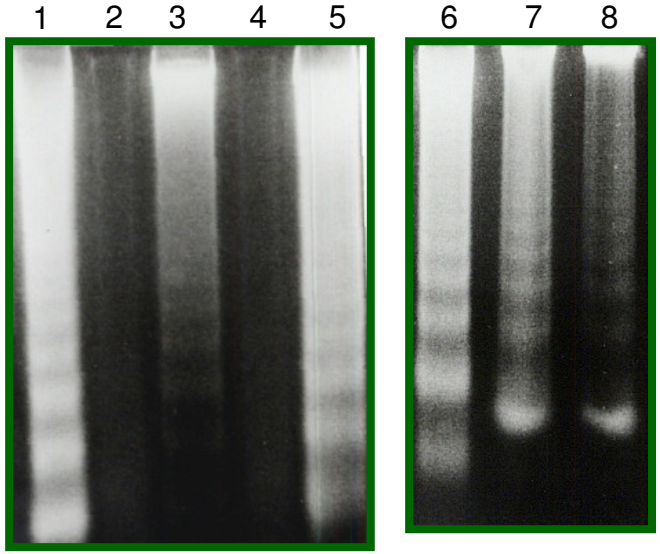

CHO cells (3 and 7) and
Baby Hamster Kidney (BHK)
(5 and 8) undergo DNA fragmentation

Can we apply Metabolic Engineering to Apoptosis Pathways

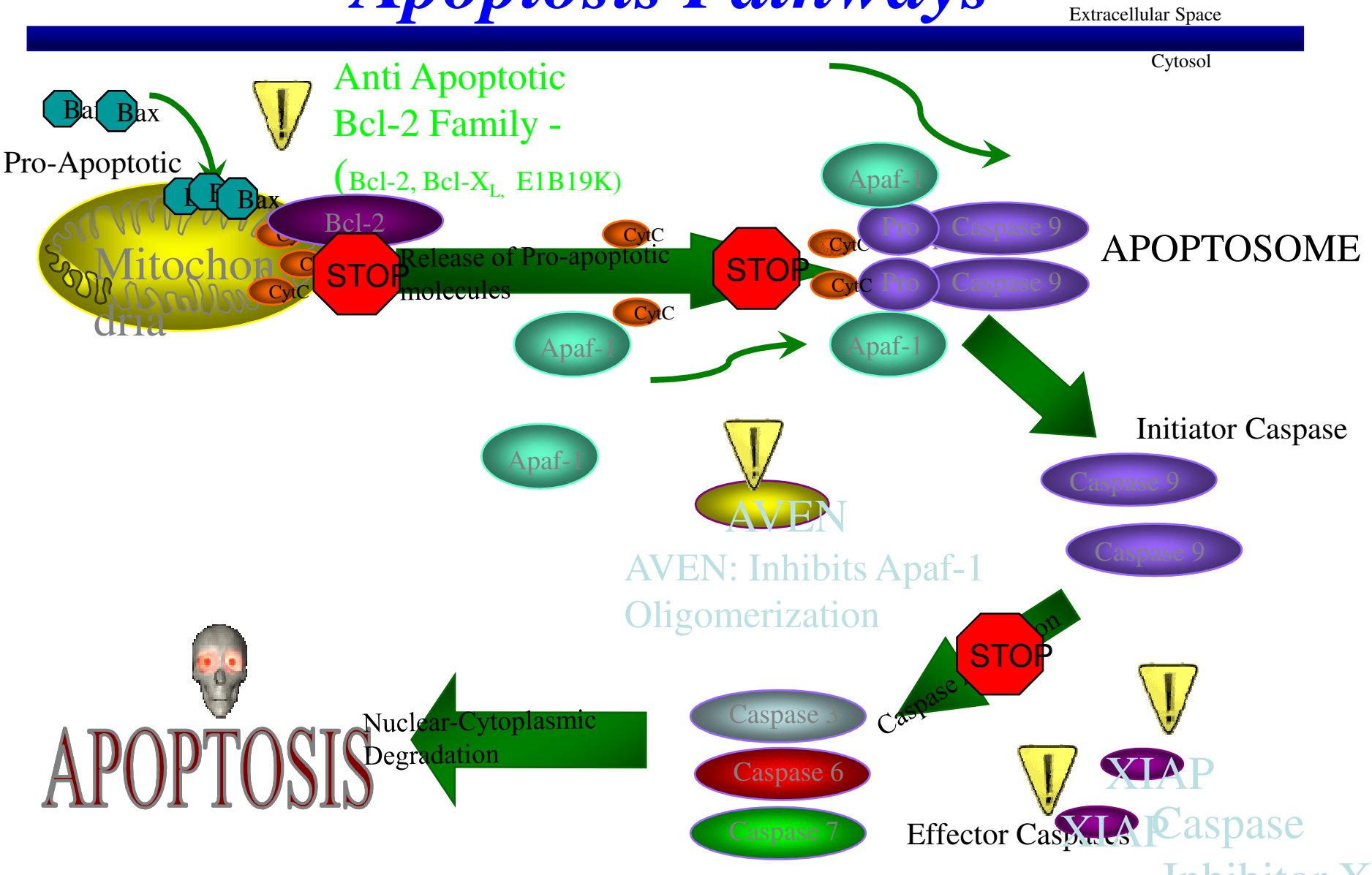

Effects of anti-apoptosis genes on Chinese hamster ovary cell apoptosis

Untreated

DMSO (Vehicle) treated

Staurosporine Treated:
-apoptosis chemical

Control Cell Line

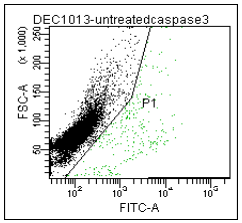

Apoptosis Positive 1%

Control Cell Line

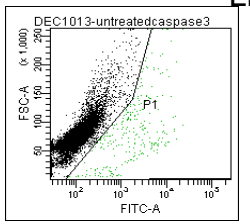

Apoptosis Positive 1%

Control Cell Line

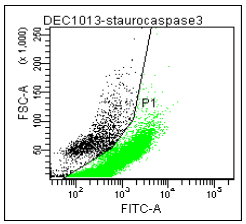

Apoptosis3

91% Positive

E1B-19K + Aven

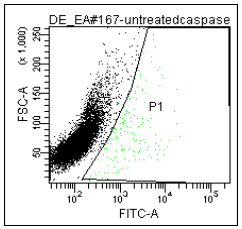

0.8% positive

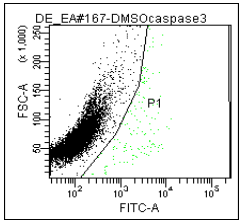

Anti-Apoptotic: E1B-19K + Aven

0.7% positive

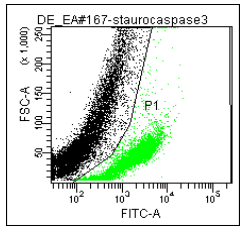

Anti-Apoptotic: E1B-19K + Aven

30% positive

E1B-Aven-Xiap

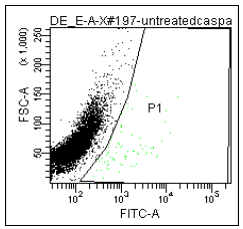

0.4% positive

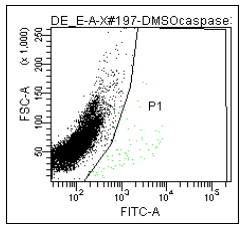

0.4% posiitve

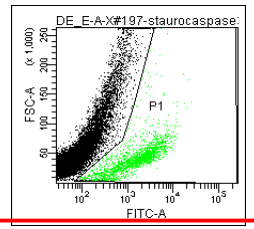

Anti-Apoptotic: E1B-Aven-Xiap

9% positive

Collaboration with Centocor: Dorai et al., Biotechnol. and Bioeng.

Higher Antibody Biotherapeutic Yields in Anti-Apoptotic Chinese hamster cells

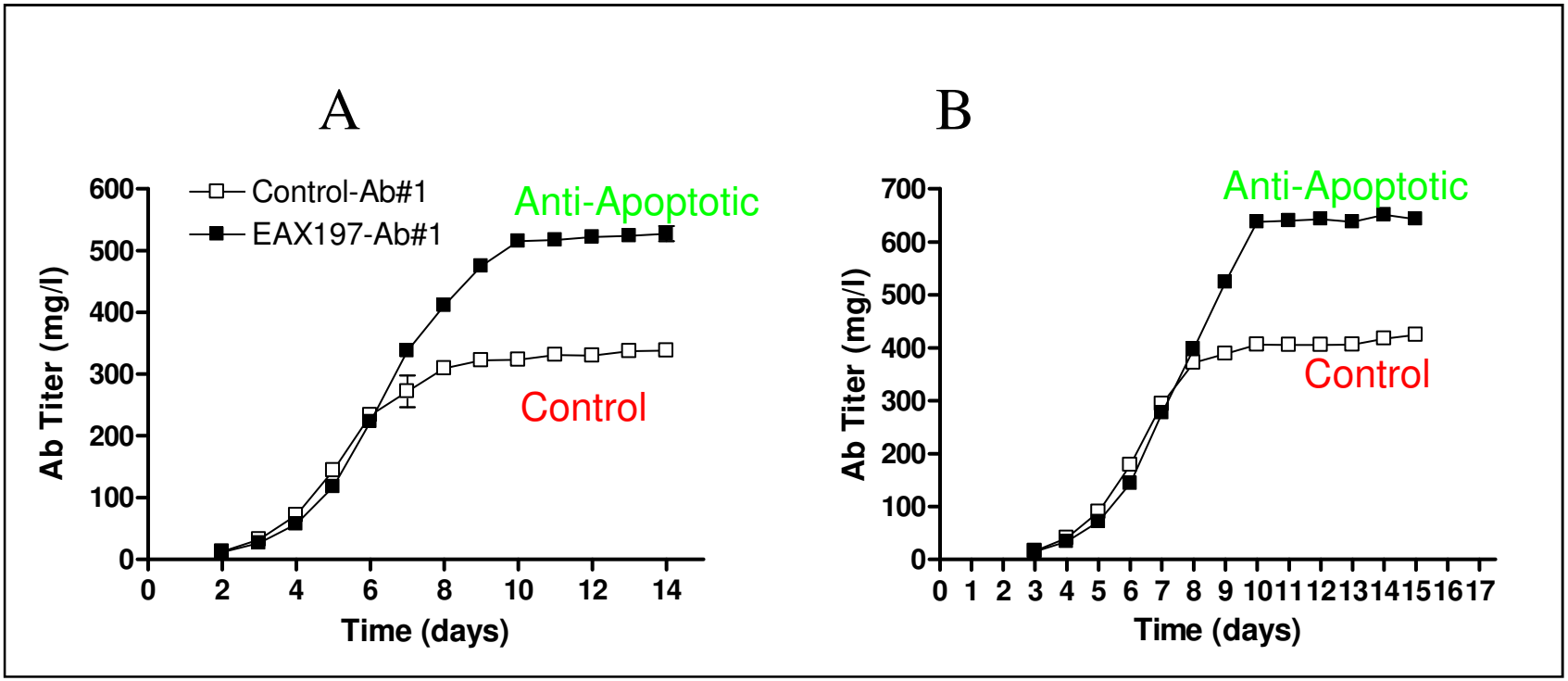

Dorai et al., Biotechnol. Bioeng.,

Licensed to Johnson & Johnson

Does Nutrient Depletion Stimulate Apoptosis

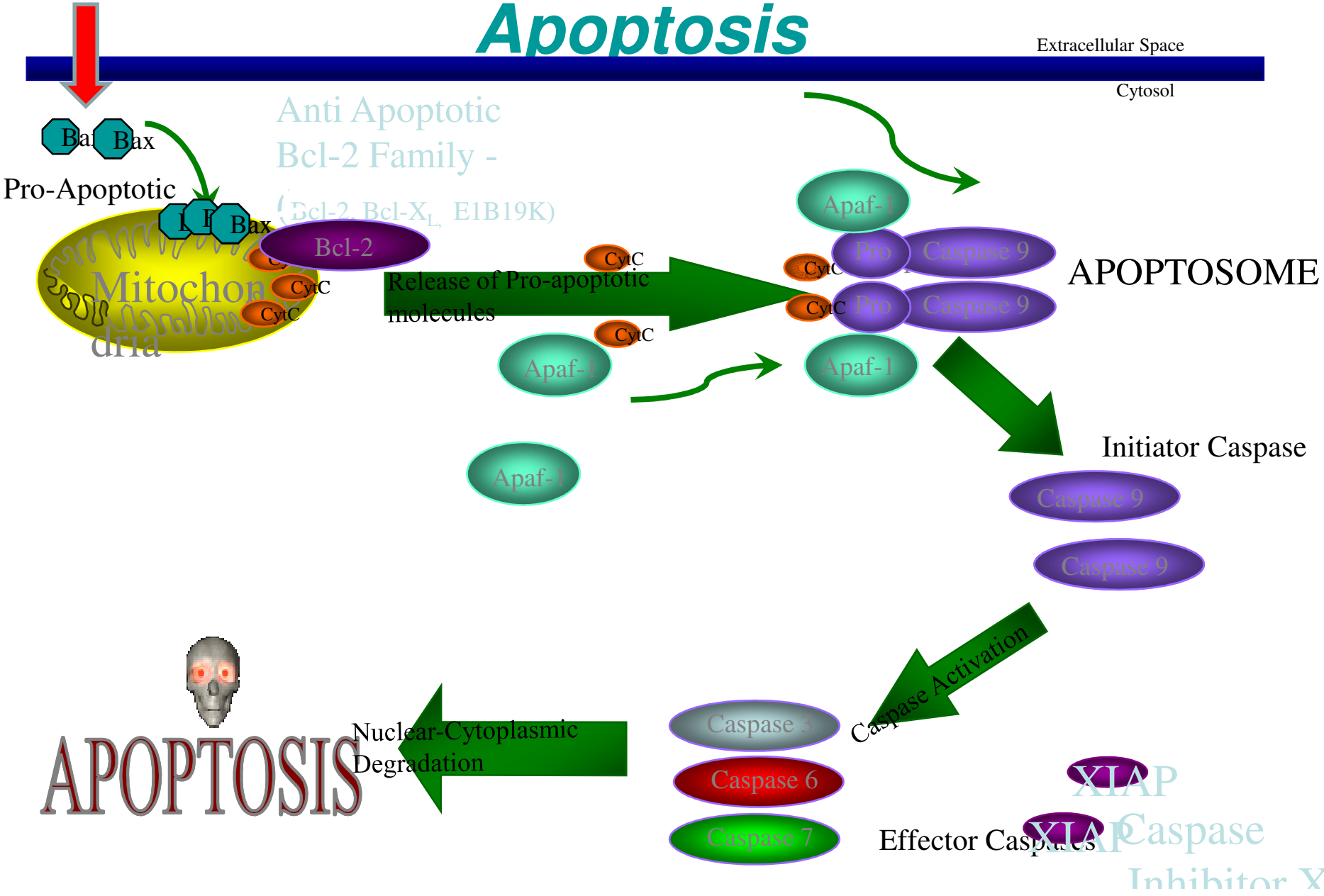

Are CHO Apoptosis Pathways activated in Depleted Media: Measurement of Caspase Activity

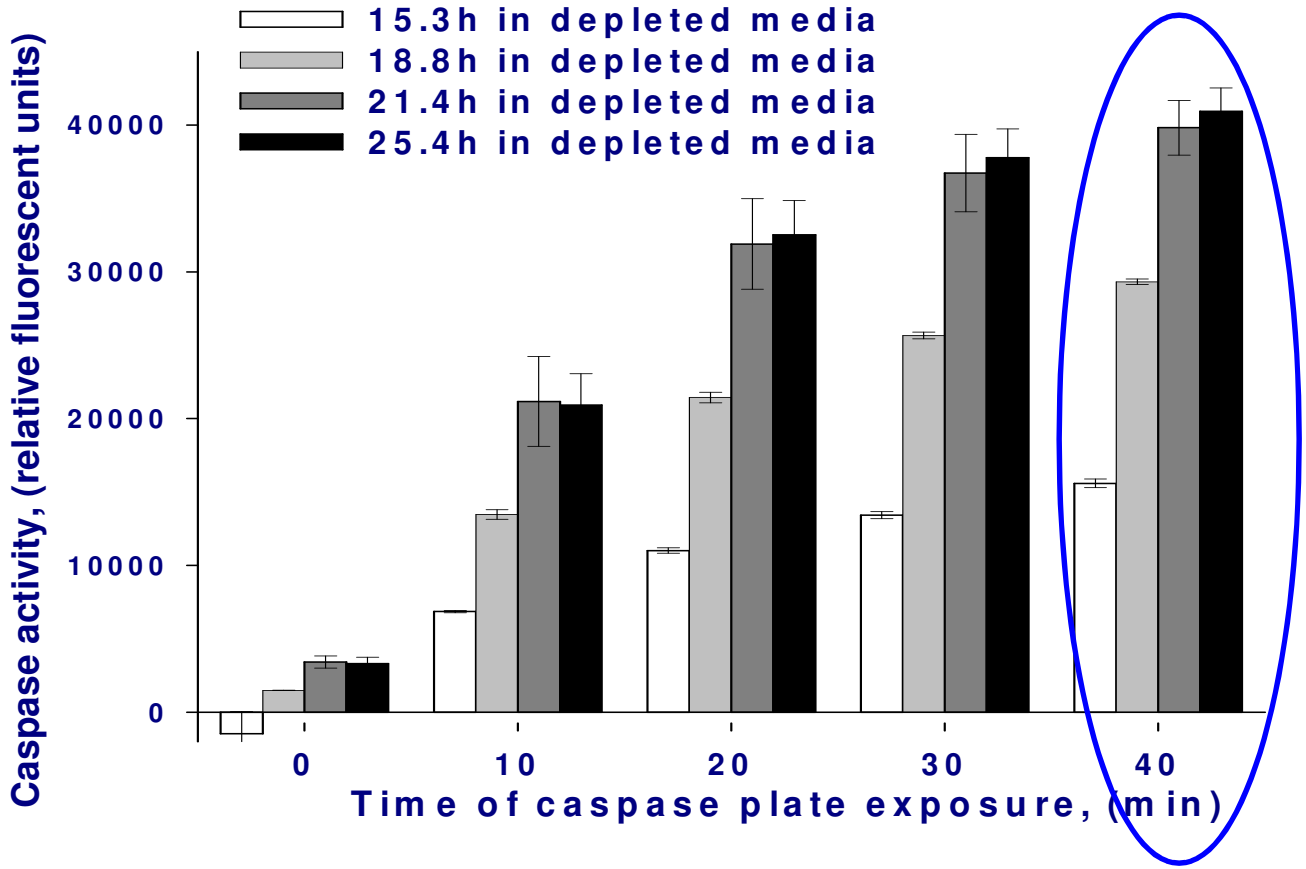

Caspase activity (apoptosis) increased for cells exposed for longer periods (20-25 hours) in depleted (spent) media

Microarray Analysis of MicroRNA: Comparison of Fresh and Depleted Media

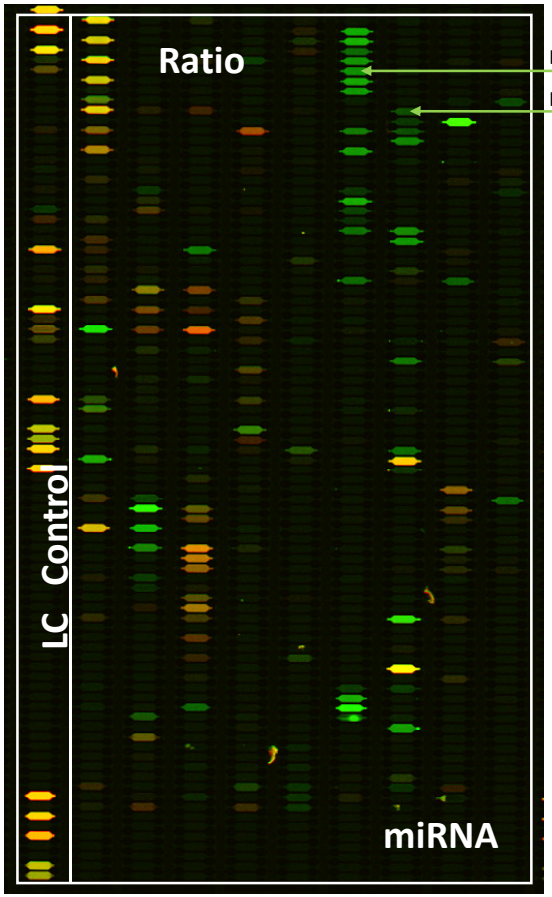

(A) Microarray map of overlaid images of miRs in fresh (labeled red) and depleted (labeled green) conditions.

MicroRNAs including mouse (mmu) microRNA (mir)-466h and mmu-mir-669c upregulated in depleted media

Quantitative PCR Analysis of MicroRNA:

esh and Depleted dia

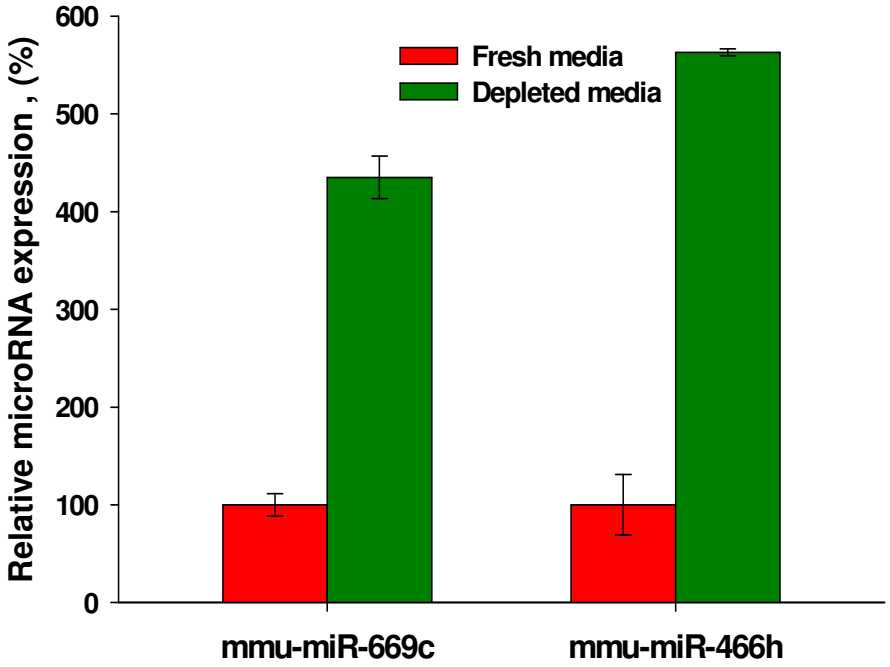

qRT-PCR of miR-669c and miR-466h in fresh and depleted conditions

Mir-669c and mir-466h upregulation in depleted conditions confirmed with quantitative PCR analysis

Potential targets of mmu-mir-466h

- 8708 mmu-miR-466h potential targets were obtained from miRecords using bioinformatics analysis

- Targets were narrowed to 38 anti-apoptotic genes with DAVID NCBI (annotation tool which classifies genes according to their biological roles)

Examine Potential targets of mmu-mir-

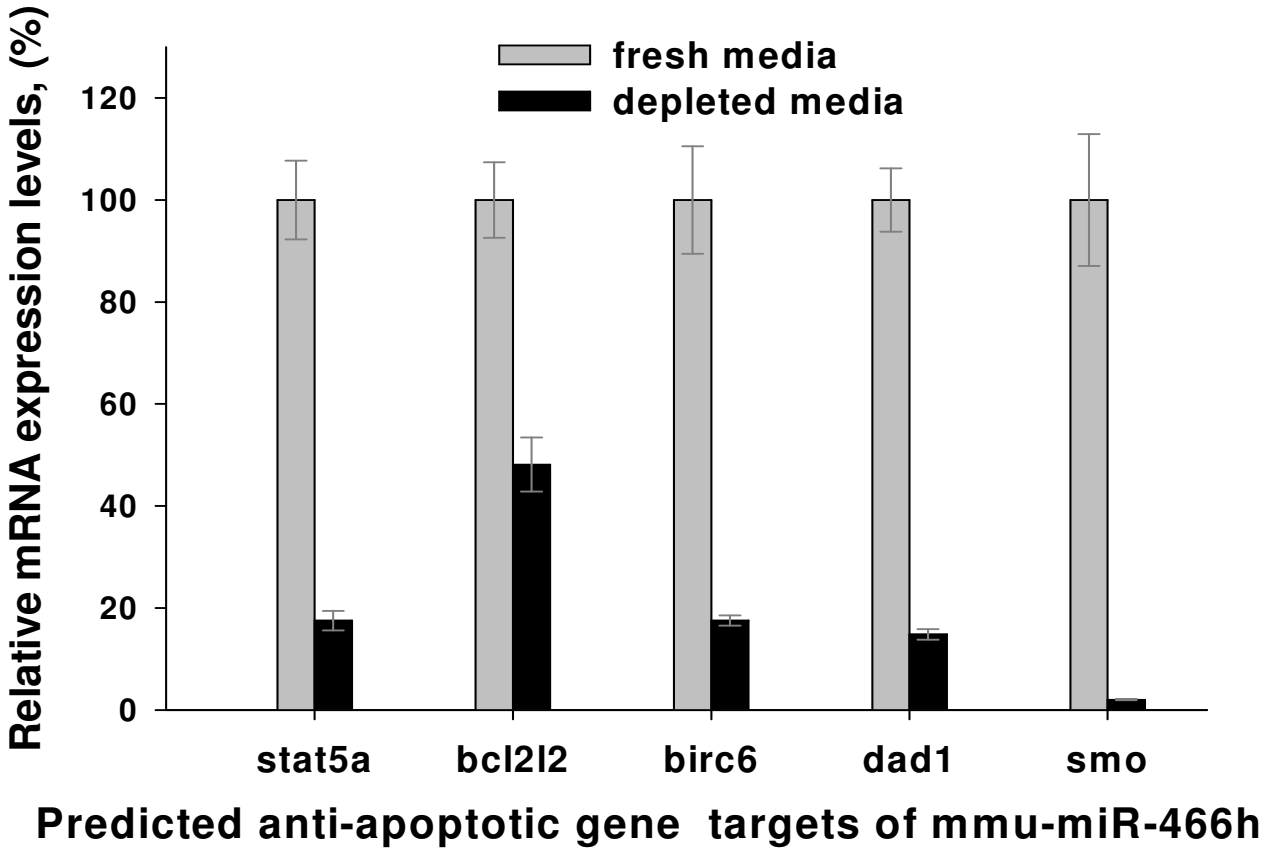

Five anti-apoptotic genes were detected in CHO and down-regulated in nutrient-depleted conditions:
stat5a, bcl2l2, birc6, dad1, smo

Effects of anti-mmu-mir466h

- A chemically modified single stranded oligonucleotide specific for mmu-miR-466h was added to the cells
- The levels of mmu-miR-466h in fresh media and in the depleted media, with or without anti-miR-466h, were measured
- **Compared with fresh media, mmu-miR-466h levels were 10 times higher in depleted media in the absence of the inhibitor**
- **Mir-466h levels were reduced by a factor of 4.5 in depleted media containing anti-miR-466h.**

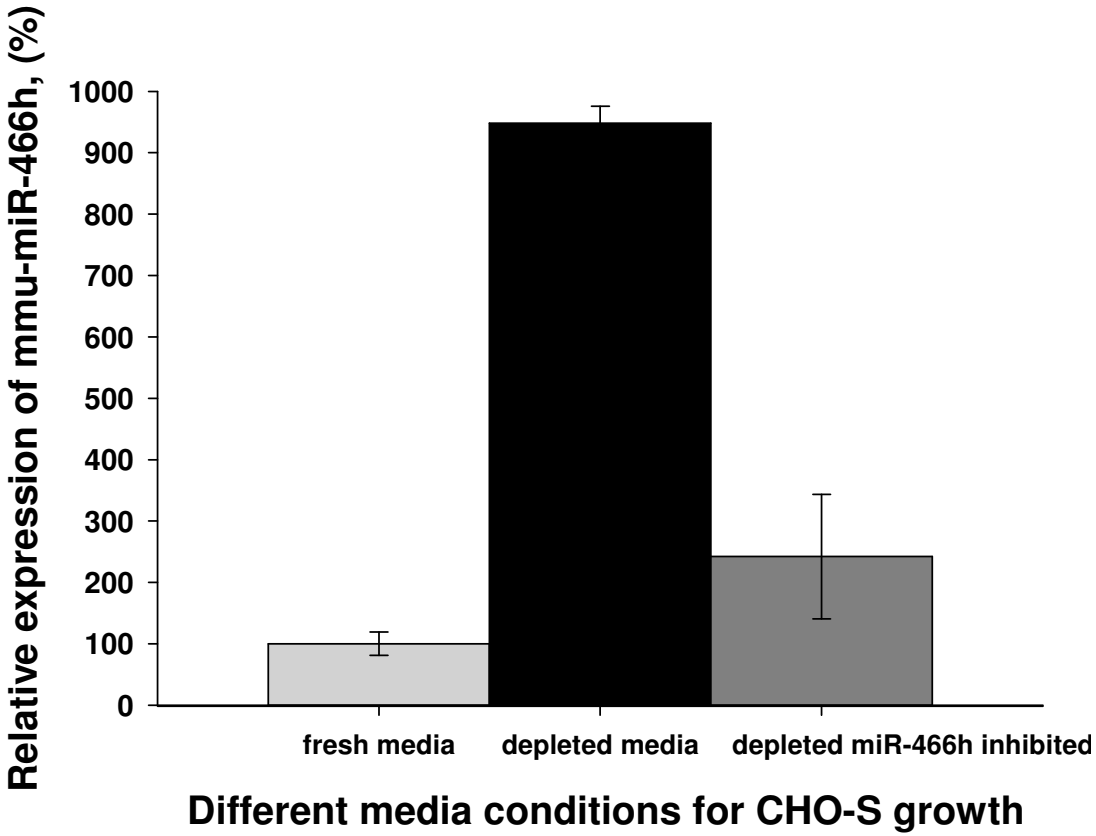

Increases in Mmu-mir-466h expression levels in depleted media are inhibited by oligonucleotide

Effects of anti-mmu-mir466h on potential anti-apoptotic targets

- **mRNA level for five anti-apoptotic targets increased between 4 and 23 fold in the presence of anti-miR-466h**
- The largest relative increases in mRNA observed in *smo* and *dad1* genes
- Addition of the negative control (irrelevant anti-miR) at the same concentration generated the respective mRNA levels that were comparable to their levels without inhibitor (data not shown).

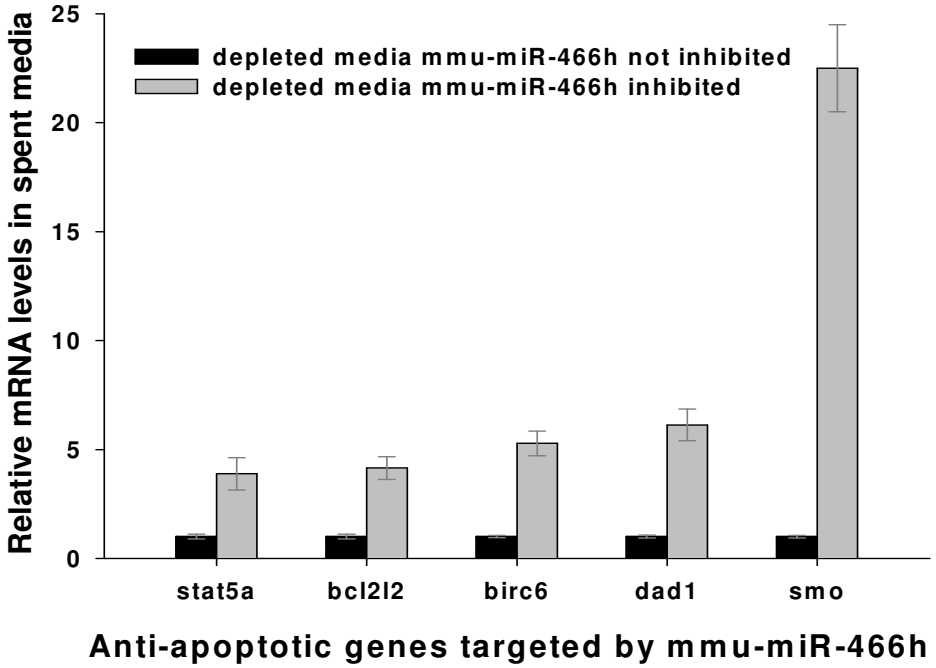

Addition of anti-mmu-mir-466h enhances mRNA levels of anti-apoptotic genes in depleted media

Does chemical inhibition of mmu-mir-466h affect apoptosis pathway?

- Caspase 3/7 activity was analyzed after 17 to 20 hours of incubation in fresh or depleted media
- Caspase activity increased only slightly in fresh medium
- No difference in caspase activity after 17 hours exposure in spent/depleted media
- After 20 hours exposure, the caspase-3/7 activity increased in depleted media
- **Addition of anti-miR-466h oligonucleotide reduced caspase activity below control**

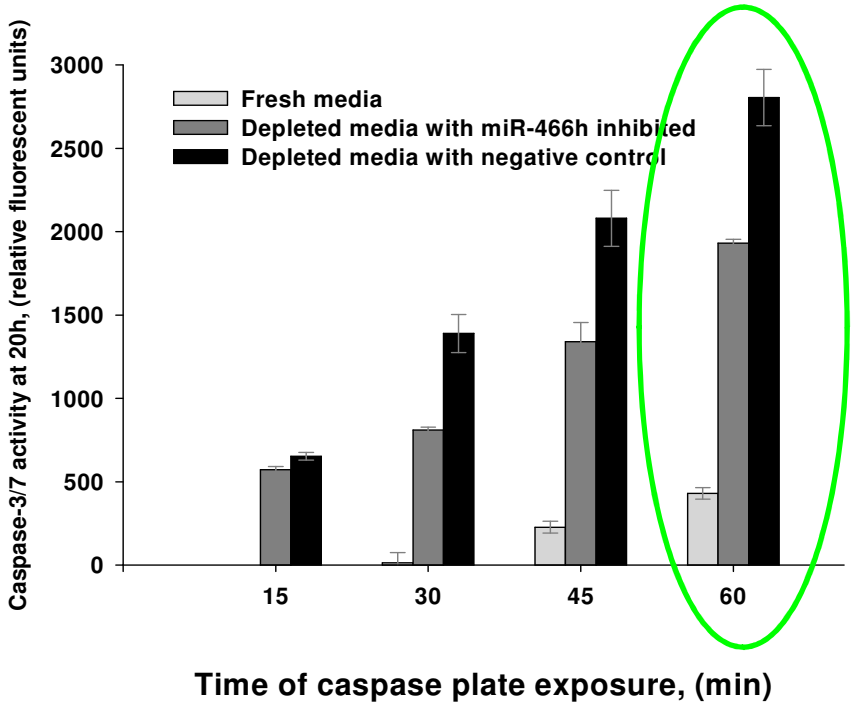

Addition of anti-mmu-mir-466h chemical to cells lowers caspase activity following nutrient depletion

Does chemical inhibition of mmu-mir-466h affect cell viability

- Cell viability in the depleted media started to decline after about 18 hours and fell to 81% by 23 hours.
- **When the cells were chemically treated with anti -miR-466h oligonucleotide, the cell viability was higher at both the 20 and 23 hours time points.**

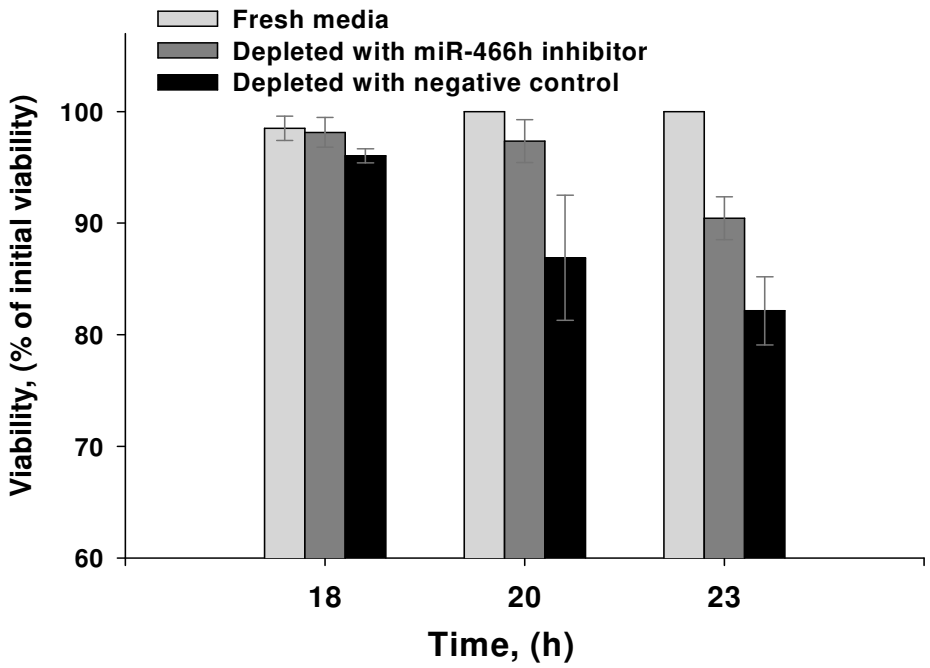

Addition of anti-mmu-mir-466h chemical to cells enhances viability following nutrient depletion

MicroRNA and Apoptosis Signaling

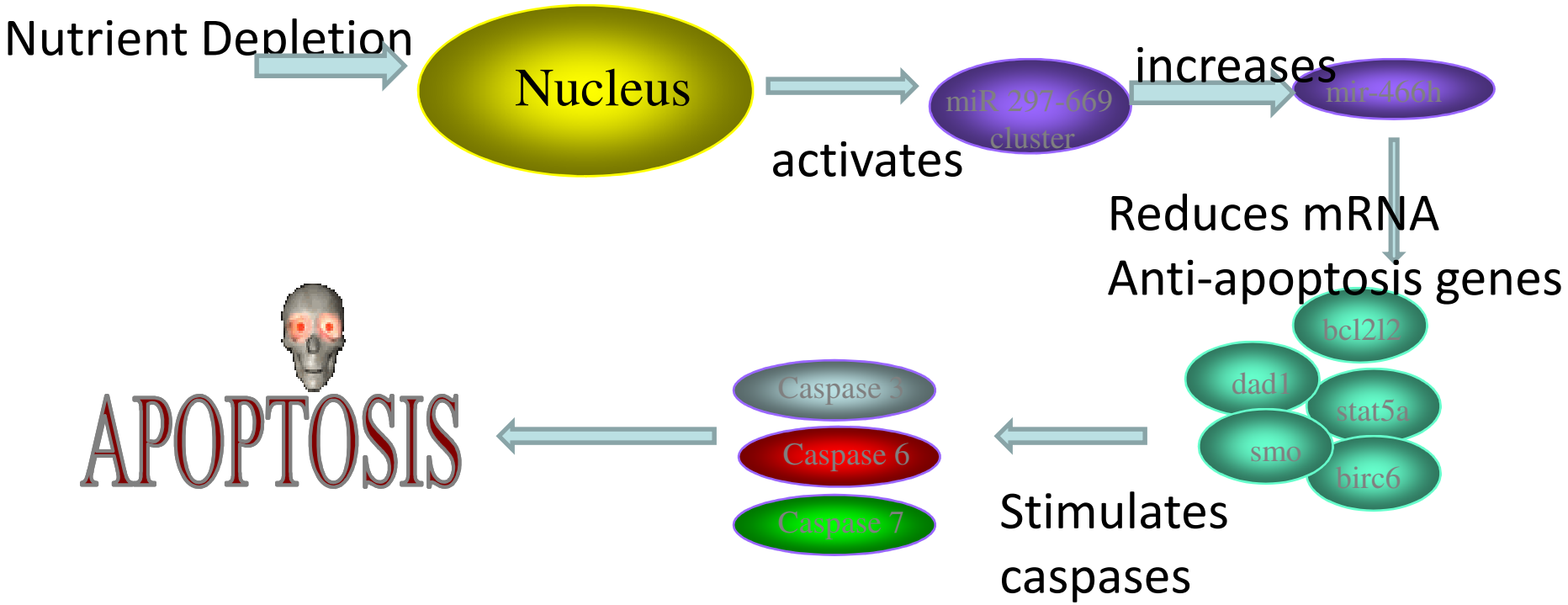

Chemical Inhibition of MicroRNA

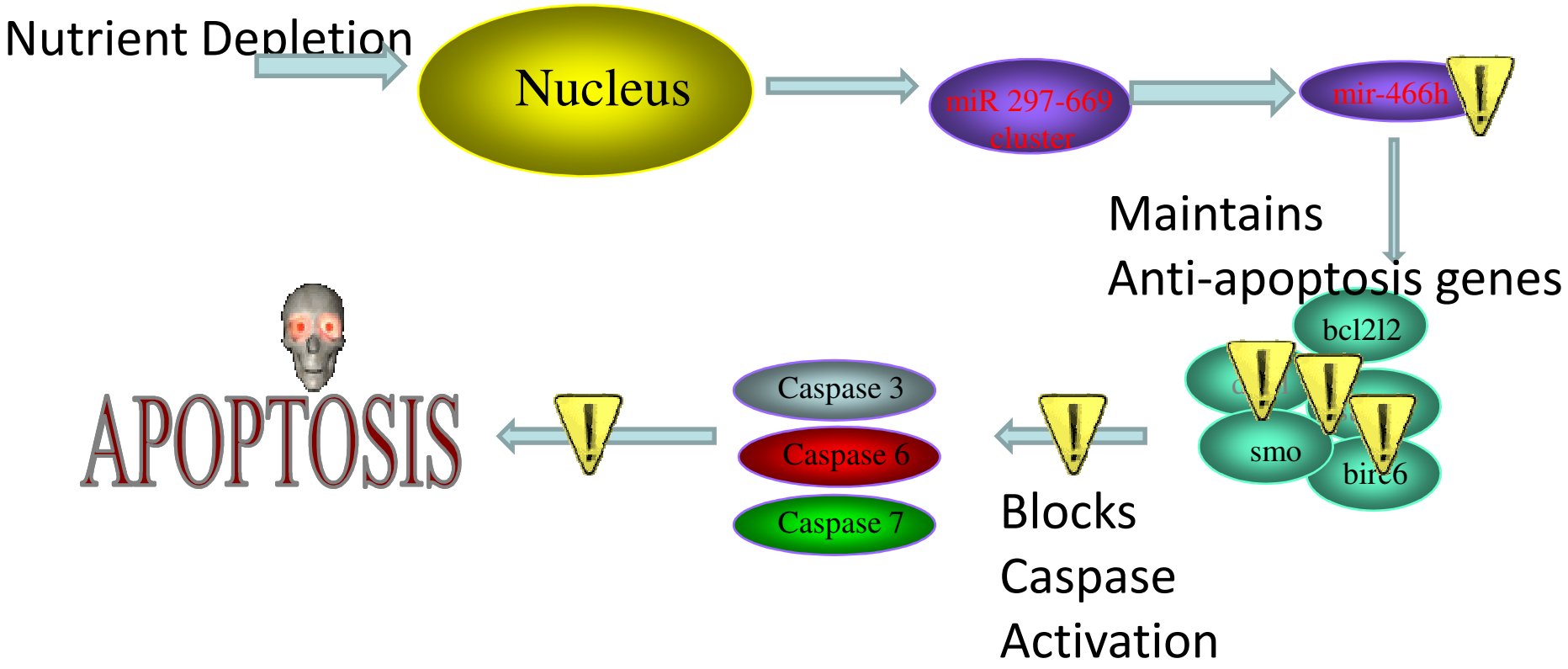

Stress In Algae?

- Photooxidative Stress
  - Intense Light → Photoinhibiton → Reactive Oxygen Species
  - Intense Light + O_2 Build-Up in Closed PBRs → ROS
  - *Reduced Photosynthetic Efficiency*
  - *Is there Cell Damage & Death or even Apoptosis?*

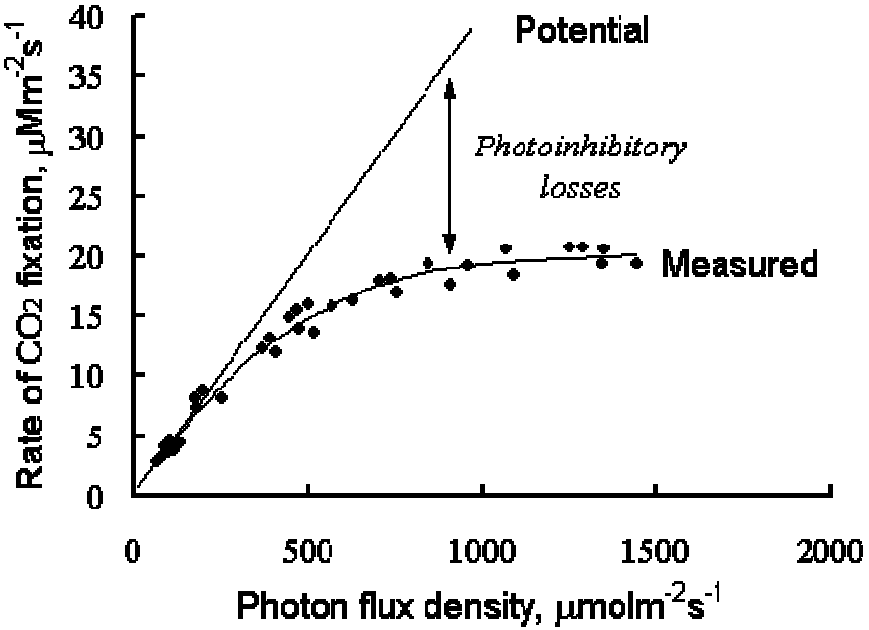

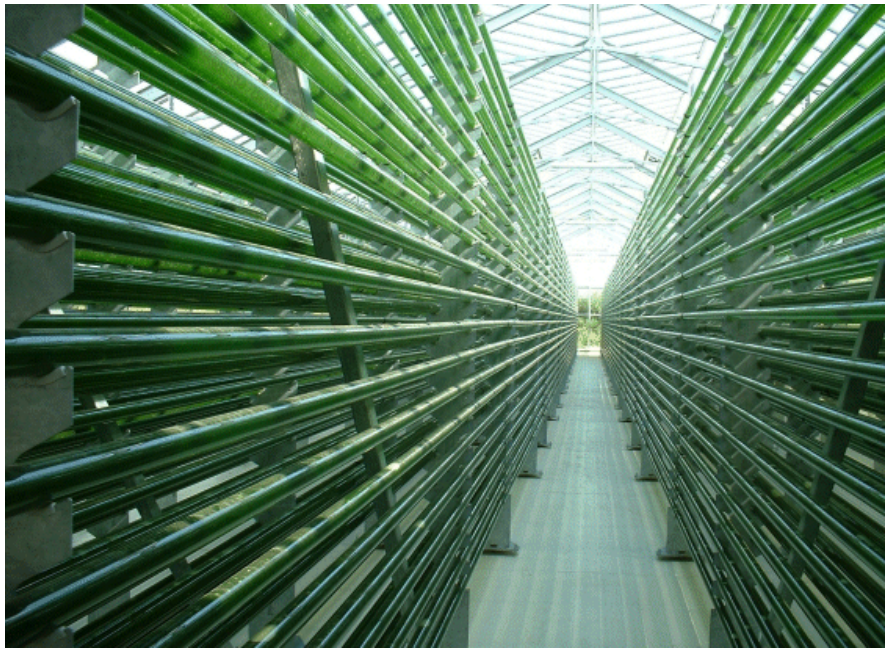

Representative Algae

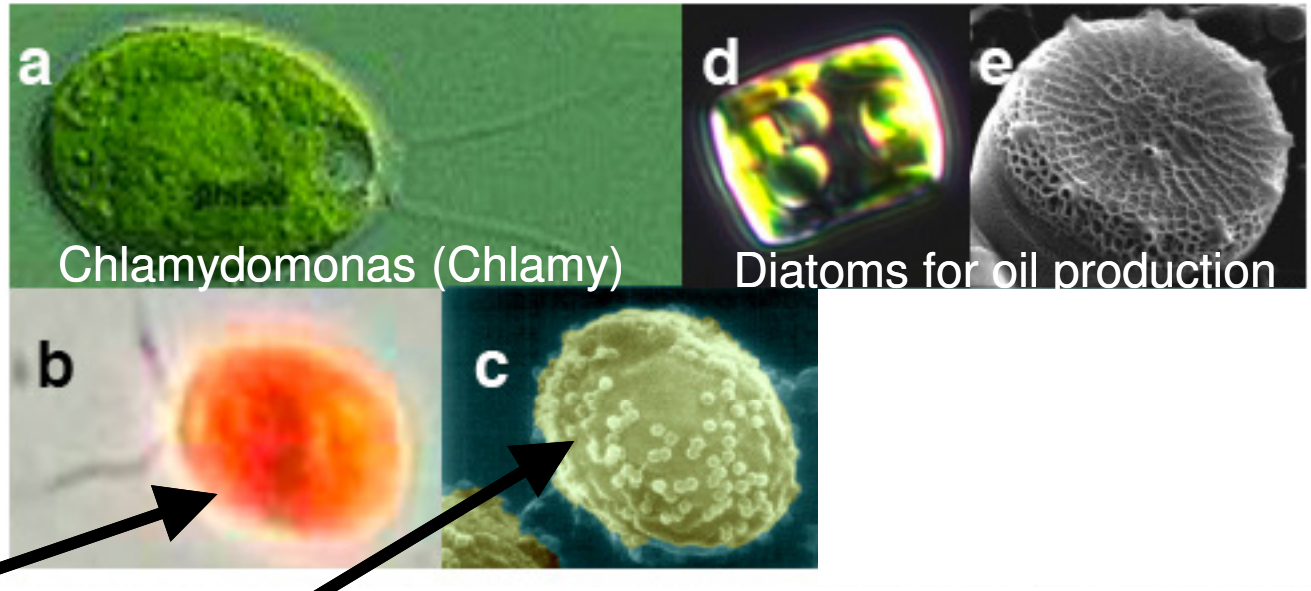

Dunaliella

Chlorella with virus on surface

Examine Algal Response to Model Stress Insult

Camptothecin-Model Insult for DNA damag

In Chlamydomona reinhardtii

- Camptothecin binds to Topoisomerise I and prevents DNA re-ligation
  - Creates 'nicks' in DNA resulting in permanent DNA damage and subsequent apoptosis
- Wanted to test whether pRelax would rescue cells from undergoing apoptosis upon Camptothecin treatment
- Hoescht Nuclear Staining
  - DNA fragmentation
- Guava Viacount viability

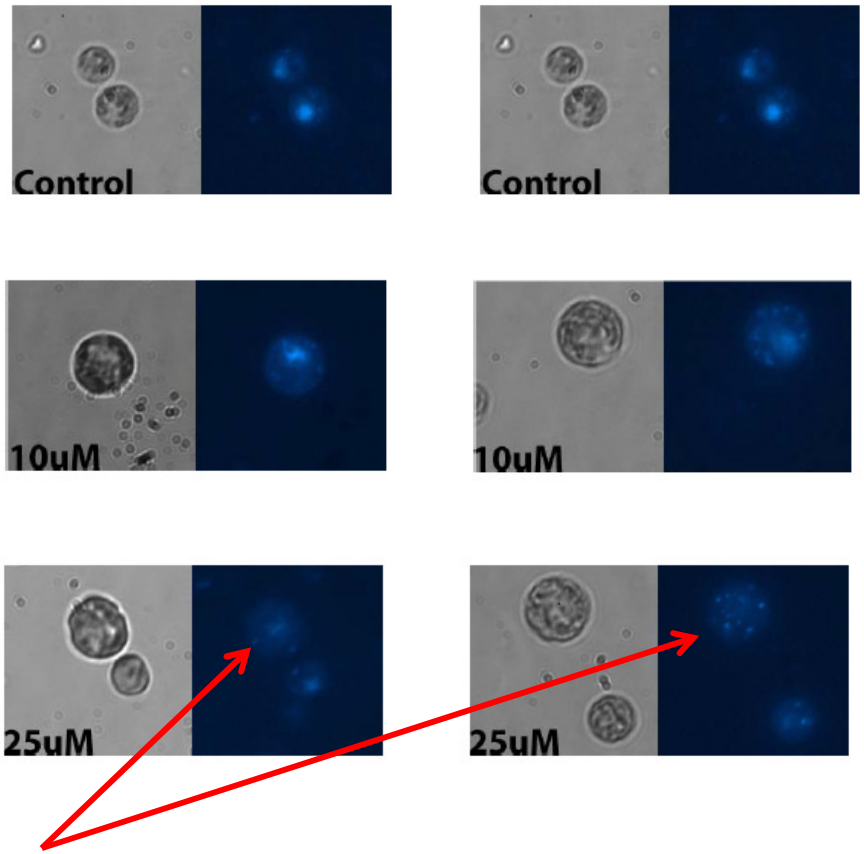

DNA fragmentation in Algae ?

Effect of other Environmental Stresses

Other stress imposition on wild-type (UTEX 2244) Chlamy

NaCl

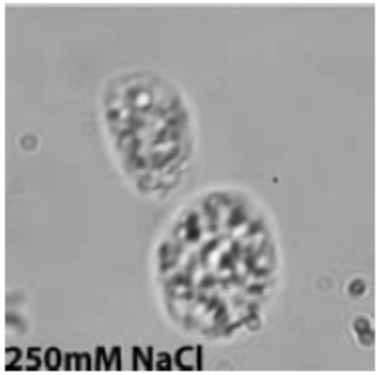

UV

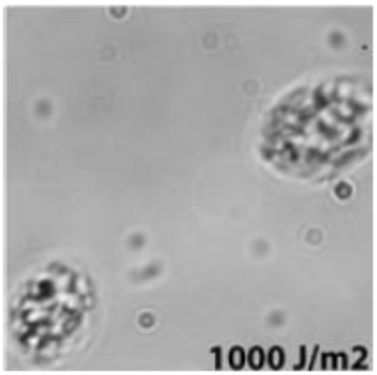

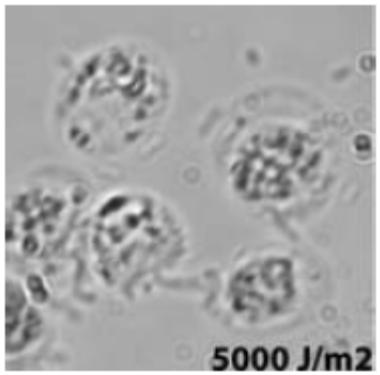

C.Reinhardtii after 3 days of stress

Other Stresses Reduce Cell Survival

Abiotic stress imposition on wild-type (UTEX 2244) C.reinhardtii

- 200mM NaCl, 300mM NaCl, 42°C Heat Shock (2h)

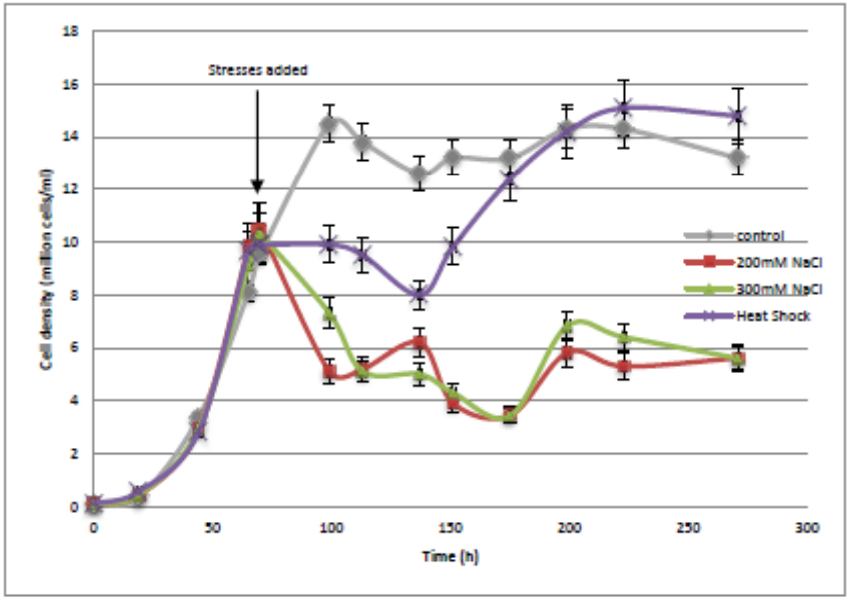

Figure 32: Wild-type *C.reinhardtii* growth curves - Multiple abiotic stress imposition

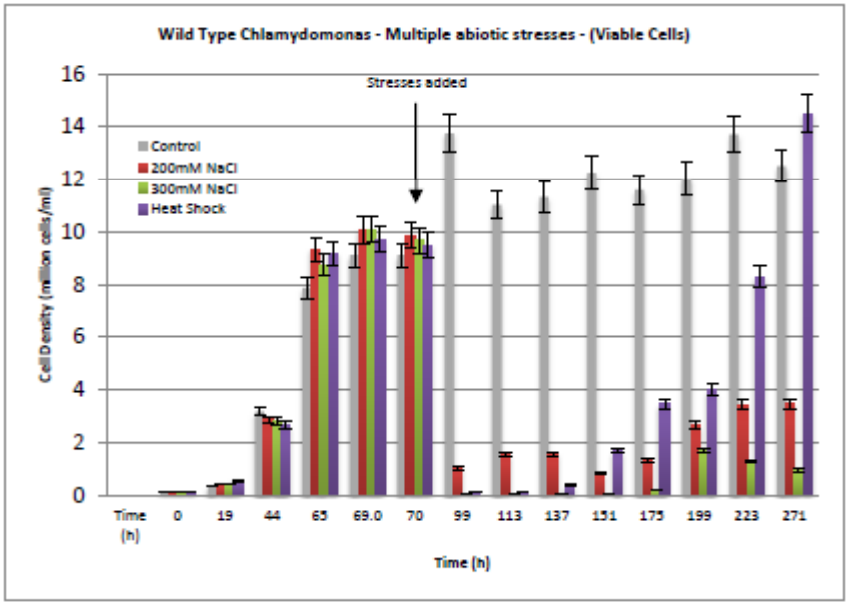

Figure 33: Wild Type Chlamydomonas - Multiple abiotic stresses (viability)

PHOTOOXIDATIVE STRESS TEST

Chlamydamonas
Control

Cell Density
(10^6 cells/ml)

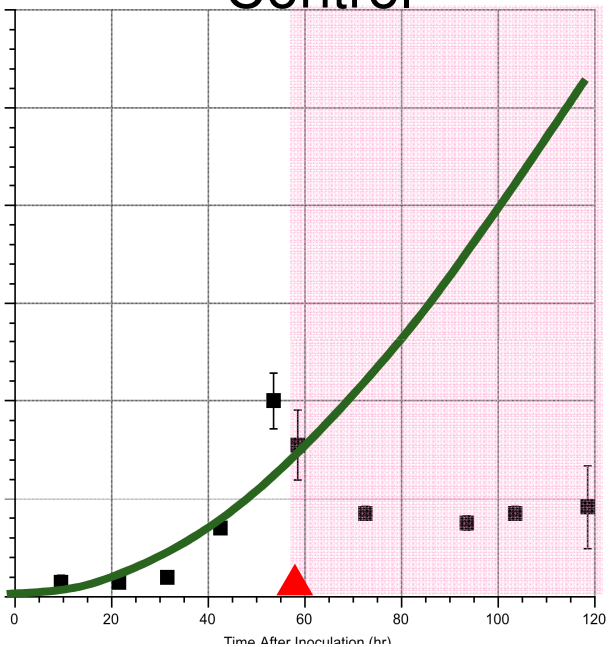

Generation of Reactive Oxygen Species with 2 μM Rose Bengal

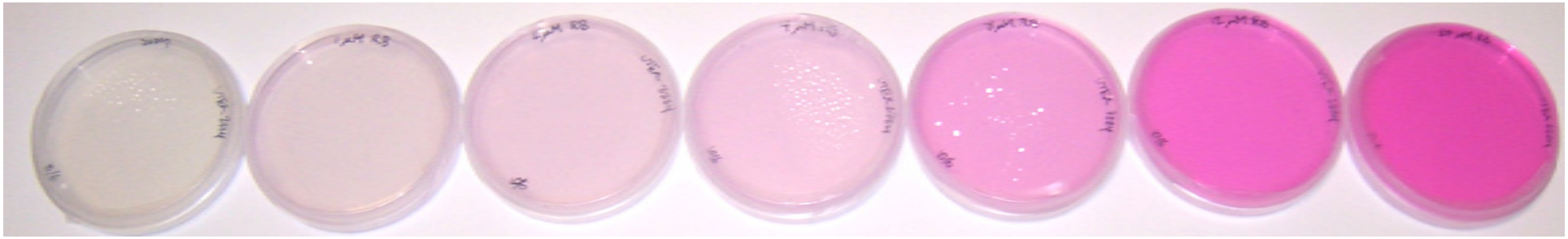

Effect of anti-apoptosis genes: Relative Reduction in growth rate

Abiotic stress imposition on pBcl-x transformants (UTEX 2244) to determine tolerance

- **NaCl:** 50mM, 75mM, 100mM, 150mM, 250mM

Wild-Type

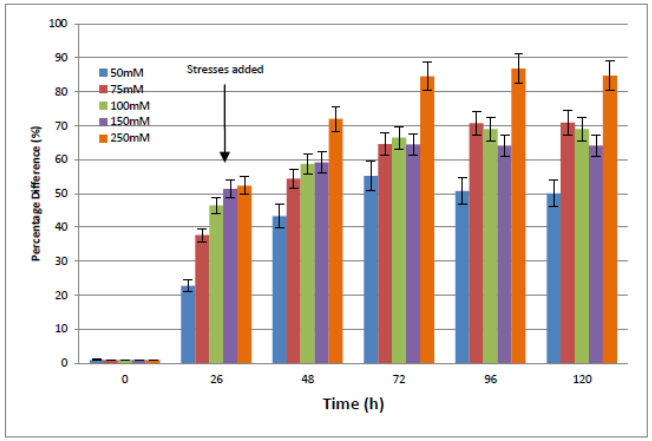

Figure 38: Wild-type cell density difference to control (%) of NaCl stress curves

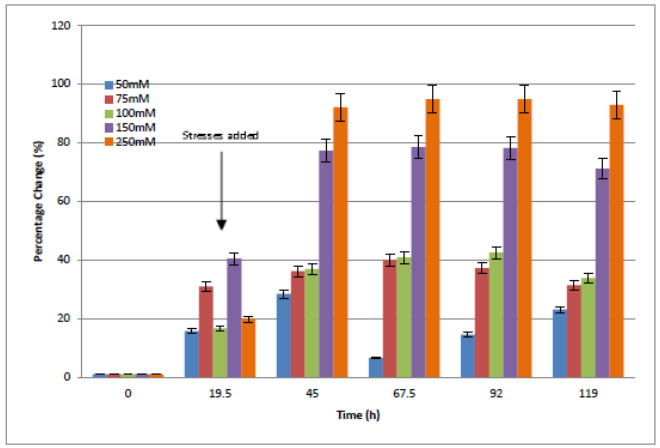

pBcl-x #2

Figure 39: pRelax#2 cell density difference to control (%) of NaCl stress curves

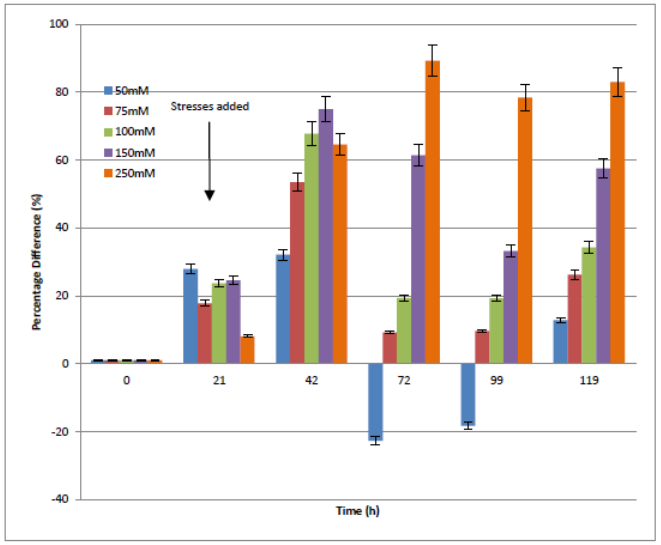

pBcl-x #8

Figure 40: pRelax #8 cell density difference to control (%) of NaCl stress curves

Average growth reductions:

- **WT:** **50.8%**
- **pBcl-x-2:** **31%**
- **pBcl-x-8:** **26.1%**

Effect of anti-apoptosis genes At high salt concentrations

- NaCl range 175mM, 200mM, 225mM, 250mM

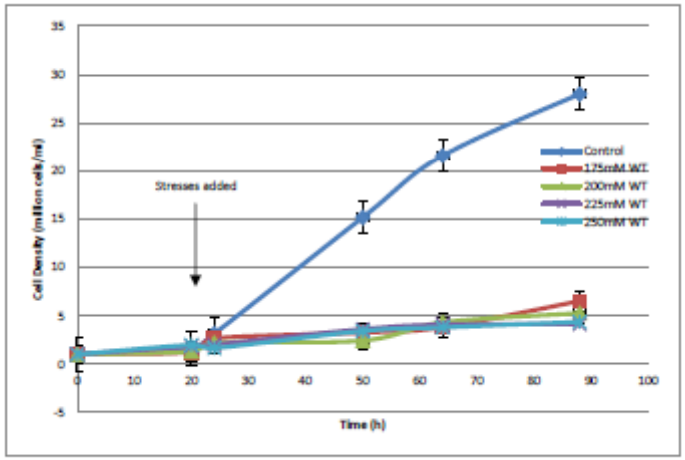

Figure 61: Growth curves of Wild-Type *C.reinhardtii* under High NaCl stress

Wild-Type

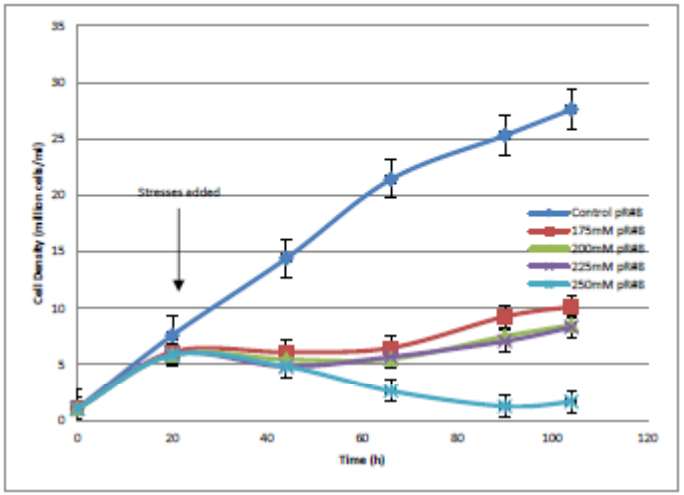

Figure 62: Growth Curves of pRelax#8 under High NaCl Stress

pBcl-x8

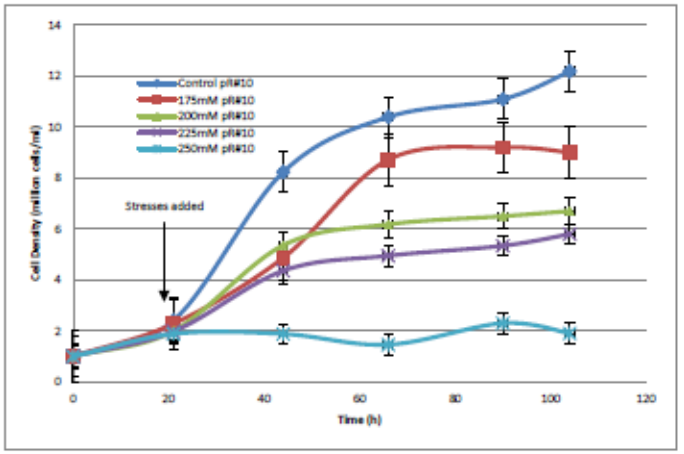

Figure 63: Growth Curves of pRelax#10 under High NaCl Stress

pBcl-x #10

Stress analysis on flow cytometer- Guava?

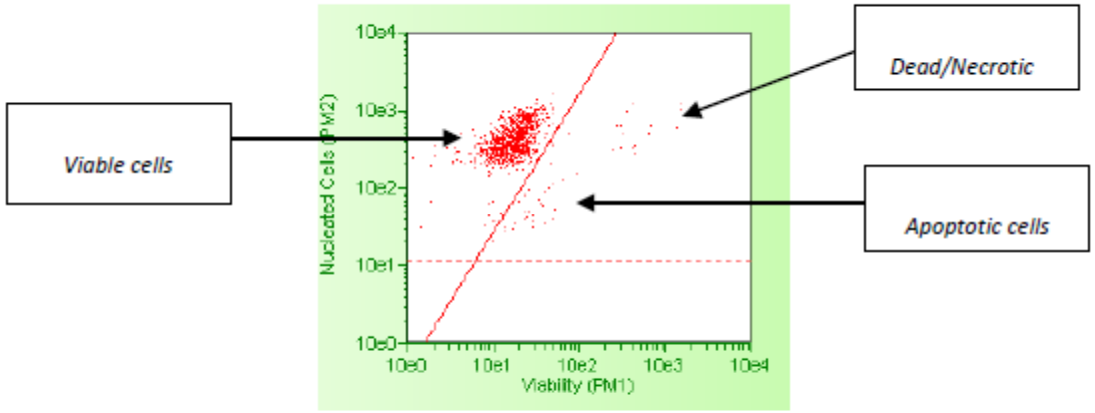

Screenshot from ViaCount software of C.Reinhardtii

Percent viable of wild-type and algae expressing Bcl-x – High NaCl – (Day 3) on flow cytometer (Guava)

Wild-Type **pBclx-#8**

Control

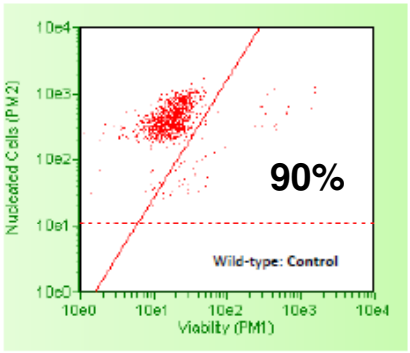

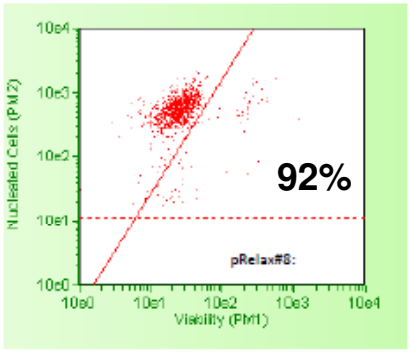

Control

175mM

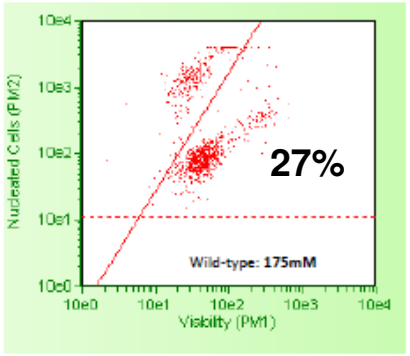

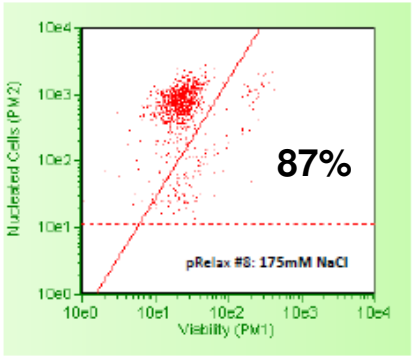

175mM

Percent viable of wild-type and algae expressing Bcl-x – High NaCl – (Day 3) on flow cytometer (Guava)

Wild-Type **pBcl-x #8**

200mM

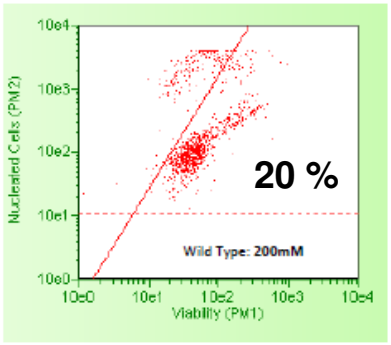

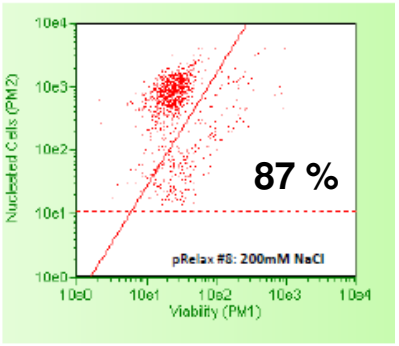

200mM

225mM

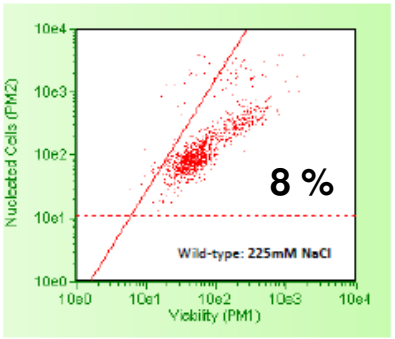

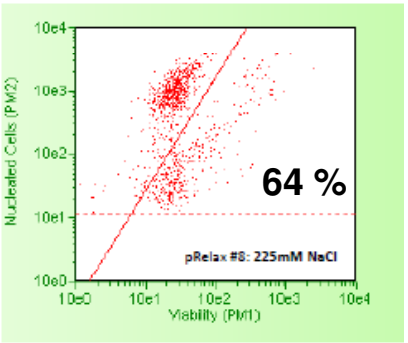

225mM

250mM

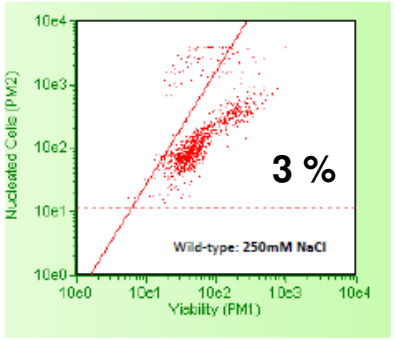

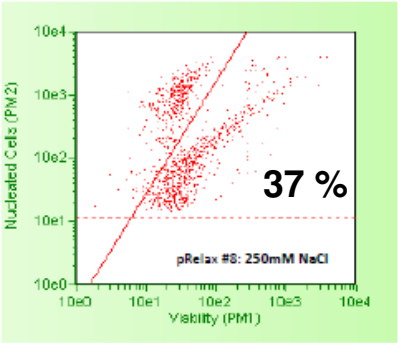

250mM

PHOTOOXIDATIVE STRESS TEST

Chlamydamonas Control

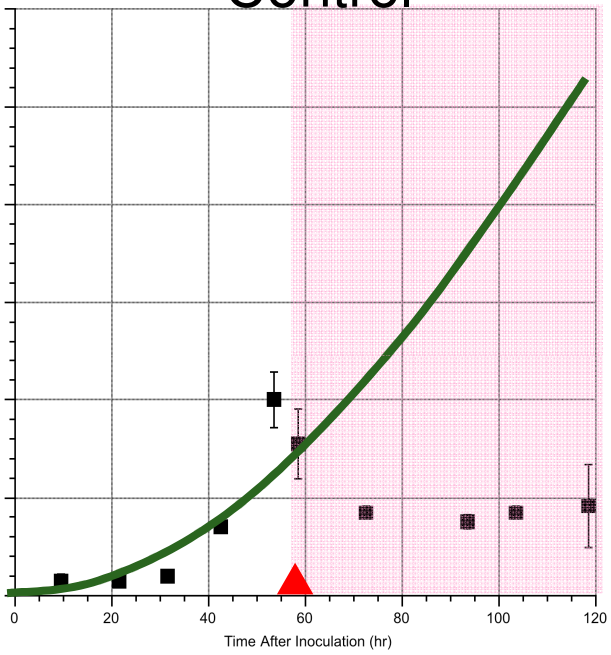

Anti-apoptotic 1

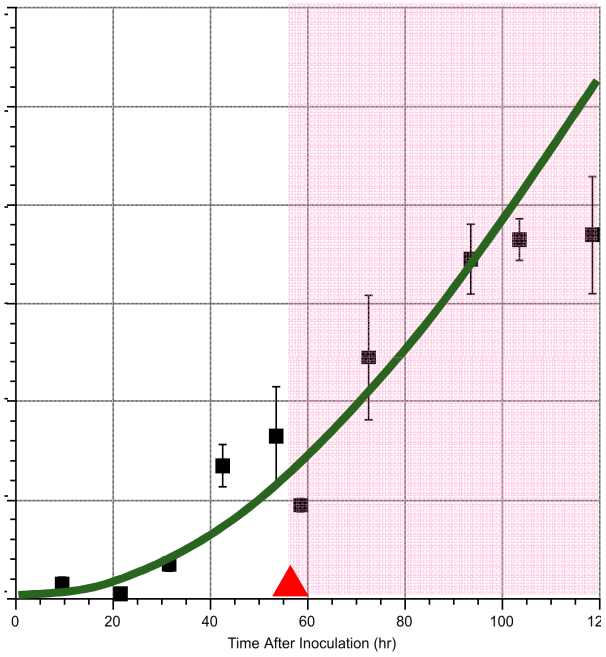

Anti-apoptotic 2

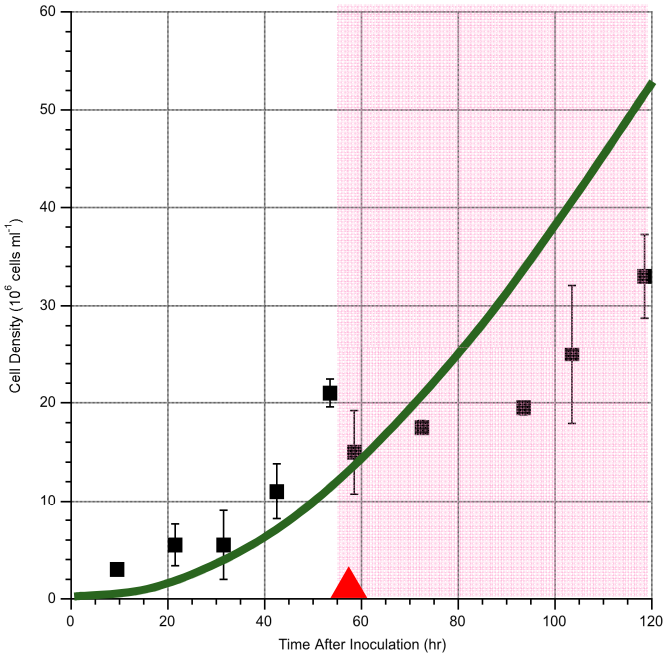

Generation of Reactive Oxygen Species with 2 μM Rose Bengal

Expression of anti-apoptotic gene inhibits algae death by photosensitizing dye Rose Bengal similar to photoxidative stress

Microalgae and Stress Response

- Microalgae appear to respond to different stresses through cell death pathways
  - Salt stress
  - Photooxidative stress
  - UV Stress
- Some of the cell death pathways may be conserved between microalgae and mammalian cell lines
- Anti apoptosis strategies may also be appropriate for some microalgae at least for some stresses
  - Salt Stress
  - Photooxidative Stress
  - Does not work for high UV stresses

Algae Growth in Different Environments

- Photoautotrophic: CO_2 and Light
- Mixotrophic: Carbon Source and CO_2
- Heterotrophic: Carbon Source Alone

Chlorella protothecoides - Autotrophic & Heterotrophic

Collaboration with CSU-Minxi Wan

Mixotrophic and Photoautotrophic growth of algae species

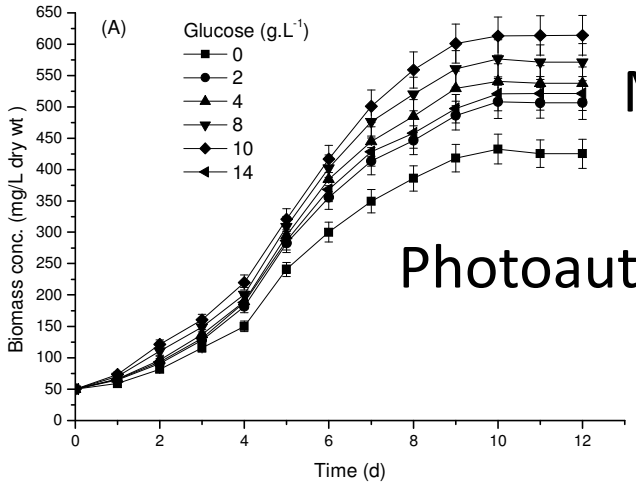

Mixotrophic

Photoautotrophic

Nannochloropsis oculata
HQW03

Mixotrophic

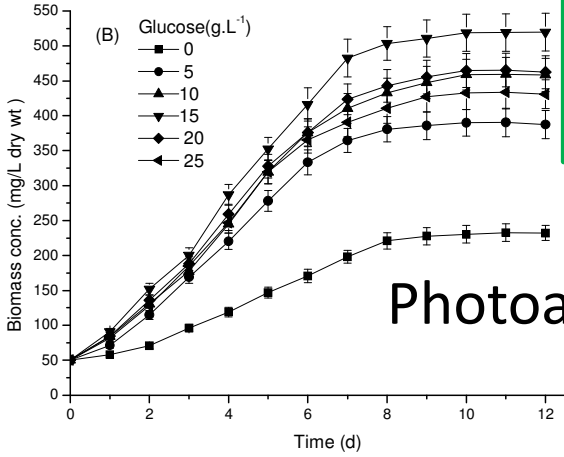

Photoautotrophic

Dunaliella salina
HQW04

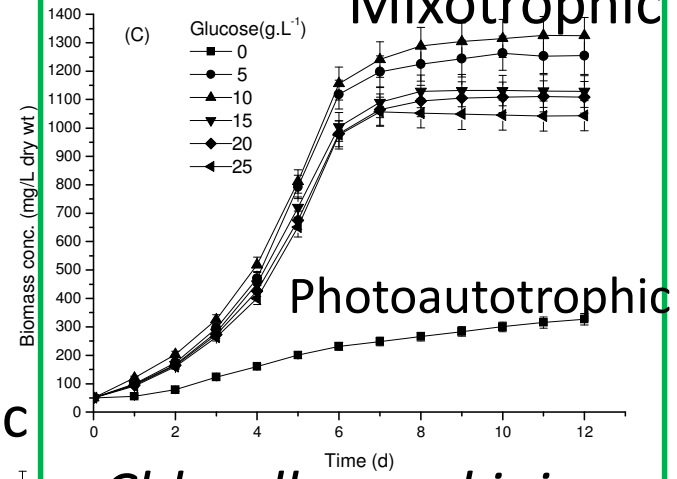

Mixotrophic

Photoautotrophic

Chlorella sorokiniana
CS-01

Effect of nitrogen source and carbon source during heterotrophic growth

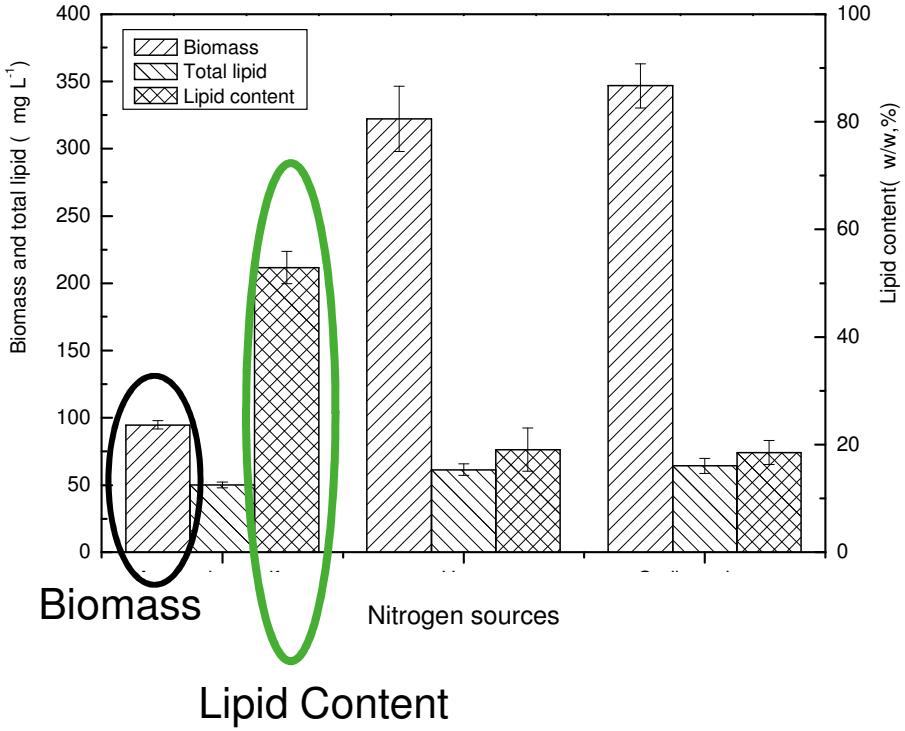

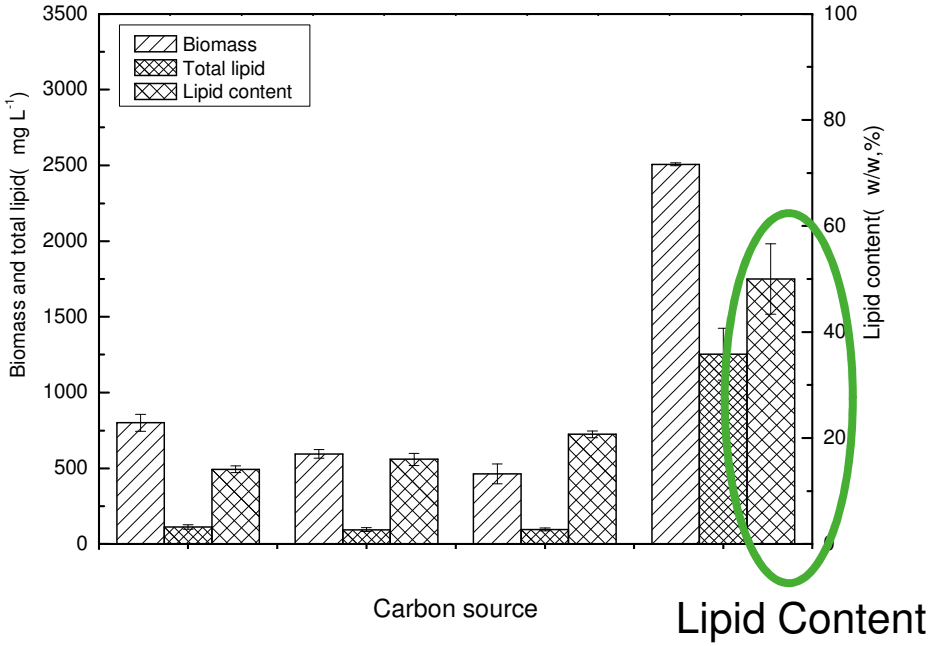

The nitrogen and carbon source can alter the biomass/lipid content

Substrate growth inhibition of *Chlorella sorokiniana* in mixotrophy

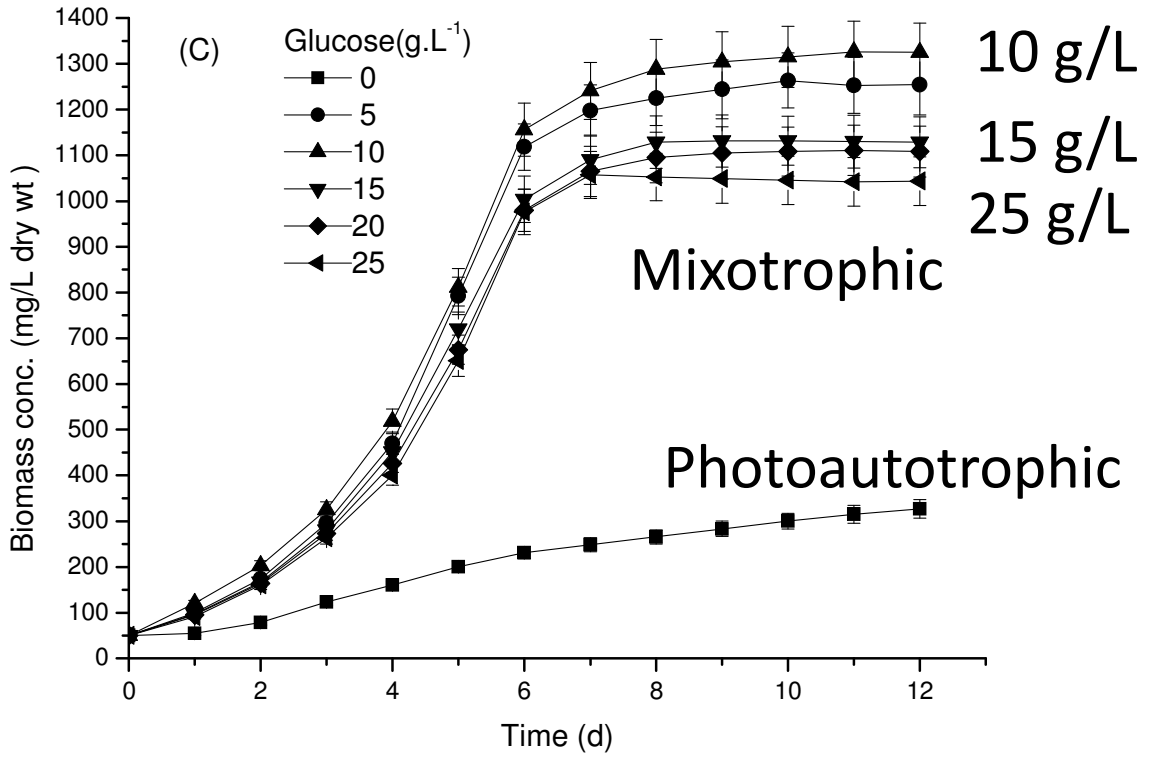

Lipid and Protein Content under Mixotrophic Conditions

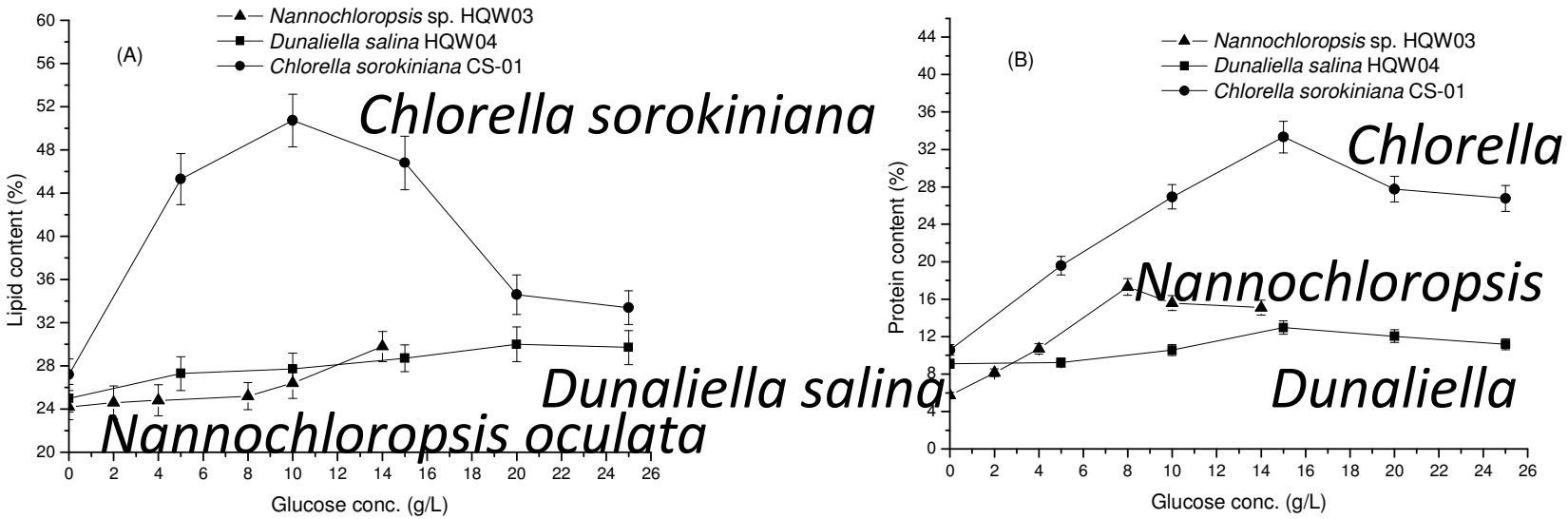

Chlorella exhibits a lipid maximum under mixotrophic conditions

Comparison of Chlorella Lipid Content in Logarithmic and Stationary Phase

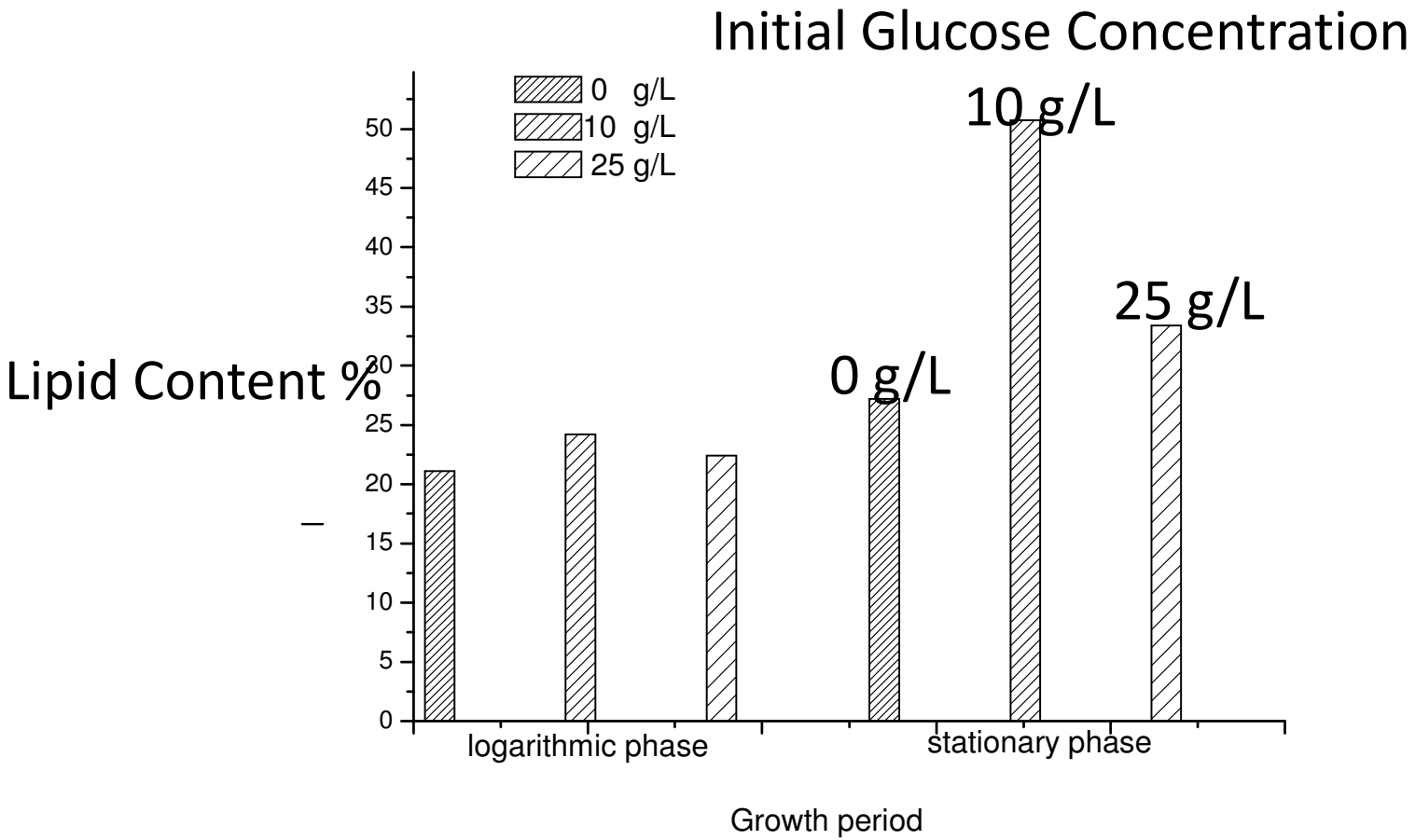

Lipid content increases from log to stationary phase

Change in Chlorella Gene Expression Photoautotrophy vs. Mixotrophy

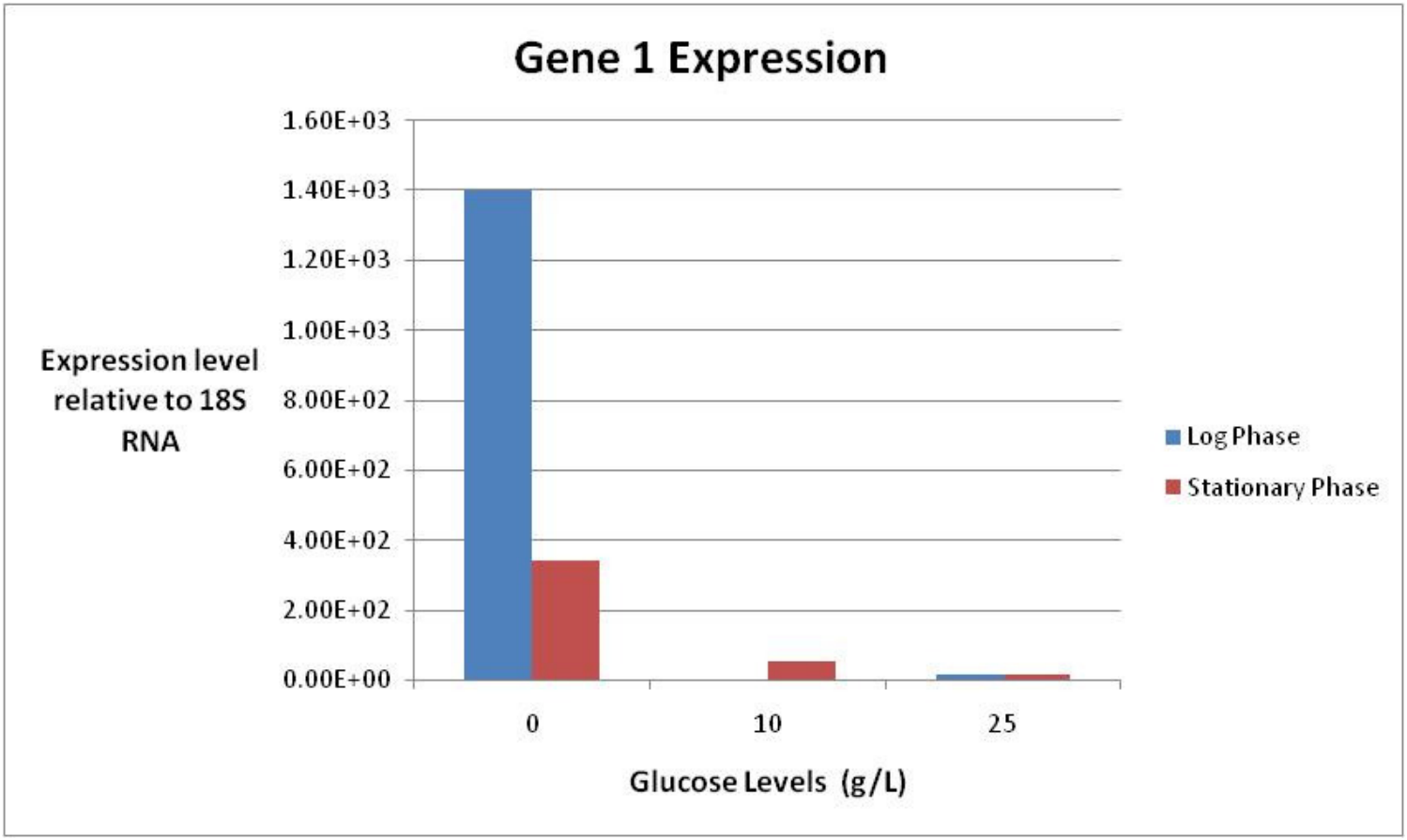

Gene 1 expression decreases from photoautotrophic to mixotrophy

Change in Chlorella Gene 3 Expression in Logarithmic and Stationary Phases

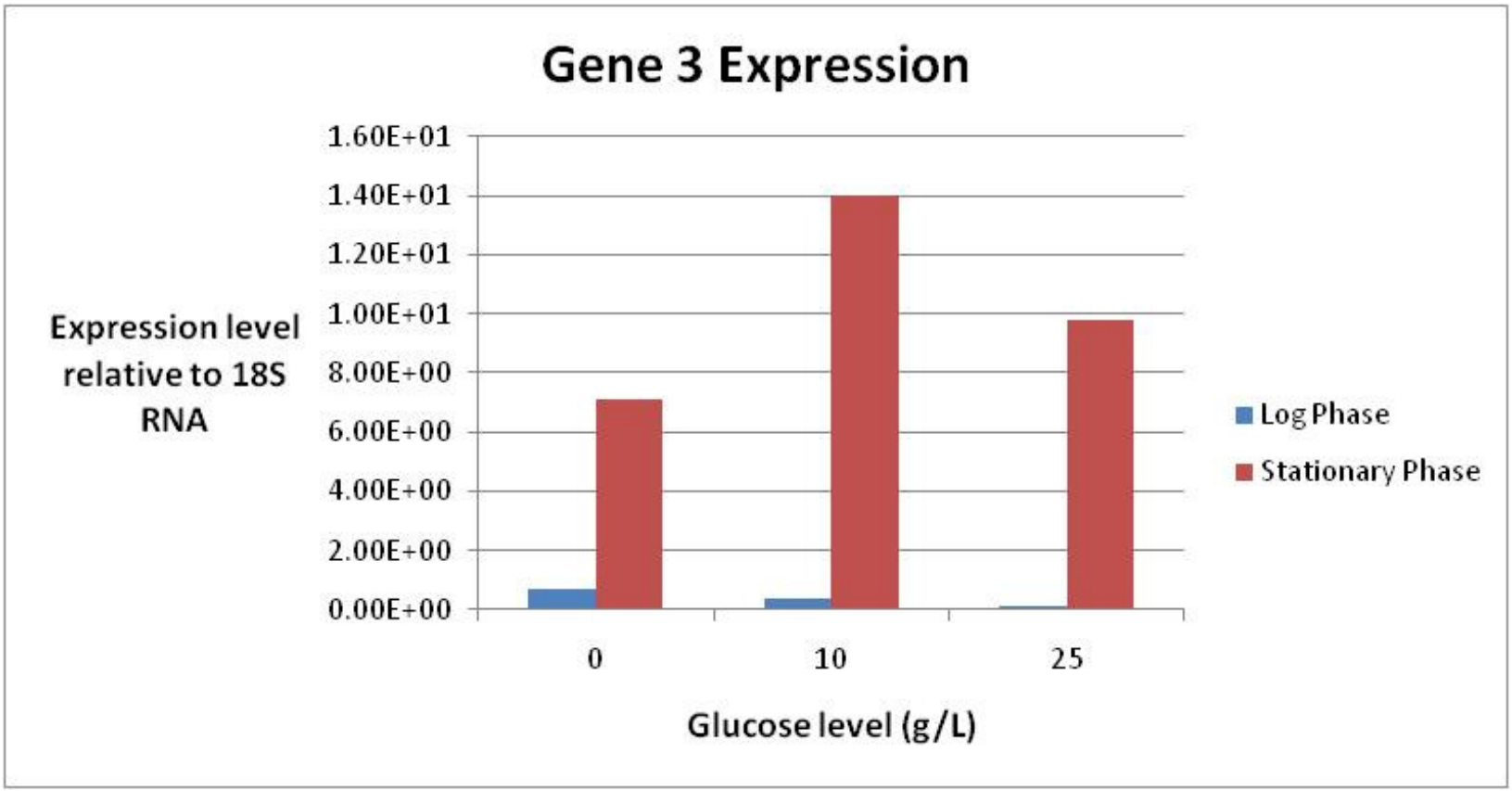

Gene 3 expression increases from logarithmic to stationary phase

CONCLUSIONS

- Metabolic Engineering has been used to improve cell performance
  - Improving Product Quality through Changes in Glycosylation Patterns
  - Improving Yields of Cells and Target Biotherapeutics

- Genomics and other ‘omics tools will be an integral part of metabolic engineering
  - CHO genome has yielded information on potential Met. Eng. targets
  - MicroRNA is an emerging genomic control tool that can alter expression of multiple factors including anti-apoptosis genes simultaneously.

- Cell Engineering of Bcl-x_L Protects both Mammalian Cells and Microalgae from a Variety of Stresses that may be found in Bioreactor Environments

Other Glycosylation Observations:
NO Bisecting GlcNAc to Blocks Fucose

ß4 GlcNAc from GnTIII:

No observed bisecting (ß4) N-acetylglucosamine (found on 10% of human IgG glycoforms)

GnTIII observed in genome, but not transcriptome

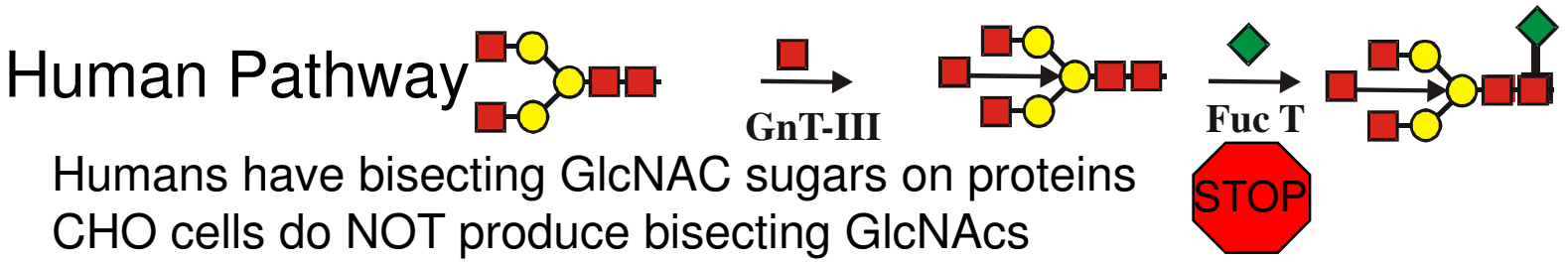

Humans have bisecting GlcNAC sugars on proteins
CHO cells do NOT produce bisecting GlcNAcs
10% of human antibodies include bisecting GlcNAcs

Biological Function?
-Bisecting GlcNAc will inhibit the binding of fucose
-Absence of fucose will increase the antibody-delivered cytotoxicity
-Antibodies from CHO cells will be LESS active in humans (have fucose)
-Antibodies from Humans will be more active (less fucose)

Targets of mmu-mir-466h

Mouse gene symbol	mmu-miR-466h binding site(s) in mRNA 3'-UTR	Anti-apoptotic role of targeted gene
bcl2l2	GCACAC TGCACA	Inhibits formation of permeability transition pore and release of cytochrome C by binding to bax
birc6	GCACA	Inhibits apoptosome by binding to active-site pocket of Caspase-9. Functions as E2 ubiquitin conjugase for Caspase-9 and Smac/Diablo.
dad1	2 of TGCACA	Component of N-oligosaccharyl transferase catalyzing transfer of oligosaccharide from lipid-linked donor to nascent polypeptide chain. Loss of dad1 triggers apoptosis
smo	TGCACAC GCACAC	Uninhibits gli-1 transcriptional factor which stimulates up-regulation of bcl2
stat5a	GCACAC	Stat5a dimers are transcriptional factors for *bcl-x*$_L$ and *bcl2* genes

Five anti-apoptotic genes :

stat5a, bcl2l2, birc6, dad1, smo

What factors cause can cell death in mammalian bioreactors?

- Nutrient limitations
- Oxygen limitation
- Toxin accumulation
- Virus infection
- Hydrodynamic Stress
- Recombinant Protein Expression

Morphological/Physical Changes Associated with Apoptosis

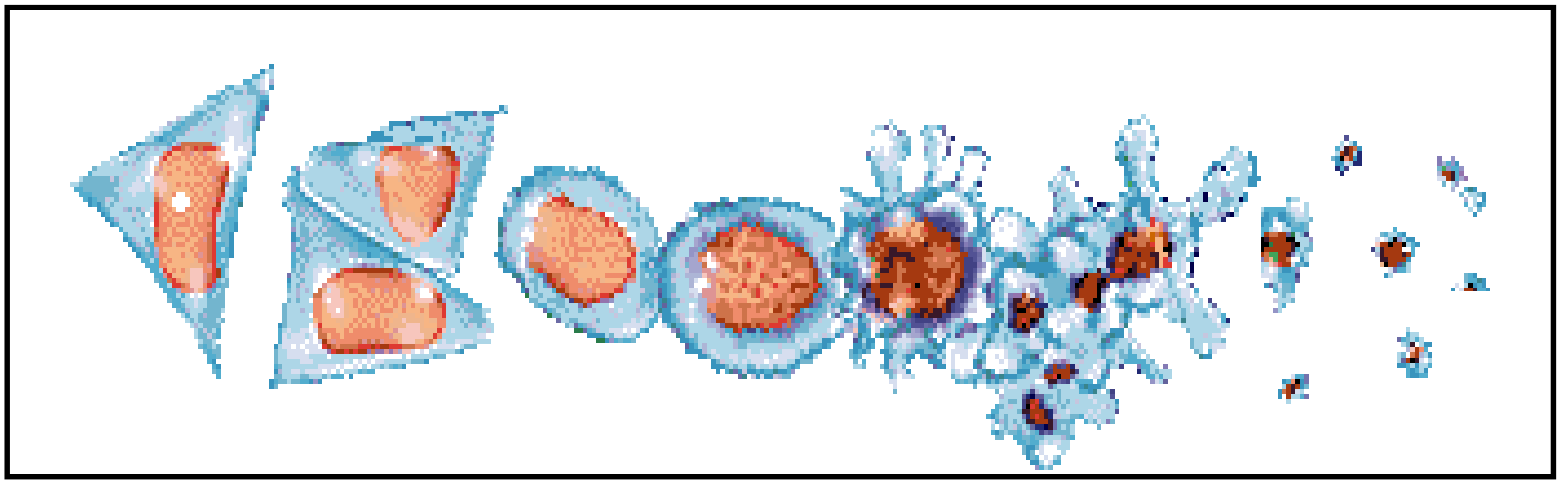

CHO Genome Assembly Strategy

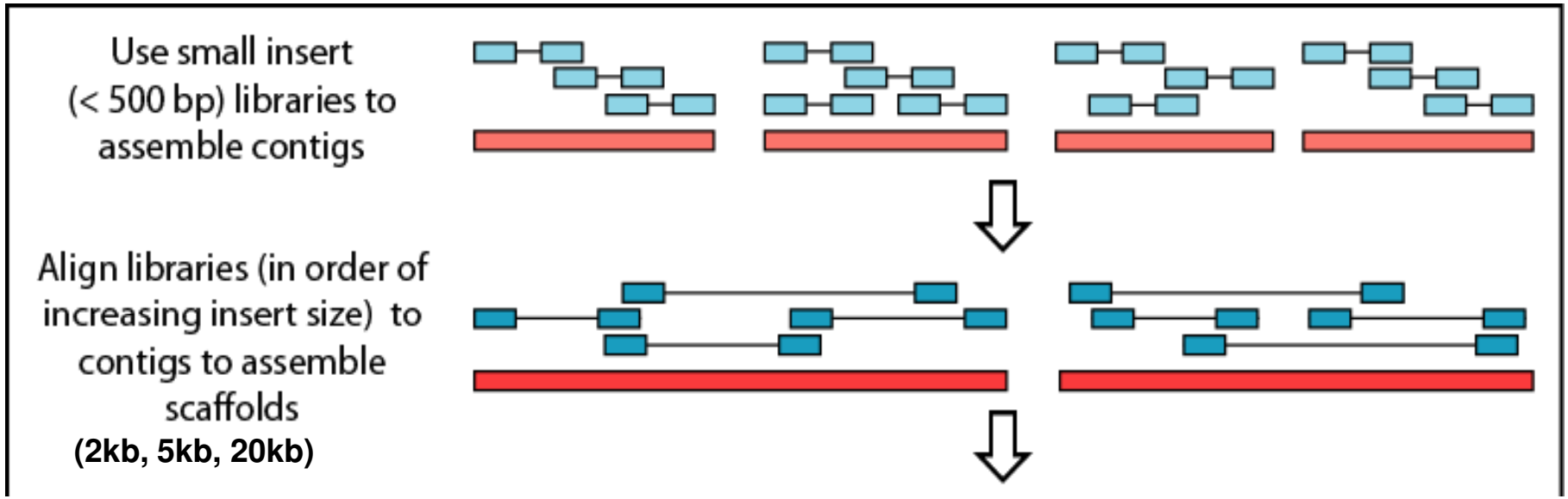

- **CHO-K1 genome assembly**
  - **2.45 Gb of estimated 2.6 Gb genome assembled**

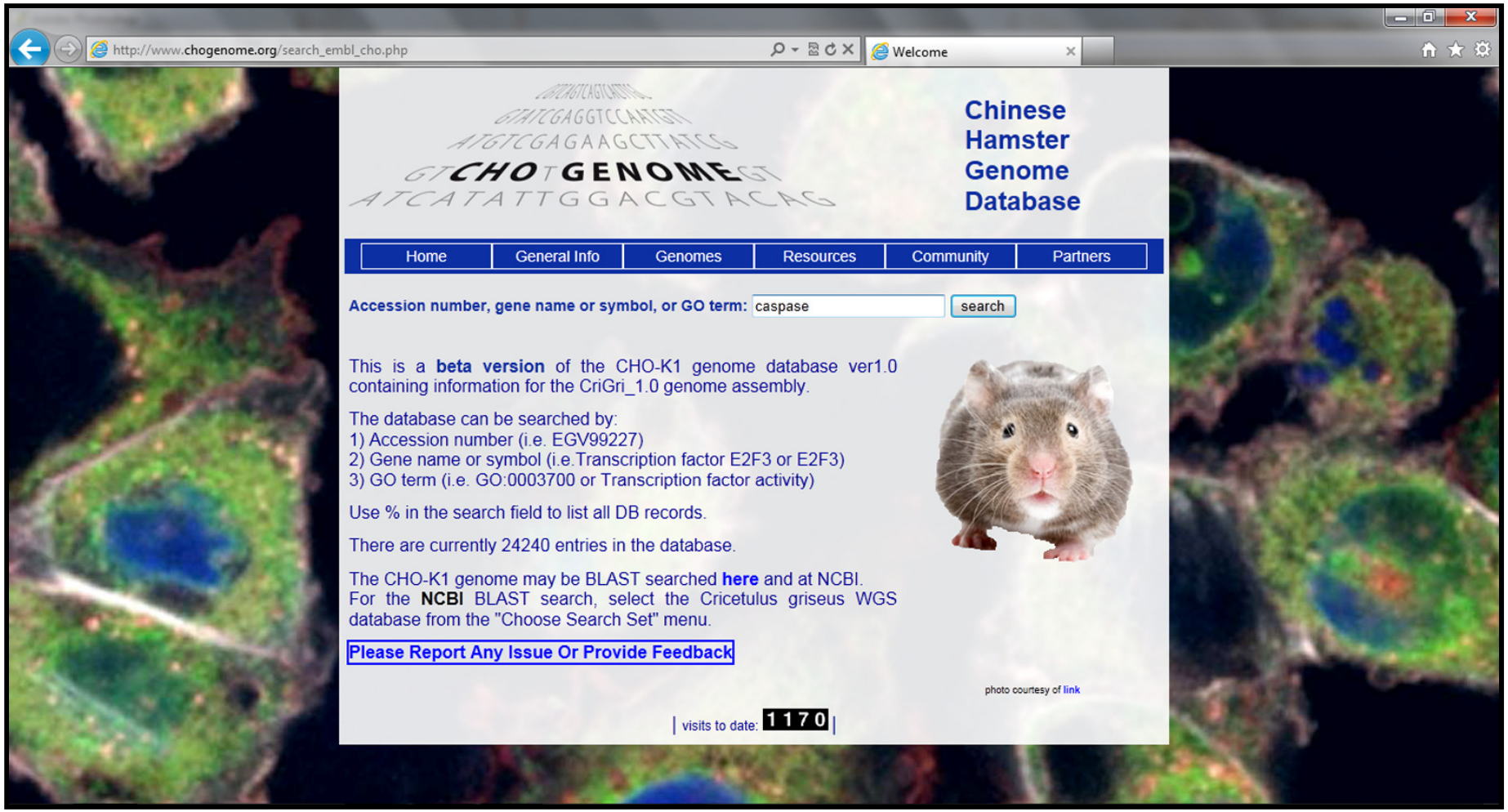
http://www.chogenome.org/search_embl_cho.php
Welcome
CHO GENOME
Chinese Hamster Genome Database
Home
General Info
Genomes
Resources
Community
Partners
Accession number, gene name or symbol, or GO term:
caspase
search
This is a beta version of the CHO-K1 genome database ver1.0 containing information for the CriGri_1.0 genome assembly.
The database can be searched by:
1) Accession number (i.e. EGV99227)
2) Gene name or symbol (i.e.Transcription factor E2F3 or E2F3)
3) GO term (i.e. GO:0003700 or Transcription factor activity)
Use % in the search field to list all DB records.
There are currently 24240 entries in the database.
The CHO-K1 genome may be BLAST searched here and at NCBI.
For the NCBI BLAST search, select the Cricetulus griseus WGS database from the "Choose Search Set" menu.
Please Report Any Issue Or Provide Feedback
photo courtesy of link
visits to date: 1170

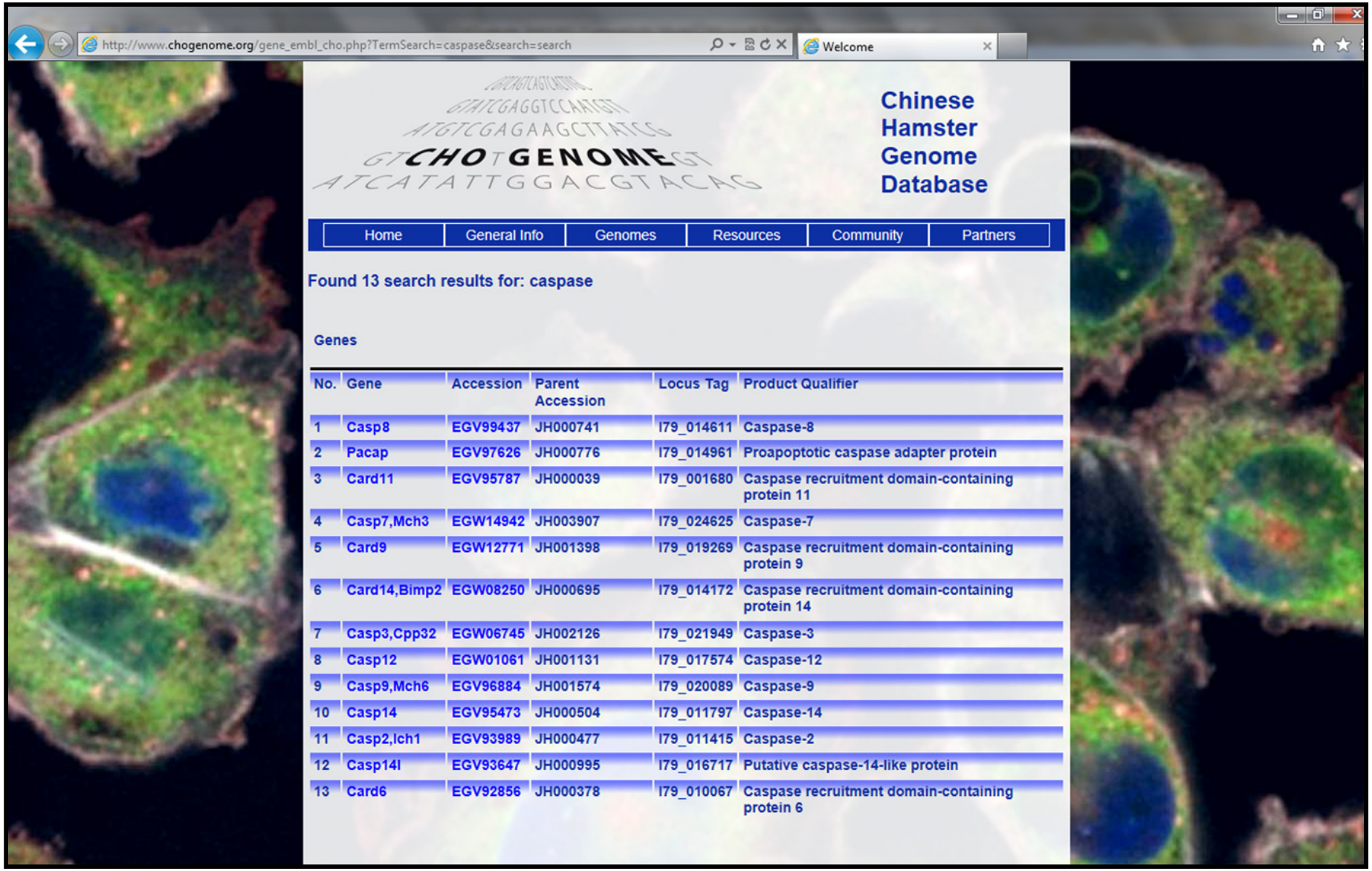

No.	Gene	Accession	Parent Accession	Locus Tag	Product Qualifier
1	Casp8	EGV99437	JH000741	I79_014611	Caspase-8
2	Pacap	EGV97626	JH000776	I79_014961	Proapoptotic caspase adapter protein
3	Card11	EGV95787	JH000039	I79_001680	Caspase recruitment domain-containing protein 11
4	Casp7,Mch3	EGW14942	JH003907	I79_024625	Caspase-7
5	Card9	EGW12771	JH001398	I79_019269	Caspase recruitment domain-containing protein 9
6	Card14,Bimp2	EGW08250	JH000695	I79_014172	Caspase recruitment domain-containing protein 14
7	Casp3,Cpp32	EGW06745	JH002126	I79_021949	Caspase-3
8	Casp12	EGW01061	JH001131	I79_017574	Caspase-12
9	Casp9,Mch6	EGV96884	JH001574	I79_020089	Caspase-9
10	Casp14	EGV95473	JH000504	I79_011797	Caspase-14
11	Casp2,Ich1	EGV93989	JH000477	I79_011415	Caspase-2
12	Casp14l	EGV93647	JH000995	I79_016717	Putative caspase-14-like protein
13	Card6	EGV92856	JH000378	I79_010067	Caspase recruitment domain-containing protein 6

Change in Chlorella Gene 2 Expression Photoauto/Mix and Log/Station

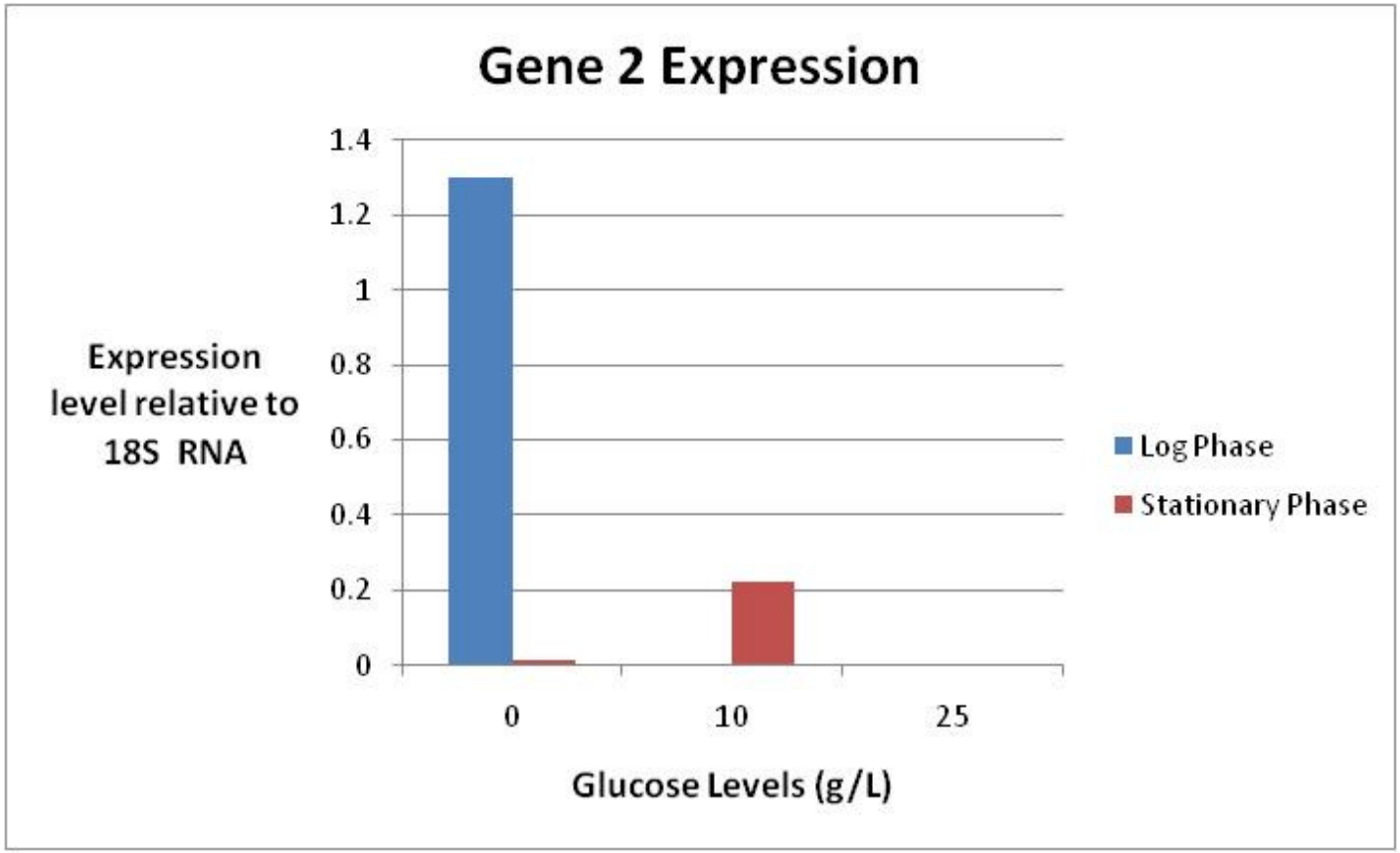

Lack of a consistent trend for Gene 2 expression in stages

CHLORELLA SPECIES GROWTH

***Chlorella sorokiniana* UTEX 1669**

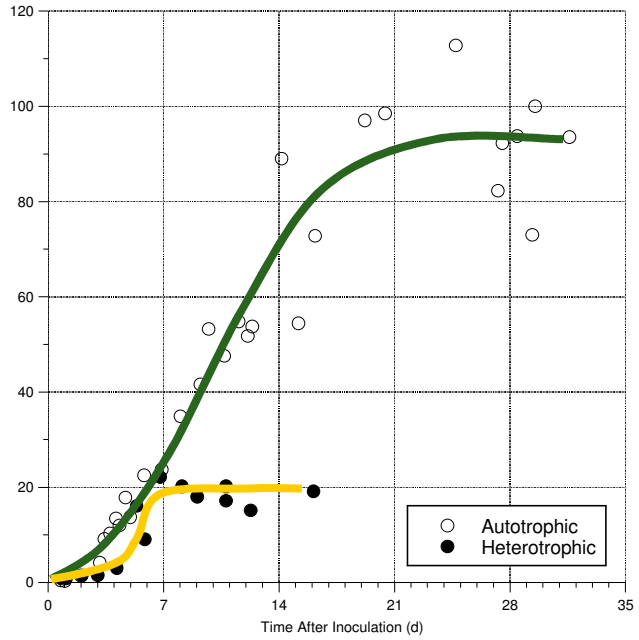

***Chlorella vulgaris* UTEX 265**

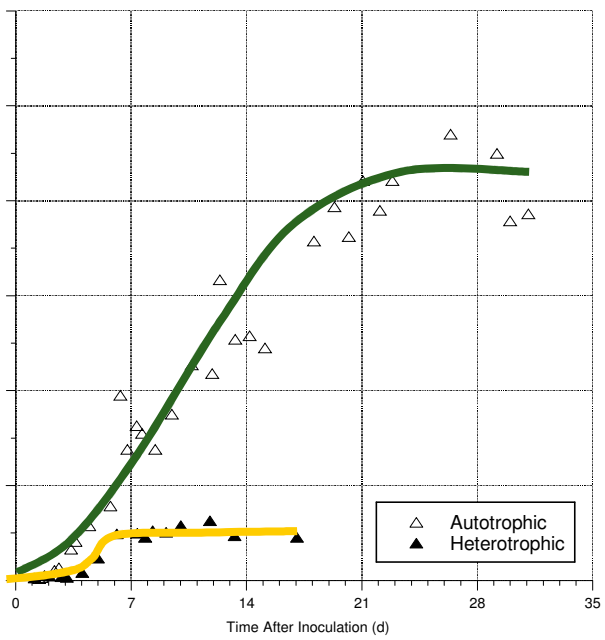

***Chlorella sorokiniana* UTEX 1230**

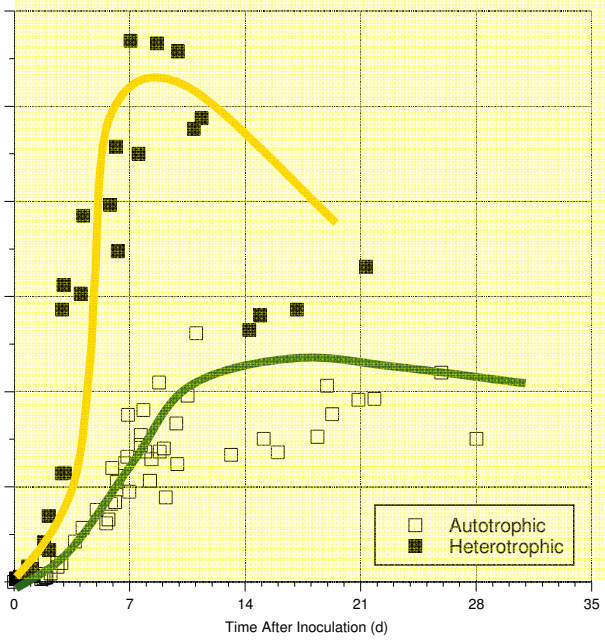

Strain	UTEX 265	UTEX 411	UTEX 1669	UTEX 1230
Species	*C. vulgaris*	*C. protothecoides*	*C. sorokiniana*	*C. sorokiniana*
Specific Growth Rate, *K'* (d^{-1})	0.84 ± 0.09	0.48 ± 0.01	0.77 ± 0.10	1.77 ± 0.04
	0.23 ± 0.01	0.32 ± 0.05	0.19 ± 0.02	0.36 ± 0.05
Doubling Time (hr)	20 ± 2.0	35 ± 1.4	21 ± 2.2	9.2 ± 1.0
	72 ± 3.0	52 ± 3.8	89 ± 2.6	46 ± 3.2
Divisions per Day (d^{-1})	1.2 ± 0.1	0.69 ± 0.04	1.1 ± 0.1	2.6 ± 0.1
	0.33 ± 0.04	0.46 ± 0.07	0.27 ± 0.03	0.52 ± 0.07

Effect of Temperature and pH on heterotrophic growth of Chlorella

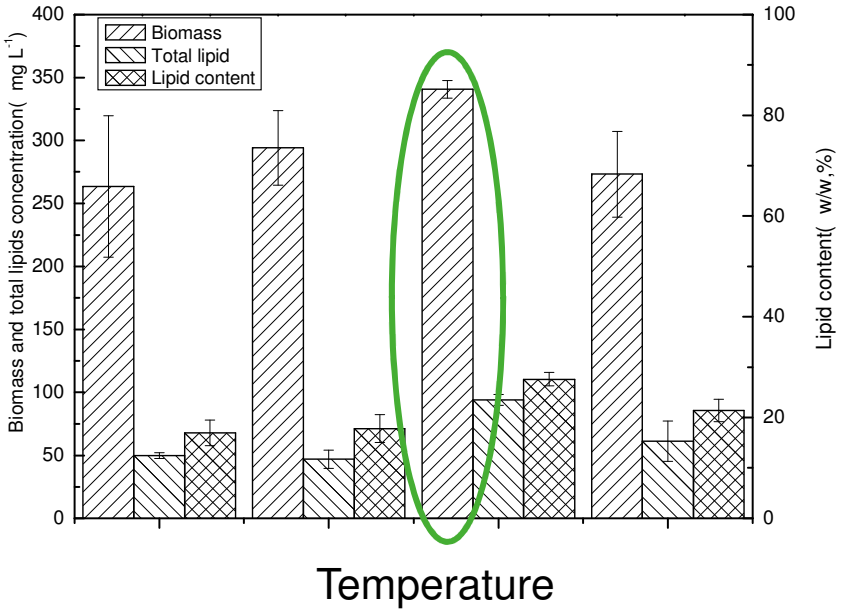

Temperature

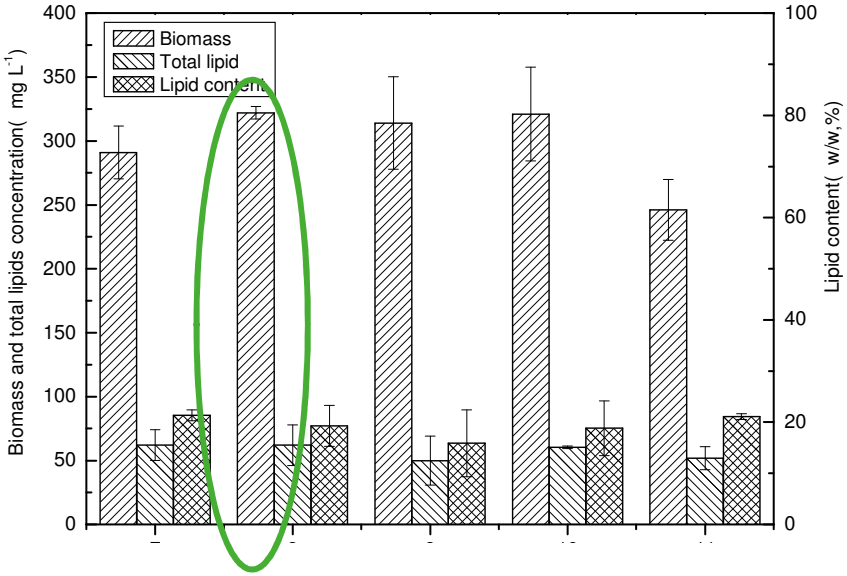

pH

Chlorella exhibits Temperature and pH optimums for biomass

Interpreting Algal Dynamics: Kinetic Model of *C. reinhardtii*

- **15** Pathways were included for a total of:

  320 Biochemical Reactions
  218 Compounds

- **376** kinetic constants were retrieved from the BRENDA enzyme database, while **216** (36% of total) were estimated.
- In addition, **275** turnover numbers were obtained and **45** (14% of total) are estimated.
- Numerical integration was accomplished using an adaptive 4th order Runge-Kutta with adaptive step size (max error 1E-4)

Goncalo Maia and Mariajose Castellanos-University of Maryland, Collaborators

Effect of nitrogen on growth and lipid content during heterotrophic growth

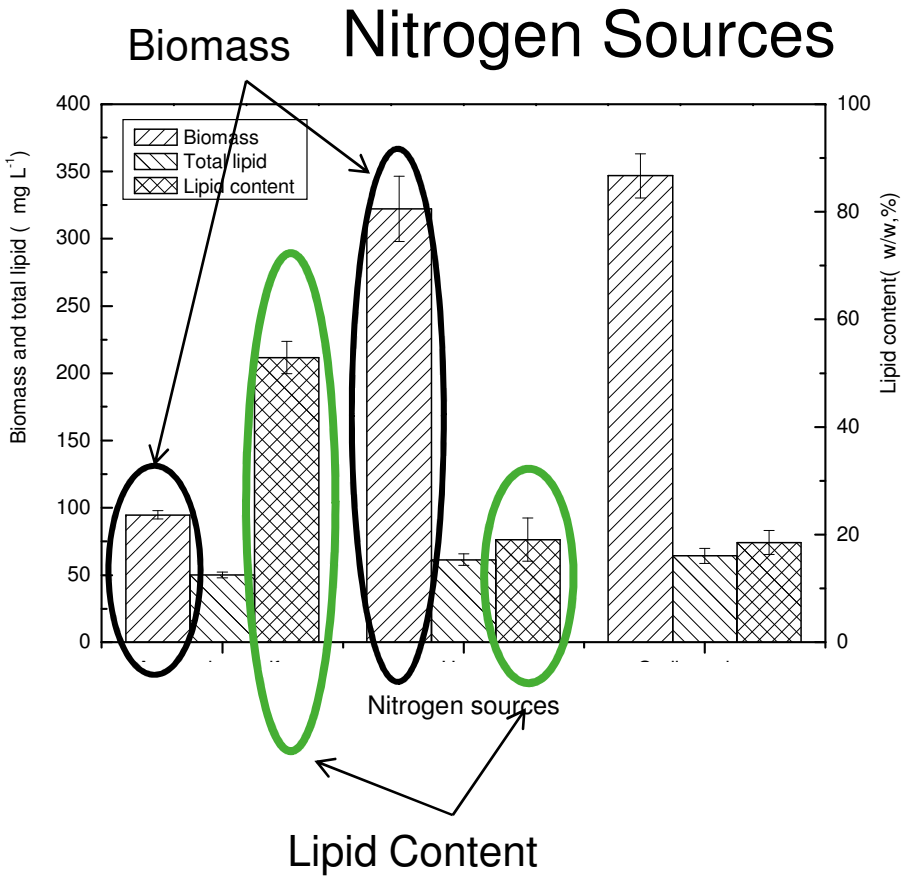

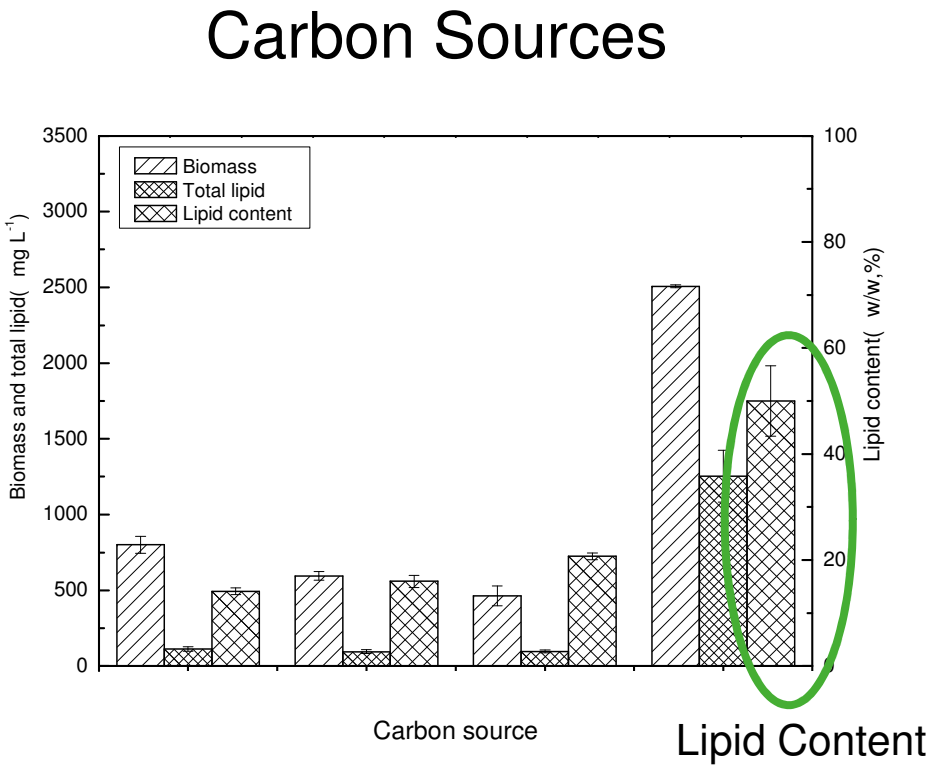

The nitrogen and carbon source can alter the biomass/lipid content

Abiotic stress imposition on pBcl-x transformants (UTEX 2244) to determine tolerance

- **Ultra-Violet:** 1000J,2000J, 3000J, 4000J, 5000J

- No effect of Bcl-xL on protection

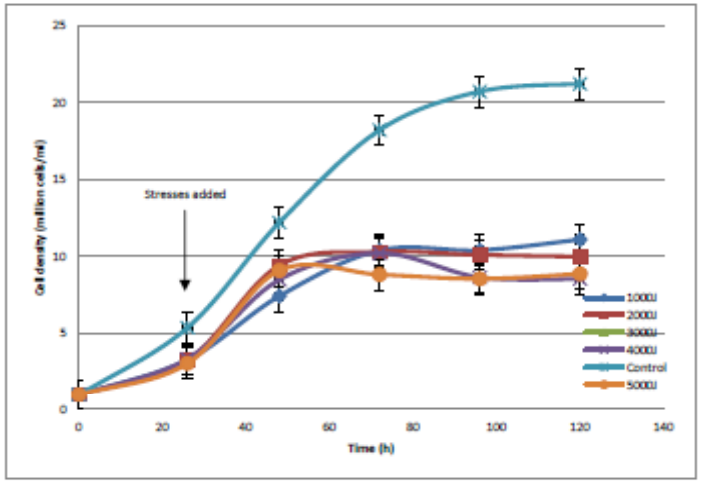

Figure 41: Wild-type *C.reinhardtii* exposed to UV stress (1000J/m² – 5000J/m²)

Wild-Type

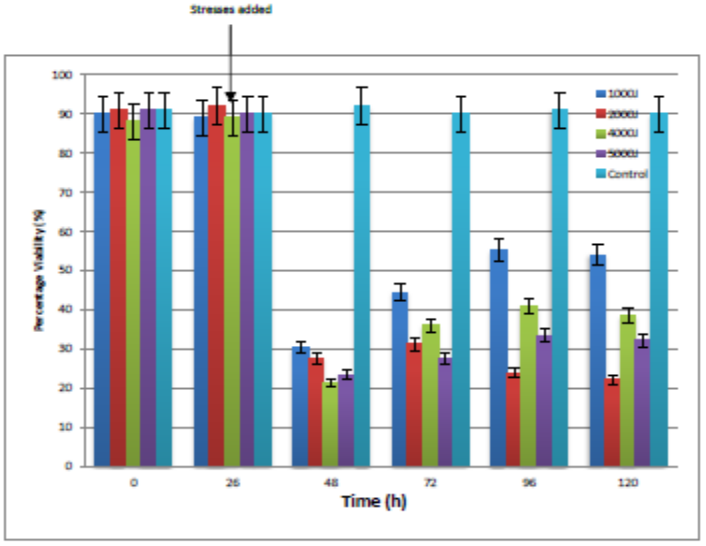

Figure 43: Wild-type UV viabilities over 1000J/m² – 5000J/m² stress range

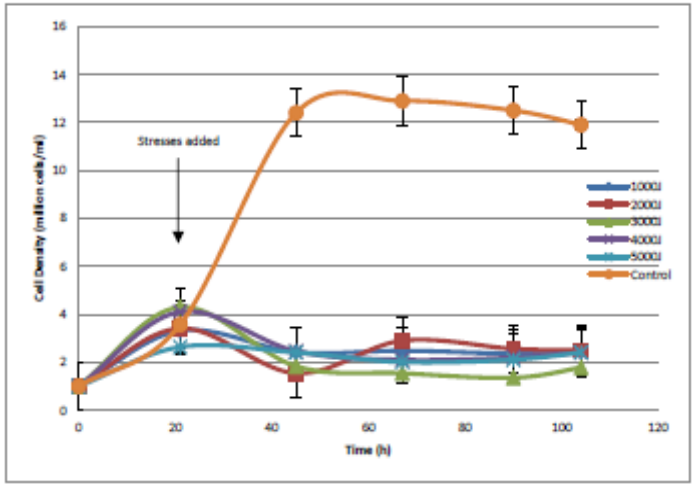

Figure 42: pRelax#8 exposed to UV stress (1000J/m² – 5000J/m²)

pBcl-x

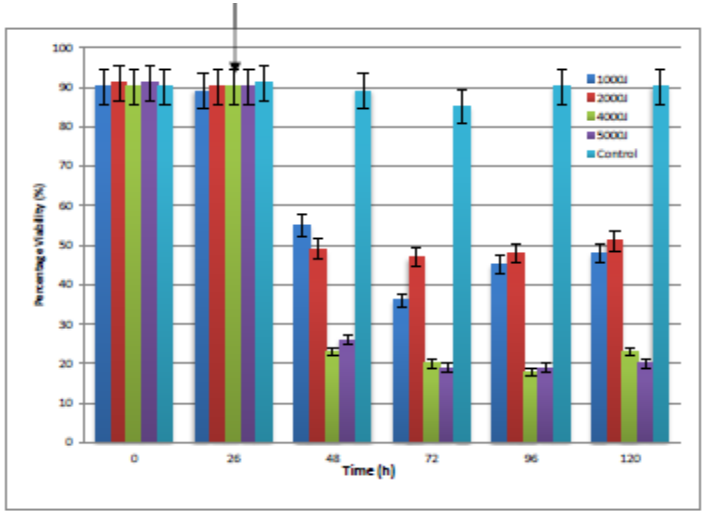

Figure 44: pRelax#8 UV viabilities over 1000J/m² – 5000J/m² stress range

5. Tolerance and Adaptation

Stresses on previously Heat-shocked microalgae *Chlamy*

- Algae are able to adapt to new abiotic stresses after prior shock
- I ex

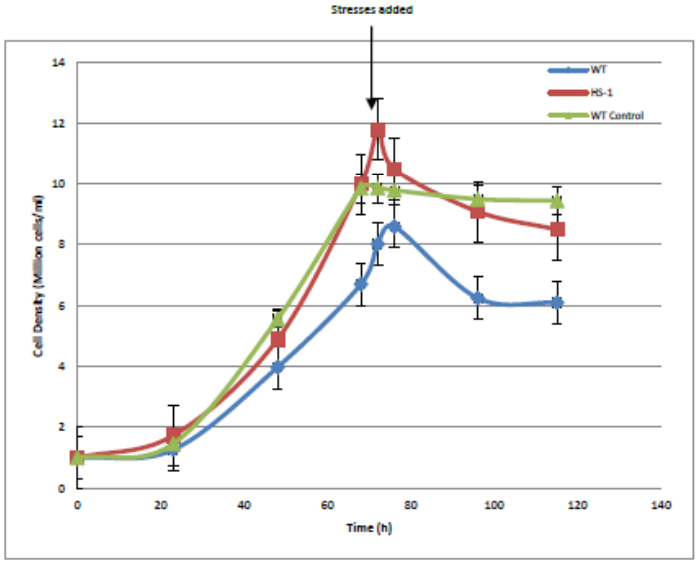

Figure 50: Wild-Type and previously heat shocked cells (HS-1) exposed to 200mM NaCl

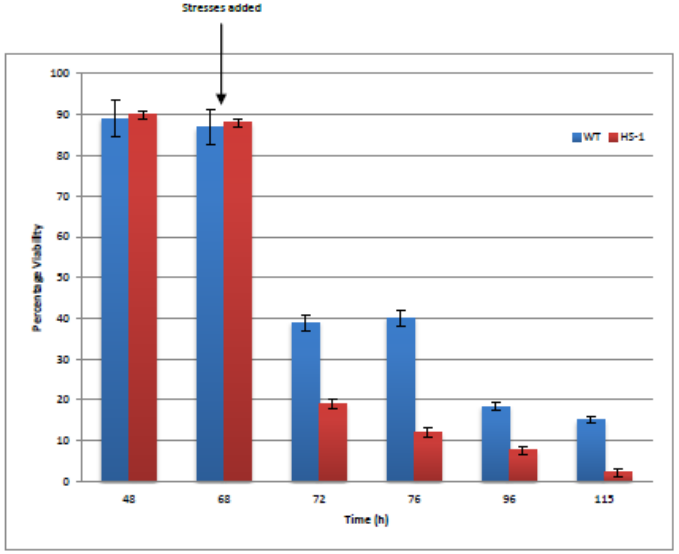

Figure 49: Viabilities of Wild-Type and previously heat shocked cells (HS-1) exposed to 200mM NaCl

200mM NaCl

5. Tolerance and Adaptation

Stresses on previously Heat-shocked *C.reinhardtii*

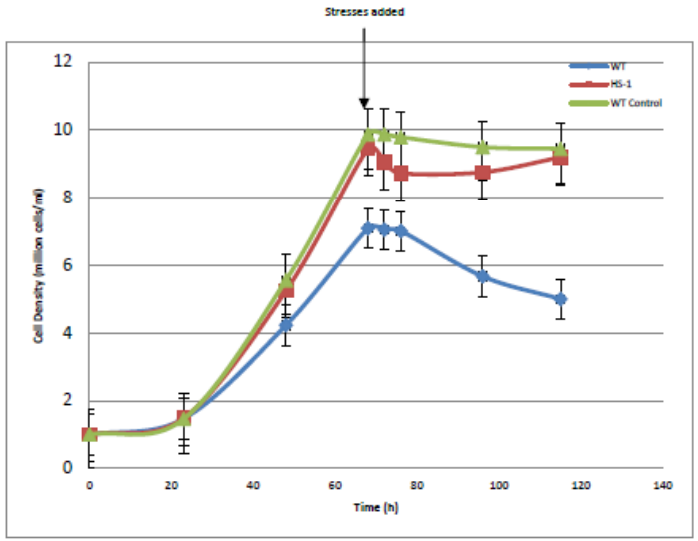

Figure 73: Wild-Type and previously heat shocked cells (HS-1) exposed to 42^{0}C heat shock

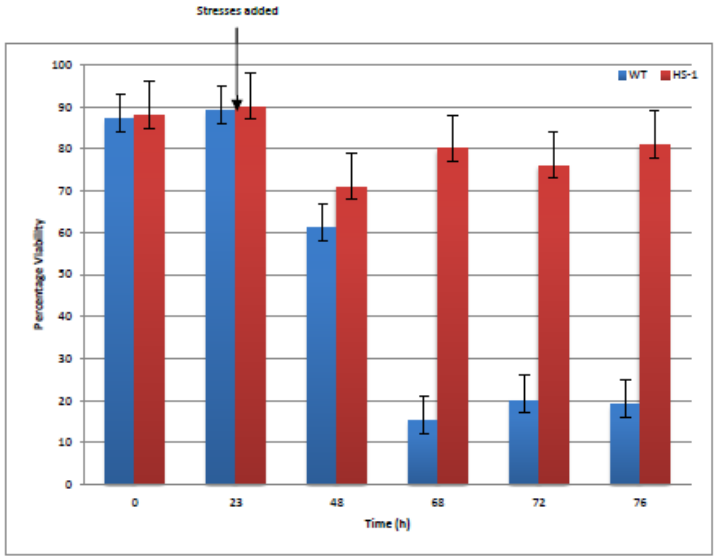

Figure 74: Viabilities of Wild-Type and previously heat shocked cells (HS-1) exposed to 42^{0}C heat shock

Heat Shock # 2

Effect of other Environmental Stresses

- Plants and Algae must weather High Irradiance (**UV**) , pH fluctuations, **NaCl changes** and **Peroxide stresses** and **Heat**

Photooxidation and Reactive Oxygen Species

- Reactive Oxygen Species (ROS) produced by Photosystems/ETS upon various stresses
- Damage intracellular components
- Can induce apoptosis through signaling
- Bcl-x_L can possibly inhibit apoptosis from ROS induction

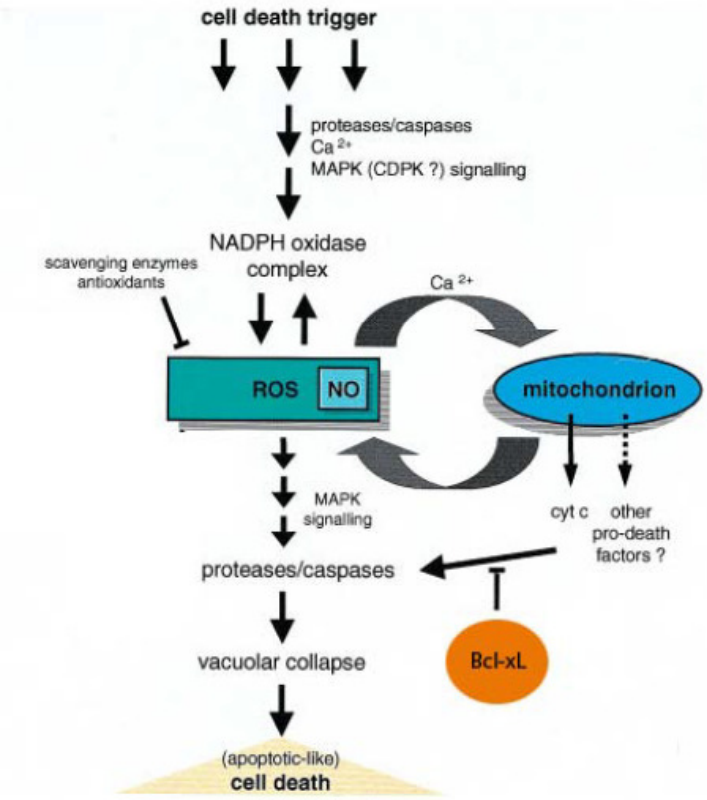

APPROACH: APPLY ANTI-APOPTOSIS GENES TO ALGAE

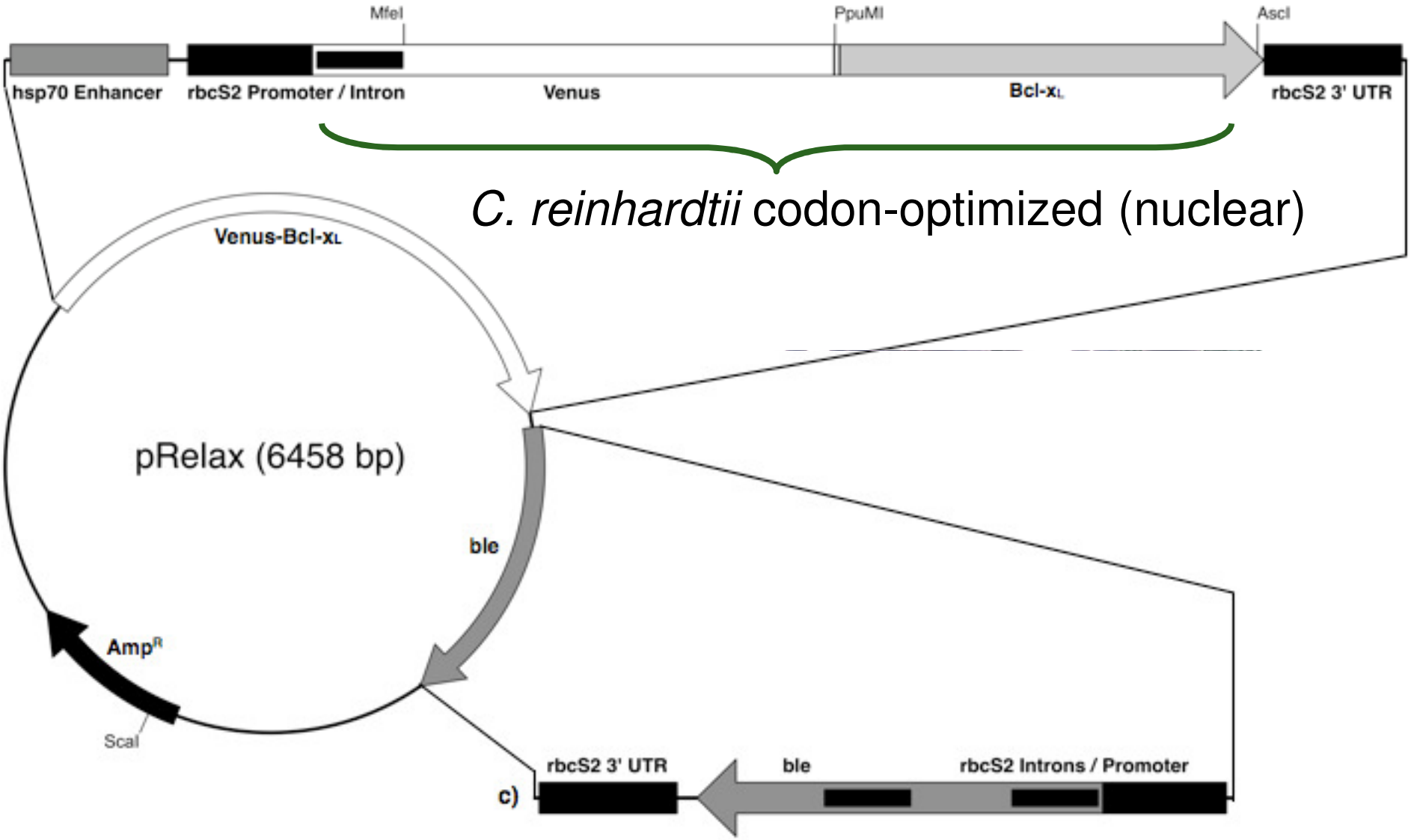

CONFIRMATION OF GENE EXPRESSION

- Reverse Transcriptase (RT)-PCR
  - Total RNA Extraction
  - cDNA Synthesis (oligo-dT_{18} Primers)
  - PCR (200 bp of Venus)

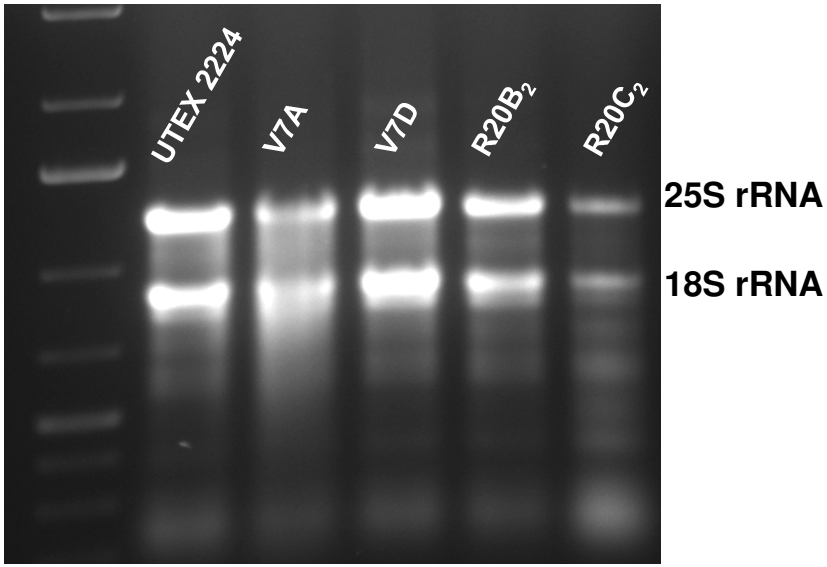

RNA Preparation

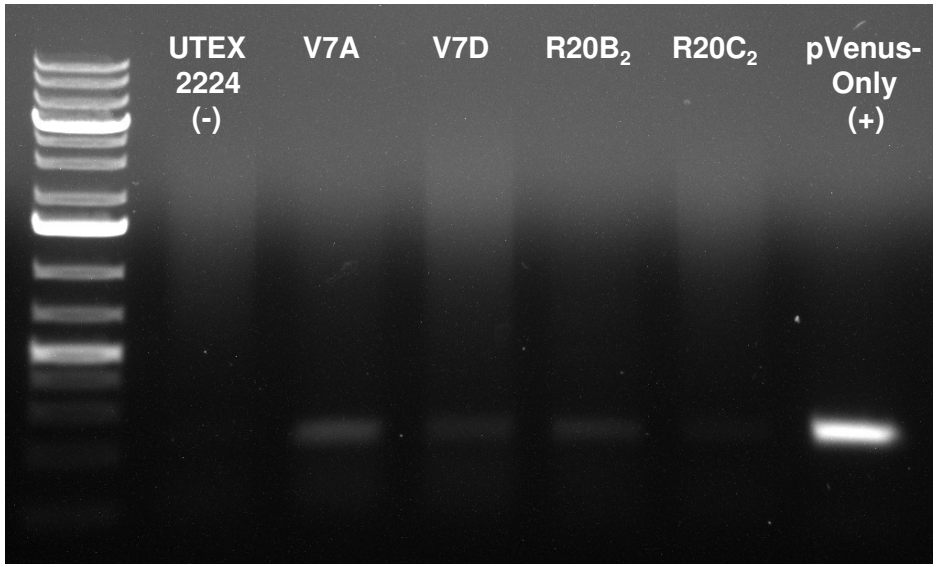

RT-PCR Products

Effect of Model Insult on Algae and Anti-Apoptosis Genes:

Camptothecin-induced cell death in wild-type wall-less *C.reinhardtii*

- Range: 10µM, 25µM, 50µM, 100µM, 200µM
- 51% reduction in growth rate in 10µM
  90.1%+ reduction after 25µM
- Same test was applied for Wall-less with and without pBclx but *no significant difference* in apoptosis reduction
- Perhaps death from DNA damage in Chlamy (C. Reinhardtii) occur by *Mitochondria-independent pathway* through which Bcl-x_L has no effect

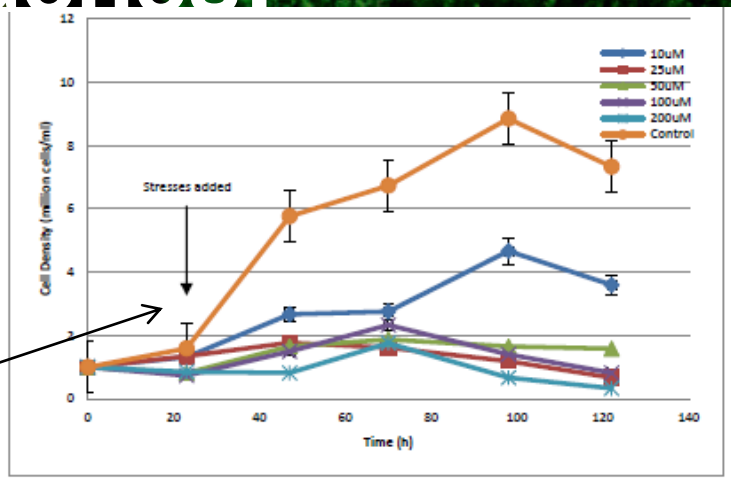

Figure 27: Wild Type *C.reinhardtii* (CW-15+) growth curves (Campthothecin application)

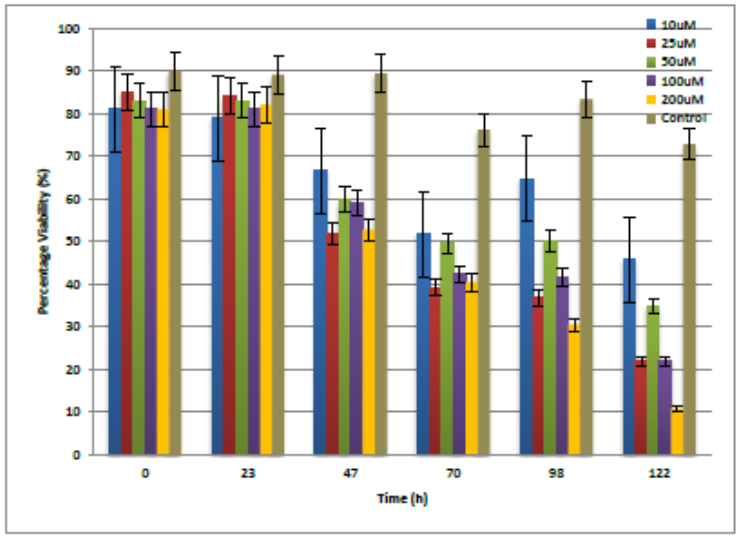

Figure 27: Wild type *C.reinhardtii* (UTEX 2337) Viability (Camptothecin application)

CHO N-linked Glycosylation Pathways

Sialylation
α(2,6) linkage possible
Not expressed.

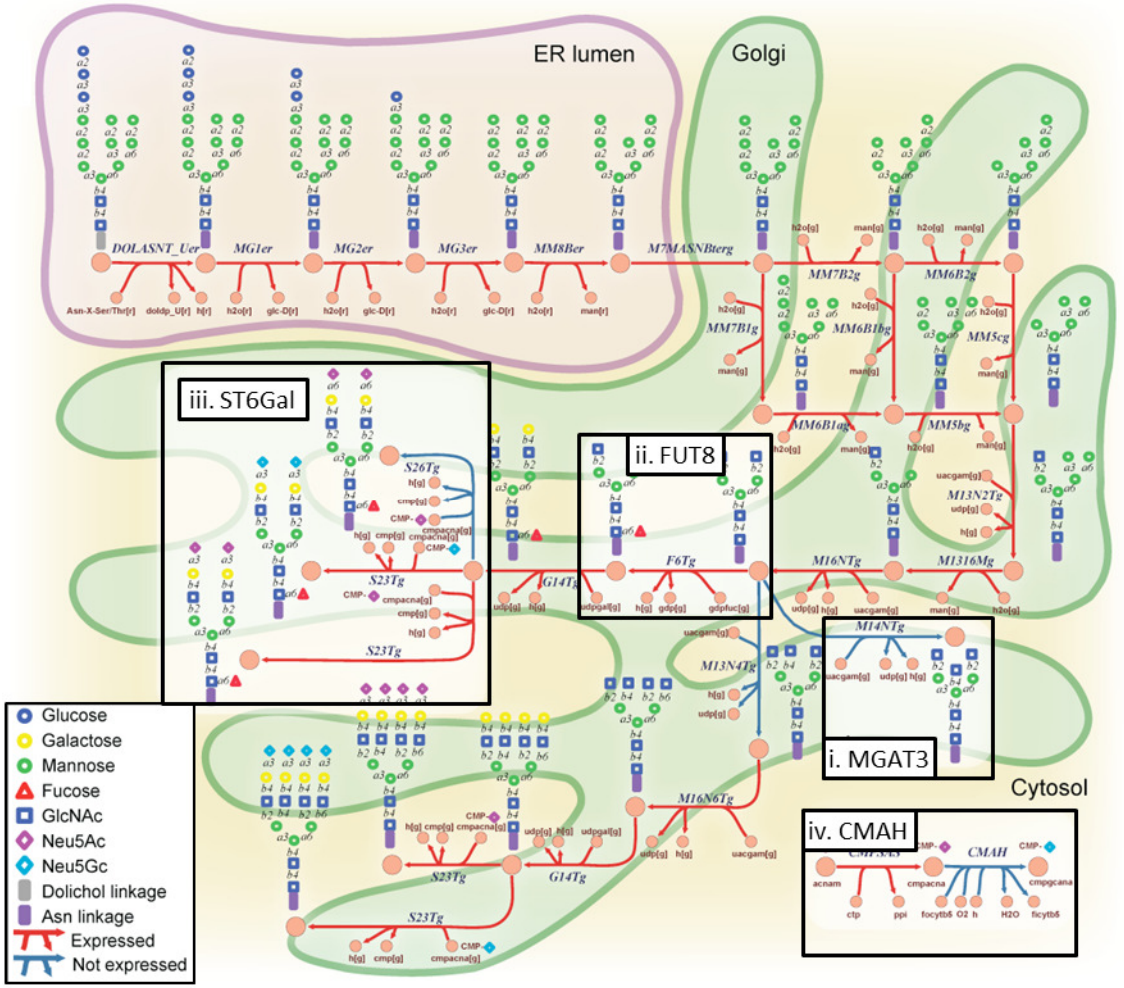

Only fucosyltransferases FUT8 and O-FUT

Bisecting (ß4) GlcNAc
LEC10 gain of function

Neu5Ac->Neu5Gc
No expression,
lower Neu5Gc less
immunogenic
response in humans.

Xu et al , Nature Biotechnol., (2011)

Glycosylation Processing Events in cells

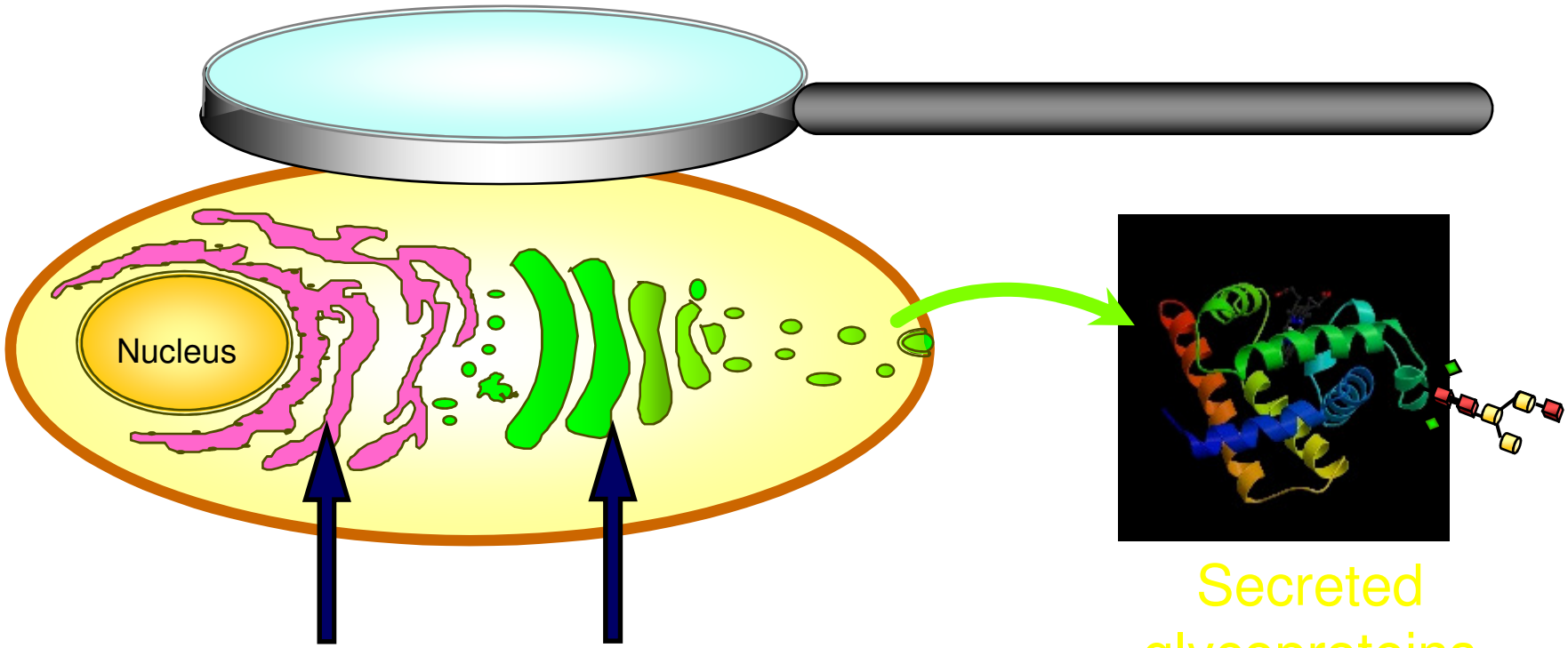

Nature versus the Drug Approval Process

Nature Desires Diversity and Variability

Biopharma Demands Consistency and Reproducible

Analysis of Gene Function in Chinese Hamster Ovary Cells

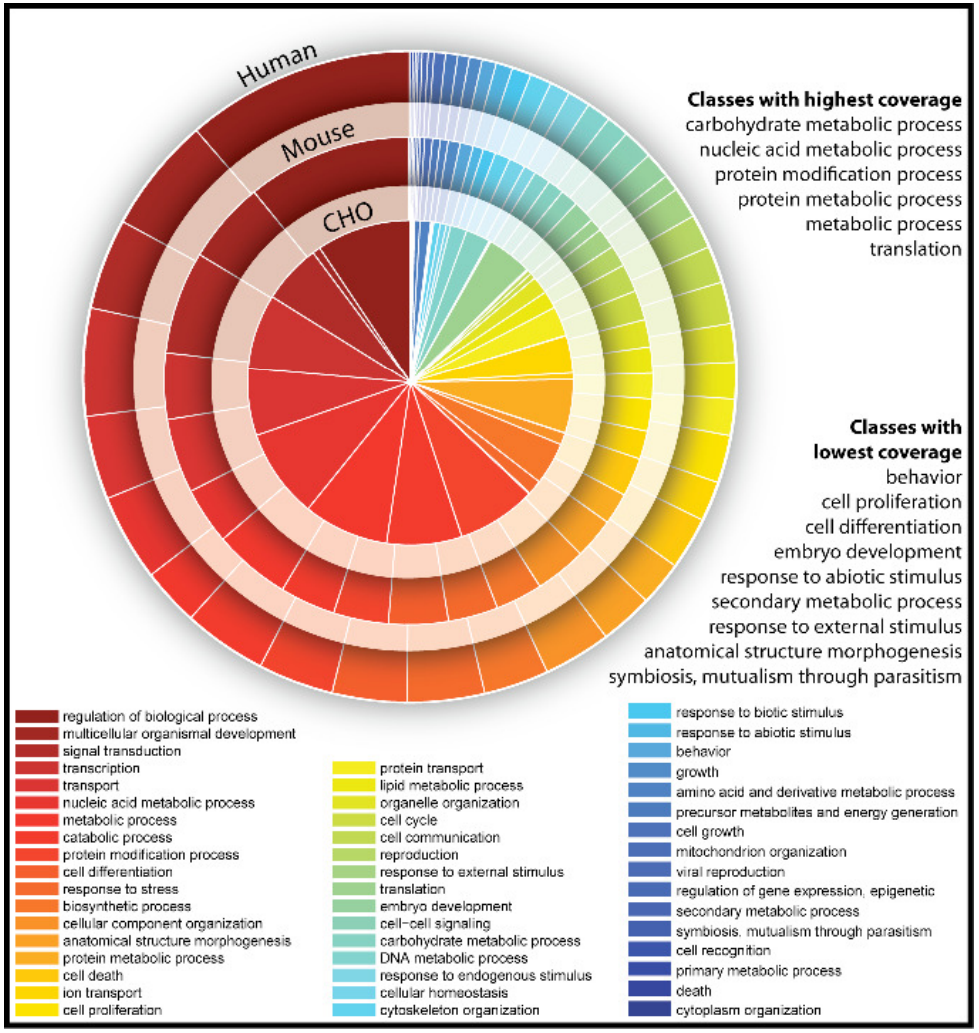

Xu et al , Nature Biotechnoloy (2011)

5. Metabolic Engineering

Metabolic Flux Analysis (MFA) overview

- Use stochiometric reactions of metabolic networks to determine fluxes

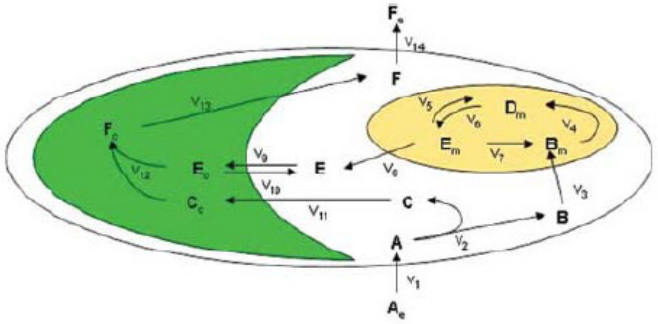

Figure75: Pathways in a hypothetical algal cell with three compartments, the mitochondria, cytosol and chlorophyll, the v values indicate the fluxes in the particular reactions and the bold capital letters (A,B,C etc.) are the metabolites.

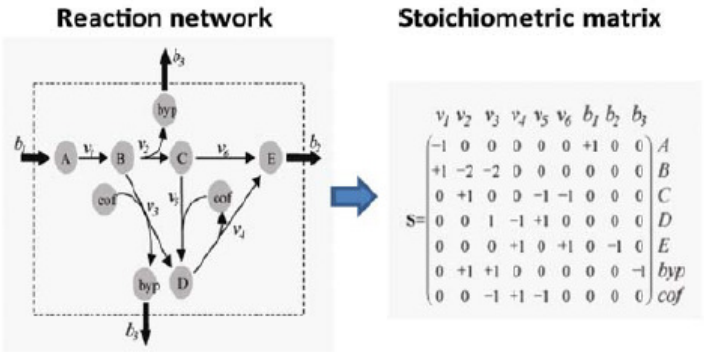

Algae Growth in Different Environments

- Photoautotrophic: CO_2 and Light
- Mixotrophic: Carbon Source and CO_2
- Heterotrophic: Carbon Source Alone

Chlorella protothecoides - Autotrophic & Heterotrophic

Collaboration with CSU-Minxi Wan

Mixotrophic and Photoautotrophic growth of algae species

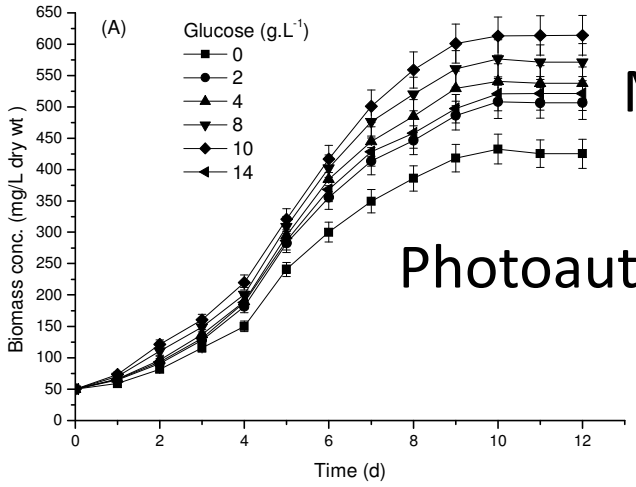

Mixotrophic

Photoautotrophic

Nannochloropsis oculata
HQW03

Mixotrophic

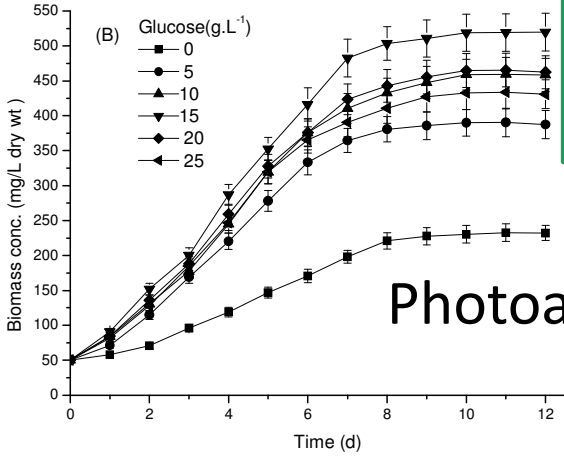

Photoautotrophic

Dunaliella salina
HQW04

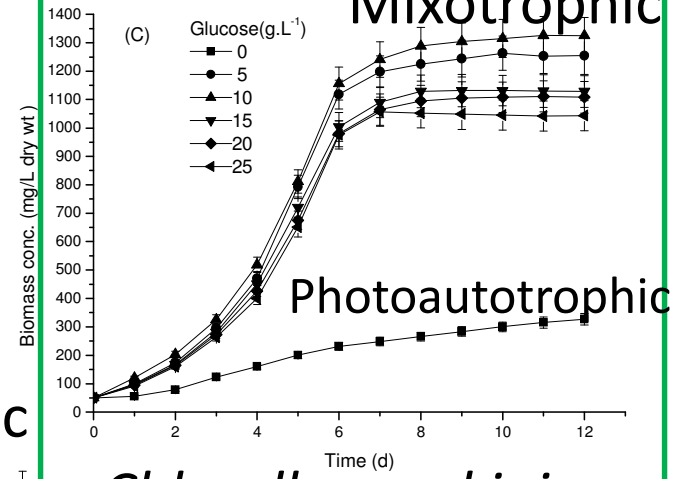

Mixotrophic

Photoautotrophic

Chlorella sorokiniana
CS-01

CHLORELLA SPECIES GROWTH

***Chlorella sorokiniana* UTEX 1669**

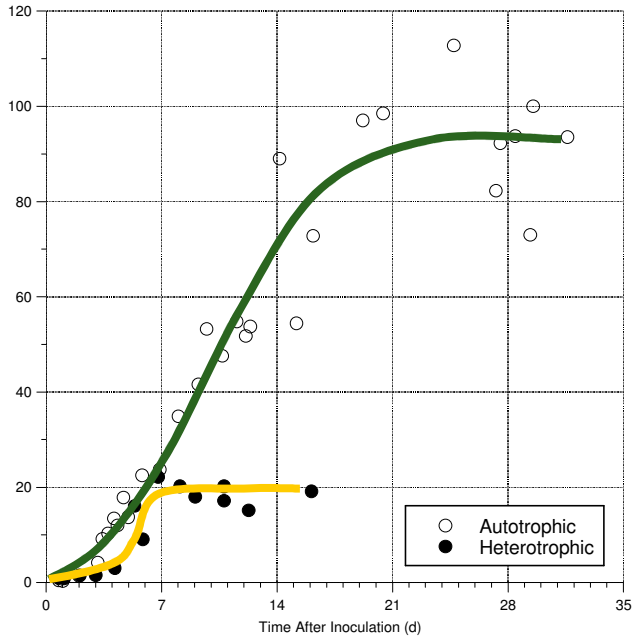

***Chlorella vulgaris* UTEX 265**

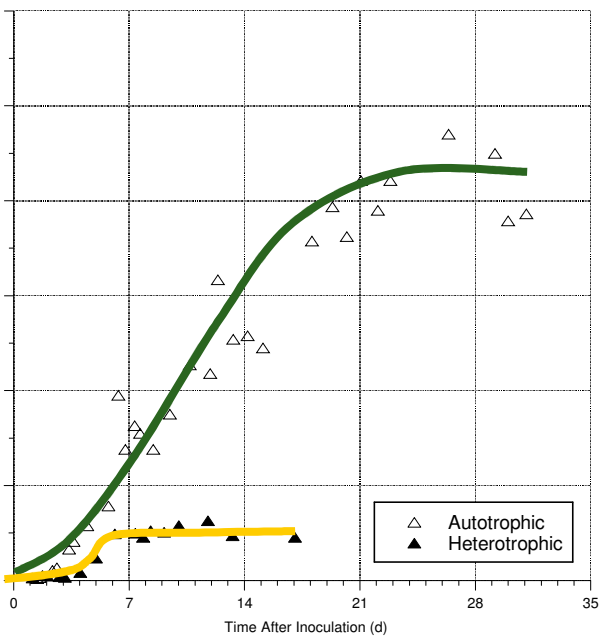

***Chlorella sorokiniana* UTEX 1230**

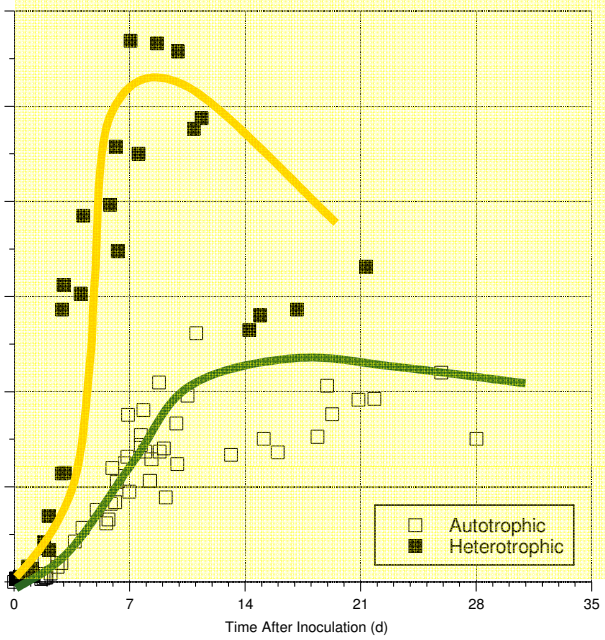

Strain	UTEX 265	UTEX 411	UTEX 1669	UTEX 1230
Species	*C. vulgaris*	*C. protothecoides*	*C. sorokiniana*	*C. sorokiniana*
Specific Growth Rate, *K'* (d^{-1})	0.84 ± 0.09	0.48 ± 0.01	0.77 ± 0.10	1.77 ± 0.04
	0.23 ± 0.01	0.32 ± 0.05	0.19 ± 0.02	0.36 ± 0.05
Doubling Time (hr)	20 ± 2.0	35 ± 1.4	21 ± 2.2	9.2 ± 1.0
	72 ± 3.0	52 ± 3.8	89 ± 2.6	46 ± 3.2
Divisions per Day (d^{-1})	1.2 ± 0.1	0.69 ± 0.04	1.1 ± 0.1	2.6 ± 0.1
	0.33 ± 0.04	0.46 ± 0.07	0.27 ± 0.03	0.52 ± 0.07

Effect of Temperature and pH on heterotrophic growth of Chlorella

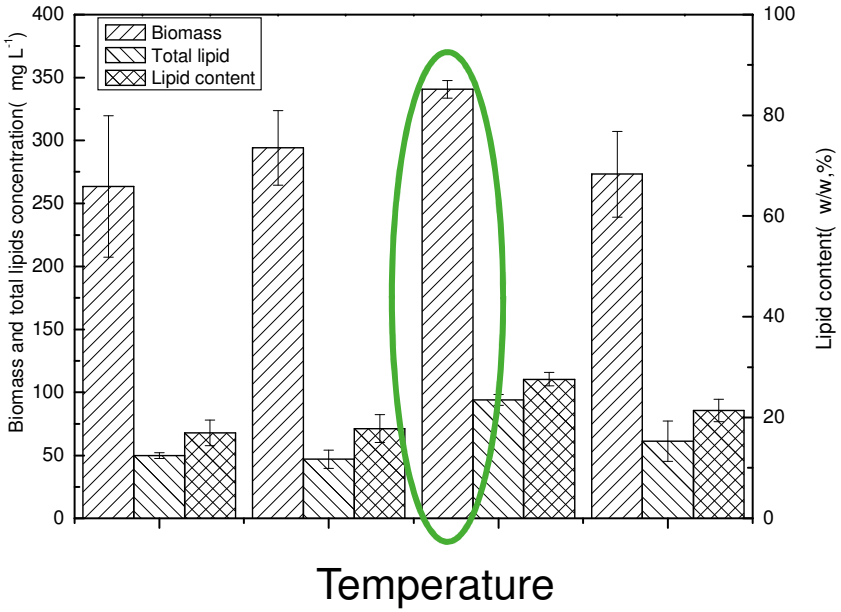

Temperature

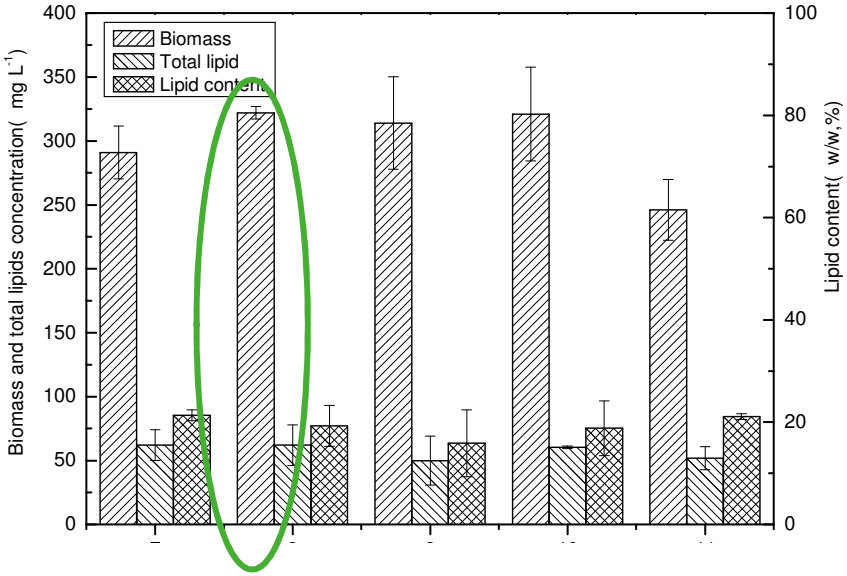

pH

Chlorella exhibits Temperature and pH optimums for biomass

Effect of nitrogen source and carbon source during heterotrophic growth

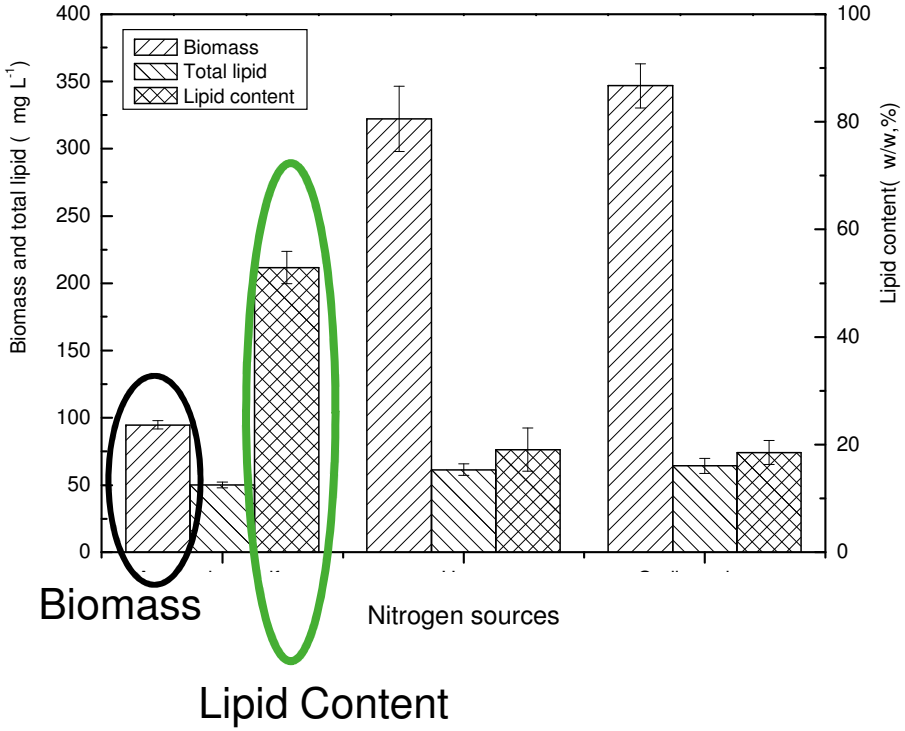

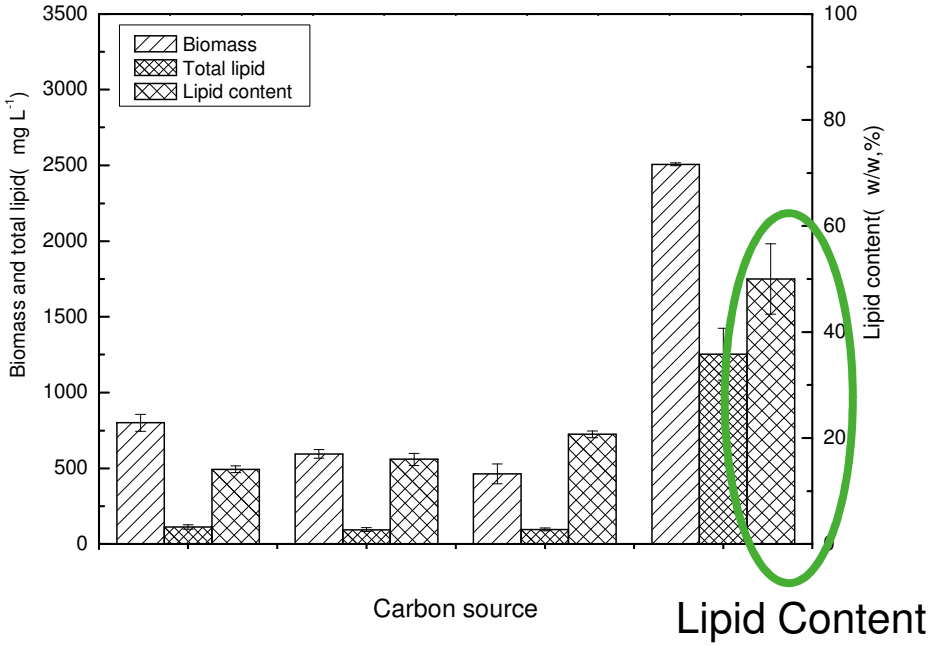

The nitrogen and carbon source can alter the biomass/lipid content

Substrate growth inhibition of *Chlorella sorokiniana* in mixotrophy

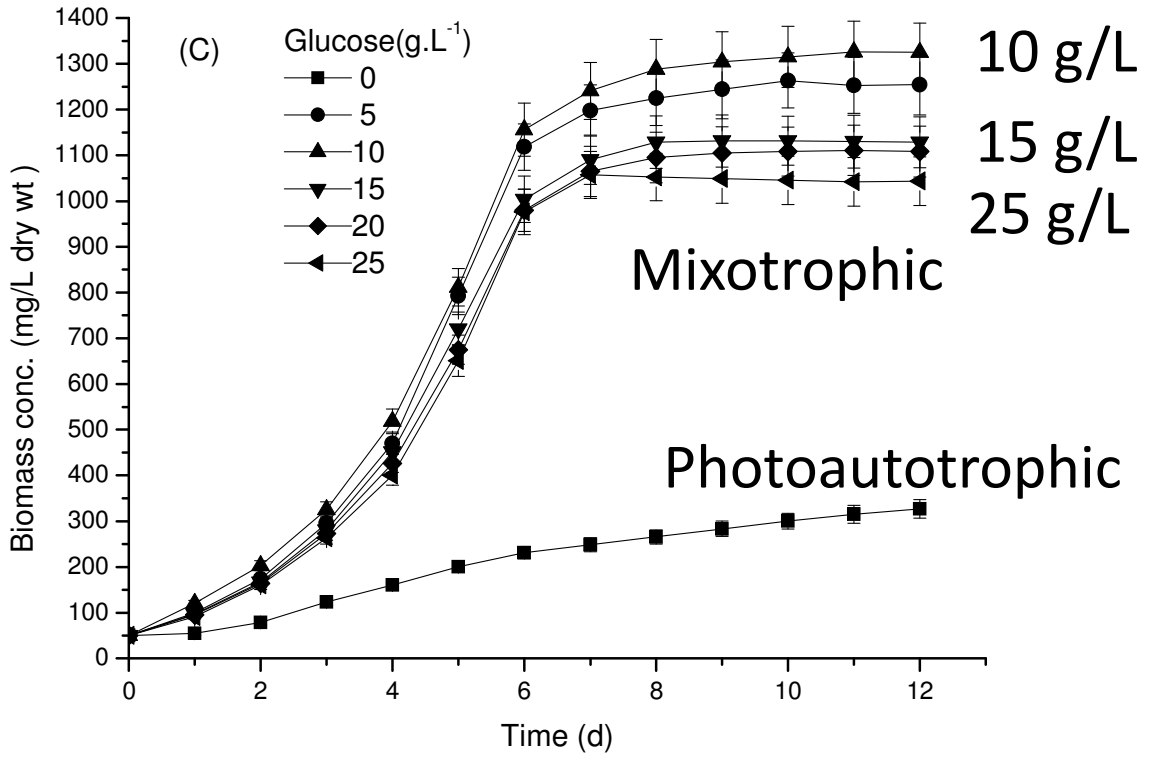

Lipid and Protein Content under Mixotrophic Conditions

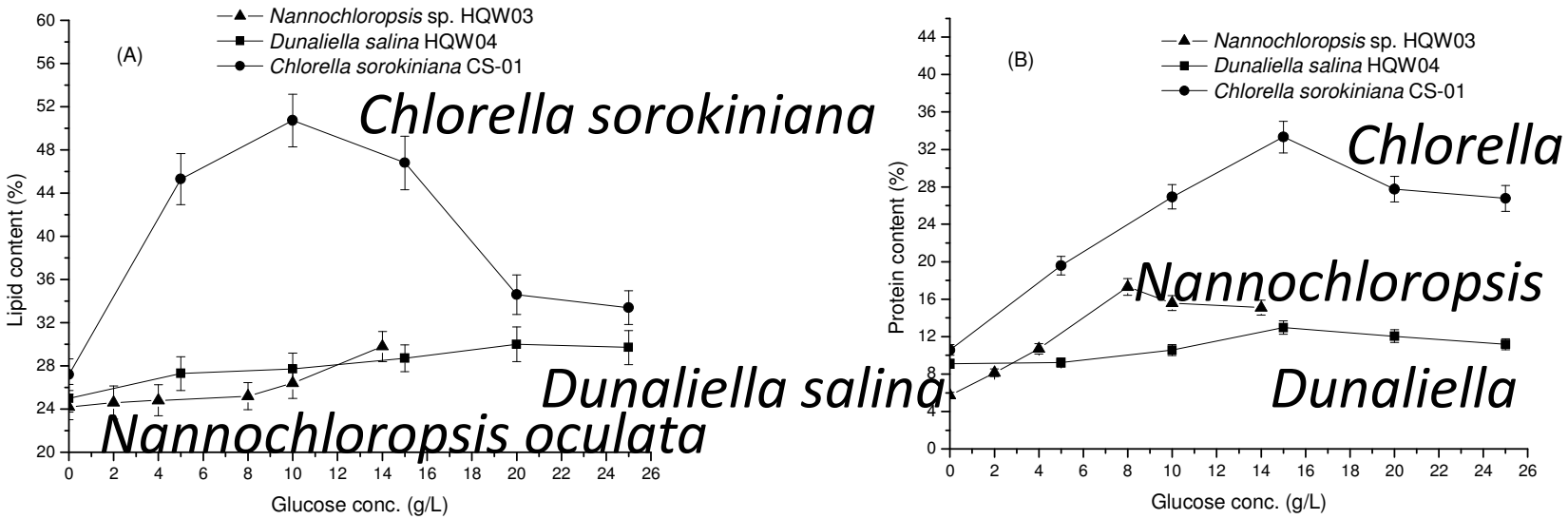

Chlorella exhibits a lipid maximum under mixotrophic conditions

Comparison of Chlorella Lipid Content in Logarithmic and Stationary Phase

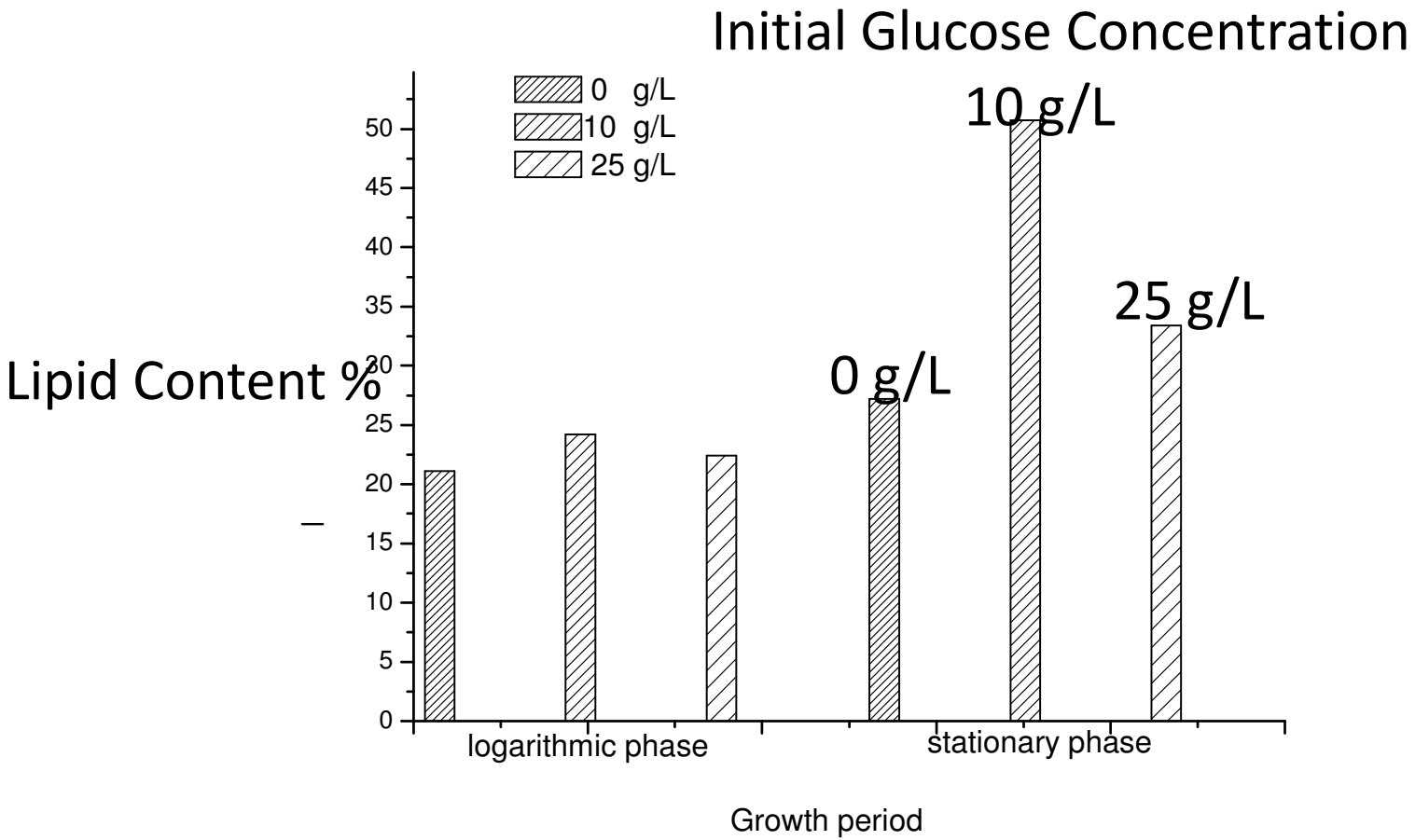

Lipid content increases from log to stationary phase

Change in Chlorella Gene Expression Photoautotrophy vs. Mixotrophy

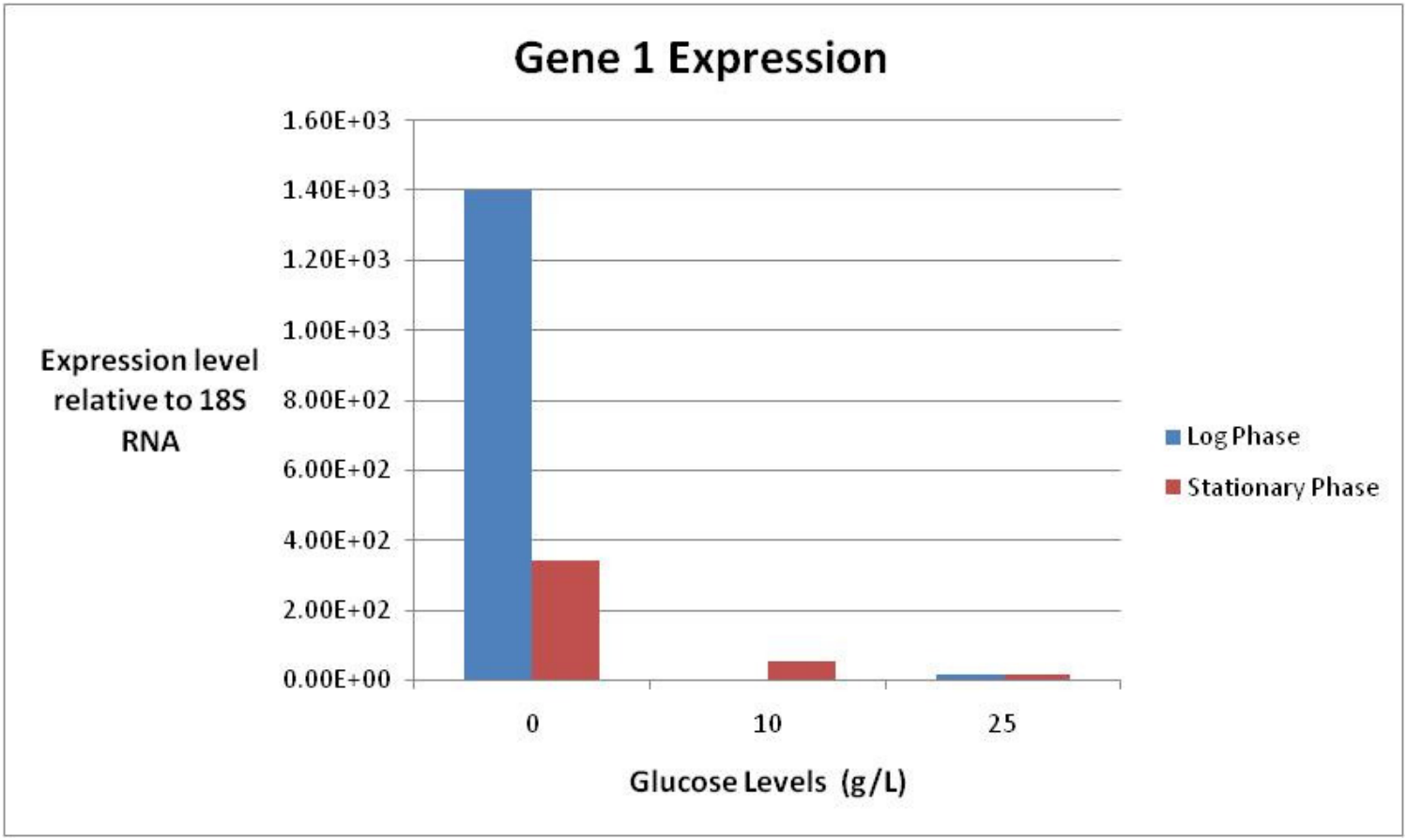

Gene 1 expression decreases from photoautotrophic to mixotrophy

Change in Chlorella Gene 2 Expression Photoauto/Mix and Log/Station

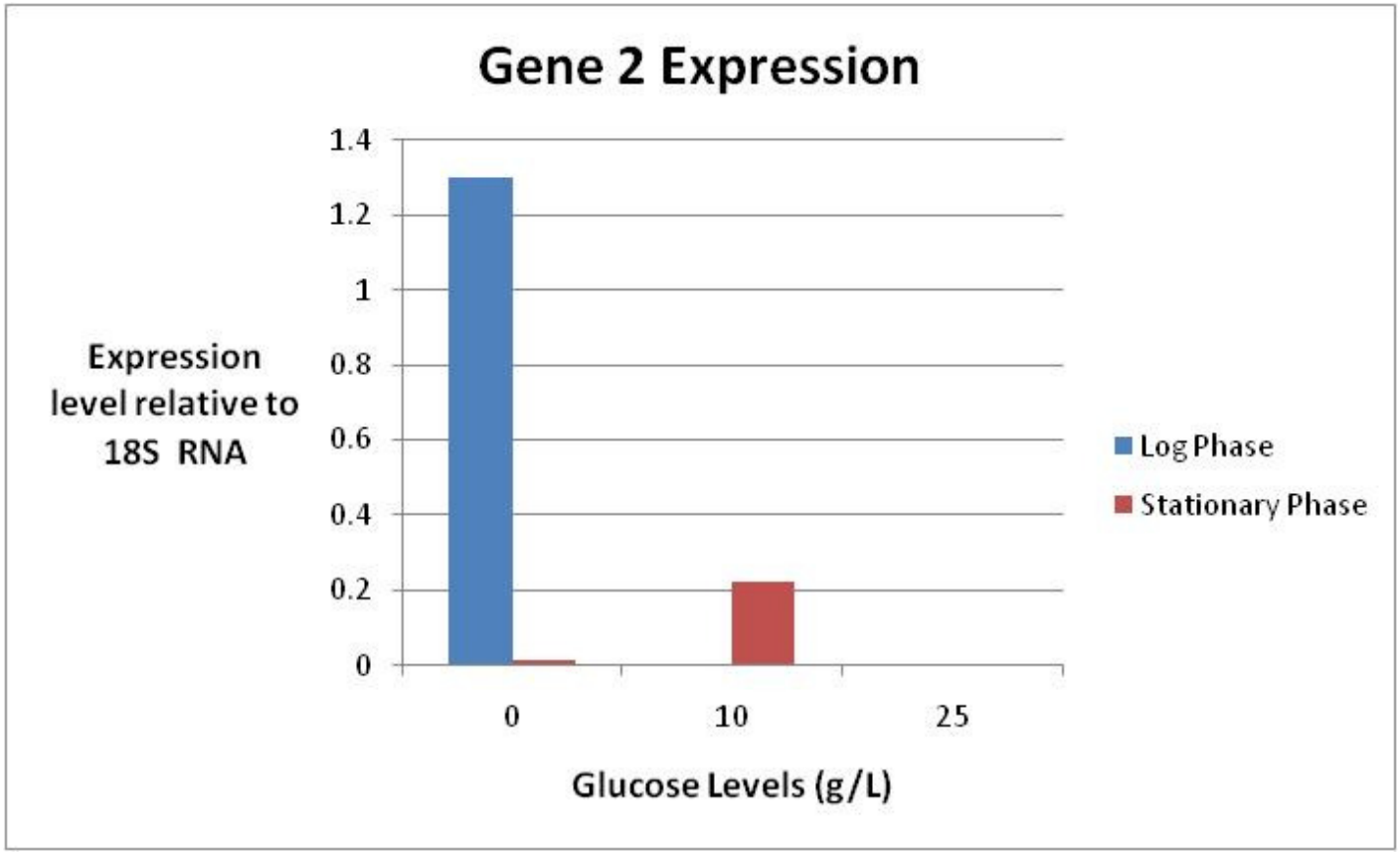

Lack of a consistent trend for Gene 2 expression in stages

Change in Chlorella Gene 3 Expression in Logarithmic and Stationary Phases

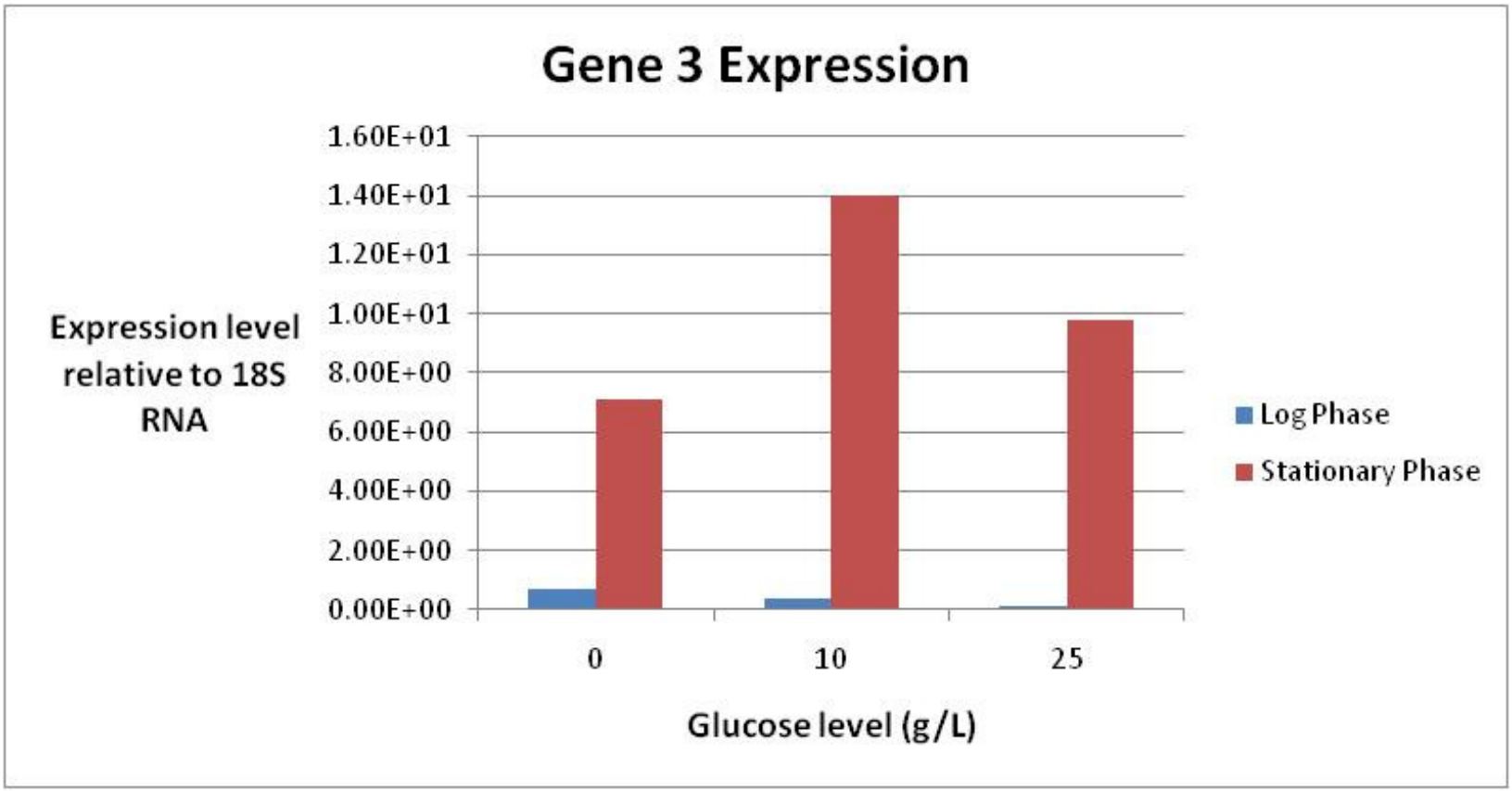

Gene 3 expression increases from logarithmic to stationary phase

Interpreting Algal Dynamics: Kinetic Model of *C. reinhardtii*

- **15** Pathways were included for a total of:

  320 Biochemical Reactions
  218 Compounds

- **376** kinetic constants were retrieved from the BRENDA enzyme database, while **216** (36% of total) were estimated.
- In addition, **275** turnover numbers were obtained and **45** (14% of total) are estimated.
- Numerical integration was accomplished using an adaptive 4th order Runge-Kutta with adaptive step size (max error 1E-4)

Goncalo Maia and Mariajose Castellanos-University of Maryland, Collaborators

Effect of nitrogen on growth and lipid content during heterotrophic growth

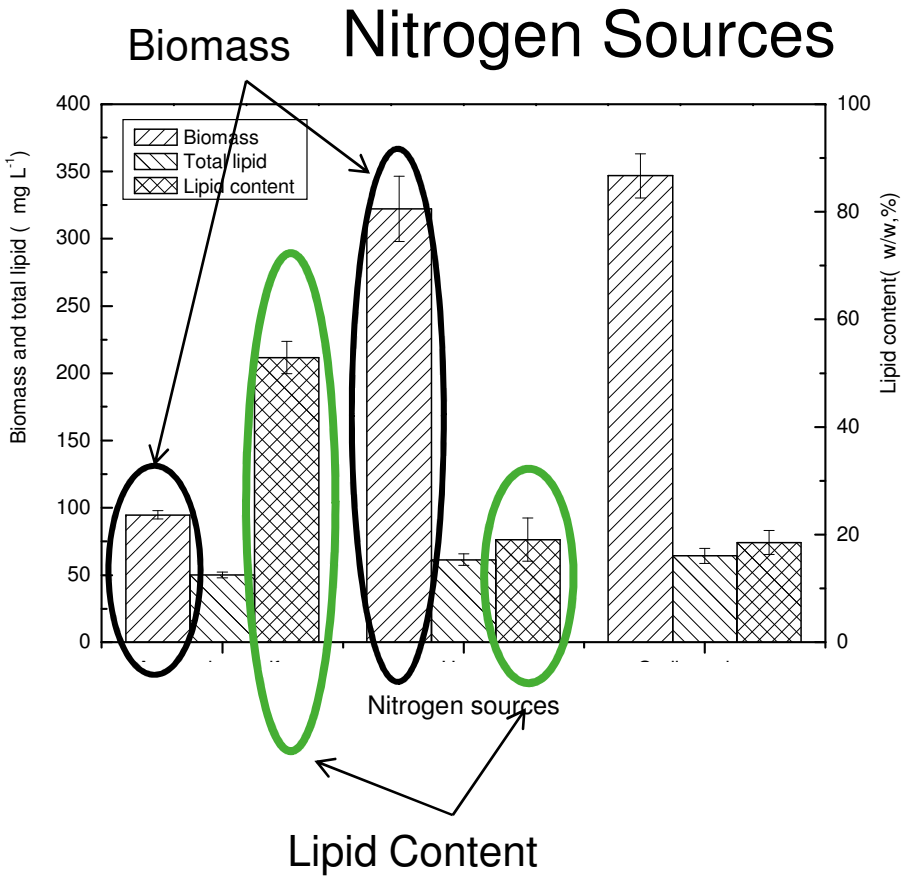

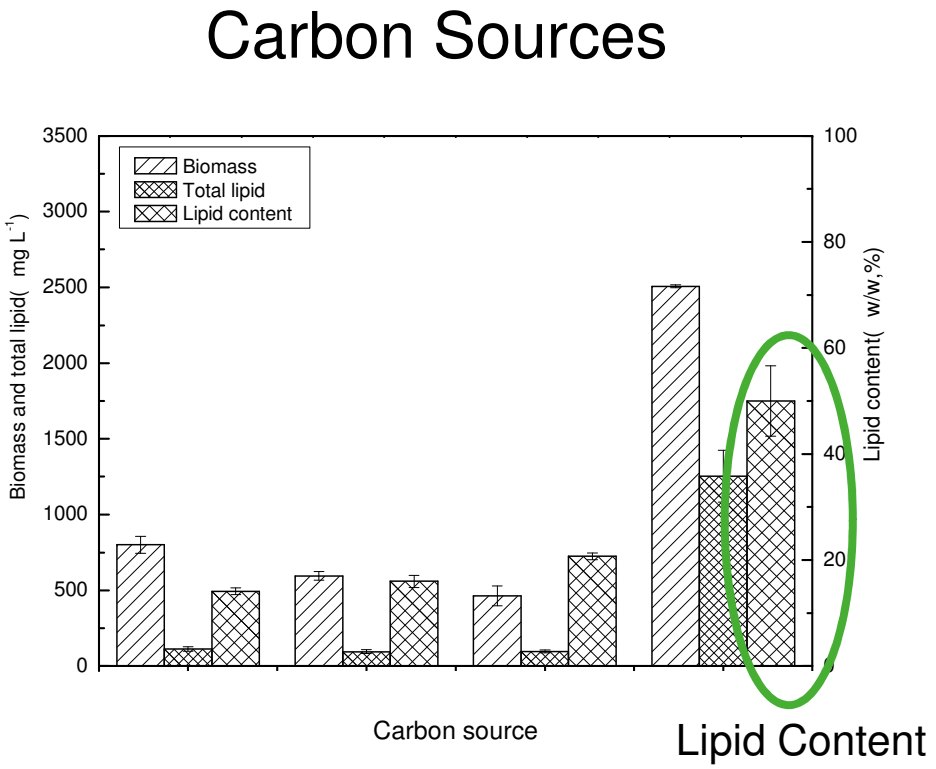

The nitrogen and carbon source can alter the biomass/lipid content

Higher nitrogen supply leads to higher growth

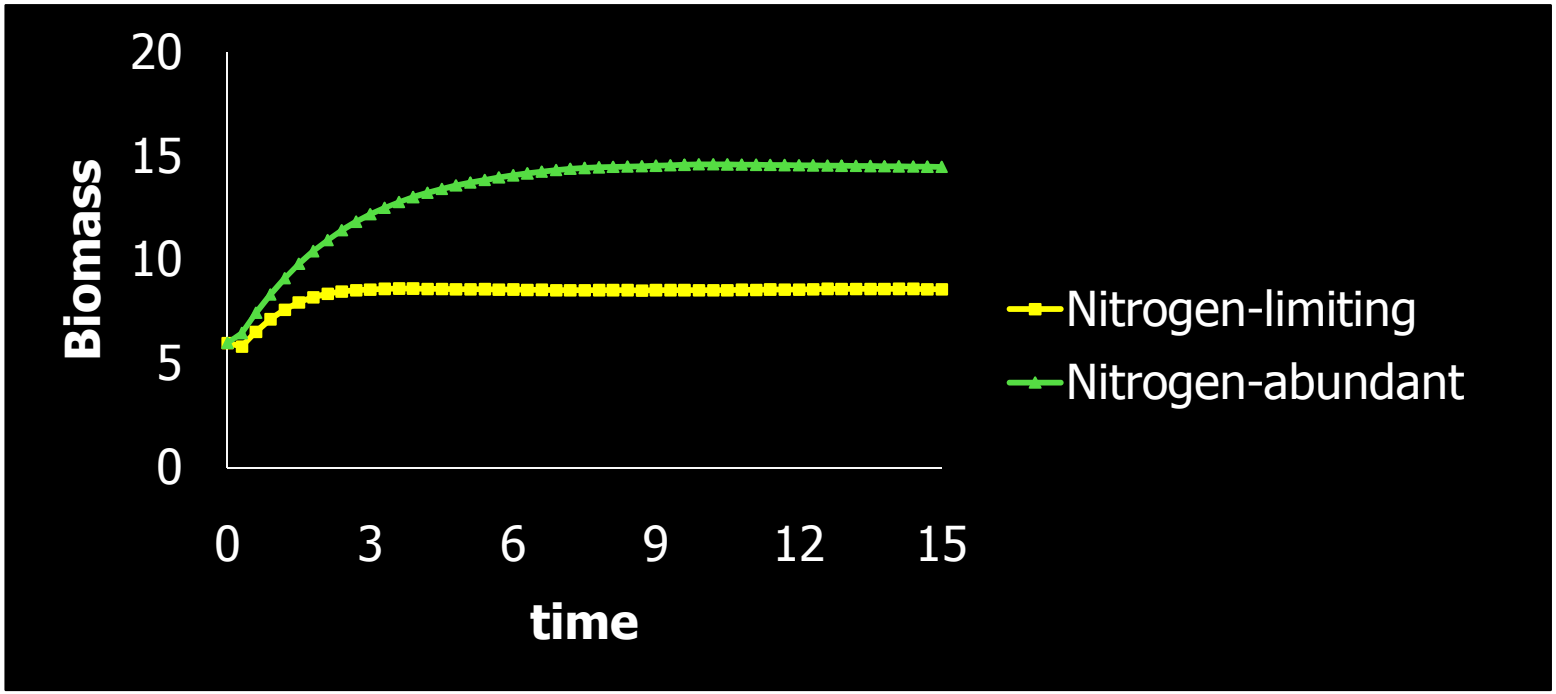

- Nitrogen-abundant conditions exhibit a biomass generation factor about 45% higher than in the nitrogen-limiting scenario
- Experimentally, it has been reported 35-43% increase[1]

[1] *Shobha et al, Applied Biochemistry and Biotechnology, 1990*

Effect of nitrogen supply leads on lipid intermediates

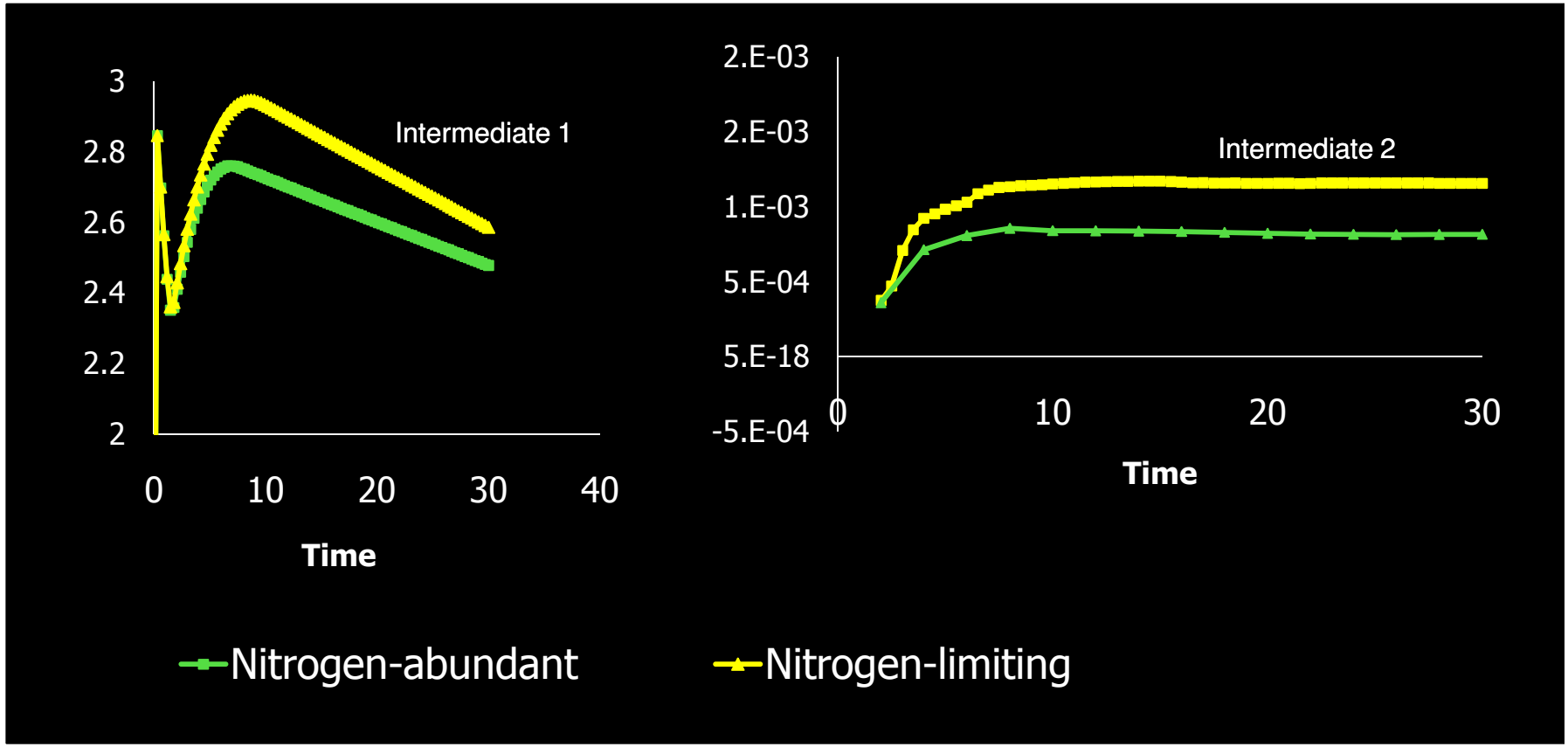

- nitrogen-limiting conditions leads to a higher concentration of intermediates when compared with the standard or nitrogen-abundant case

Consumption of ATP

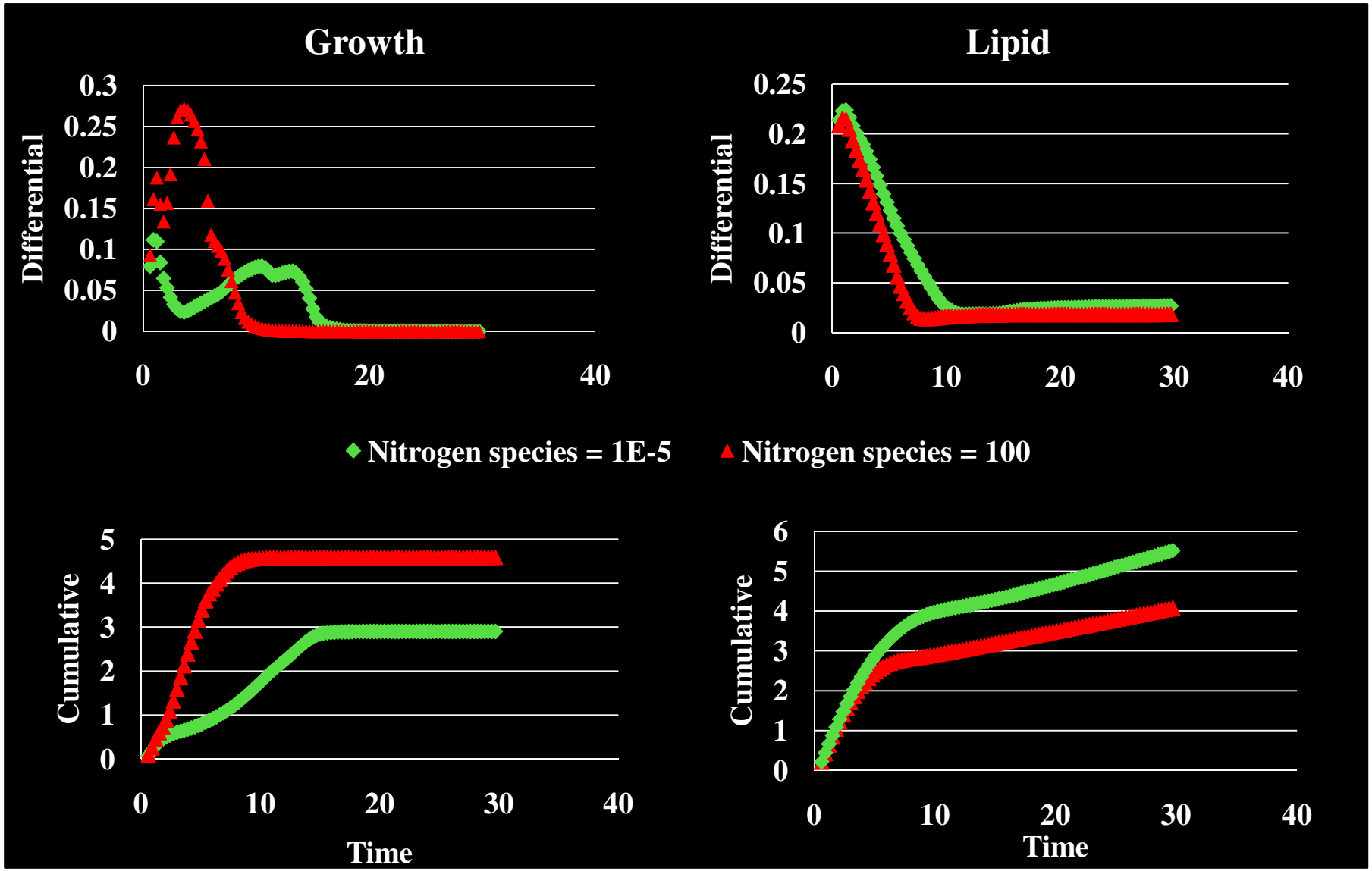

Effect of Nitrogen, Higher Lipid Intermediate Production

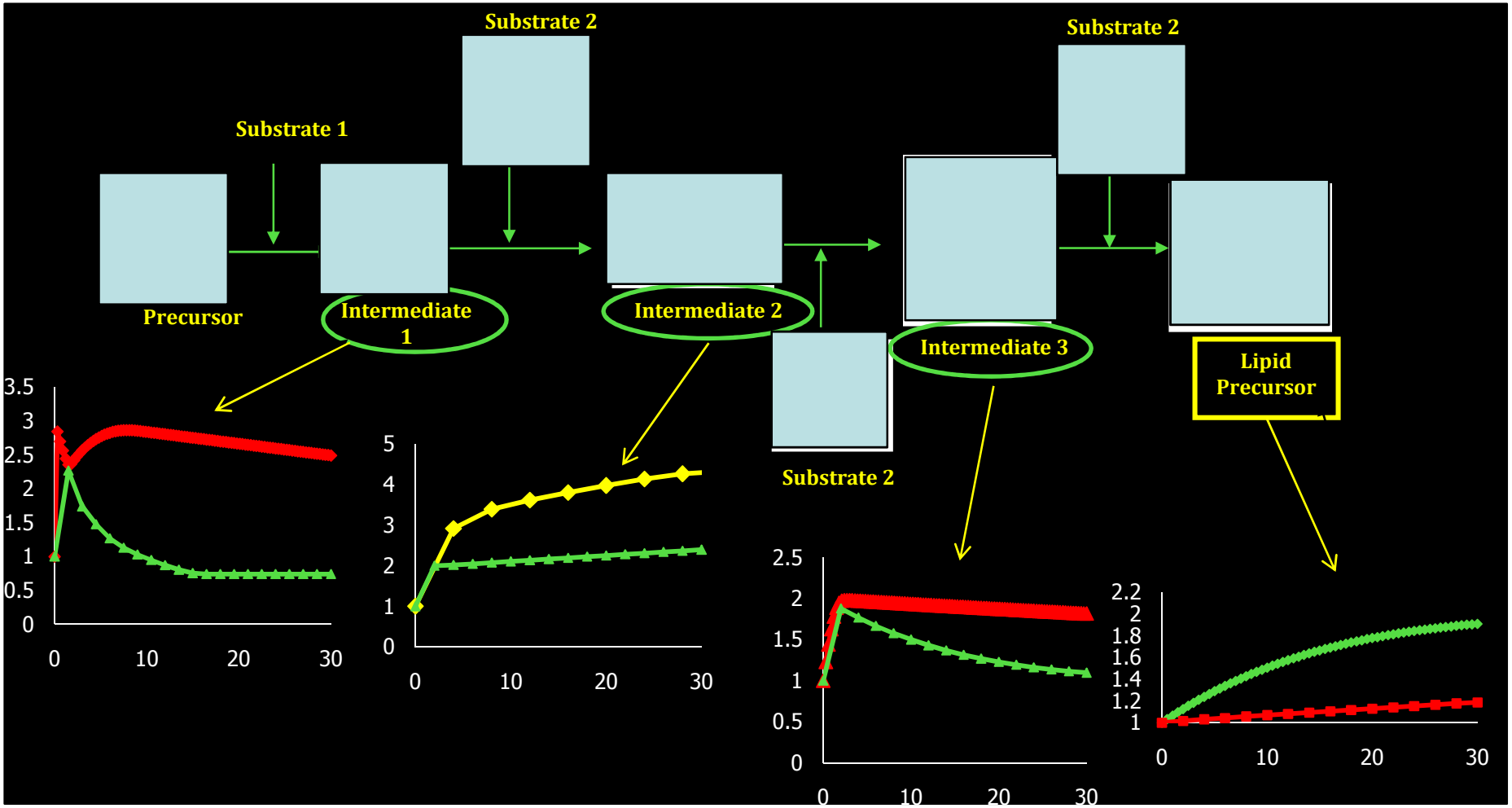

N at 100

N at 100, ATP change

N at 100, ATP change, Enzymes changed

Analysis of Intracellular Pathways: Metabolic Flux Analysis

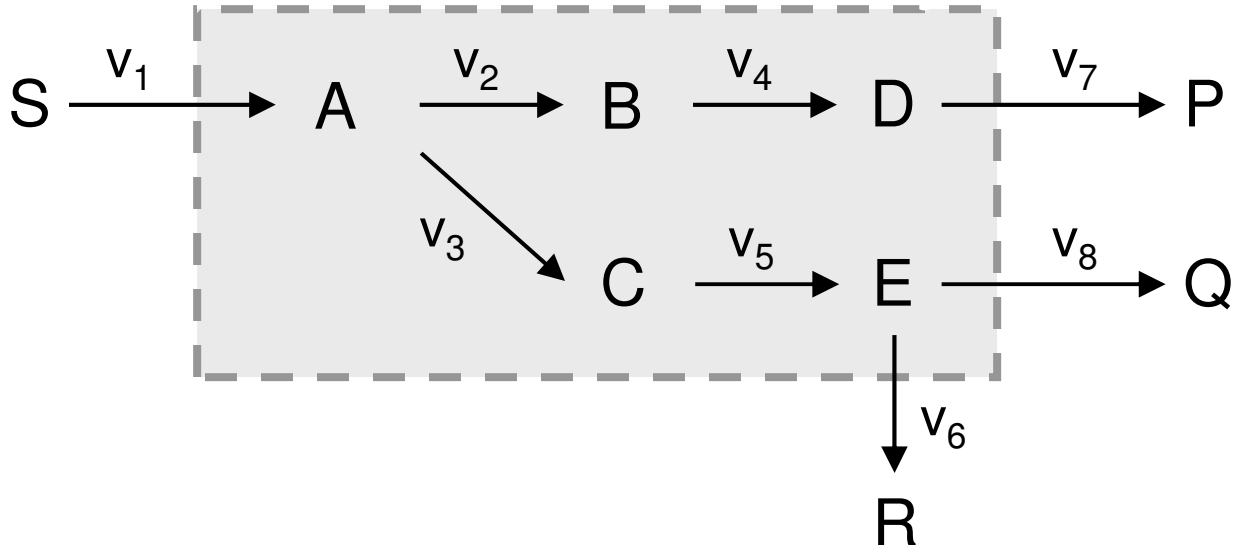

$$
\begin{array}{c}
 \\
A \\
B \\
C \\
D \\
E \\
\hline
S \\
P \\
Q \\
R
\end{array}
\begin{array}{c}
\begin{array}{cccccccc} v1 & v2 & v3 & v4 & v5 & v6 & v7 & v8 \end{array} \\
\left(\begin{array}{cccccccc}
1 & -1 & -1 & 0 & 0 & 0 & 0 & 0 \\
0 & 1 & 0 & -1 & 0 & 0 & 0 & 0 \\
0 & 0 & 1 & 0 & -1 & 0 & 0 & 0 \\
0 & 0 & 0 & 1 & 0 & 0 & -1 & 0 \\
0 & 0 & 0 & 0 & 1 & -1 & 0 & -1 \\
\hline
-1 & 0 & 0 & 0 & 0 & 0 & 0 & 0 \\
0 & 0 & 0 & 0 & 0 & 0 & 1 & 0 \\
0 & 0 & 0 & 0 & 0 & 0 & 0 & 1 \\
0 & 0 & 0 & 0 & 0 & 1 & 0 & 0
\end{array}\right)
\end{array}
* \left(\begin{array}{c} v1 \\ v2 \\ v3 \\ v4 \\ v5 \\ v6 \\ v7 \\ v8 \end{array}\right)
= \left(\begin{array}{c} 0 \\ 0 \\ 0 \\ 0 \\ 0 \\ \hline r_S \\ r_P \\ r_Q \\ r_R \end{array}\right)
$$

Collaborator: Maciek Antoniewicz, University of Delaware

Flux Determination using ^{13}C-Labeled Tracers

(1)
Grow cells with
^{13}C-labeled substrate

[1-^{13}C]glucose &
[U-^{13}C]glucose
often used

(2)
Measure ^{13}C-labeling

GC-MS
LC-MS
NMR

(3)
Estimate Fluxes

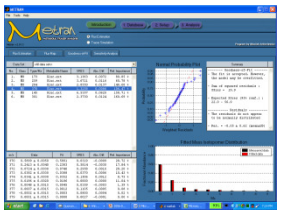

Least-squares
parameter estimation

Collaborator: Maciek Antoniewicz, University of Delaware

Determine Metabolite Mass Isotopomer Distribution

^{13}C ^{12}C ^{12}C ^{12}C

Metabolic conversion

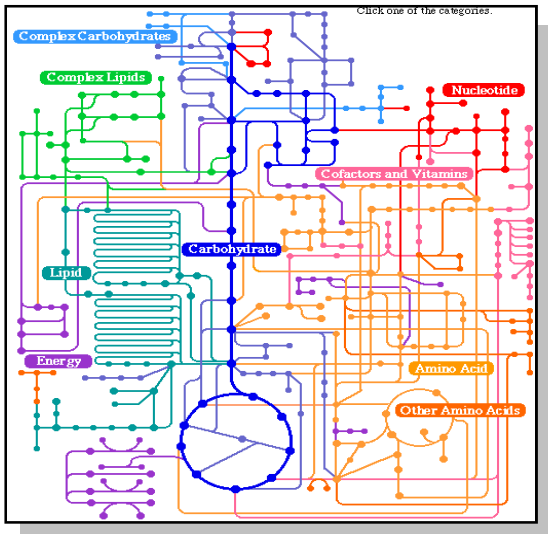

GC/MS analysis

Mass isotopomers

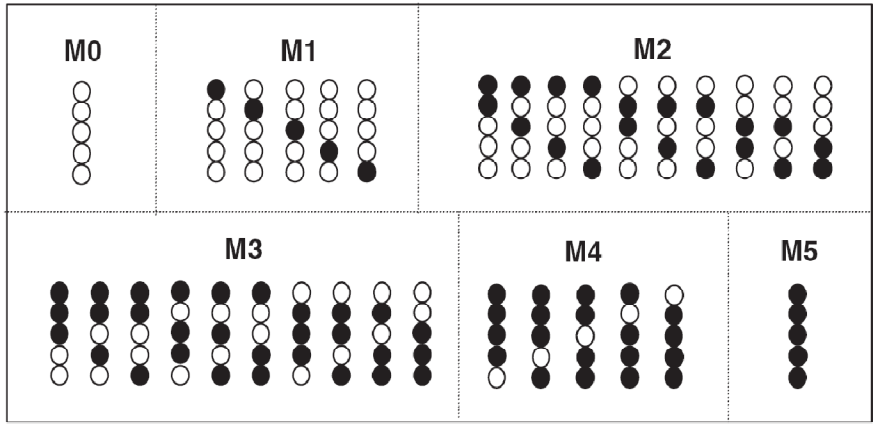

Collaborator: Maciek Antoniewicz , University of Delaware

Determination of Fluxes

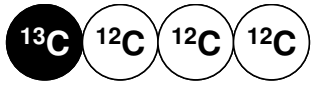

Metabolic conversion

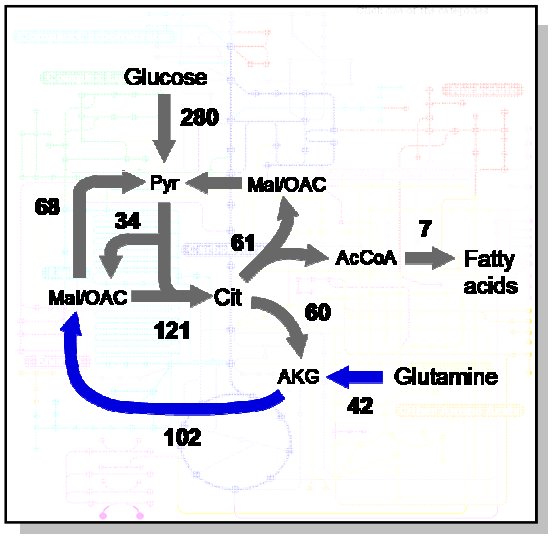

GC/MS analysis

Flux Analysis

(least-squares regression)

Mass isotopomers

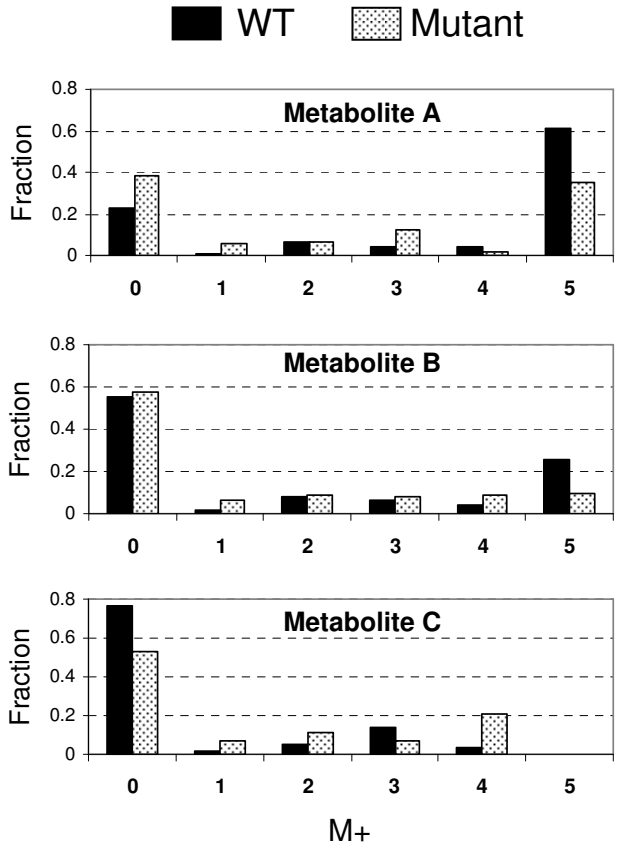

Collaborator: Maciek Antoniewicz, University of Delaware

Model Prediction: Effects of Nitrogen, ATP, Enzymes on Biomass and Lipids

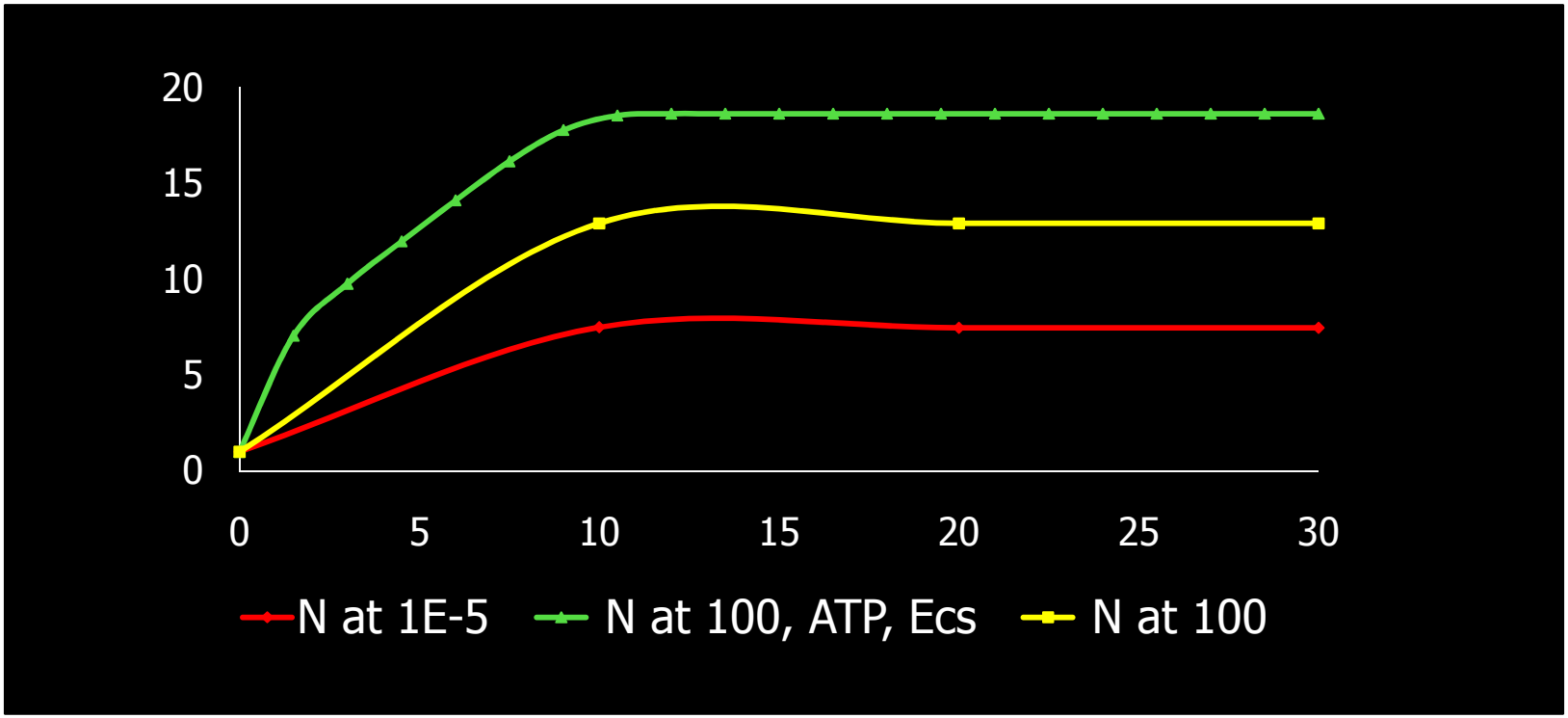

- Coupling nitrogen changes and ATP changes together with enzyme changes can increase biomass and provide for high lipid production

Separations of Lipids from Algae

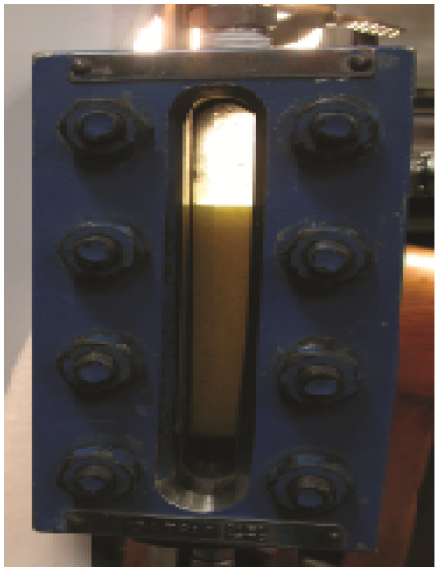

Fig. 4: Disrupted Algae in Separation Chamber

Separations of Lipids from Algae

Test Sample

Control

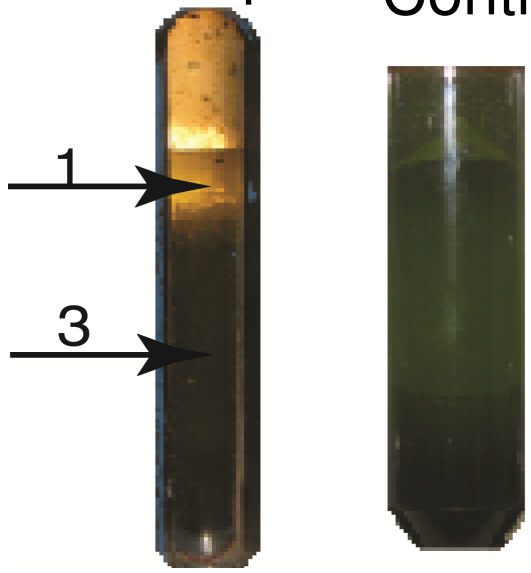

Lipid and Biomass are separated into two separate phases after several hours in test sample versus the control sample

Test Sample 2

Control

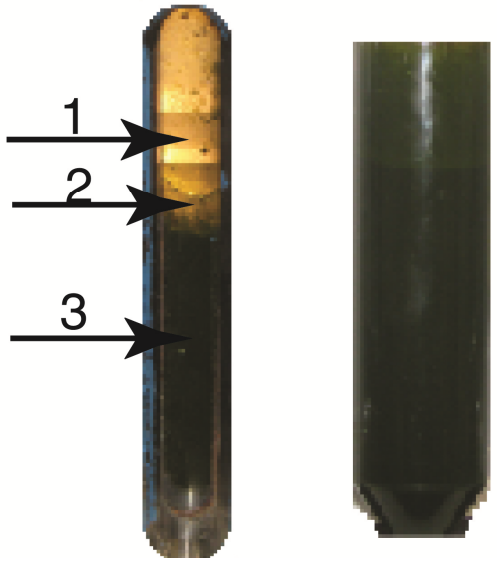

Lipid and Biomass are separated into three separate phases after variable treatment in test sample as compared to no separation in control sample

CONCLUSIONS

- Metabolic Engineering has been used to improve cell performance
  - Improving Product Quality through Changes in Glycosylation Patterns
  - Improving Yields of Cells and Target Biotherapeutics

- Genomics and other ‘omics tools will be an integral part of metabolic engineering
  - CHO genome has yielded information on potential Met. Eng. targets
  - MicroRNA is an emerging genomic control tool that can alter expression of multiple factors including anti-apoptosis genes simultaneously.

- Cell Engineering of Bcl-x_L Protects both Mammalian Cells and Microalgae from a Variety of Stresses that may be found in Bioreactor Environments

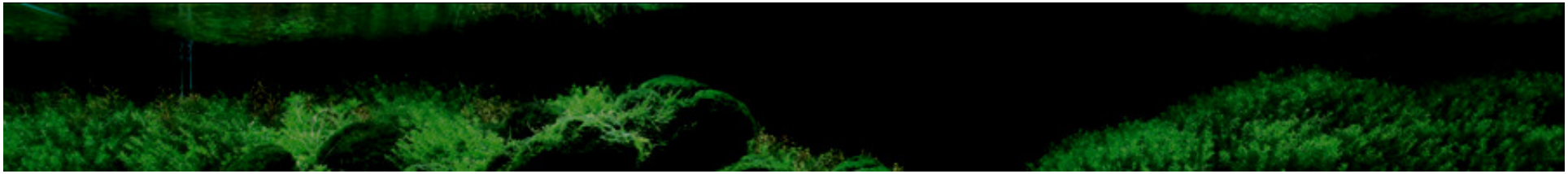

谢谢大家

欢迎提问(请用英文)

pRelax stress imposition – High NaCl

- NaCl range 175mM, 200mM, 225mM, 250mM

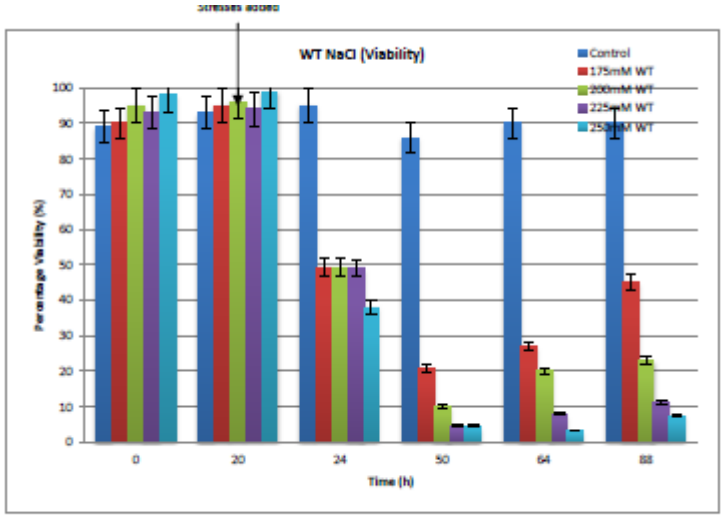

Figure 64: Viabilities of Wild-Type *C.reinhardtii* under High NaCl stress

Wild-Type

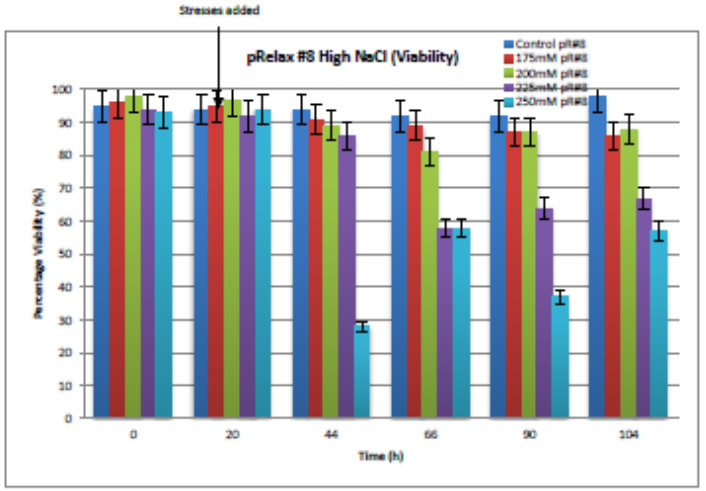

Figure 65: Viabilities of pRelax# 8 under High NaCl stress

pRelax #8

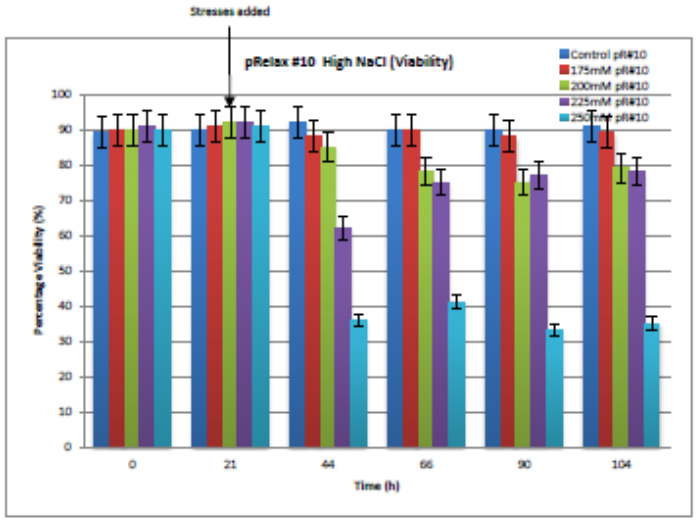

Figure 66: Viabilities of pRelax# 10 under High NaCl stress

pRelax #10

CONCLUSIONS

- Metabolic Engineering has been used to improve cell performance
  - Solving the Product Quality and Yield Paradox
  - Improving Yields of Target Biotherapeutics

- Cell Engineering of Bcl-x_L Protects *C. reinhardtii* from Photooxidative Stress due to Rose Bengal and Improves Cell Densities

- Mixotrophic/Heterotrophy vs Photoautotrophy

  Stationary vs Exponential
  - Optimize Growth Rate and Cell Density
  - Optimize Carbon and Nitrogen Sources
  - Alter Lipid and Protein Content
  - Determine Gene Expression Important to Productivity

Conclusions

- Modeling can be used to indicates effects of nitrogen limiting conditions and illustrate trade-off between biomass and lipid content
- ATP plays a relevant role in metabolism and is important to lipid generation and growth
- A efficient lipid-producing, high growth microalgae is possible in an optimized cellular environment
- Metabolic flux analysis will provide insights into production bottlenecks for both biomass and biofuels
- Algal biological products will require proper integration of biology, modeling, and engineering systems to realize full potential

Acknowledgements

- Students and Post-Docs: Julian Rosenberg, Minxi Wan, Adam Cohen, Sandra Bennum, Shawn Lawrence, Karthik Viswanathan, Goncalo Maia

- Collaborators: George Oyler, Frederick Krambeck, Marc Donohue, Karen Palter, Mariajose Castellanos, Maciek Antoniewicz, Haimanti Dorai

- Funding: NIH, DOE, Centocor Johnson and Johnson

SPECIES SELECTION: *CHLORELLA* SPP.

- Four strains suggested to grow heterotrophically (lipids & lutein):
  - *C. sorokiniana* UTEX 1669
  - *C. sorokiniana* UTEX 1230
  - *C. vulgaris* UTEX 265
  - *C. protothecoides* UTEX 411

- Analyzed heterotrophic growth supplemented with 10 g glucose L^{-1}
  - Growth Rate
  - Metabolic Efficiency
  - Relative Lipid Content

- Compared to autotrophic growth
  - BBM (Bold's Basal Medium)
  - Aerated with Ambient CO_2

Chlorella protothecoides - Autotrophic & Heterotrophic

Algal Biotechnology Alliance

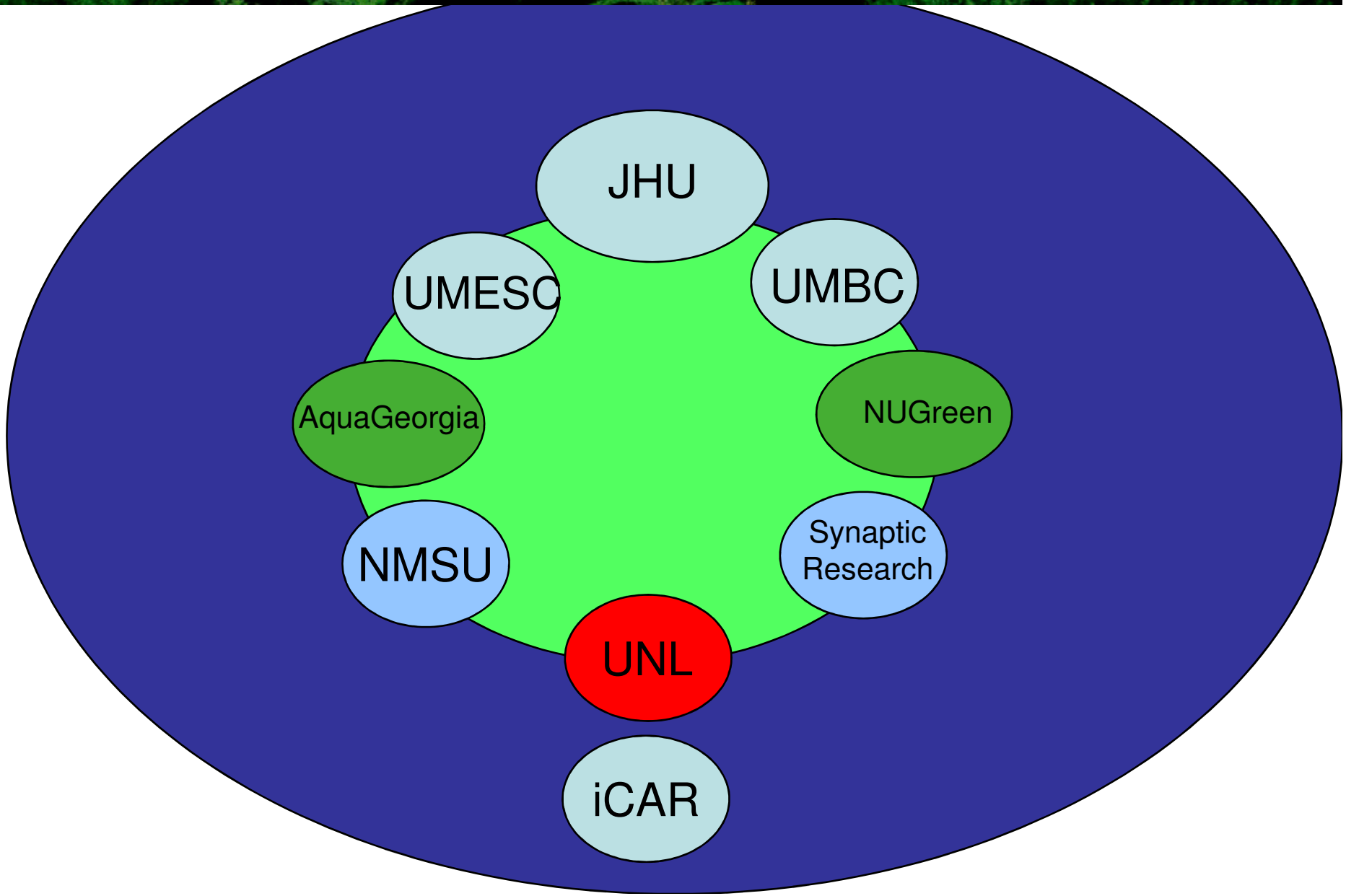

Insect and Mammalian Metabolic Processing Diverges in Golgi

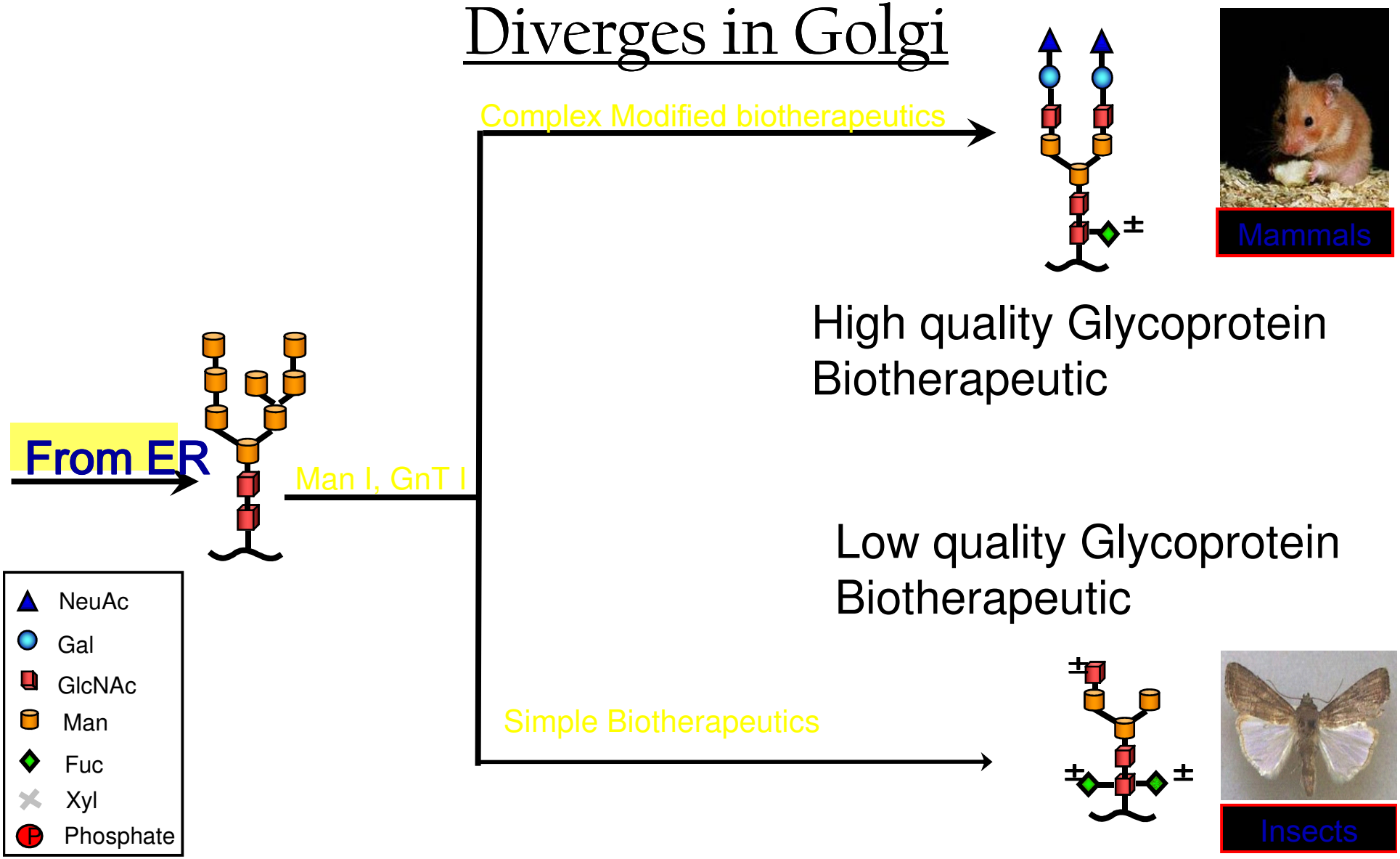

Metabolic Flux Analysis

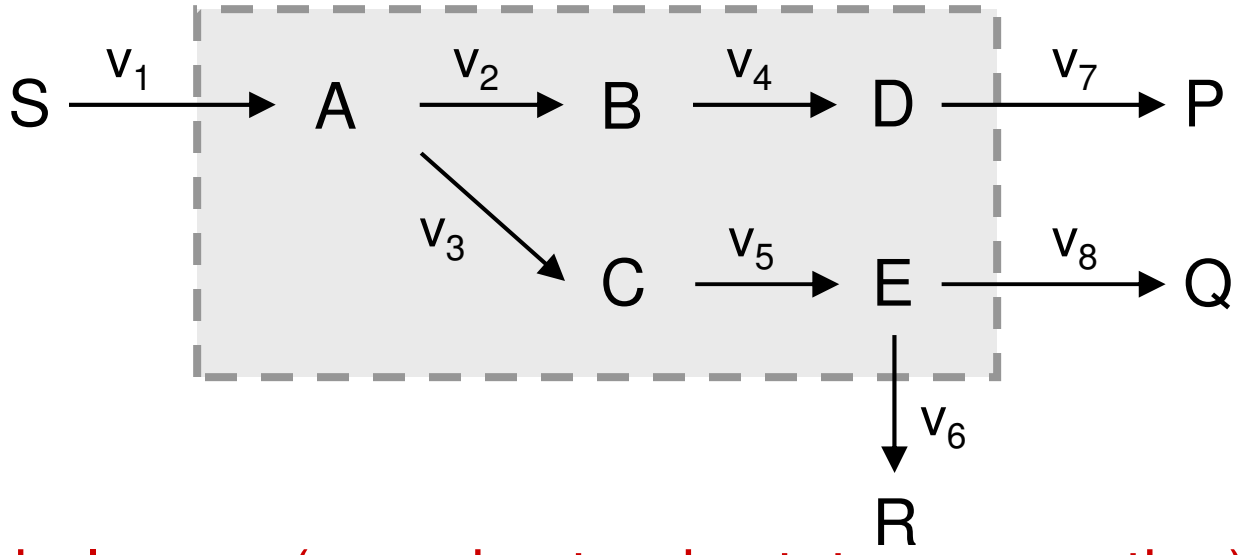

Metabolite balances (pseudo steady state assumption):

Balance for A : v1 = v2 + v3 (FLUXES IN = FLUXES OUT)

Balance for B : v2 = v4

Balance for C : v3 = v5

Balance for D : v4 = v7

Balance for E : v5 = v6 + v8

Collaborator: Maciek Antoniewic, University of Delaware


100 ml
APPROX.
80
60
40

Biodiesel is a fatty acid ester with a short carbon alcohol (methanol or ethanol). The conversion is accomplished by transesterification.

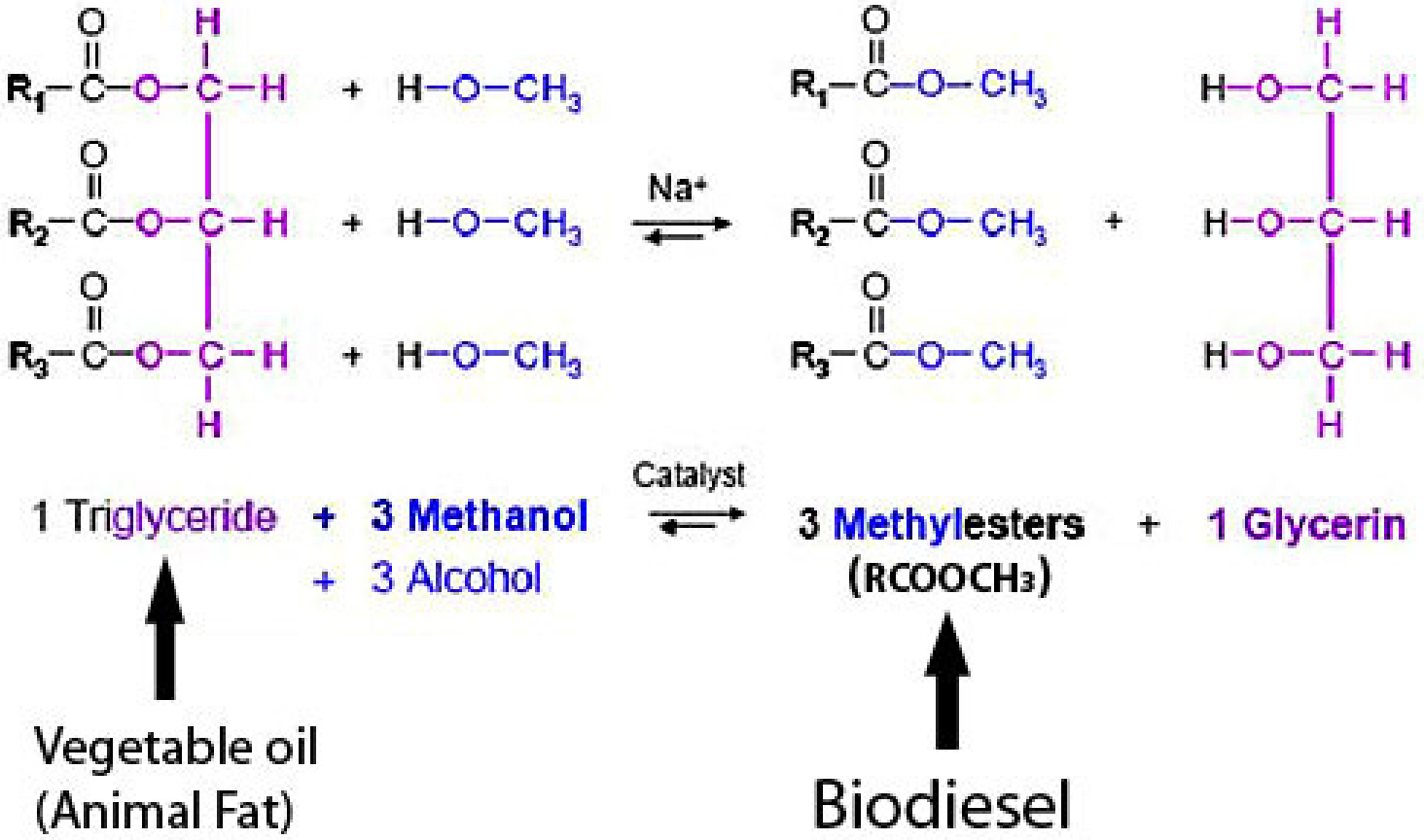

Dry Weights & Relative Lipid Content

Nile Red Fluorescent Analysis of Neutral Lipids

***Chlorella* spp. Dry Weights**

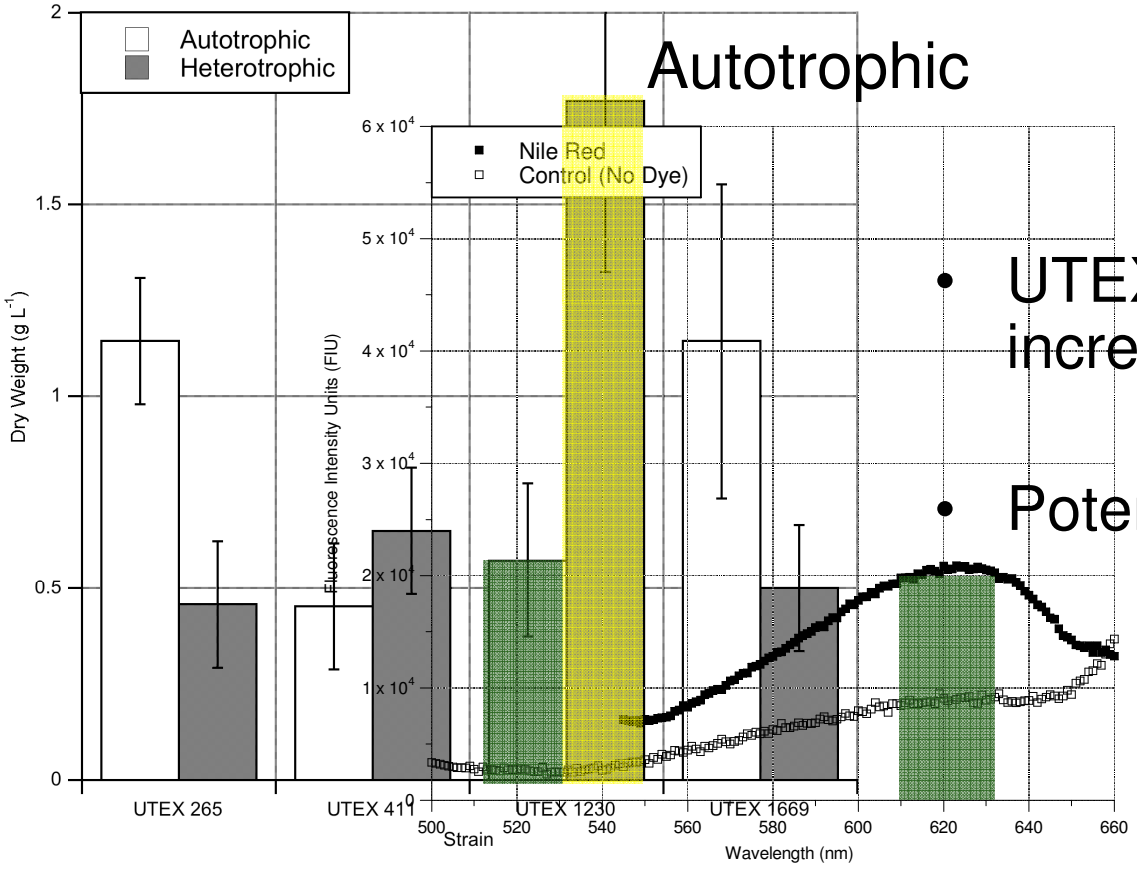

Autotrophic

Heterotrophic

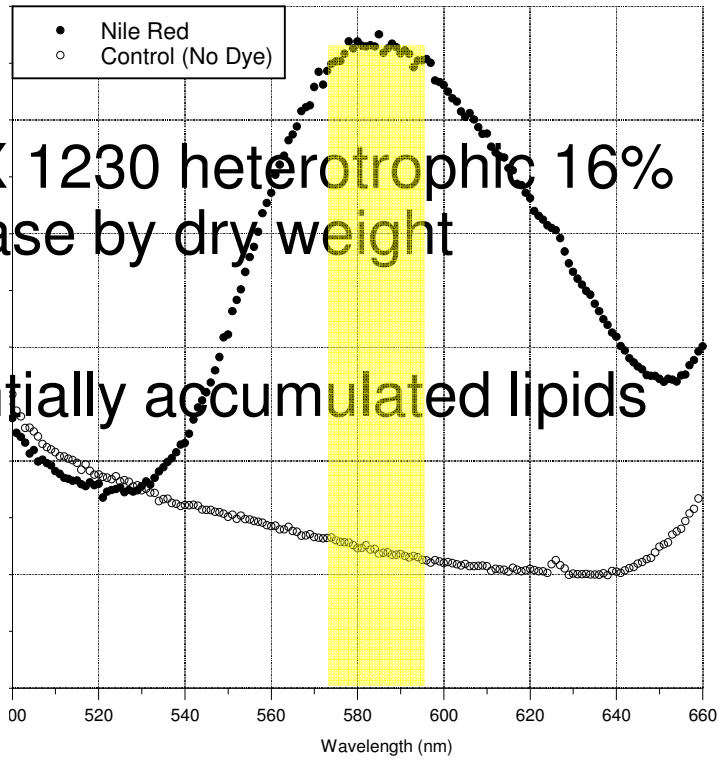

- UTEX 1230 heterotrophic 16% increase by dry weight
- Potentially accumulated lipids

NR: Excitation = 486 nm, Emission = 570-590 nm

Chesapeake Bay offers great potential for application of Algae Technology

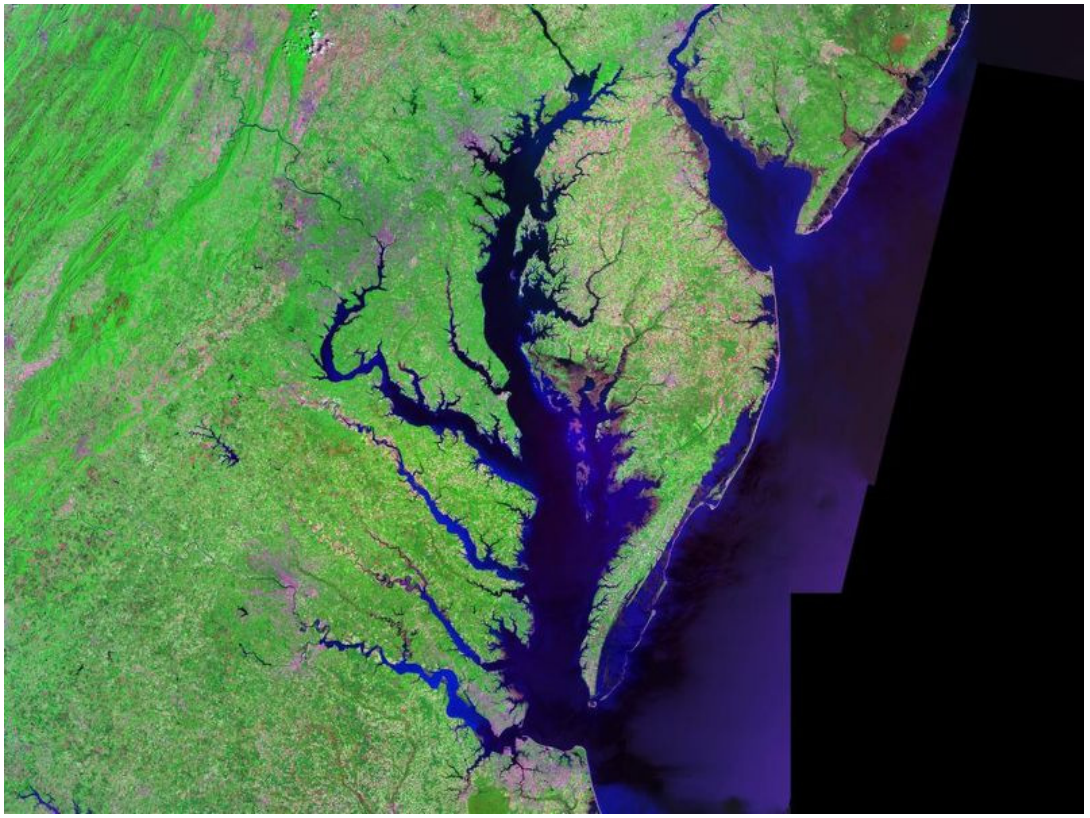

Focus on environmental improvement with algal systems as well as biofuels and coproducts

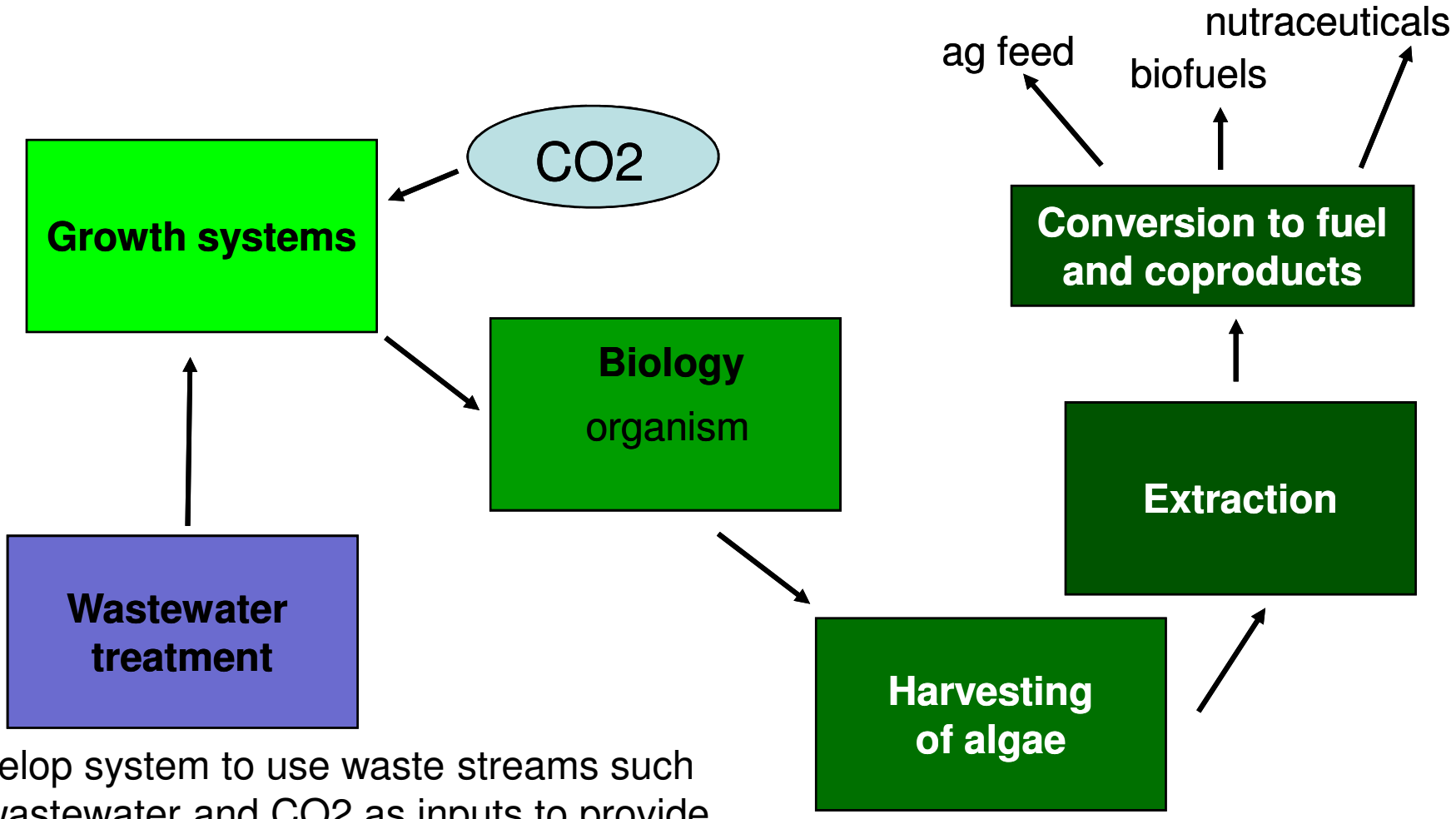

Develop system to use waste streams such as wastewater and CO2 as inputs to provide environmental improvement.

Develop for co-products leads to multiple value streams.

Algae have the great potential biofuels yield

Table 1 Potential oil yields per acre per year

Crop	Gallons of oil/acre/year
Soybeans	43
Sunflower	86
Canola	171
Jatrjopha	214
Palm oil	641
Microalgae	up to 6,000 (with future technology)

Algal Biotech focus on Chesapeake

- Improve water quality while enhancing economic viability of Chesapeake basin development.
- Support sustainable agriculture
- Reduce greenhouse gas emissions
- Provide significant biofuels to reduce dependence on fossil fuels

Technology under consideration will be usable throughout the United States and world-wide

Photobioreactor design and growth systems keys to economic viability

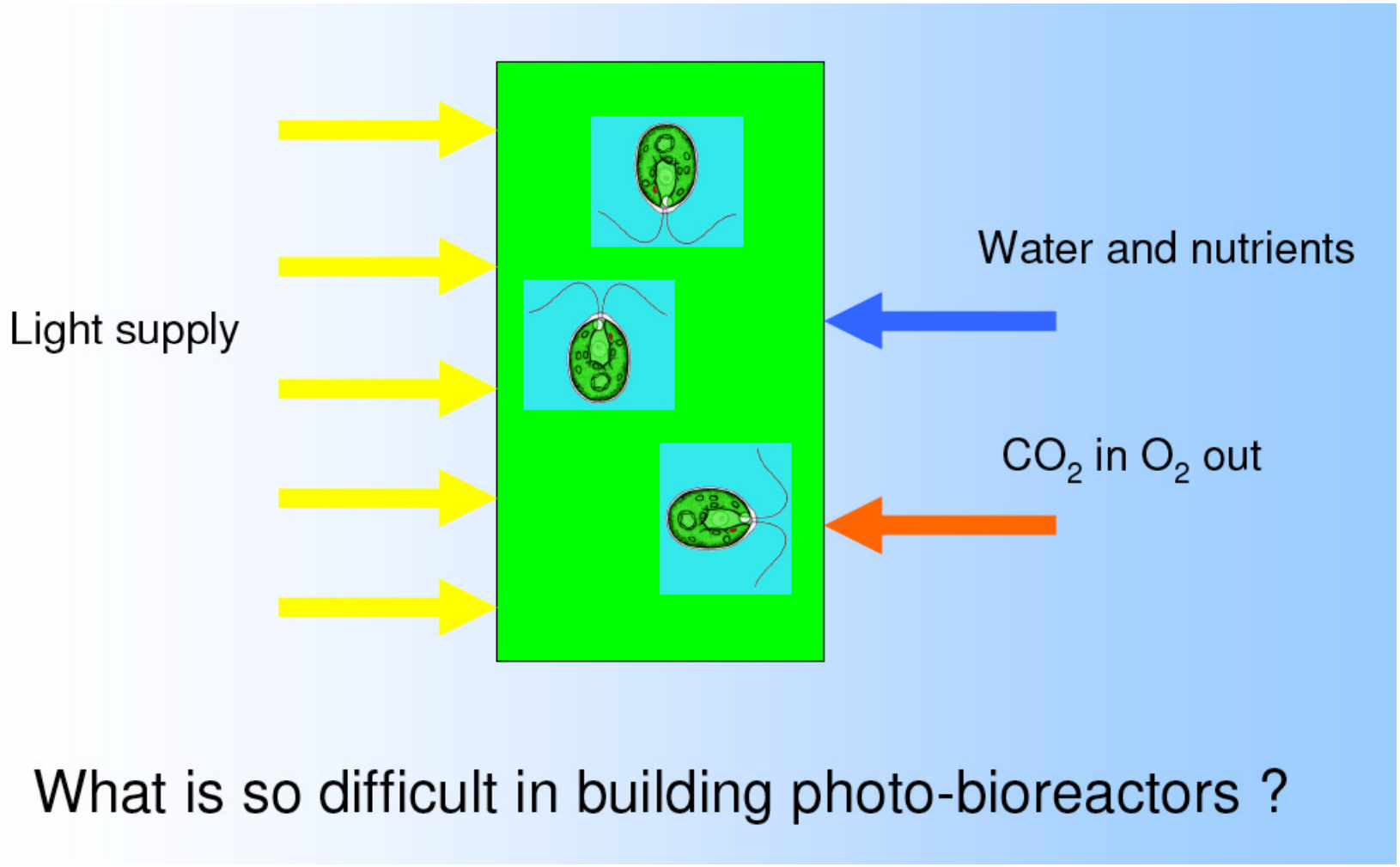

A focus of the JHU Critical Pathway will be PBR development

Why Algae for Biofuels?

Algae have great potential in biofuels and GHG abatement

Caveats:

- Despite these virtues, algae biofuels are not yet economically viable.
- Major breakthroughs in both engineering and biology are required.

JHU and ABA will apply a Critical Pathway approach to providing transformational algal biofuels technology.

Algae Biotechnology and Chesapeake Bay Preservation

- Largest Estuary in US with large diverse ecosystem but under stress.
- 8 Billion spent over 10 years for environment remediation – will continue to grow.
- Nitrogen run off and input from development and agriculture important sources.
- CO2 Emissions from energy production are important concerns.
- Chesapeake Bay region rich in biotechnology base.

- Most recently EPA has assumed clean-up authority!

CONCLUSIONS FROM *CHLORELLA* STUDY

- Characterized four *Chlorella* strains auto- & heterotrophically
- Recognized diversity of algal strains within species
  - *C. sorokiniana* UTEX 1669 & UTEX 1230
- Desire to study genetics of *Chlorella* spp.
  - *Chlorella* virus host NC64A genetics
  - Need strain specific genomic information

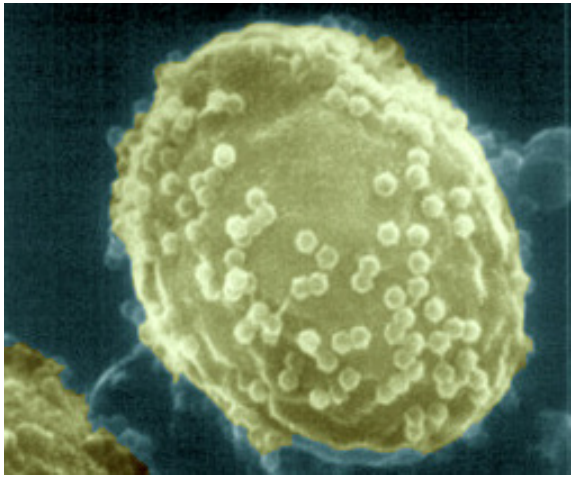

Chlorella sp. NC64A infected with surface-bound virus particles

Growth System: 2 stage Concept for Wastewater Treatment

Photobioreactor: highly controlled monoculture

Raceway: high nutrient influx and polymicrobial community with wastewater input. Maintain a relative monoculture due to high inoculum from PBR.

Images from Lab of Dr Boussiba, MBL, Ben Gurion University

Hypoxic Zones : Algal environmental enhancement and Biofuels production can have worldwide impact

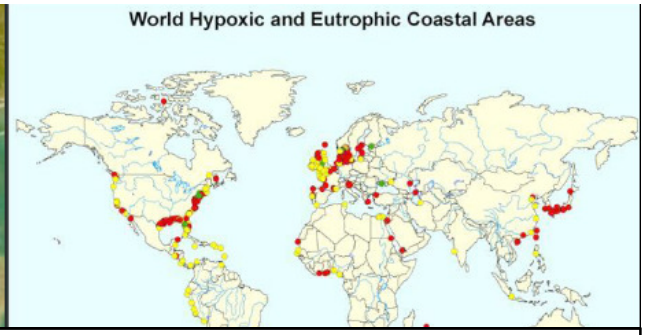

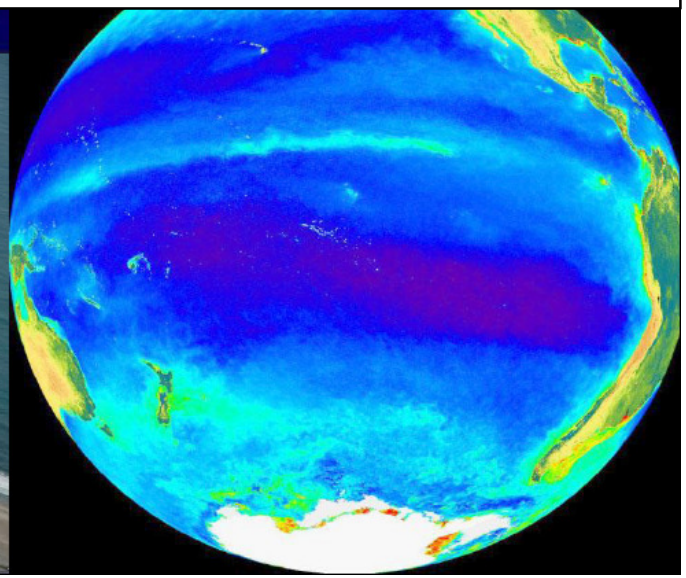

JHU AND ABA Algal Environmental Enhancement Vision

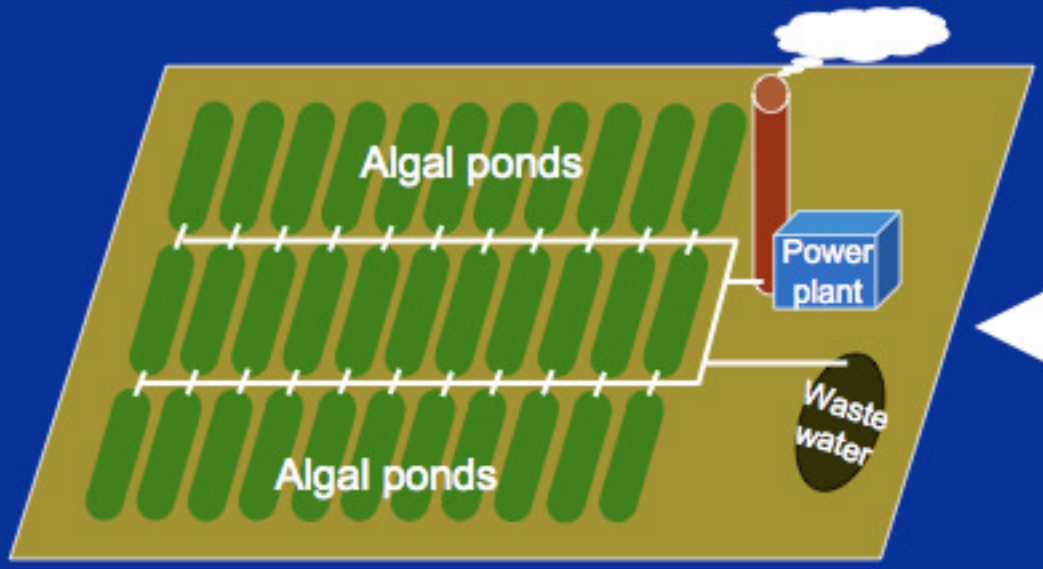

Adapted from Feng Chen, COMB

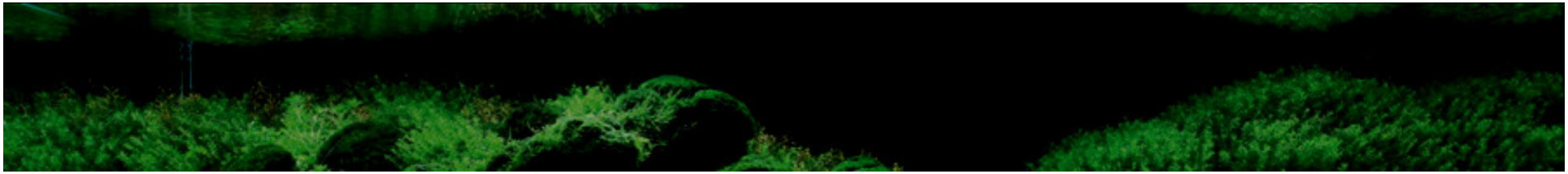

Algae have great potential in biofuels and green house gas abatement

- High potential biofuel productivity.
- Algae sequester CO_2 from a point source of emission.
- Algae do not compete with food crops.
- Algae do not require premium farm land.
- Algae can grow on waste, salty, and brackish water.
- Algae for wastewater treatment offers value added potential.
- Algae biomass for aquacultural and animal feed.

Algae Bioprocessing Issues

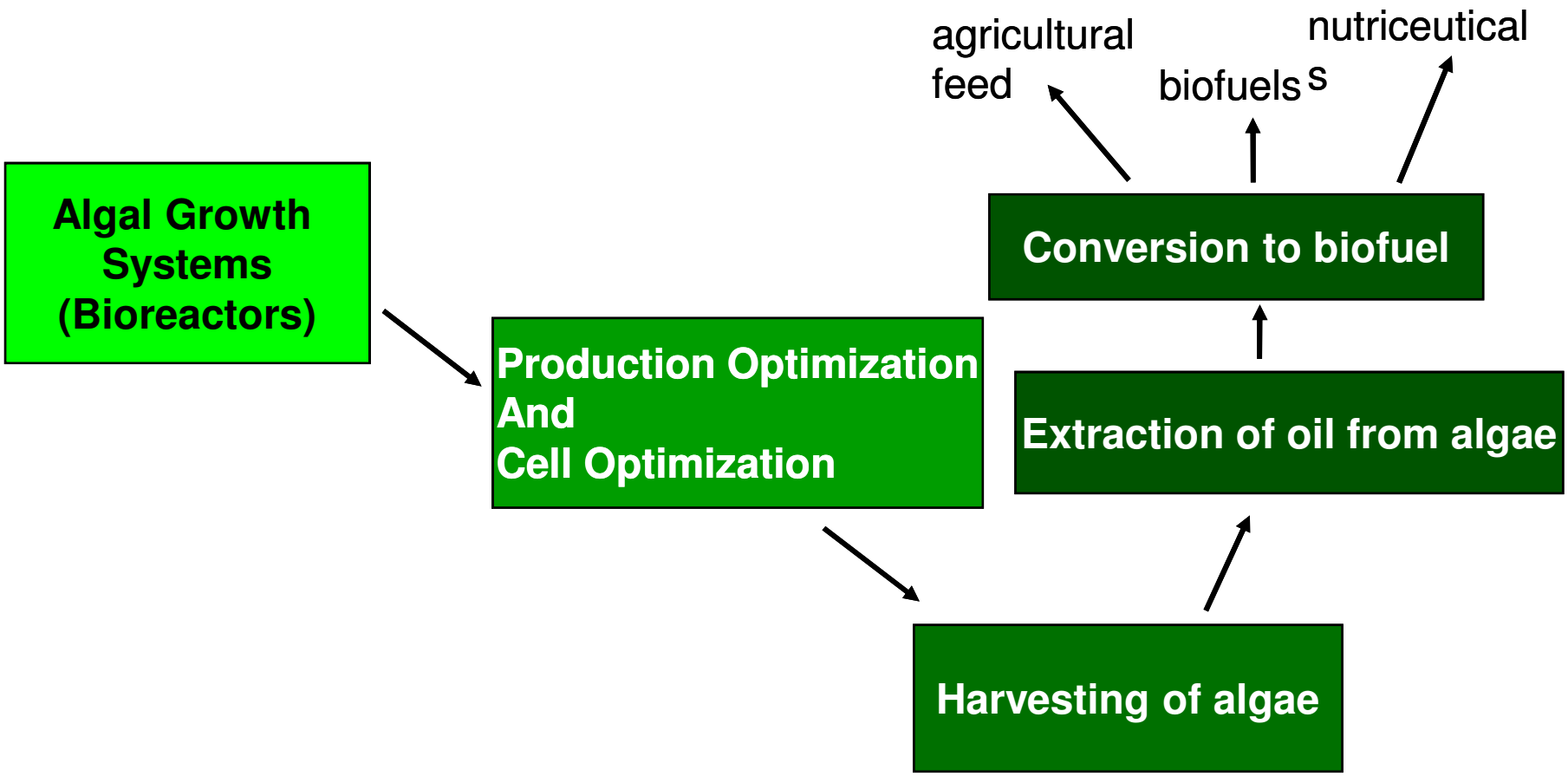

- Technological and biological barriers at many levels.
- Solution: Systems integration and Analysis of Multiple Issues

Comparing Expression Systems: An Engineering Problem

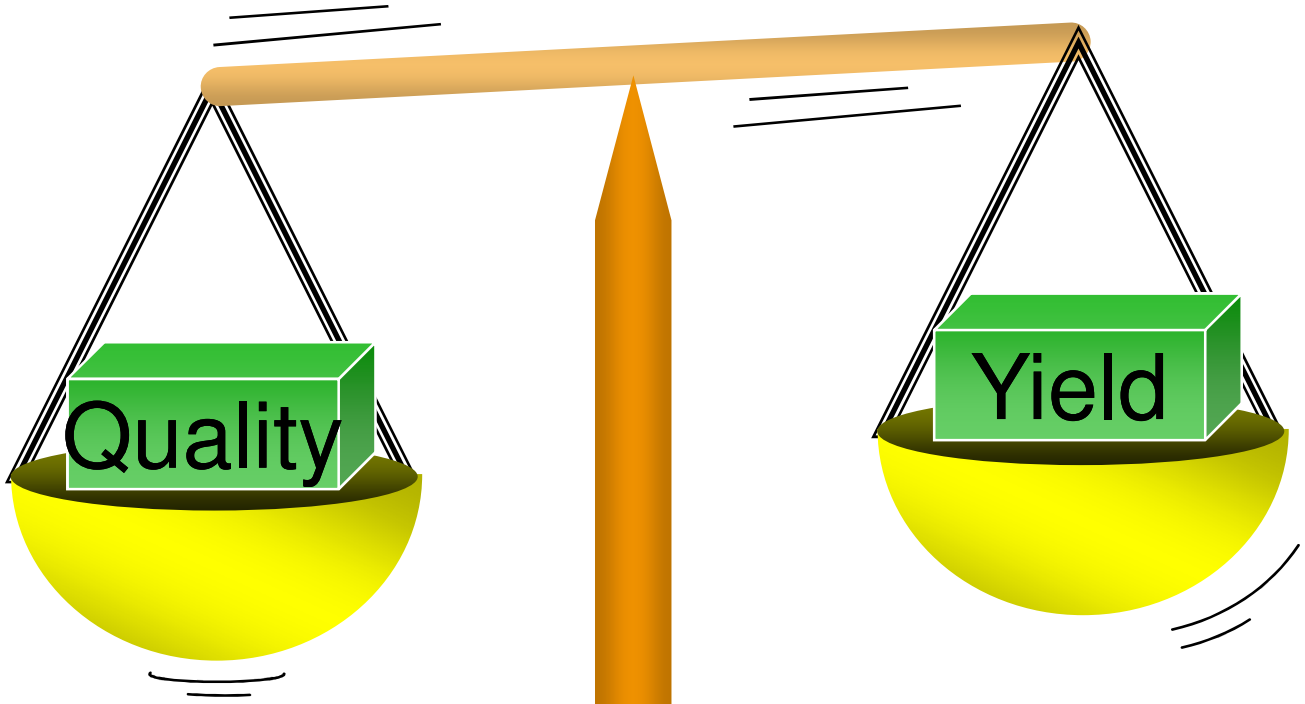

Desirable product properties

Efficient and inexpensive production scheme

Some Glycosylation Observations

ß4 GlcNAc from MGAT3:

No observed bisecting (ß4) N-acetylglucosamine (found on 10% of human IgG glycoforms)

MGAT3 observed in genome, but not transcriptome

Fucosylation:

Most mammals have 5 primary types:
α(1,2), α(1,3), α(1,4), α(1,6), and protein O-fucosyltransferases

Only α(1,6) and protein O-fucosyltransferases expressed.

Sialylation:

CHO K1 homologs to all six human ST3Gal enzymes (α(2,3)) sialic acid to galactose.) All expressed.

CHO K1 homologs to human ST6Gal genes (α(2,6)) but not expressed.

CHO Genome Assembly Strategy

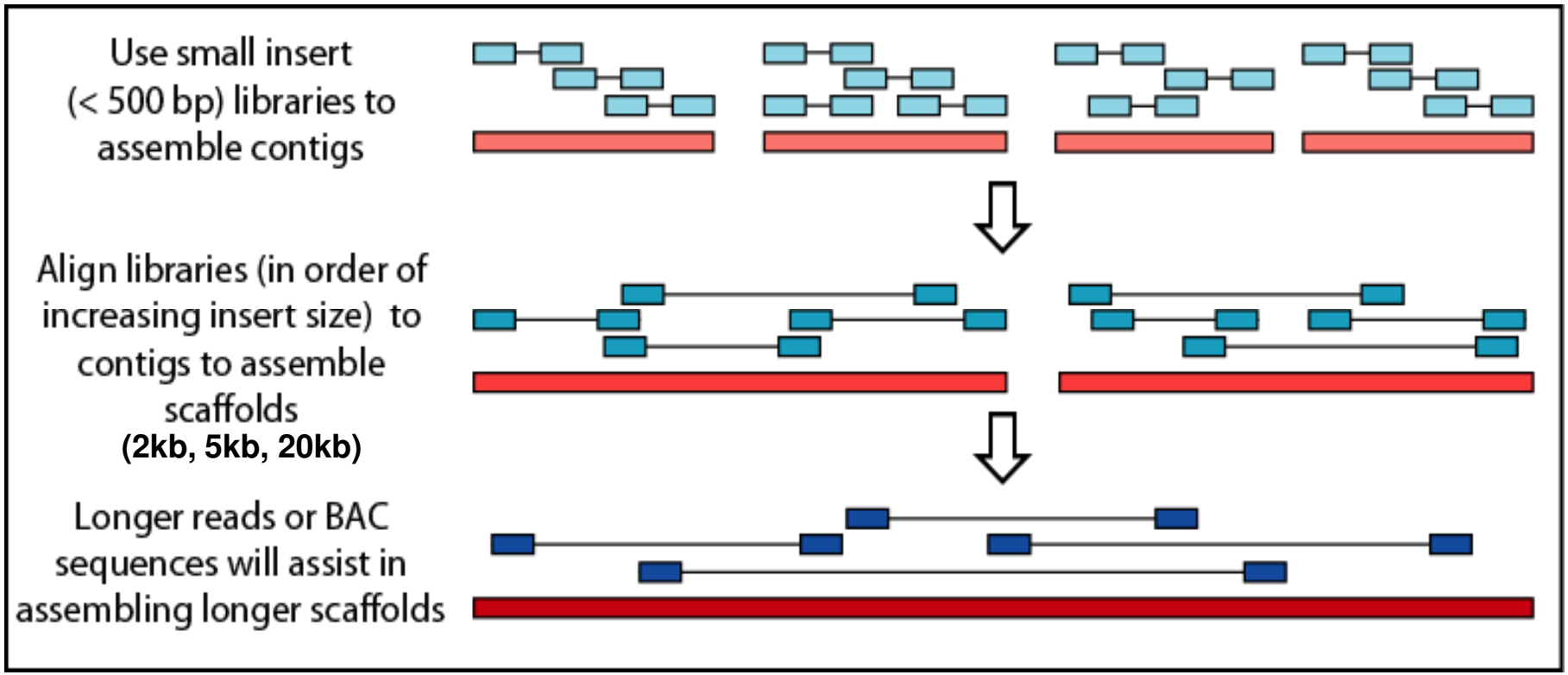

Comparative Genomic Features

	CHO-K1	Mouse	Rat	Human
Genome size	**2.6 Gb**	**2.6 Gb**	**2.75 Gb**	**2.9 Gb**
Chromosomes (2n)	**21**	**40**	**42**	**46**
Average GC content	**41.3%**	**41.5%**	**41.8%**	**40.9%**
Repeat content*	**38%**	**37%**	**40%**	**46%**
Predicted genes^	**24,383**	**21, 662**	**22, 416**	**20, 935**

*Repeat content: RepeatMasker against Repbase transposable element library and RepeatModeller to construct *de novo* repeat library.

^Genscan, Augustus, GlimmerHMM to predict genes which are aligned to Ensembl rel. 58). GLEAN used to reconcile gene set that was augmented with transcriptome data using Tophat and Cufflinks.

Xu et al (2011)

Global Analysis of Viral Resistance

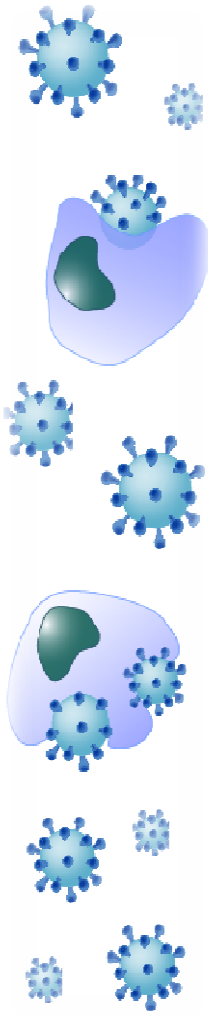

CHO genome contains homologs to 99% of the ~388 human genes important for viral infection (IL1A, SNRPC, MT1X, CD58)

CHO cells express ~ 60% of these genes (226 of 384)

Viral resistance due to reduced expression (GO)

- Glycoprotein binding, T-cell activation.
- Membrane receptors and cell adhesion molecules
- Genes involved in T-cell activation
- EGFR expressing CHO cells susceptible (HSV entry), but wildtype CHO resistant.

Xu et al (2011)

CHO Genome: Where do we go from here?

It's time to open up the black box of CHO

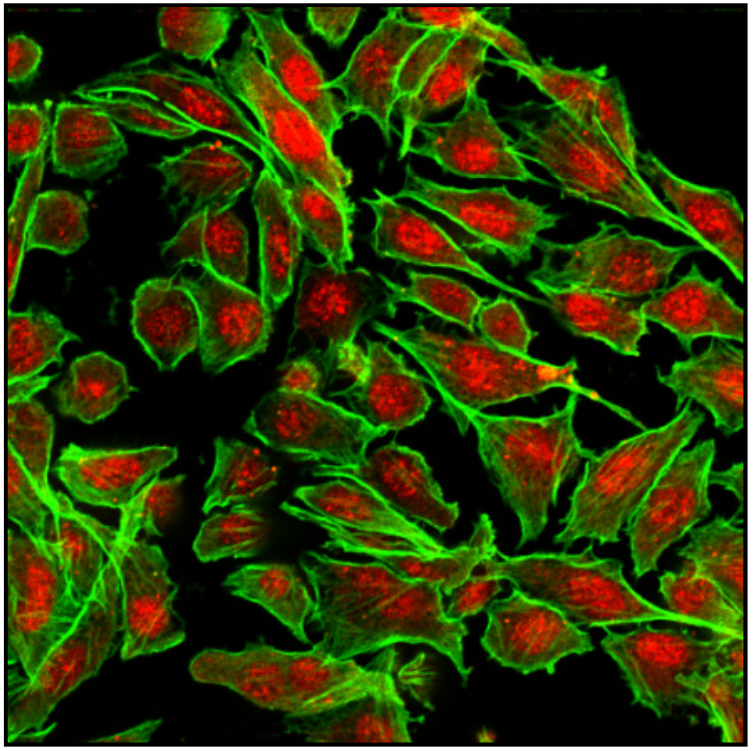

The Next Phase for CHO-Understanding and Improving Your Production Machinery

CHO protein expression

- We screen thousands of hosts for optimal producers
  - What are the genetic causes for enhanced production
  - Can we incorporate these improvements into future hosts
  - What are the best “hot spots” for expression and why
- Gene expression and regulation
  - Transcriptome sequencing
  - Small RNA and microRNA discovery
- Genome sequencing and assembly
  - Global analysis of pathway function and regulation
  - Understanding metabolic and signaling pathways
- Cell Engineering to upregulate or downregulate targeted pathways

Gene Annotation

Genes functionally annotated using Swissprot, GO, TrEMBL, InterPro, and KEGG.

83% of CHO-K1 genes were functionally annotated.

Significant coverage (GO) of translation, metabolism, and protein modification compared to human and mouse.

Less coverage of human/mouse genes for behavior, embryo development, and anatomical structure morphogenesis.

Xu et al (2011)

Comparative Analysis of Gene Function

Functional Analysis of CHO Genes

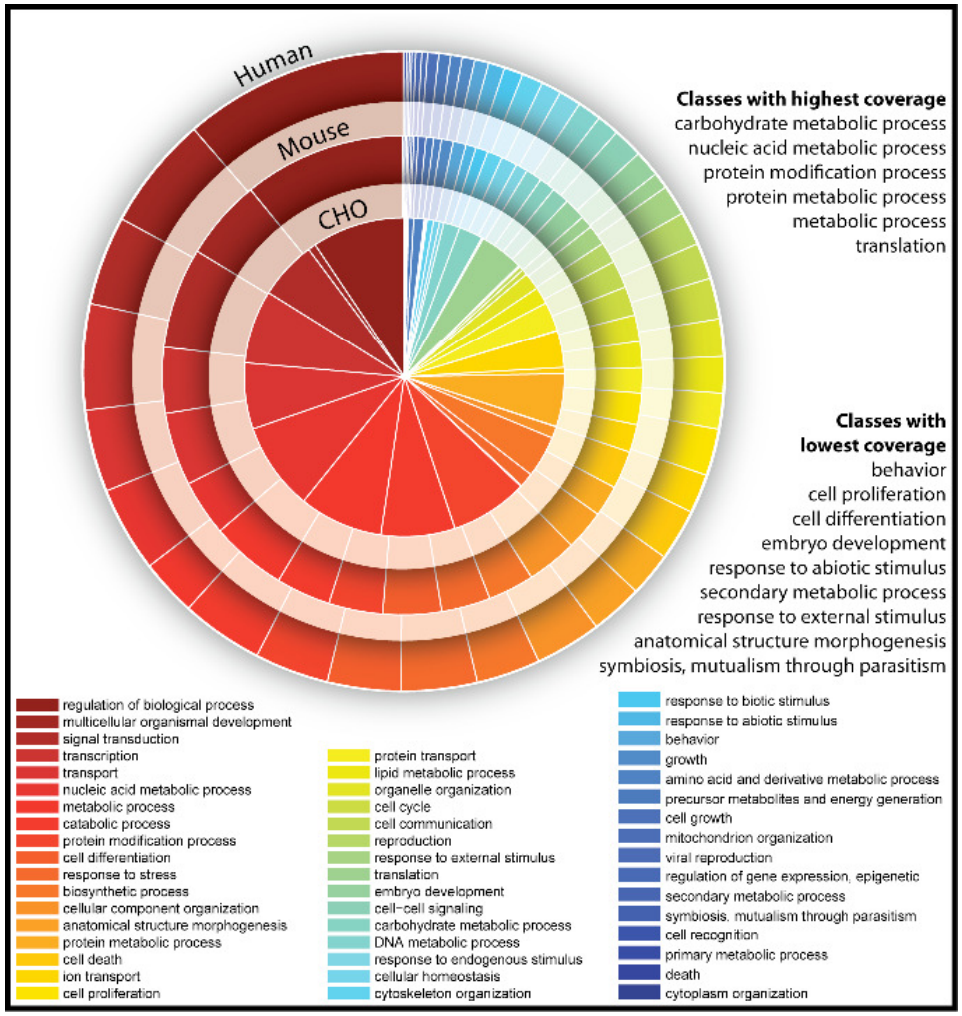

Orthologous Clusters

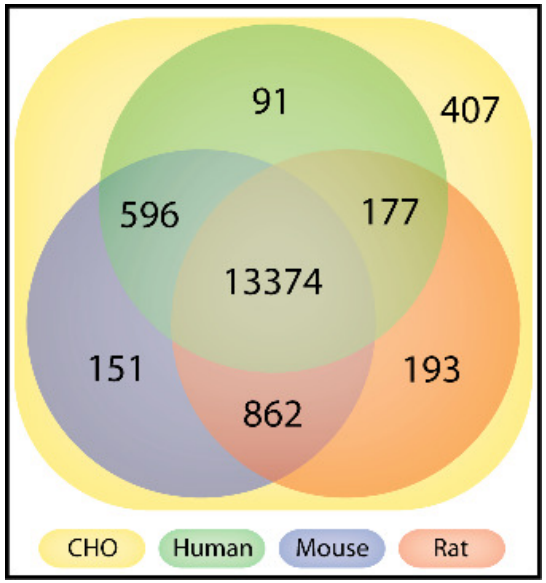

80-87% of genes have orthologs.

2428 Gene clusters contained human, mouse, and rat, but not CHO K1.

Xu et al (2011)

The International Community's assembled to sequence the CHO Genome

BGI: Xu Xun, Shengkai Pan, Xin Liu, Wenbin Chen, Min Xie, Wenliang Wang, Jun Wang

UCSD / GT Life Science: Harish Nagarajan, Nate Lewis,
Iman Famili, Bernhard Palsson

Stanford University: Norma Neff, Benjamin Passarelli, Winston Koh, Steve Quake

Johns Hopkins Univ: Michael Betenbaugh, Amit Kumar

DTU: Mikael Andersen

Delaware / Cornell: Kelvin Lee, Stephanie Hammond,

CHO K1 Genome Assembly and Annotation

- CHO-K1 (ATCC CCL-61)
- CHO-K1 genome sequence
  - Total of 343 Gb sequence generated
  - >95-fold coverage of the CHO genome
- CHO-K1 genome assembly
  - 2.45 Gb of estimated 2.6 Gb genome assembled
- CHO-K1 genome annotation
  - 24,383 predicted genes
  - 29,291 predicted transcripts
  - 416 ncRNAs predicted

Xu et al (2011)

Chinese Hamster Genome Database

Chinese hamster database ver1.0

- **Host CriGri_1.0 genome assembly**
- **Sequence and annotation retrieved from NCBI, EMBL-EBI, and UniProt databases**

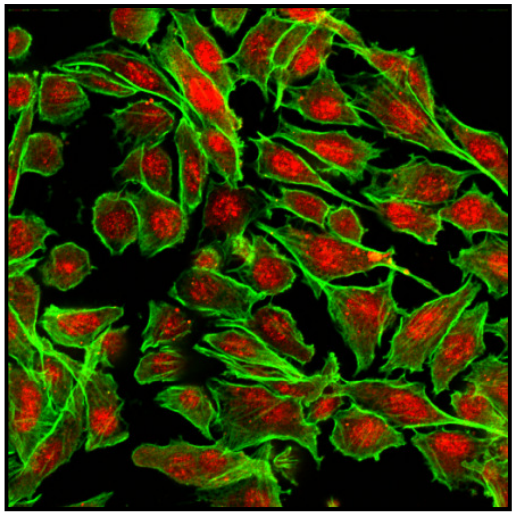

Current database contents

- 24,240 protein-coding gene products
- Gene symbols for 18,729 gene products
- Gene Ontology terms for 11,895 gene products

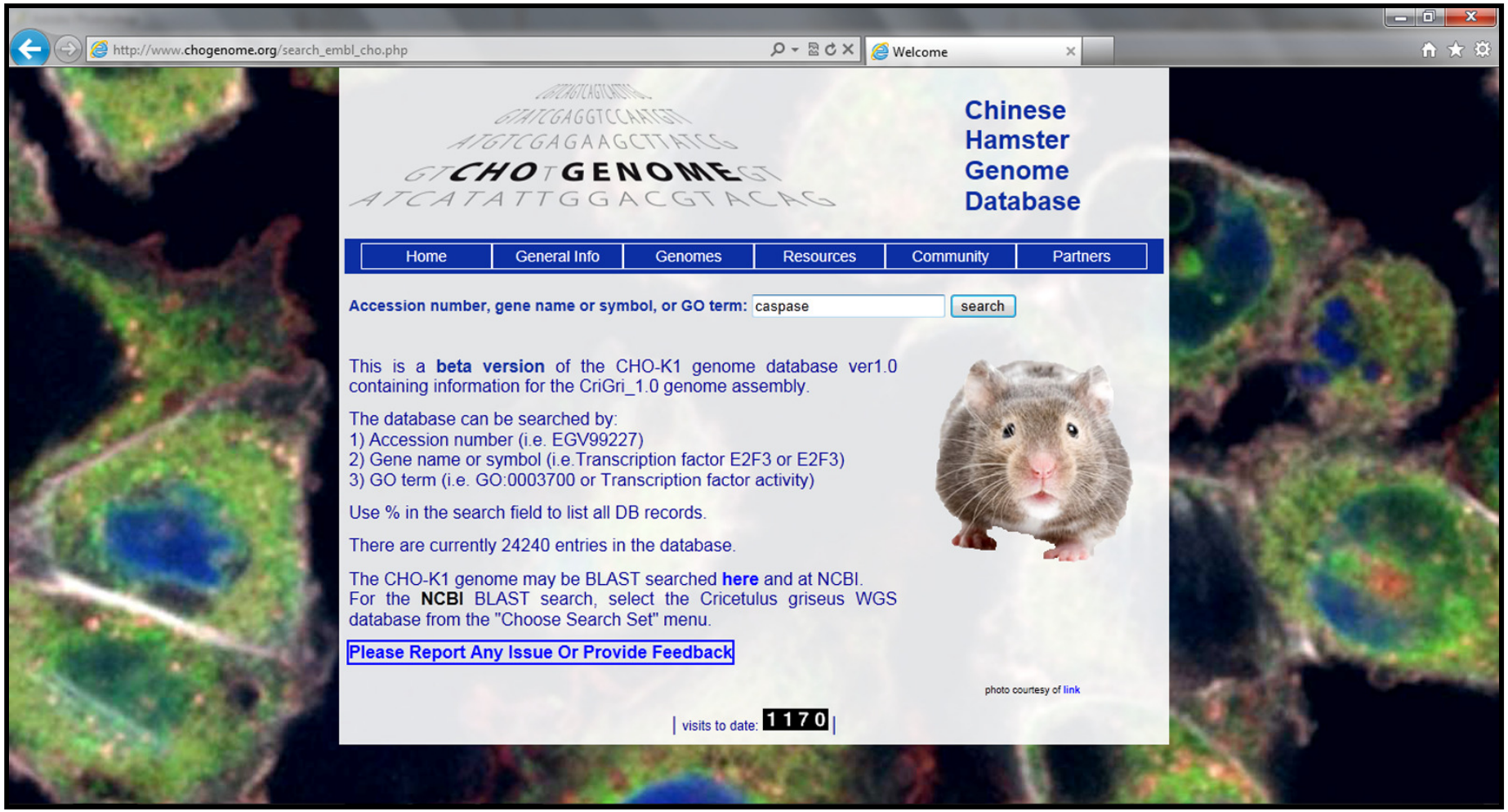
http://www.chogenome.org/search_embl_cho.php
Welcome
CHO GENOME
Chinese Hamster Genome Database
Home
General Info
Genomes
Resources
Community
Partners
Accession number, gene name or symbol, or GO term:
caspase
search
This is a beta version of the CHO-K1 genome database ver1.0 containing information for the CriGri_1.0 genome assembly.
The database can be searched by:
1) Accession number (i.e. EGV99227)
2) Gene name or symbol (i.e.Transcription factor E2F3 or E2F3)
3) GO term (i.e. GO:0003700 or Transcription factor activity)
Use % in the search field to list all DB records.
There are currently 24240 entries in the database.
The CHO-K1 genome may be BLAST searched here and at NCBI.
For the NCBI BLAST search, select the Cricetulus griseus WGS database from the "Choose Search Set" menu.
Please Report Any Issue Or Provide Feedback
photo courtesy of link
visits to date: 1170

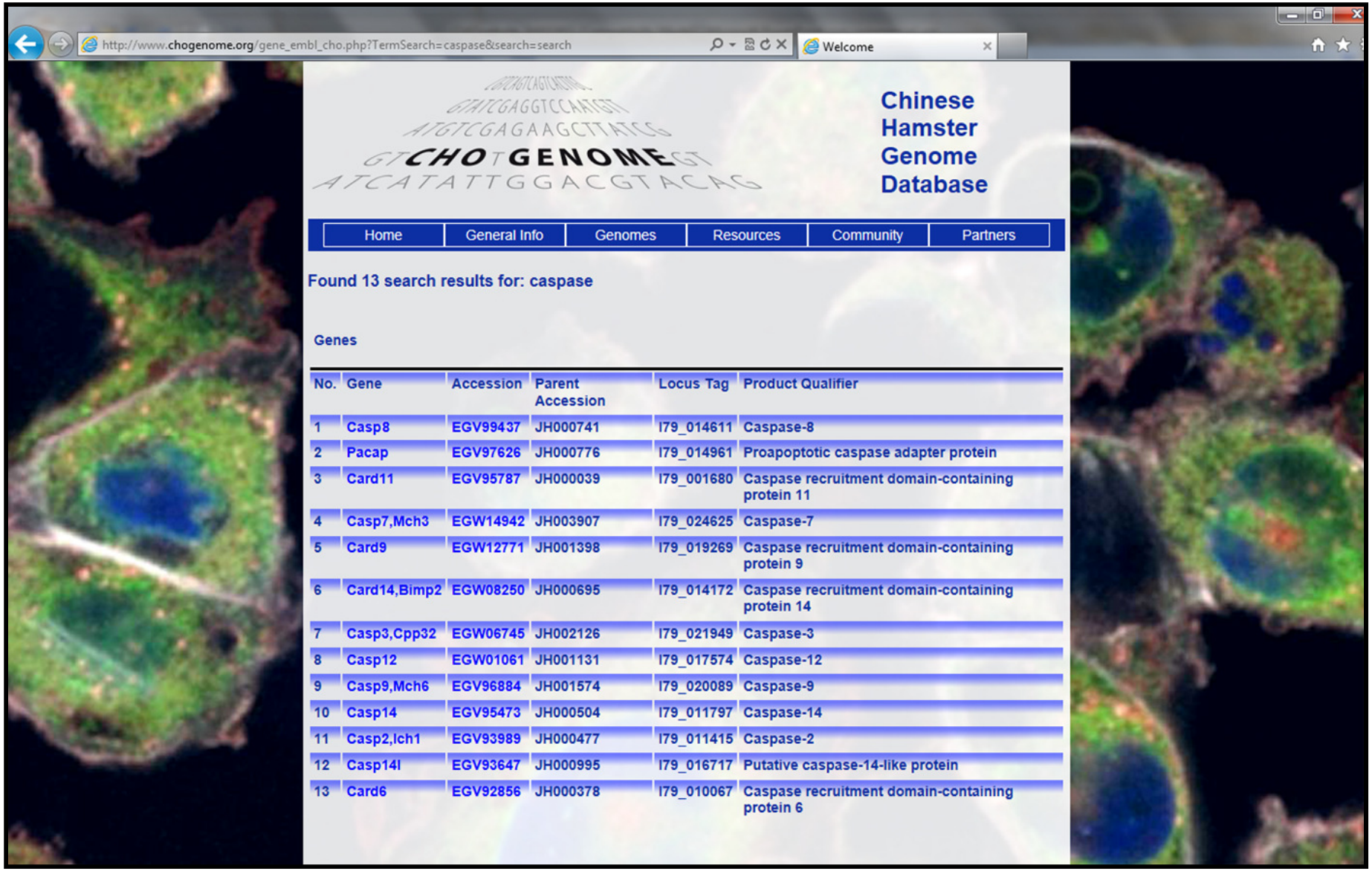

No.	Gene	Accession	Parent Accession	Locus Tag	Product Qualifier
1	Casp8	EGV99437	JH000741	I79_014611	Caspase-8
2	Pacap	EGV97626	JH000776	I79_014961	Proapoptotic caspase adapter protein
3	Card11	EGV95787	JH000039	I79_001680	Caspase recruitment domain-containing protein 11
4	Casp7,Mch3	EGW14942	JH003907	I79_024625	Caspase-7
5	Card9	EGW12771	JH001398	I79_019269	Caspase recruitment domain-containing protein 9
6	Card14,Bimp2	EGW08250	JH000695	I79_014172	Caspase recruitment domain-containing protein 14
7	Casp3,Cpp32	EGW06745	JH002126	I79_021949	Caspase-3
8	Casp12	EGW01061	JH001131	I79_017574	Caspase-12
9	Casp9,Mch6	EGV96884	JH001574	I79_020089	Caspase-9
10	Casp14	EGV95473	JH000504	I79_011797	Caspase-14
11	Casp2,Ich1	EGV93989	JH000477	I79_011415	Caspase-2
12	Casp14l	EGV93647	JH000995	I79_016717	Putative caspase-14-like protein
13	Card6	EGV92856	JH000378	I79_010067	Caspase recruitment domain-containing protein 6

Chinese Hamster Genome Database

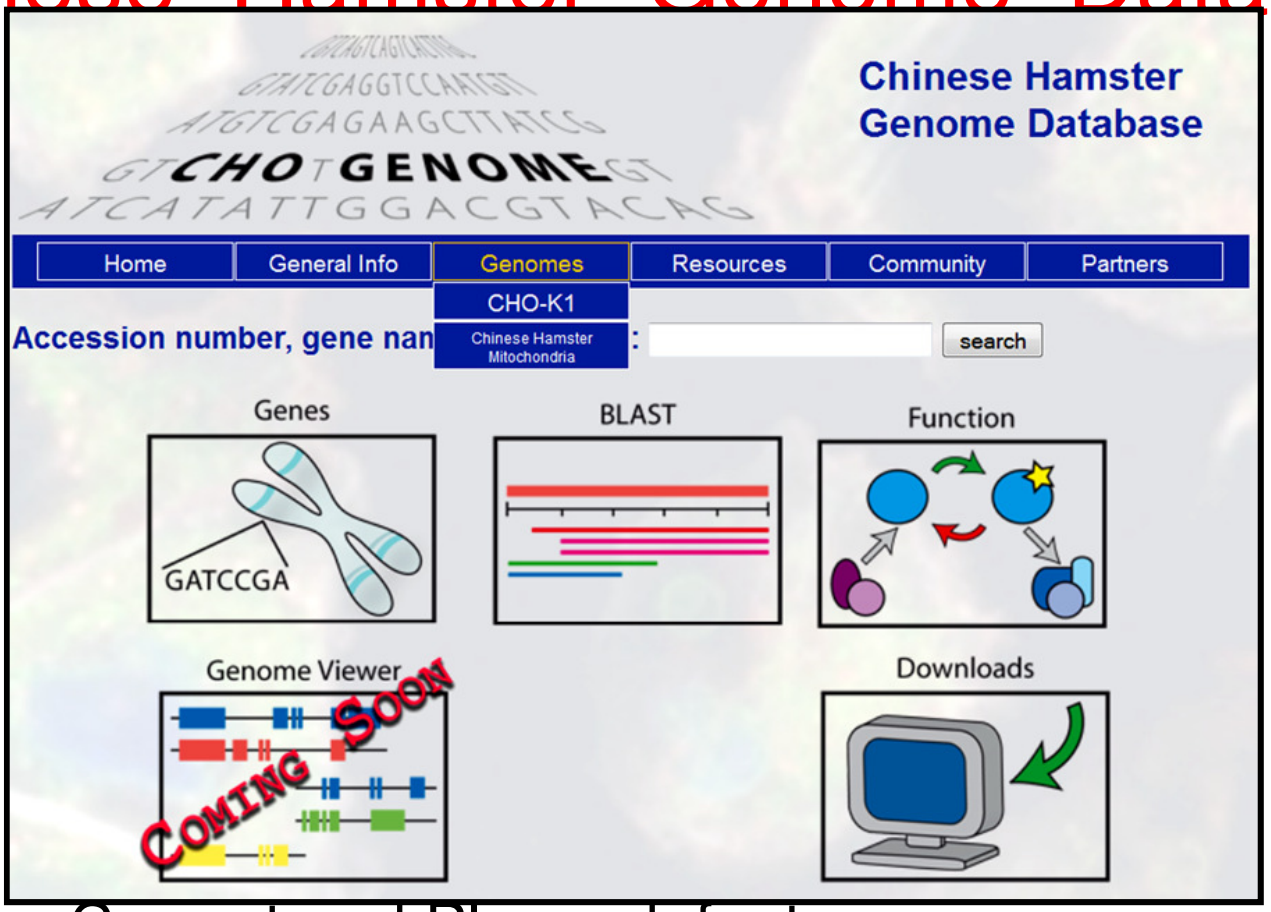

Current and Planned features:

- Host genome sequence
- Develop genome browser
- Integrate protein, transcript, metabolic data
- Provide community resources

Functional Analysis of Gene Expression

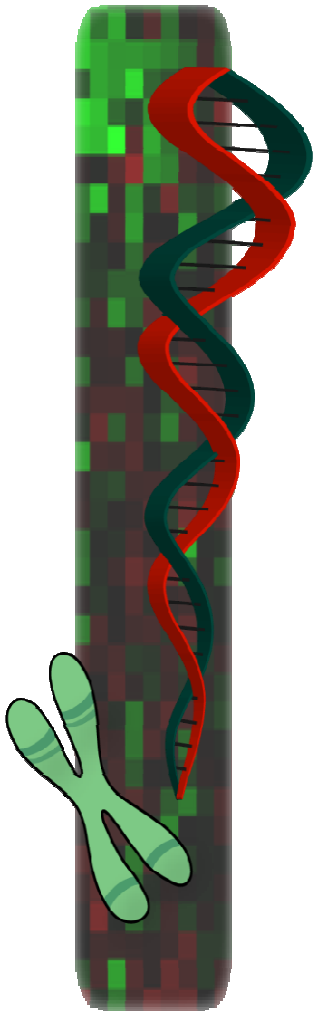

CHO cells are preferred hosts because

- Human-like glycosylation patterns
- Resistance to viral infection

Analysis of global gene expression

- Identify human genes in these pathways
- Look for CHO homologs in genome
- Examine gene expression using RNA-Seq data

Develop an organism database for CHO to facilitate

- **Improved understanding of your host organism**
- **Data accessibility for the CHO community**
- **Development of genome-scale tools**
- **Collaboration between groups**
- **Incorporation of new datasets**

Apoptotic Morphology in Cell Culture

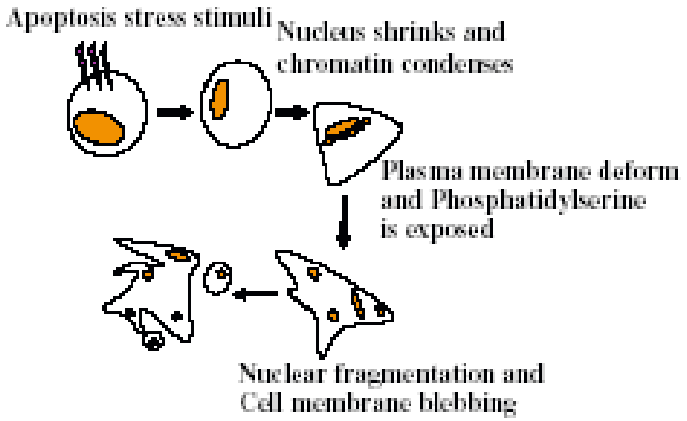

Fig. 1 Schematic describing the various morphological features associated with apoptosis. An initially healthy cell encounters either intracellular or extracellular stress leading to the initiation of apoptosis which is followed by cell and nuclear shrinkage. As the cell progresses to later stages of apoptosis, the plasma membrane begins to deform and the membrane lipid, phosphatidylserine is exposed. This is followed by nuclear fragmentation and the breaking off of the cell membrane also referred to as blebbing

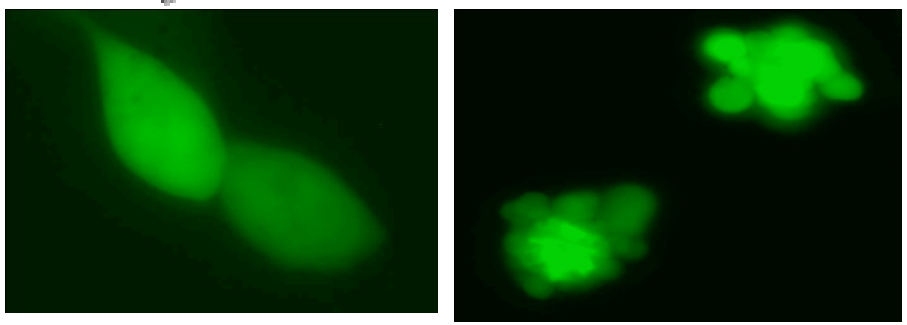

Wild type CHO Apoptotic CHO

Apoptosis is a genetically controlled process and can be morphologically recognized by cell and chromatin shrinkage followed by plasma membrane blebbing. Blebbing involves the shedding of membrane fragments from the whole in the form of apoptotic bodies that often include cytosolic and nuclear contents. Apoptotic Chinese hamster ovary (CHO) cells exhibiting membrane blebbing and chromatin shrinkage are compared to wild-type CHO cells either expressing

Targets of mmu-mir-466h

Mouse gene symbol	mmu-miR-466h binding site(s) in mRNA 3'-UTR	Anti-apoptotic role of targeted gene
bcl2l2	GCACAC TGCACA	Inhibits formation of permeability transition pore and release of cytochrome C by binding to bax
birc6	GCACA	Inhibits apoptosome by binding to active-site pocket of Caspase-9. Functions as E2 ubiquitin conjugase for Caspase-9 and Smac/Diablo.
dad1	2 of TGCACA	Component of N-oligosaccharyl transferase catalyzing transfer of oligosaccharide from lipid-linked donor to nascent polypeptide chain. Loss of dad1 triggers apoptosis
smo	TGCACAC GCACAC	Uninhibits gli-1 transcriptional factor which stimulates up-regulation of bcl2
stat5a	GCACAC	Stat5a dimers are transcriptional factors for *bcl-x*$_L$ and *bcl2* genes

Five anti-apoptotic genes :

stat5a, bcl2l2, birc6, dad1, smo

MicroRNA and Apoptosis Signaling

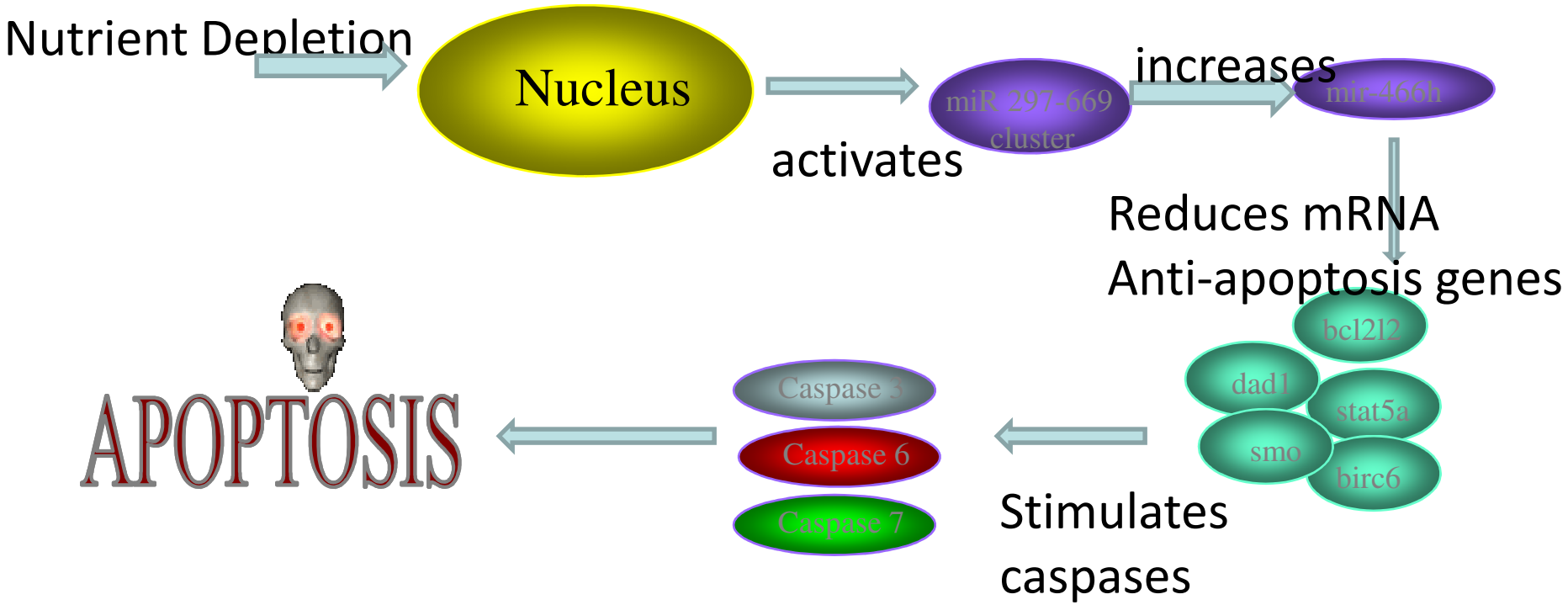

Chemical Inhibition of MicroRNA

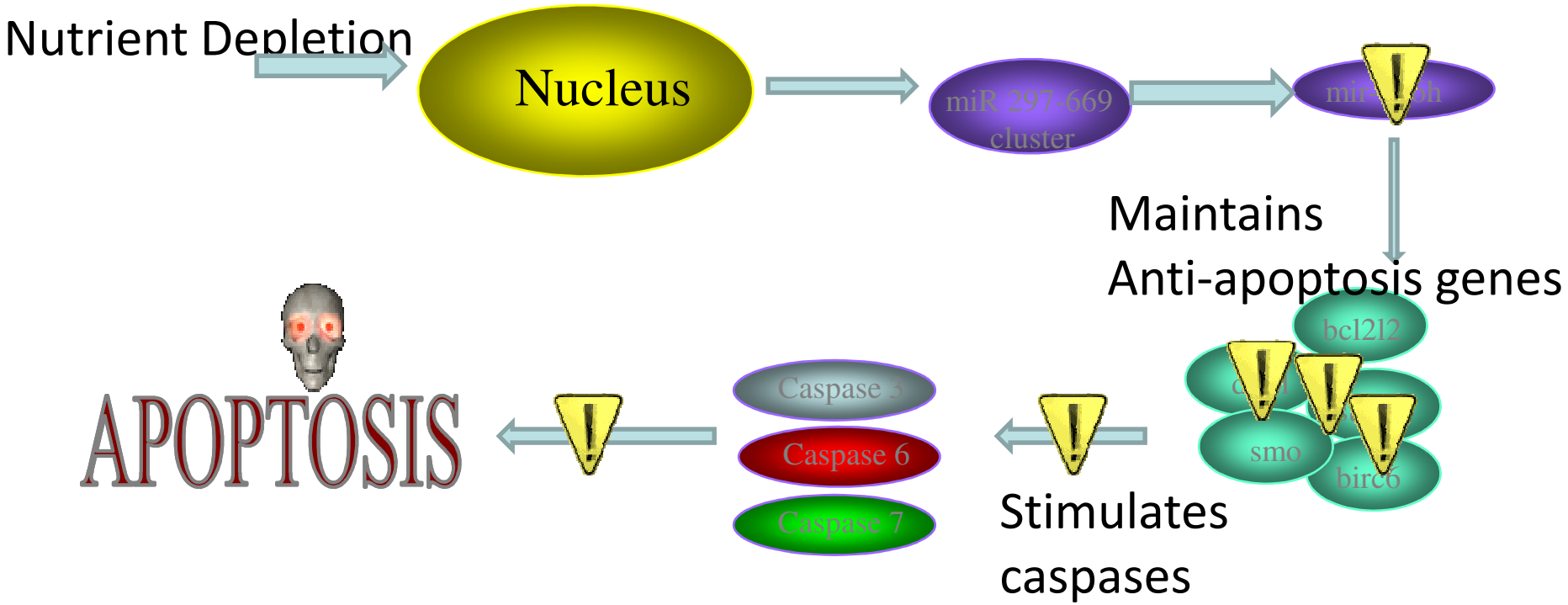

Concluding Remarks and Future Work

Conclusions:

- **MicroRNAs are activated in CHO cells under nutrient depleted conditions**
- **Many of these, including mmu-miR-466h and mmu-miR-669c, are contained within the mmu-297-669 microRNA cluster**
- **The microRNA mmu-mir-466h has a number of anti-apoptotic gene targets including bcl2l2, birc6, dad1, stat5a and smo**
- **Inhibition of mmu-miR-466h lowers CHO caspase activity and increases cell viability**

Future work:

- **Develop stress-tolerant CHO cell lines through continuous inhibition of mmu-miR-466h**
- **Identify genomic location and pathways for upregulation of pro-apoptotic microRNAs**
- **Examine the role of other microRNAs in CHO cells apoptosis and other cell functions**

Effect of Anti-apoptosis genes on survival

Abiotic stress imposition on pRelax transformants (UTEX 2244) to determine tolerance

- **NaCl**: 50mM, 75mM, 100mM, 150mM, 250mM

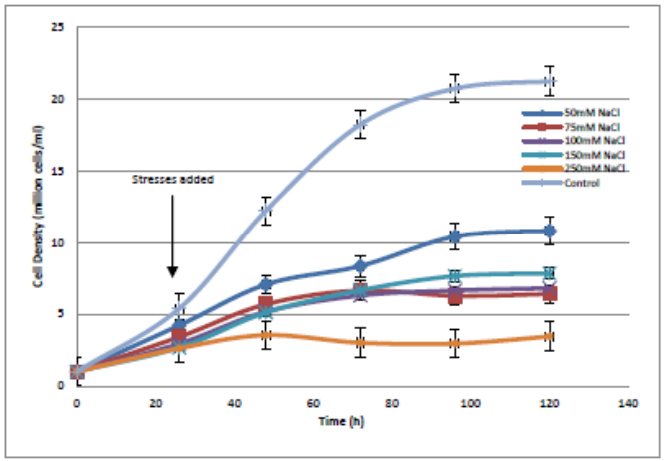

Figure 35: Wild-type *C.reinhardtii* exposed to NaCl over 5 days

Wild-Type

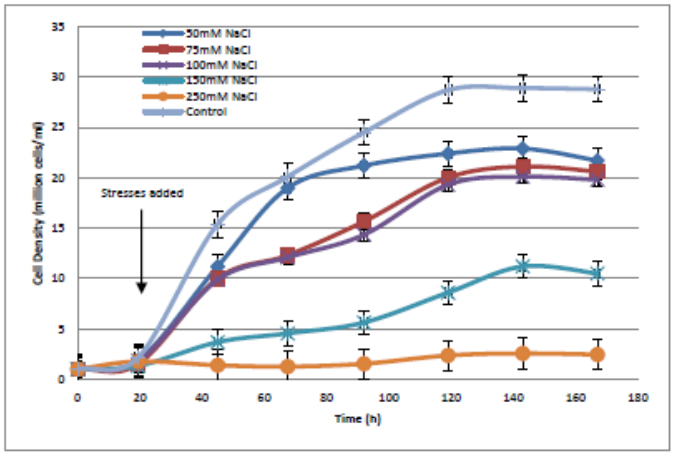

Figure 36: pRelax#2 exposed to NaCl over 7 days

pBclX-1

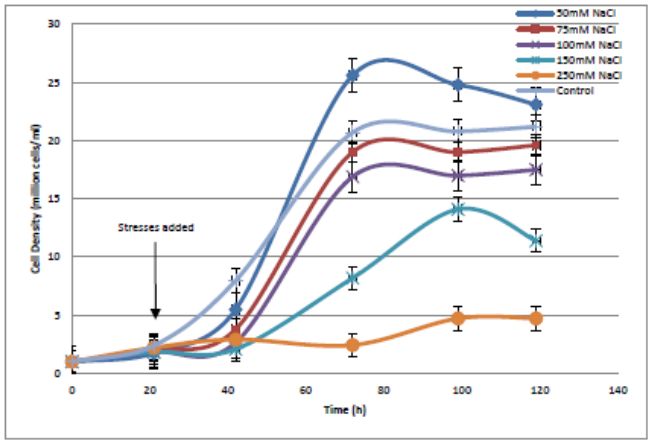

Figure 37: pRelax# 8 exposed to NaCl over 6 days

pBclX-2

Growth reductions:

- WT: 50.1% - 84.7%
- pBcl-x1: 12.8% - 82.9%
- pBcl-x2 22.9% - 92.7%

GENETIC TRANSFORMATION WITH BCL-X_L

- Microparticle Bombardment (Biolistic Transformation)
  - DNA-Coated Gold Particles, Diameter < 10 µm
  - Venus-Bcl-x (1.7 kb), Venus (1.0 kb), ble (0.75 kb)
  - Selection on 1 mg L^{-1} Bleocin Plates, 1 Week

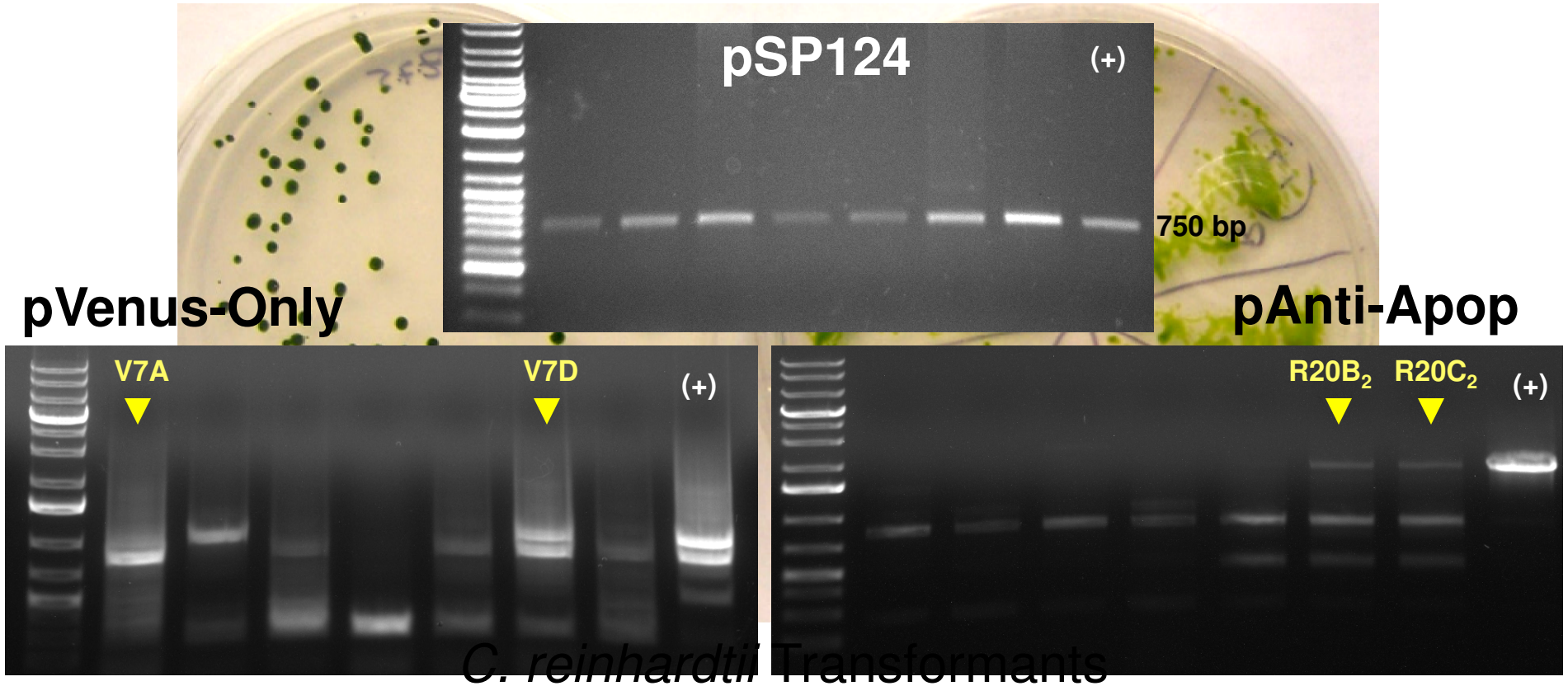

C. reinhardtii Transformants

Abiotic stress imposition on pRelax transformants (UTEX 2244) to determine tolerance

- **Peroxide:** 1mM, 2mM, 4mM, 8mM

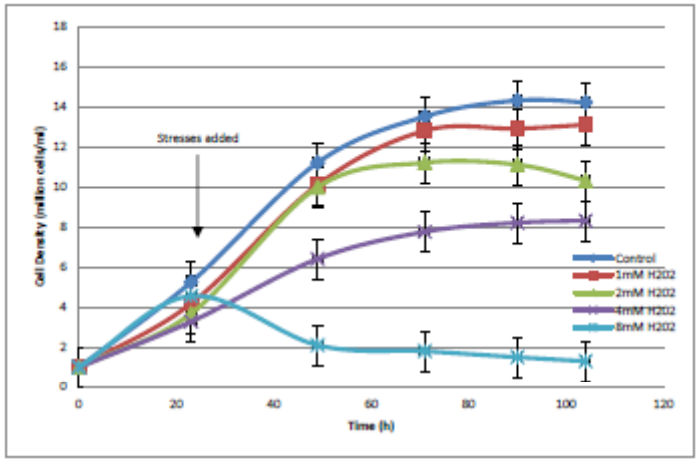

Wild-Type

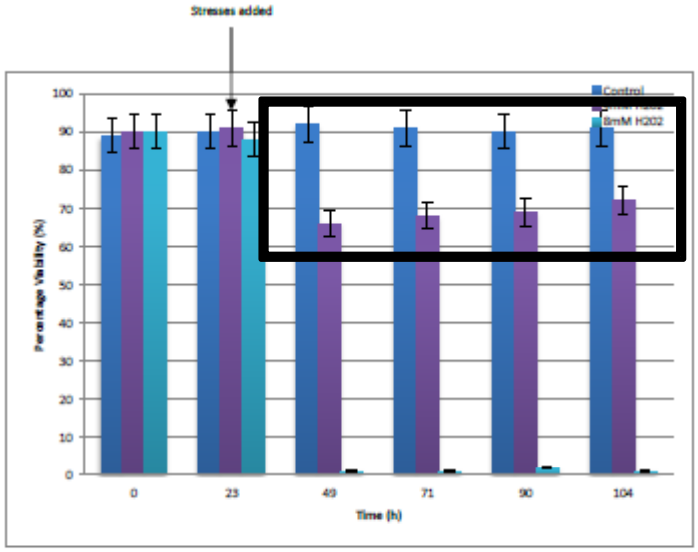

Figure 45: Wild-Type *C.reinhardtii* exposed to range of H_2O_2 stresses

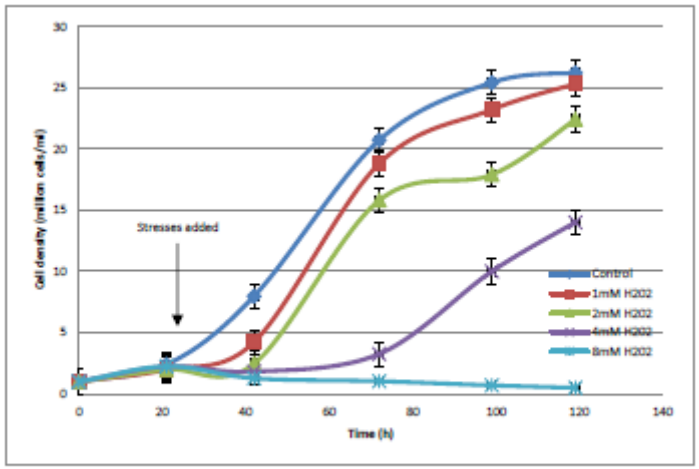

pRelax #8

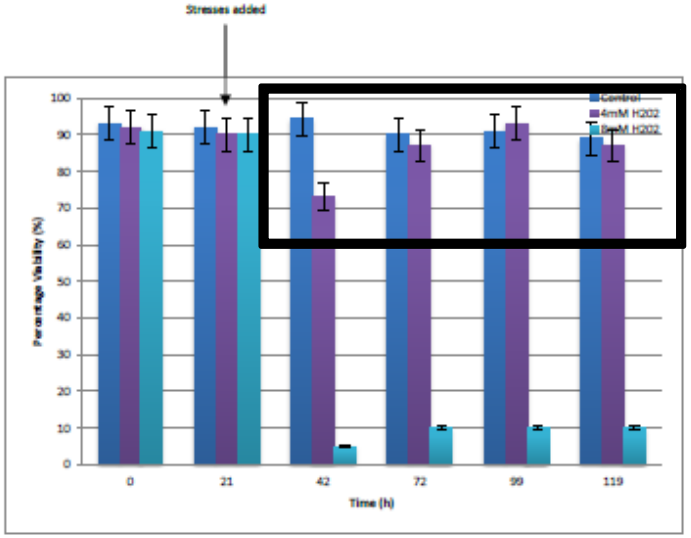

Figure 46: pRelax#8 exposed to range of H_2O_2 stresses

Figure 48: pRelax#8 viabilities over H_2O_2 stress range

Metabolic Engineering in Algae?

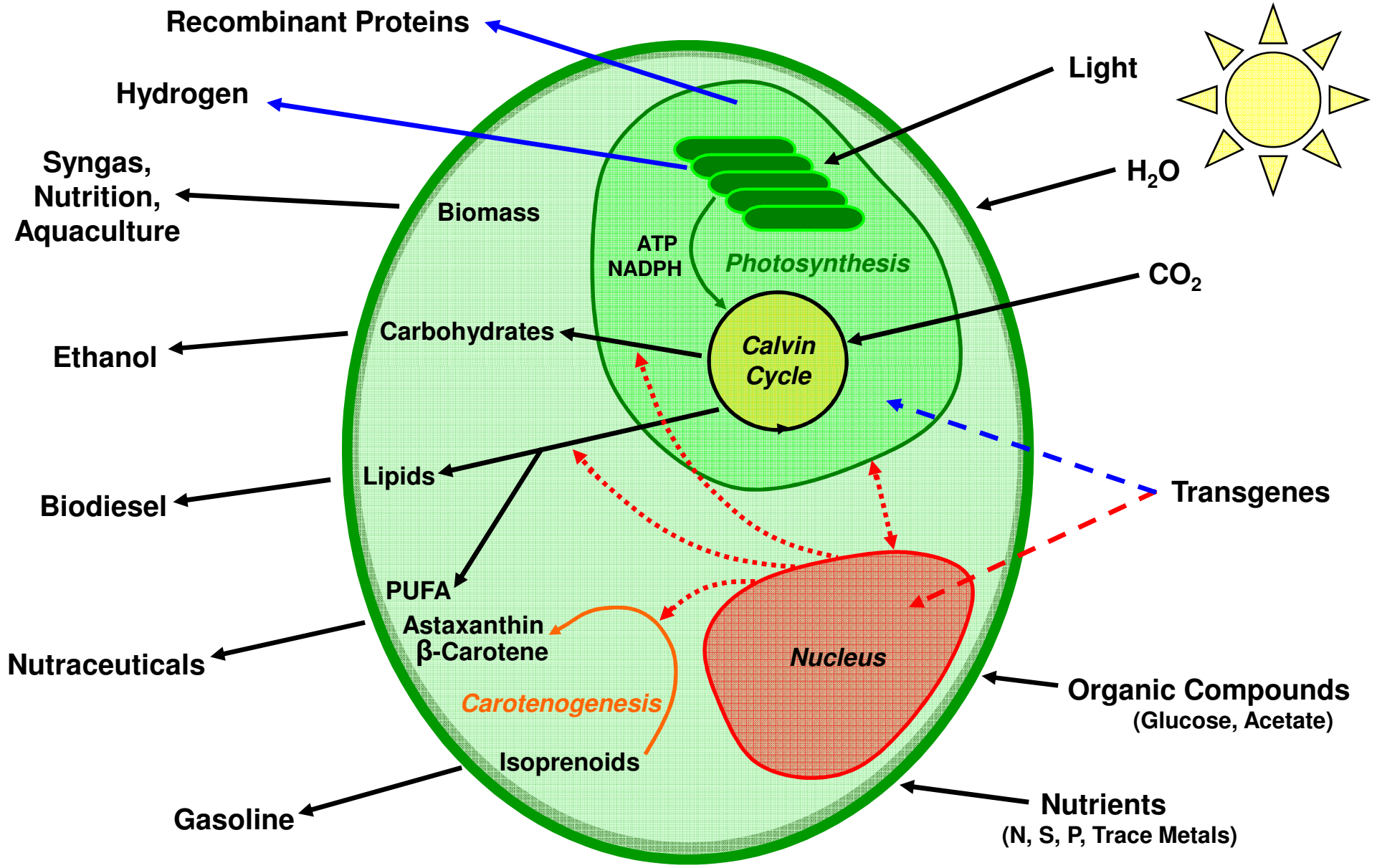

Results and Discussion (High NaCl)

- pRelax #8 and #10 show high tolerance to High NaCl stress
- 49.3% overall higher tolerance to NaCl stress than wild type
- Growth rate seems to be significantly affected in both pRelax and WT
- pRelax cells seem to maintain integrity of cell walls
  - Prevention of apoptotic cell disintegration

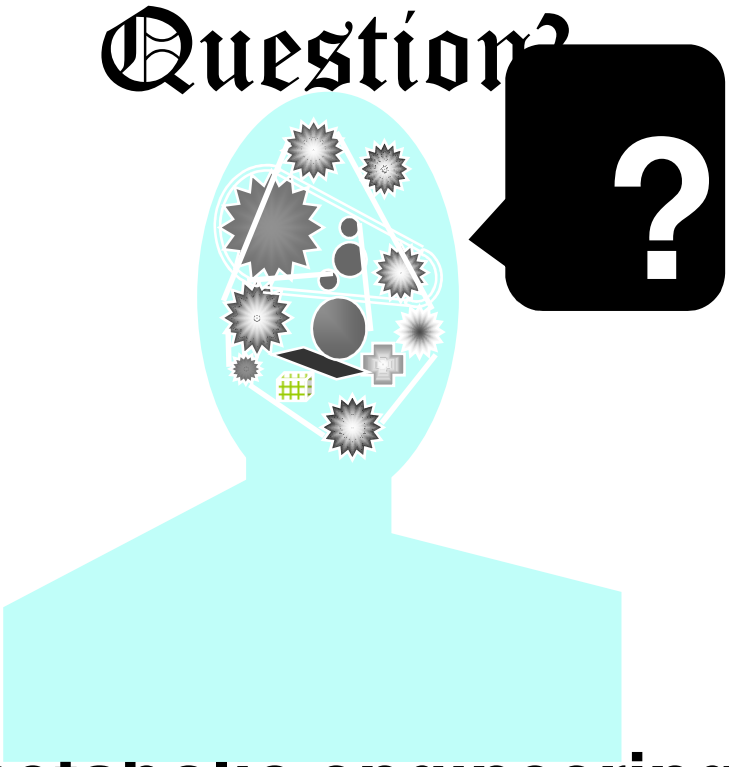

Can metabolic engineering solve problems of yield and quality?

Can we use metabolic eng. to achieve high yields and high quality?

Importance of Quality: Glycosylation Pathways

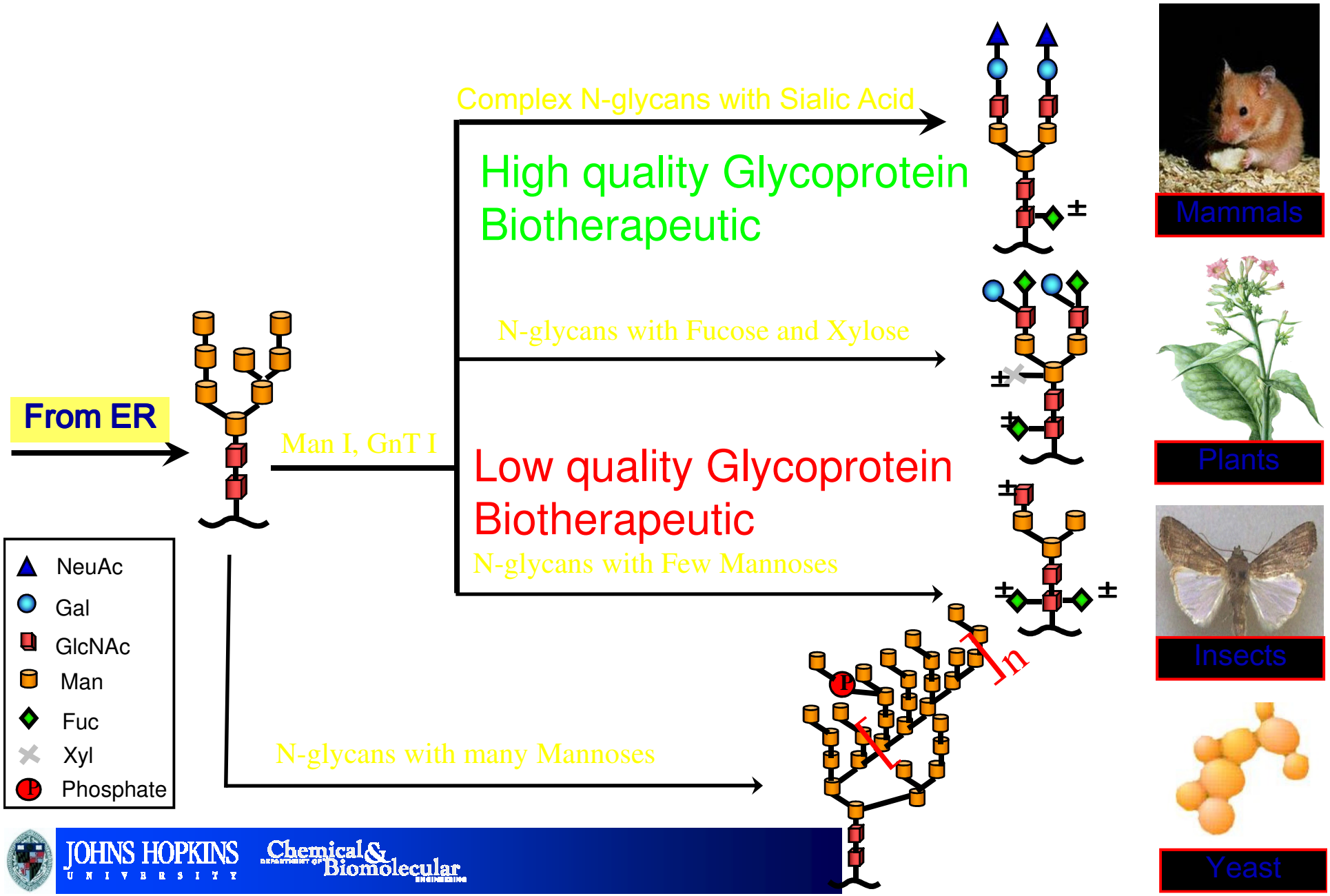

How can we engineer better production hosts?

Product Yield?

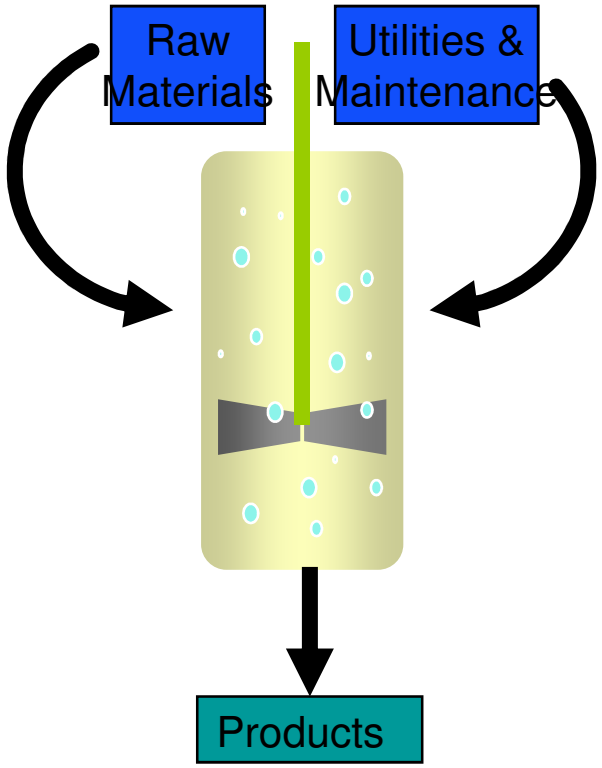

Bacteria (*E. coli*)
Yeast
Plants and Algae Cells
Insect Cells
Mammalian

Product Quality ?

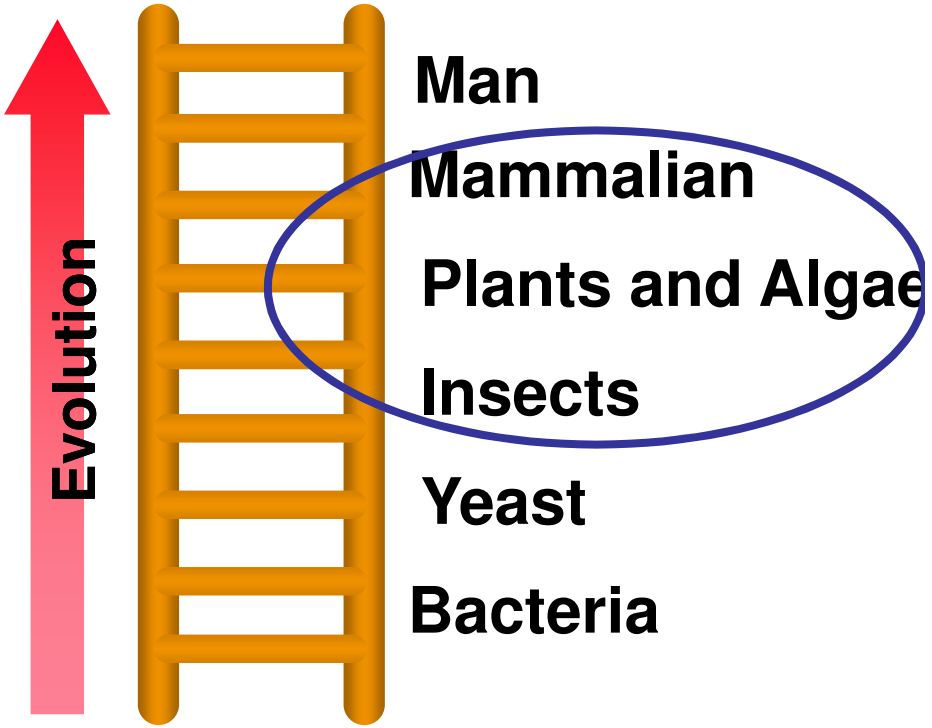

Insect Cells

Apply metabolic engineering to alter glycosylation in insect cells?

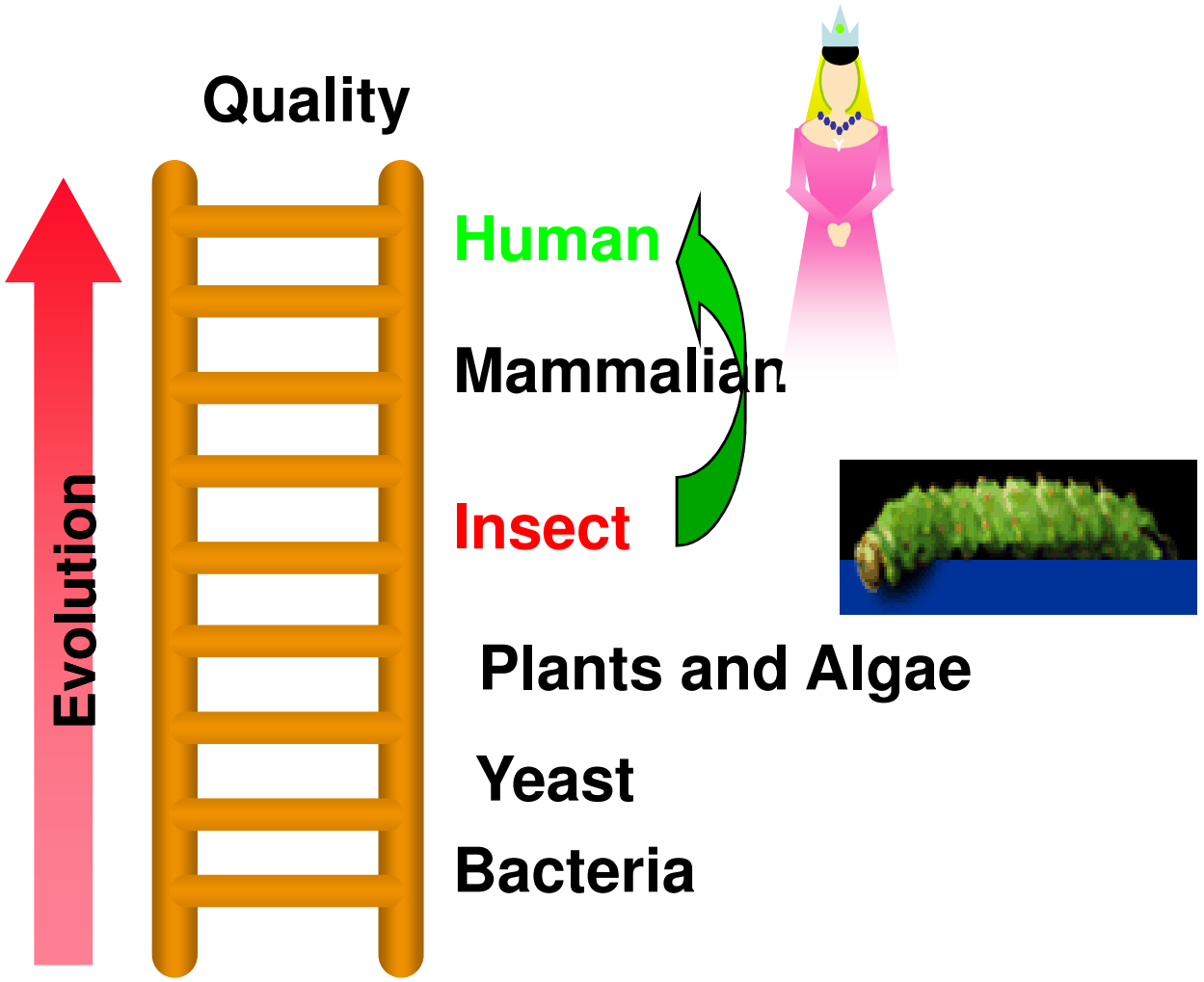

Engineered Insect Cells:

Humanized Biotherapeutics

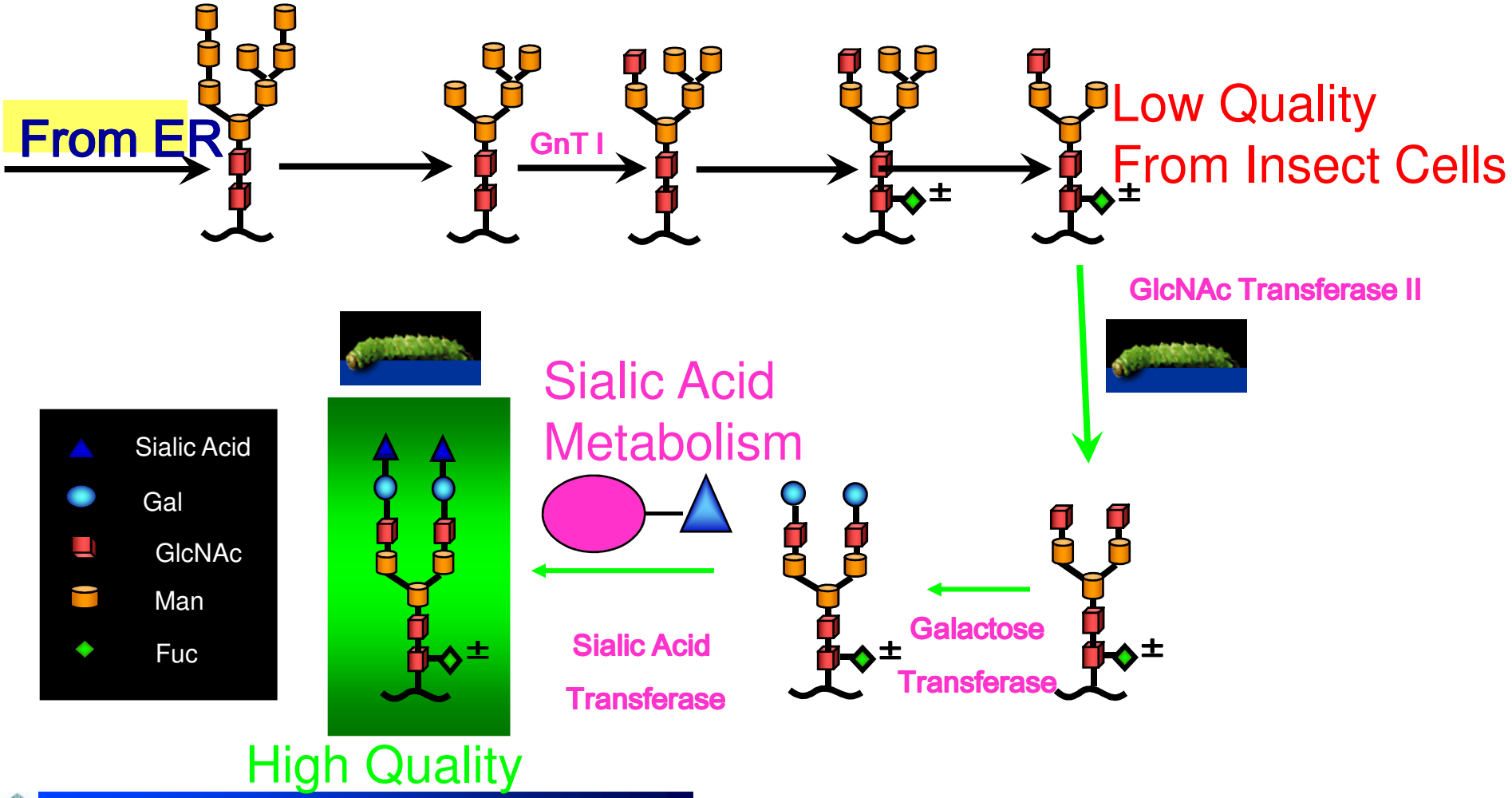

Licensed to Merck, 2009

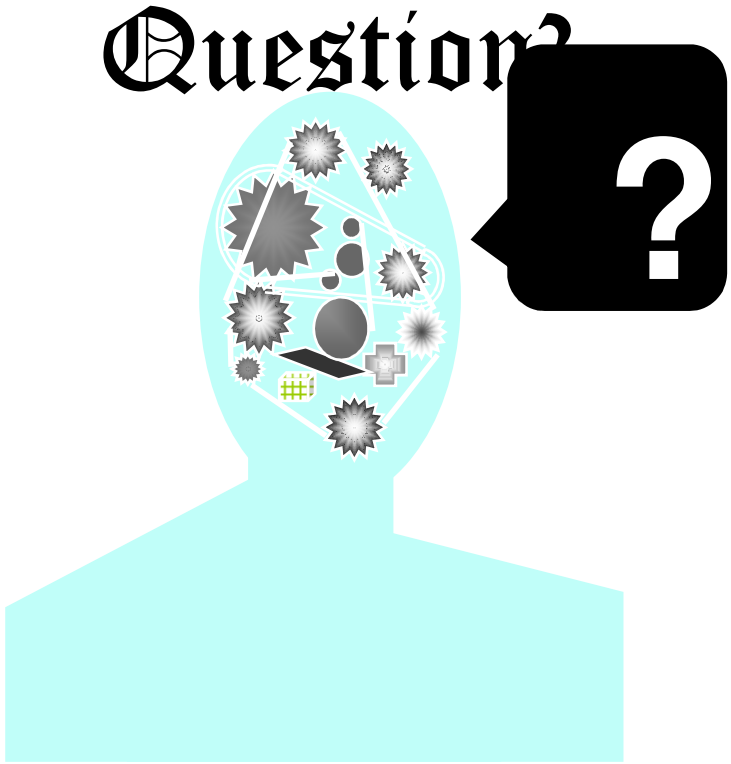

How do we apply genomics to metabolic engineering problems: Mammalian cell culture

One problem:
No Chinese Hamster Ovary Genome

Global Analysis of Glycosylation

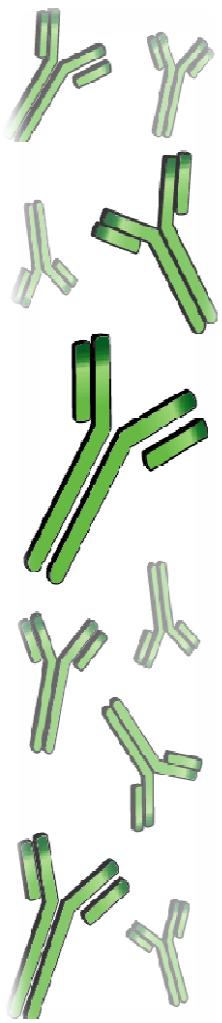

CHO genome contains homologs to 99% of human glycosylation genes (297 of 300, missing ALG13, CHST7, CHST13)

CHO cells express ~ 50% of these genes (141 of 297)

- **Includes genes involved in construction and localization of core glycan structure**

Xu et al (2011)

Glycosylation Genes Expressed in K1

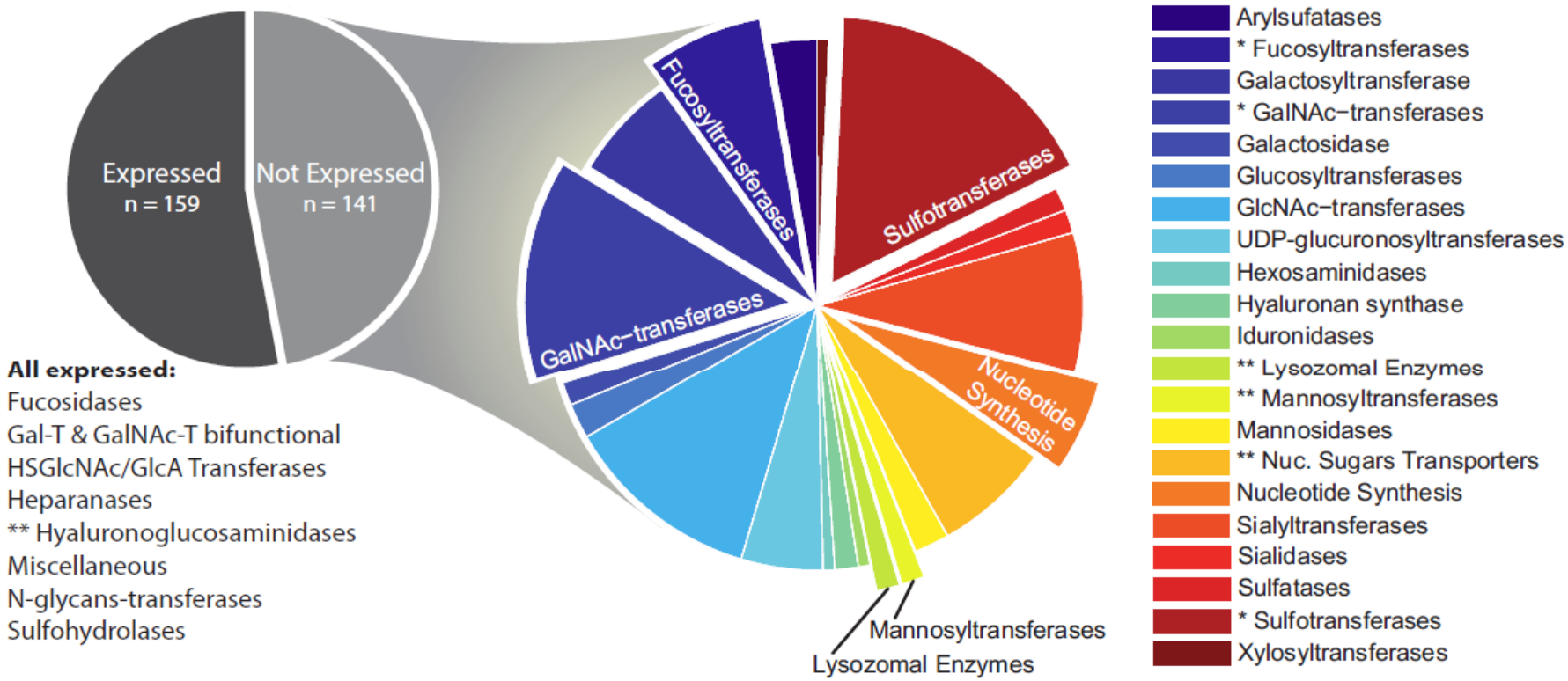

CHO N-linked Glycosylation Pathways

Sialylation
α(2,6) linkage possible
Not expressed.

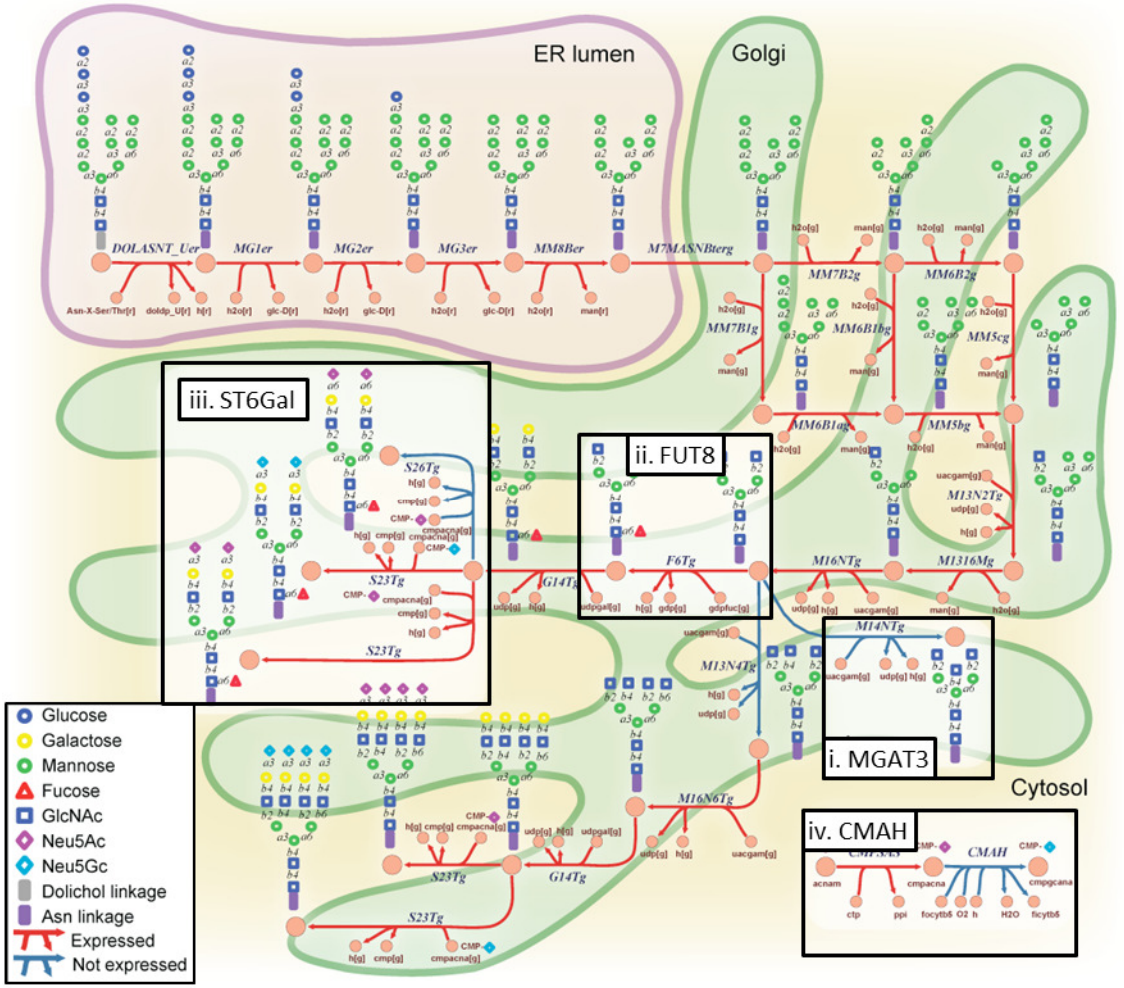

Only fucosyltransferases FUT8 and O-FUT

Bisecting (ß4) GlcNAc
LEC10 gain of function

Neu5Ac->Neu5Gc
No expression,
lower Neu5Gc less
immunogenic
response in humans.

Xu et al , Nature Biotechnol., (2011)

Some Glycosylation Observations

Sialylation:

CHO K1 homologs to all six human ST3Gal enzymes (α(2,3)) sialic acid to galactose.) All expressed.

ST6Gal genes (α(2,6)) not expressed.

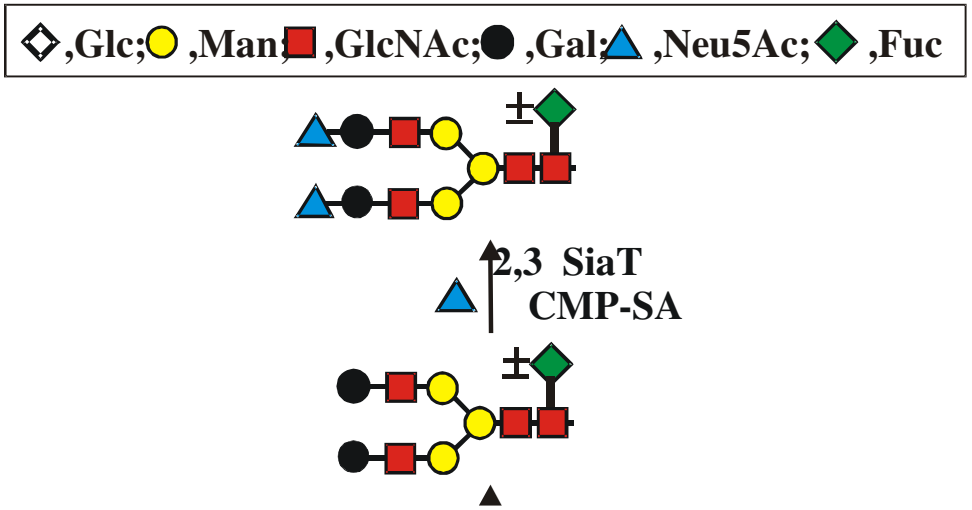

Human contains two types of sialic acid linkages.
CHO cells can only make one of those.
Sialic acids linkages can affect binding such as with influenza virus infection

Other Glycosylation Observations:
NO Bisecting GlcNAc to Blocks Fucose

ß4 GlcNAc from GnTIII:

No observed bisecting (ß4) N-acetylglucosamine (found on 10% of human IgG glycoforms)

GnTIII observed in genome, but not transcriptome

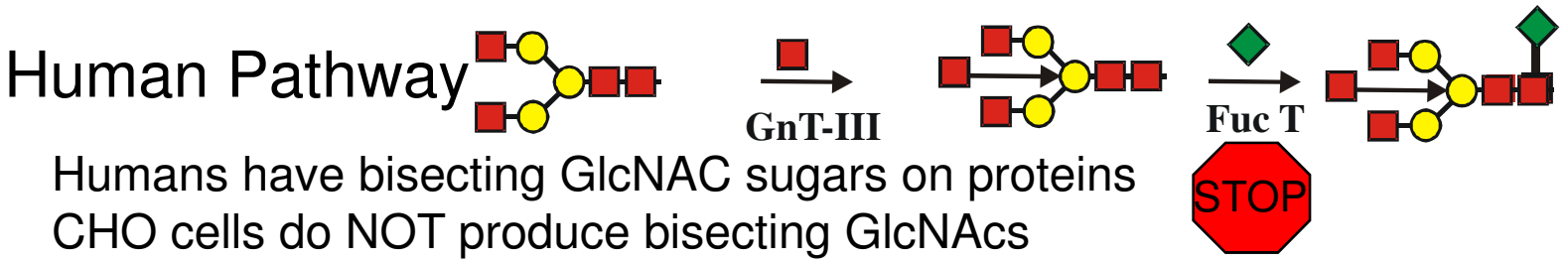

Humans have bisecting GlcNAC sugars on proteins
CHO cells do NOT produce bisecting GlcNAcs
10% of human antibodies include bisecting GlcNAcs

Biological Function?
-Bisecting GlcNAc will inhibit the binding of fucose
-Absence of fucose will increase the antibody-delivered cytotoxicity
-Antibodies from CHO cells will be LESS active in humans (have fucose)
-Antibodies from Humans will be more active (less fucose)

www.CHOgenome.org

Can the community come together to assemble CHO ‘omics information?.

A community website sponsored by academic, government and industrial collaborators has organized and financially committed to share and host genome-scale information about CHO and activities for the biotechnology community.

flybase.org
wikipedia
etc.

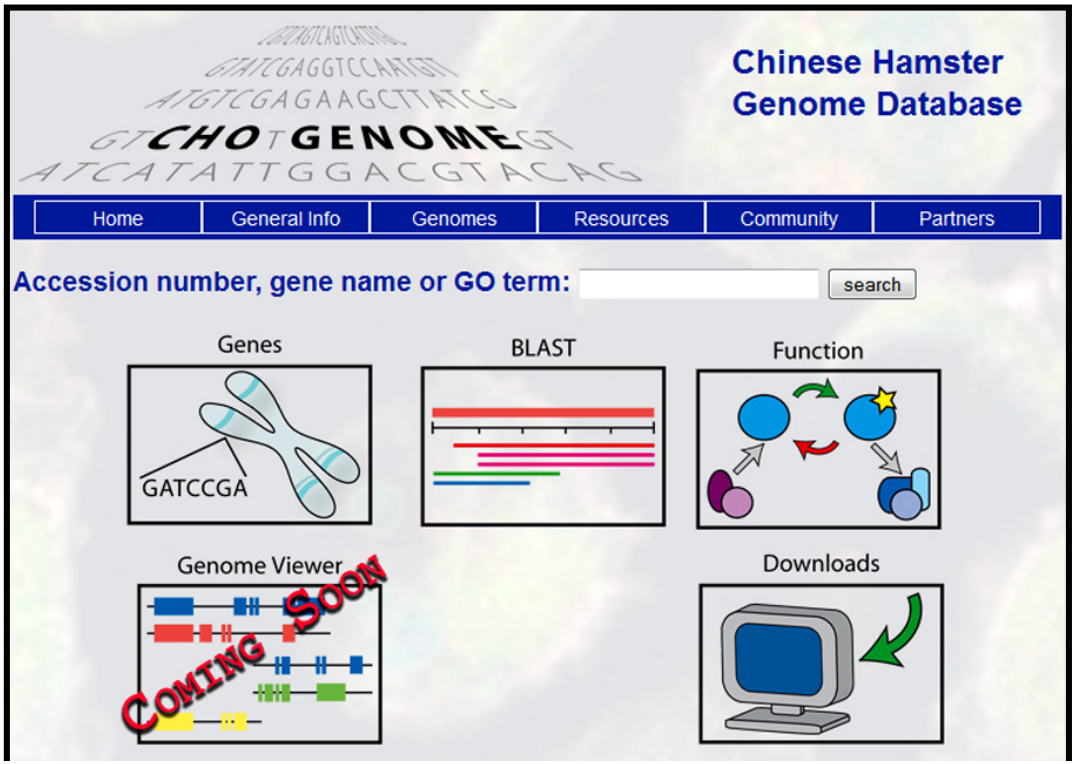

CHO GENOME

Chinese Hamster Genome Database

Home | General Info | Genomes | Resources | Community | Partners

CHO Genome Community

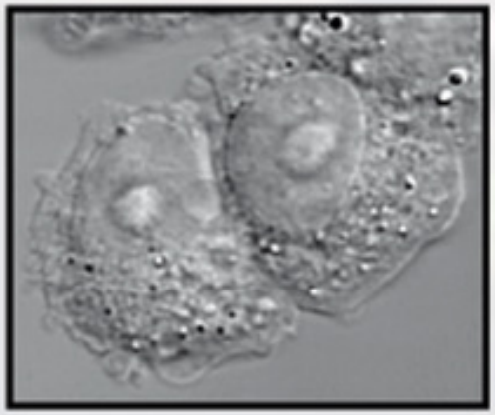

The Chinese hamster (*Cricetulus griseus*) ovary (CHO) cell line was first isolated by Puck (J. Exp. Med. 1958; 108: 259-271) more than 50 years ago. Currently, CHO cells are the most important cell line for production of biopharmaceutical proteins ($100 billion USD in annual revenue) and they offer tremendous promise for production of vaccines as well as in their ongoing critical role as a transfection host for understanding gene function. Despite the scientific and economic importance of this cell line, there is no publicly available genome sequence information for CHO cells.

A Resource for CHO cell genomics

Based on an open source model, the mission of the CHOgenome.org User Group is to share genome-scale information on Chinese Hamster Ovary cells to the international scientific community.

This website, currently hosted at the University of Delaware, is dedicated to hosting data and resources to support the international community working with CHO cells.

We are building the infrastructure to support genome sequencing activities through an international not-for-profit community-based effort.

For more information, feel free to contact:

Kelvin Lee (Univ. Delaware; KHL at udel dot edu)
Nicole Borth (BOKU; nicole dot borth at boku dot ac dot at)
Michael Betenbaugh (Johns Hopkins Univ.; beten at jhu dot edu)

www.CHOgenome.org